

Nature and the Origin of Ein Feshcha Springs (NW Dead Sea)

By
Jawad Ali Hasan
From Jerusalem / Palestine

A thesis for the degree of Doctor of Natural Sciences submitted to the
Faculty of Civil Engineering, Geosciences and Environmental
Sciences

University of Karlsruhe, Germany

Date of thesis defense: 04.02. 2009

Supervisors:

Prof. Dr. Heinz Hötzl, Karlsruhe University
Prof. Dr. Akiva Flexer, Tel Aviv University
Prof. Dr. Amer Marei, Al-Quds University

Declaration

I hereby certify and confirm that this thesis is entirely the result of my own work and that no other than the cited aid and sources have been used.

Erklärung

*Hiermit bestätige ich, dass die vorliegende
Dissertations-Arbeit selbstständig und nur unter
Verwendung der genannten Hilfsmittel
angefertigt wurde*

(Jawad Ali Hasan)
Karlsruhe, February 2009

Dedication

*To my mother and father who supported me and lights up my
life since my birth to this date*

*To my lovely wife "Missa" for her efforts, moral
support and endless encouragement*

*To my children, for there understanding during my absence,
with my love to them all.*

Fawad

ACKNOWLEDGMENTS

This piece of research took a lot of efforts by many people whom I am acknowledging in this dissertation, and will also carry their kindness and support with me when I build my professional life. This support by my professors, colleagues, and friends, was translated through different ways. I was very lucky to receive the wonderful encouragement from all, in addition to financial and psychological support.

I would like to express my deepest thanks and gratitude to my supervisors; Prof. Dr. H. Hoetzl (Faculty of Civil Engineering, / Karlsruhe University), Prof. Dr. Akiva Flexer (Faculty of Science / Tel Aviv University) and Prof. Dr. Amer Marei (Faculty of Science / Al-Quds University) for their kindness, guidance, support, fruitful suggestions and their independence oriented supervision that has given me more insight into the field of scientific research.

The author would like to thank the German Federal Ministry of Education and Research (BMBF) and Dr. Metzger (PTWT) for supporting and funding my work; and for the Country and people of Germany for their continuous support of the Palestinian people and peace in the Middle East.

Special thanks should go to my best promoter and friend Dr. Wasim Ali for his kindness and almost daily assistance, scientific guidance and support. Wasim Ali never forget his people specially the students, thus I was not the only Palestinian student whom Wasim Ali has provided help for him to complete his study in Germany.

I would like to thank *Al-Quds* University represented by its president *Prof. Dr. Sari Nusaiba* for his trust and support. Not to forget my friends Dr. Adnan Rasheed, Dr. Mustafa Kamies, Mr. Mohannad Quri, the staff of the Center for Chemical and Biological Analyses and the Environmental Research Lab for their help and facilitating my work.

Finally, I am indebted to everyone who contributed to completing this work whom I have failed to mention.

ABSTRACT

Groundwater is the primary source of water for the Palestinians and Israelis in West Bank. Efficient management of this resource requires a well developed understanding of the groundwater flow systems so that the quantity of good quality groundwater that can be abstracted on a sustainable basis will be determined.

This study focuses on a small area of the West Bank (Marsaba-Feshcha), since it is considered as one of the few places of the region where additional limited amounts of the groundwater can be developed. This area is arid and suffers from an acute shortage of fresh water; the outlet of this Eastern Aquifer basin is the Ein Feshcha springs group which is located on the upper north-western shore of the Dead Sea, whose discharge amounts to about 60 MCM/Y of saline water. Recent studies have identified the possibility of increasing ground water extraction from Ein Feshcha springs group (Guttman et al., 1995, Guttman, 1998 and Wolfer, 1998).

To understand the hydrodynamics of the Ein Feshcha spring system, water samples were conducted for hydrochemical and isotopic analysis, field studies and geophysical analysis were carried out in order to answer an opened questions regarding water flow and mixing mechanisms. This thesis present the results of hydrochemical, hydrogeological, geomorphological and geophysical studies conducted between 2005 and 2008 on Marsaba-Feshcha study area.

The results of the chemical and isotope analyses interpretation (Na-K-Mg, Schoeller and Durov diagrams, the ionic ratios, the positive relationships between Cl and other elements, heavy metals, Ra, Rn, 18O and 2H relations) used in attempt to identify the water source and mixing processes taking place at the vicinity of the springs strongly suggest variable scenarios controlling springs salinization. In some cases, it is due to mixing with paleo-brines at the fresh saline water interface, while in other cases deep seated brines emerge along regional faults. With the geochemical analysis, radioactive- and stable isotopes no clear evidence show that evaporation brine plays an important role for salinization of groundwater within the rift graben but there is more evidence for dissolution of salts which may explain the high content of Ba and Pb. Nevertheless it is believed that the water receives its salinity in the direct vicinity of the springs, being of better quality in the Cretaceous mountain reservoir. This finds its expression in EC values, from 0.7 to >15 mS/cm and Cl concentrations of 137 to >11048 mg/l.

A salt diaper was recognized in the study area, due to this salt diaper the conducted waters through the fractures and faults exhibit a wide range of major cations; major anions and trace element concentrations leading to dissolution, evaporation and/or precipitation processes which takes place along the water flow path and in the vicinity of the springs.

The use of VES-method proved the horizontal migration of fresh/saline water interface as a result of drop in Dead Sea level, which is formed due to the contact between the trapper saline pockets with the conducted fresh waters through the transversally faults. These transversal faults conduct the fresh water from West to the East finding its way at the vicinity of Ein Feshcha were local mixing between the fresh waters and significantly evaporated and isotopically modified brines trapped in between the exposed clay layers due to the retreat of Dead Sea water (paleo brines) take place. With the use of NPEMFE-method and field observations we managed to localize the transversal faults were the hydraulic connection between the lower aquifer and the upper aquifer get mixed and fined its way out at Ein Feshcha study area.

This study has practical implications regarding recent groundwater management and groundwater development for the benefit of both Palestinians and Israelis residing in the area. It is apparent that in order to intercept the fresh water before it becomes mixed with the salt diaper and / or paleo-brines, new well field at upstream need to be drilled and more water to be pumped in the Eastern flanks of Judea Mountains.

ZUSAMMENFASSUNG

Für Palästinenser und Israelis im Westjordanland ist Grundwasser die wichtigste Ressource für die Wassergewinnung. Eine nachhaltige und effektive Bewirtschaftung dieser Ressource erfordert ein gut entwickeltes Verständnis der Grundwasserfließsysteme, damit die nachhaltig entnehmbaren Wassermengen so bestimmt werden können, dass es zu keiner Beeinträchtigung der Grundwasser-Qualität kommt.

Diese Studie konzentriert sich auf den südöstlichen Teil des Westjordanlands (Marsaba-Feshcha), einem der wenigen Teilgebiete, wo noch begrenzte Mengen von Grundwasser zusätzliche erschlossen werden können. Dies obwohl das Gebiet extrem arid ist und an einem akuten Mangel an Süßwasser leidet. Die noch erschließbaren Wassermengen dokumentieren sich in der Schüttung der heute noch ungenutzten Wässer der Ein Feshcha Quellgruppe im Uferbereich des nordwestlichen Toten Meeres. Sie stellt den Auslauf des „Östlichen Aquiferbeckens“ dar und umfasst im langjährigen Mittel eine Wassermenge von rund 60 MCM/Y, allerdings von stark salzhaltigem Brackwasser. Neue Studien und Grundwasser-Modellierungen haben jedoch die Möglichkeit aufgezeigt, aus dem Grundwasserleiter der Ein Feshcha Quellgruppe unter Berücksichtigung der Herkunft der hochsalinaren Wässer und deren Vermischungszonen mit dem Süßwasser letztere für die Wassergewinnung zu erschließen (Guttman et Al., 1995, Guttman, 1998 und Wolfer, 1998).

Zur Abklärung der komplexen hydrodynamischen Verhältnisse und zum besseren Verstehen der bei der Vermischung der unterschiedlichen Wässer wirksamen Mechanismen und Prozesse wurde ein umfangreiches Untersuchungsprogramm im Umfeld und Einzugsgebiet des Ein Feshcha Systems im Rahmen diese Doktorarbeit gestartet. Es umfasste geologische, strukturelle und hydrogeologische Feldstudien, geophysikalische Sondierungen und Auswertungen sowie ein umfangreiches Beprobungs- und Analysenprogramm zur Untersuchung der verschiedenen Quellwässer. In dieser Dissertation werden die Ergebnisse dieser in der Zeit von 2005 bis 2008 durchgeführten Untersuchungen im Gebiet Marsaba-Feshcha zusammengefasst.

Die Ergebnisse der chemischen und Isotopen-Analysen wurden unter Heranziehung der Ionen-Verhältnisse, insbesondere der Na-K-Mg-Verhältnisse sowie der positiven Beziehungen zwischen Cl und anderen Elementen, ferner mittels Schoeller- und Durov-Diagrammen, sowie den Konzentrationen von Schwermetallen, Ra, Rn und dem ^{18}O und ^2H Verhältniss

bewertet und hinsichtlich der Mischungsprozesse analysiert. Die Ergebnisse lassen erkennen, dass stark veränderliche Szenarien im direkten Umfeld der Einzelaustritte die Mischungsverhältnisse und damit die Versalzung der Wässer beeinflussen. In einigen Fällen kommt es direkt im Interface der aufsteigenden Paläo-Solen zur Vermischung mit den geringmineralisierenden Grundwässern, während in anderen Fällen Salzwässer aus tieferen Salzwasserkörpern entlang einzelner lokaler Störungszonen nach oben steigen. Mittels der hydrogeochemischen Analysen sowie der radioaktiven und stabilen Isotope ist nicht zu belegen, dass der Verdunstung eine größere Rolle für die Versalzung der betrachteten Grundwässer zukommt, hingegen spricht mehr für die Auflösung von Salzkörpern, wodurch die erhöhten Werte von Ba und Pb erklärt werden können. Unabhängig davon ist von einer Vermischung der Salz- und Süßwässer in der direkten Umgebung der Quellen auszugehen. Dies findet seinen Ausdruck in den hohen Streuwerten der EC Werten, von 0,7 zu >15 mS/cm, und der Cl-Konzentrationen, von 137 zu >11048 mg/l, im Umfeld der Quellen, während die Versalzung in den Bohrungen des Kreideaquifer rasch nach Westen abnehmen.

Eine Salzdiapir-Struktur wurde im Untersuchungsgebiet erkannt. Aufgrund dieses Diapirs weisen die verschiedenen Wässer entlang der Brüche und Störungen sehr hohe Konzentrationen bei den Hauptionen auf, wobei es im weiteren an der Oberfläche entlang des Wasserablaufpfades wieder zu Verdunstung und Ausfällungen im Umfeld der Quellen kommt.

Der Einsatz der VES-Methode belegte die horizontale Migration der Salz/Süßwasser-Interfacefront im Quellbereich als Folge der rezenten Absenkung des Toten Meeres von Westen nach Osten. Hierbei spielt die Wassernachführung über transversale Störungen in den Festgesteinen eine große Rolle. Diese Wässer lösen zum Teil die in den jungen Tonsedimenten des Toten Meeres eingeschalteten Salztaschen und bedingen eine weitere Ursache für die zunehmende Versalzung der aus Westen aus dem Kreideaquifer nachströmenden Süßwässer. Mittels des Einsatzes der NPEMFE-Methode und weiterer geophysikalischer Feldmessungen konnten die transversalen Störungen lokalisiert werden. Über diese erfolgt im Wesentlichen auch die hydraulische Verbindung zwischen dem unteren und dem oberen Aquifer sowie der weitere Abfluss aus dem engeren Quellgebiet der Einflüsse.

Diese Ergebnisse und Befunde haben praktische Auswirkungen zum Vorteil der Palästinenser und Israeli betreffend der weiteren Grundwasserexploration sowie der Bewirtschaftung dieses

Grundwasservorkommens. Es ist offensichtlich, um das Süßwasser zu gewinnen, dass es vor der Versalzung durch Vermischung mit den Paläo-Solen oder dem Kontakt mit dem Salzdiapir gefasst werden muss. Die Untersuchungen zeigen, dass neue Brunnenfelder weiter westlich im Anstrombereich der Süßwasser zu bohren sind. Damit wäre es möglich das durch Niederschlagsinfiltration in den hohen Kammlagen zwischen Hebron-Jerusalem-Ramallah einsickernde Wasser, das im Wesentlichen den „Eastern Aquifer“ in der östlichen Flanke der Judäischen Berge generiert, wesentlich intensiver zu nutzen.

TABLE OF CONTENTS

Declaration		i
Dedication		ii
Acknowledgment		iii
Abstract		iv
German Abstract		vi
Table of Contents		ix
List of Figures		xii
List of Tables		xvii
List of Symbols		xix
1	INTRODUCTION	1
1.1	Study Area	2
1.2	Land use & Land Cover	3
1.3	Motivation and Problem	5
1.4	The Importance of the Eastern Basin of the Mountain Aquifer	7
1.5	Previous Studies	8
1.5.1	The Saline Water Formation	8
1.5.2	Previous Studies carried out in the Study Area	9
1.6	The Main Objective of the Study	13
1.7	The study assumptions and Hypothesis	13
1.8	Sources of Data	15
2	GEOLOGY AND TECTONIC SETTING	16
2.1	Overview on the Geology of the West Bank	16
2.2	Regional Geological Setting	17
2.3	General Structural Geology of the Study Area	20
2.4	Lithostratigraphy of the West Bank	24
2.5	Lithostratigraphy of Marsaba-Feshcha Driange Basin	27
2.5.1	Cretaceous Rocks	31
2.5.1.1	The Kurnub Group	31
2.5.1.2	The Ajlun Group	31
2.5.1.2.1	Lower Beit Kahil Formation (Albian to Lower Cenomanian)	32
2.5.1.2.2	Upper Beit Kahil Formation (Albian to Lower Cenomanian)	32
2.5.1.2.3	Yatta Formation (Lower Cenomanian)	32
2.5.1.2.4	Hebron Formation (Upper Cenomanian)	33
2.5.1.2.5	Bethlehem Formation (Upper Cenomanian to Turonian)	33
2.5.1.2.6	Jerusalem Formation (Turonian)	34
2.5.1.3	Senonian Group (Belqa Group)	34
2.5.2	Neogene and Quaternary	35
2.5.2.1	Plio-Pleistocene Formation	36
2.5.2.2	Holocene formation	37
3	HYDROGEOLOGY & GROUNDWATER AQUIFERS	39
3.1	Climate Conditions of the West Bank	39
3.1.1	Climate Conditions of Marsaba-Feshcha Study Area	39
3.2	Drainage System	41

3.2.1	Surface Water Flow Direction of Marsaba-Feshcha Study Area	43
3.2.2	Ground Water Flow Patterns of Marsaba-Feshcha Study Area	44
3.3	Surface Water Resources	45
3.3.1	The Jordan River	46
3.3.2	The Dead Sea	46
3.3.3	Flood Water Runoff	47
3.4	Ground Water Resources	47
3.4.1	Groundwater Wells	47
3.4.2	Springs	48
3.5	The Eastern Aquifer Basin (EAB)	50
3.6	Groundwater Aquifers in the West Bank	51
3.6.1	The Shallow Aquifer	52
3.6.1.1	Pleistocene Aquifer	52
3.6.1.2	Neogene (Miocene-Pliocene) Aquifer	52
3.6.1.3	Eocene Aquifer	53
3.6.2	The Upper Aquifer	53
3.6.2.1	Cenomanian Aquifer	53
3.6.2.2	Turonian Aquifer	53
3.6.3	The Lower Aquifer	53
3.6.4	The Deep Aquifer	54
3.7	The Aquifers and Aquicludes of Marsaba-Feshcha Study Area	54
3.7.1	Regional Aquifers in Marsaba-Feshcha Area	55
3.7.1.1	The Upper Cretaceous Carbonate Aquifer	55
3.7.1.2	Hydraulic Separation between the Two Aquifers	56
3.7.1.3	The Jordan Valley Deposits [Dead Sea Group]	57
3.7.2	Wells Abstraction and Groundwater Levels	58
4	METHODOLOGIES	59
4.1	Sampling Sites and Collection Time	59
4.2	Sample Collection Methodology	65
4.3	Determination of Chemical Parameters	66
4.4	Graphical Classification Methodology	66
4.5	Isotopic Analysis	67
4.5.1	Tritium, Deuterium and Oxygen Isotopes	67
4.5.2	Radium Isotopes (Rn222, Ra223, Ra224 and 226Ra)	68
4.5.2.1	DURRIDGE RAD 7 (Rn 222, Ra226)	68
4.5.2.2	Delayed Coincidence Counter (Ra223, Ra 224)	70
4.6	Geophysical Methods	70
4.6.1	Principle of Vertical Electric Sounding (VES)	70
4.6.2	Principle of the Natural Pulse Electromagnetic Field of the Earth (NPEMFE)	72
5	HYDROCHEMISTRY	74
5.1	Hydrochemical Data	74
5.2	General Water Quality Variations	75
5.3	Groundwater Chemistry	77
5.3.1	Giggenbach Trianglar Plot	77

5.3.2	Schoeller Graph	78
5.3.3	Durov and Piper Diagram	79
5.3.4	Geochemical Behavior of Selected Trace Elements	83
5.3.5	Chemical Composition Ratios	90
5.3.6	Mineral Saturation Levels	98
5.3.7	Correlation Matrices	100
5.4	Summary of Results	102
6	ISOTOPIC ANALYSIS	108
6.1	Water Isotopes Composition	108
6.2	$\delta^{18}\text{O}$ and $\delta^2\text{H}$ vs. Cl and TDS	113
6.3	The Radioactive Isotope Tritium	116
6.4	The Radioactive Isotopes Radium and Radon	120
6.4.1	Radium (Ra) and Radon (Rn)	121
6.5	Summary of Results	127
6.5.1	Water Isotopes composition in Selected Water Samples (^2H , ^{18}O , ^3H , Rn and Ra)	127
7	GEOPHYSICAL RESISTIVITY ANALYSIS	130
7.1	Vertical Electric Sounding	130
7.1.1	Profile I	133
7.1.2	Profile II	137
7.1.3	Profile III	138
7.2	Electromagnetic Radiation (EMR)	140
7.3	Summary of Results	143
8	DISCUSSION AND CONCLUSIONS	146
8.1	Discussion	146
8.2	Conclusions	153
8.3	Recommendations	155
9	REFERENCES	158
10	APPENDICES	173
	CURRICULUM VITAE OF THE AUTHOR	186

LIST OF FIGURES

Figure No.	Figure title	Page
Figure 1.1	A map of the studied area, showing the Marsaba-Feshcha Basin.	3
Figure 1.2	Land Use of the West Bank Marsaba-Ein Feshcha 2006, (after Arij 1995).	5
Figure 1.3	A map of the study area showing the location of the springs at the western shore of the Dead Sea. (the map coordinates refer to the Israel grid system).	8
Figure 2.1	Distribution and configuration of the geological settings in the Middle East, (after: Johnson, 1998).	18
Figure 2.2	Geological overview of West Bank and adjacent areas (modified after: Bender, 1968 and Bayer, 1986).	19
Figure 2.3	Schematic fault structure of the Dead Sea transform which forms a pull apart graben structure, (similar to the Dead Sea depression). (after: Garfunkel and Ben-Avraham, 1996).	20
Figure 2.4	Major geological structures of the West Bank showing the main folds and faults. (after: Rofe & Raffety, 1965 and Fleischer, 1996).	21
Figure 2.5	Regional Structural Map Of The West Bank/Palestine Within The Plate Tectonics Theory (modified after: Fruend & Garfunkel, 1980 and Bayer, 1980).	23
Figure 2.6	Geological cross section across the Dead Sea Depression and the graben geological structure (after: Fruend & Garfunkel, 1980).	23
Figure 2.7	Lithostratigraphic classification of the outcropped geologic formations of the West Bank (after: Geological Survey of Israel, 1973).	27
Figure 2.8	Geological cross section A-A` illustrating the structural features of the study area. (modified after: Neev & Hall, 1976 and Exact, 1999).	29
Figure 2.9	Geological formations exposed in the study area (after: Kafri et al., 1997).	37
Figure 2.10	Ideal columnar stratigraphic section indicating various formations in the study area. (modified after: Geological Survey of Isreal, 1973).	38
Figure 3.1	Average annual precipitation rate in mm in the Jordan Valley Area (EXACT, 1999).	40

Figure 3.2	Potential evapo-transpiration map of the West Bank. (modified after: SUSMAQ, 2001).	41
Figure 3.3	Topographical map of West Bank which shows the distribution and variation in altitude in the topography of the study area and the West Bank, (SUSMAQ, 2001).	43
Figure 3.4	A map showing the Marsaba-Feshcha main drainage systems.	44
Figure 3.5	A geological map showing the wells and springs location in the study area.	48
Figure 3.6	Figure 3.6: East-West cross section from Marsaba area to the Dead Sea through Ein Feshcha (Guttman et al., 2004).	55
Figure 3.7	NW-SE hydrogeological cross section showing the regional aquifers and aquicludes through the Mountain Aquifer (after: CH2MHill, 2000).	57
Figure 4.1	Sample location map presenting the locations of the sampled springs and wells at Ein Feshcha study area.	61
Figure 4.2	Sample location map presenting the locations of the sampled springs and wells at (Herodion field) the catchment study area.	62
Figure 4.3	Sample filtration methodology used for Radium pre-concentration (^{223}Ra , ^{224}Ra and ^{226}Ra).	65
Figure 4.4	DURRIDGE RAD 7 device a) Photo of the RAD7 device during Rn 222 measurements. b) Schematic technical circuit for Rn 222 for water samples measurements.	69
Figure 4.5	DURRIDGE RAD 7 device a) Photo of the RAD7 device during Ra-226 measurements. b) Schematic technical circuit for Ra-226 for water samples measurements.	69
Figure 4.6	Principle of Vertical Electric Sounding.	71
Figure 4.7	SYSCAL R2 instrument ready for measurement in the field.	71
Figure 4.8	An example for data processing of the measured resistivity values and final results from Ein Feshcha study area (sounding point EFE06).	71
Figure 4.9	a) Electromagnetic radiation sensor (CERESKOP). b) Registered signal above a fracture.	73

Figure 5.1	Site map show the Cl concentration for the year 1984, 2000 and the current work (modified after: Guttman and Simon, 1984).	76
Figure 5.2	Giggenbach Na-K-Mg diagram, representing the springs and boreholes in the Marsaba-feshcha catchment area.	78
Figure 5.3	Schoeller diagram presenting the chemical composition of the Ein Feshcha springs and some samples from the catchment area during the wet season.	79
Figure 5.4	Durov diagram for the major cations and anions, illustrating the classification of the 9 zones as proposed by Lloyd and Heathcoat (1985).	80
Figure 5.5	Based on the cation and anions composition of the samples, Durov diagram illustrates the results of the analyzed water samples of dry and wet season of Ein Feshcha and the catchment area.	81
Figure 5.6	Piper diagram illustrating the results of the analyzed samples of dry and wet season of Ein Feshcha and the catchment area.	83
Figure 5.7	Values of selected ions vs. Cl observed in water samples collected from the study area, Ein Feshcha.	85
Figure 5.8	Values of selected ions (Na, K, Ca, Mg, SO ₄ , Sr, B and Li) vs. Cl observed in water samples collected from the study area, Ein Feshcha.	86
Figure 5.9	Scatter diagram presenting the effect of temperature and pH on the beaver of Ba (a) Ba vs. temperature and (b) Ba vs. pH.	88
Figure 5.10	Scatter diagram presents a linear correlations between Sr, B and TDS, a) TDS vs. Strontium, and, b) TDS vs. Boron.	89
Figure 5.11	Sr/Ca vs TDS scatter diagram of water groups presents the correlation between the TDS and Sr/Ca ionic ratios. *D.S samples for TDS divided by 100	92
Figure 5.12	Represents the cross plots of Mg/Ca vs Na/Cl in meq/l ratios for Ein Feshcha springs and samples from the catchment area. Presenting the chemical changes due to mineral/brine interactions and due to proposed mixing patterns.	97
Figure 5.13	Durov and Piper plots showing the relative proportions of major cations and anions of the study area.	106

Figure 6.1	The stable $\delta^2\text{H}$ and $\delta^{18}\text{O}$ composition relation of all samples collected from the study area plotted and compared with respect to the EMWL and to the LMWL.	112
Figure 6.2	The isotopic compositions (^2H & ^{18}O) of selected water samples, representing a possible evaporation trend and mixing trend with other source of lighter water.	112
Figure 6.3	^{18}O and ^2H vs. Cl, the two lines represent the expected variations due to mixing of present groundwaters with brine waters and due to evaporation.	115
Figure 6.4	^{18}O and ^2H vs. TDS, the two lines represent the expected variations due to mixing of present groundwaters with brine waters and due to evaporation.	115
Figure 6.5	Results of the tritium measurements at the Dead Sea (after Ilana Steinhorn 1985).	118
Figure 6.6	Scattered plot of ^{18}O versus ^3H for the samples of the study area.	119
Figure 6.7	The secondary accumulation of hydrous manganese oxides and iron oxides as thin black layers (laminae) at Ein Feshcha study area.	121
Figure 6.8	The ^{226}Rn -Cl relation of the springs and groupwaters of the study area.	124
Figure 6.9	$^{222}\text{Rn}/^{226}\text{Ra}$ activity ratios vs. Cl of the springs and groupwaters of the study area.	125
Figure 6.10	Schematic cross section showing the actors responsible for ^{226}Ra source and the mechanism leading to ^{222}Rn release and to ^{226}Ra accumulation in spring deposits.	129
Figure 7.1	Electric resistivities of different lithologies and waters with different salinities (after Palacky, 1987).	132
Figure 7.2	Photograph presenting the location site at Ein Feshcha natural reserve. It shows the location of the three profiles and the main topography of the area.	132
Figure 7.3	Satellite map with the localization of the 19 VES-soundings on three profiles.	133
Figure 7.4	Vertical section along profile I.	135
Figure 7.5	Lithological section presenting the lithological setting of borehole Feshcha-4 and Feshcha-10 (modified after GSI, 2006).	136

Figure 7.6	Late Pleistocene–Holocene sedimentary rocks exposed at Ein Feshcha study area.	137
Figure 7.7	Vertical section along profile II.	138
Figure 7.8	a) Vertical section along profile III, b) the simulated Vertical section along profile III.	139
Figure 7.9	Field observations: a) East-West transversal fault crossing the main fault at Ein Feshcha main spring, b) East-West transversal fault at Ras Feshcha.	141
Figure 7.10	Satellite map with the detected faults and fractures localized by the stress variations using NPEMEF-method, with the Cereskop instrument.	141
Figure 7.11	East-West directed cracks found in the study area.	142
Figure 7.12	Presents the results of the combination of the two geophysical methods (VES and NPEMFE).	144
Figure 7.13	General geological schematic cross section at Ein Feshcha study area showing the field relations between the different aquifers and the Dead Sea.	145
Figure 8.1	A structural map of the top Judea Group showing the main folds and faults (modified after: Fleischer & Gafsou, 1998 and Ben-Itzhak, & Gvirtzman, 2005).	152

LIST OF TABLES

Table No.	Table title	Page
Table 2.1	Generalized stratigraphic column of the West Bank describing and illustrating the Israeli and the Palestinian names of the different geological formations in the West Bank as well as their lithology. (after: Guttman et al., 2000 and Geological Survey of Israel, 1990-2002).	25
Table 2.2	Stratigraphic table of rock units at Marsaba-Feshcha drainage basin and its surrounding area (modified after: Millennium Engineering Group et al., 2000 and Guttman et al., 2000).	30
Table 3.1	The stratigraphic table of rock units in the study area. Jerusalem formations divides into three formations in the eastern part of the study area (Begin, 1974).	53
Table 4.1	Sample name, description and coordination of the samples collected during the first campaign from the springs and wells of the catchment area.	62
Table 4.5	An illustration for the used analytical methods in the determination of the various chemical parameters	66
Table 5.1	Basic field measurements, representing the basic field analyzed data cared out during the course of this study.	74
Table 5.3	Trace element composition of the analyzed water samples from Marsaba-Feshcha study area.	84
Table 5.4	Water salinity classification based on TDS, Strontium and Boron (Saxena et al 2004).	89
Table 5.5	Chemical Composition Ratios for water samples of the study area. The ionic ratios are in meq/l.	97
Table 5.7	Interpretation or predictions of dissolution / precipitation of mineral phases depending on mineral saturation indices (SI), evaluation output from table 5.8.	100
Table 5.9	Pearson's correlation matrices for data showing marked correlations at a significance level of <0.05. All values in mmol/l, EC in $\mu\text{S}/\text{cm}$	101
Table 5.10	Average ionic ratios in groundwaters in source aquifers and in the investigated springs.	107

Table 6.1	The $\delta^{18}\text{O}$ and $\delta^2\text{H}$ composition of the samples collected during the dry and wet season from the study area.	111
Table 6.2	The tritium ($\delta^3\text{H}$) concentration in the groundwater and springs of the samples collected during the courses of this study.	119
Table 6.3	Shows the ^{222}Rn concentrations and electrical conductivity for Ein Feshcha springs and the catchment area wells.	126
Table 7.1	This table presents the coordination, length, beginning and end of the detected fractures	142
Appendix Table 4.2	Sample name, description and coordination of the samples collected during the second campaign from the springs and wells of the catchment area.	173
Appendix Table 4.3	Sample name, description and coordination of the samples collected during the third campaign from the springs and wells of the catchment area.	174
Appendix Table 4.4	An illustration for the used analytical methods in the determination of the various chemical parameters.	175
Appendix Table 5.2	This table presents the field analysis and the analysis of the cations and anions of the catchment area during the course of this study.	176
Appendix Table 5.6	The ionic ratios of the sampled wells and springs in the Marsaba-Feshcha area during the years 2005, 2006 and 2007.	178
Appendix Table 5.8	Saturation indices of the end members of water chemistry in the dry season samples of Ein Feshcha.	184

LIST OF SYMBOLS

AQU	Al Quds University
Bq/kg	Becquerel per kilogram
dpm	Disintegrations per minute
D.S	Dead Sea
EMR	Electromagnetic radiation
EMWL	Eastern Meteoric Water Line
GMWL	Global Meteoric Water Line
JWC	Joint Water Committee
Km	Kilometer
Km²	Square kilometer
LMWL	Local Meteoric Water Line
m	Meter
m³	Cubic meter
m.a.s.l	Meters above sea level
m.b.s.l	Meters below sea level
MnO₂	Manganese dioxide
MO	Military Order
MCM/yr	Million cubic meters per year
Meq/l	Milliequivalents per liter
NPEMF	Natural Pulse Electromagnetic Field of the Earth
No.	Number
ND	Not determined
pCi/kg	Picocurie per kilogram
PWA	Palestinian Water Authority
SI	Saturated indices
TU	Tritium Units
μmol/l	Micromole per liter
μg/l	Microgram per liter
UNRWA	United Nation Relief and Works Agency for Palestine Refugees
VES	Vertical Electric Sounding

1 INTRODUCTION

The area between the Mediterranean Sea and the Jordan Valley comprises of two countries, Palestine and Israel, the groundwater system is shared and does not respect the political boundaries between the two countries. Groundwater is the primary source of water for the Palestinians in the West Bank. Efficient management of this resource requires a well-developed understanding of the groundwater flow systems so that the quantity of good quality groundwater that can be abstracted on a sustainable basis will be determined (SUSMAQ, 2001).

Water resources have played an important role in shaping the geopolitical boundaries of Palestine since the beginning of the twentieth century. Although water resources of Palestine are scarce due to hydrological and other natural and physical characteristics, the abnormal political conditions due to the Israeli occupation of the West Bank since 1967 have further complicated the water situation. The scarcity of the water resources in the West Bank, due to arid to semi-arid climate, overexploitation, mismanagement as well as the fact that these resources are shared with Israel, gave it a great importance. It is the most valuable and precious resource of the region. Because of this importance, water became the central issue in the bilateral and multilateral peace talks.

The groundwater resources in the surrounding area were deteriorated noticeably in the last 50 years. Salts and TDS concentrations in the aquifer systems along Jordan valley which was covered by Lake Lisan, the ancestor of the Dead Sea, indicate a general trend of increasing salinity which reach its maximum in the lower part of Jordan rift valley and threaten the groundwater resources and consequently the stability of the whole system in the area (Khayat, 2005 and Khayat et al., 2006).

This study focuses on a small area of the West Bank (Marsaba-Ein Feshcha), since it is considered as one of the few places of the region where additional limited amounts of the ground water can be exploited. This area, the Eastern Basin (Jerusalem-Dead Sea sub-basin), as well as other parts of the whole semi arid eastern slope of West Bank mountains, is arid and suffers from an acute shortage and quality deterioration for the available replenished fresh water resources; the outlet of this basin is the Ein Feshcha spring group which is located on the upper north-western shore of the Dead Sea, whose discharge amounts to about 50-80 MCM/Y of saline / brackish water. Different rough estimations were provided for the spring

annual discharge of saline water ranging between 30 and 50 MCM/Y (Fink, 1973; Shachnai et al., 1983, Greenboim, 1992, 1993); 80 MCM/Y (Guttman and Simon, 1984), 53 MCM/Y (Guttman, 1997), 80 MCM/Y (Hötzl et al., 2001), 65 MCM/Y (Rophe, 2003). During the years of 2003 and 2004 “The Israeli Hydrological Services” established a specific survey for the measurement of the spring’s recharge which resulted with the total capacity of 62-67 MCM/Y. The springs have large storage and are characterized by stable discharges with only small annual fluctuations. It has been calculated by Mazor and Molcho (1972) that rainwater falling on the Hebron Mountains emerges at Ein Feshcha about 36 years later.

Recent studies have identified the possibilities of optimizing fresh ground water extraction from Ein Feshcha spring group (Guttman et al., 1995, Guttman, 1998, Wolfer, 1998 and Bensabat et al., 2004).

1.1 Study Area

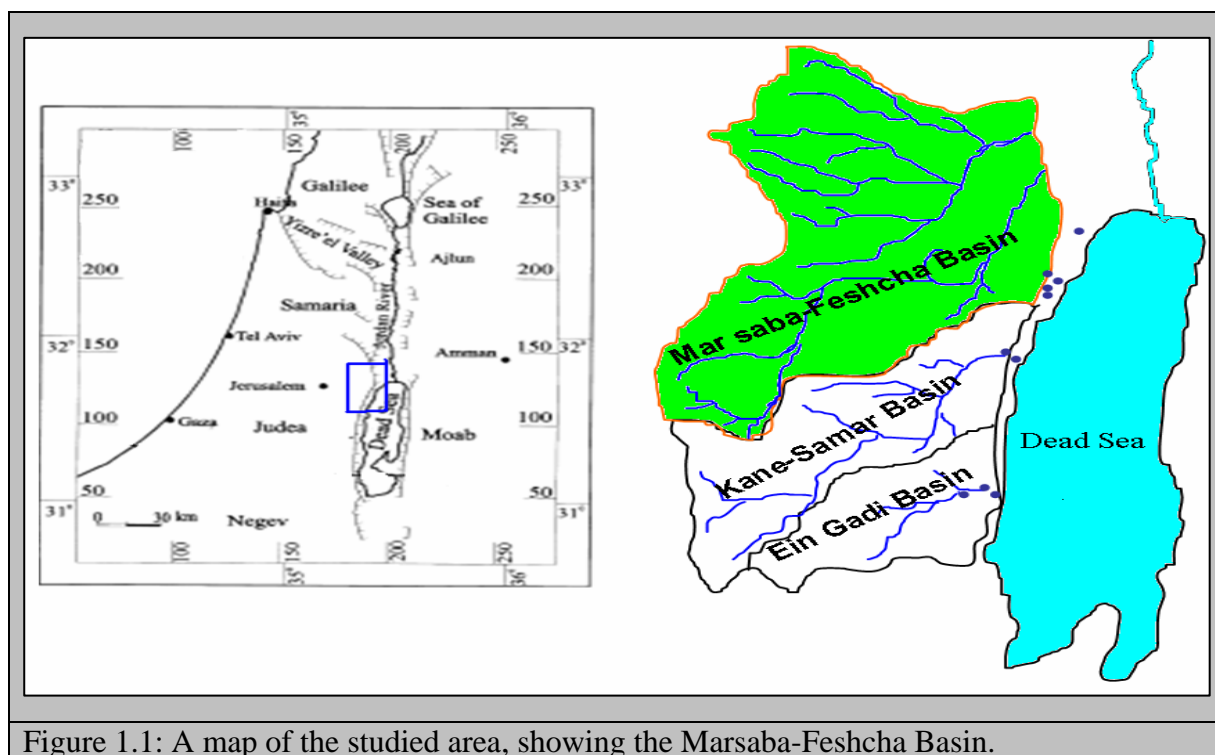
In this research, the study area considered as part of the West Bank which has an overall area of approximately 5822 km², of which 5632 km² is land area and 190 km² is the area of the Palestinian portion of the Dead Sea (ARIJ, 2000).

The study area covers a surface of approximately 800 km², extending from the eastern slopes of Jerusalem anticlinorium through the Marsaba anticline in the west to the Jordan Valley and the Dead Sea in the east, including the spring complex of Ein Feshcha in the north-west of the Dead Sea (figure 1.1). The study area is considered as part of the eastern drainage basin of the Jerusalem hills. This catchment area is part of the Eastern Basin and belongs to the sub-basin of the Jordan River-Dead Sea basin.

According to Reifenberg and Whittles (1947), the study area includes within its boundary different geological formations. In the Jordan Valley; the main rock type are Lisan marls. They are deposits of a former inland lake and consist of loose diluvial marls. The Lisan marl soils are generally of a rather light nature, their clay content varies from approximately 10 to 20%. High concentration of lime content is present, which varies between 25 and 50%. Where there is no possibility for irrigation, the Lisan marls are covered with a very sparse growth of halophytic plants. In the Eastern Slopes region, the main soil types are the semi-desert soils, the secondary soil types are the mountain marls. For the semi-desert soils, the formation of

sand and gravel is characteristic of desert weathering (Reifenberg and Whittles, 1947, Dudeen, 2000).

The study area can be defined as semi-arid to arid and suffers from acute shortage of freshwater. The main discharge of the groundwater in the Eastern Basin of the Mountain Aquifer flows into the Dead Sea at the Ein Feshcha springs. At an elevation of approximately 413m below sea level, that is, a head of 860m over a lateral distance of about 20 km. The main aquifer is bordered along the Dead Sea by an active fault zone, the Gulf of Aqaba-Jordan Valley transform fault, as well as accompanied by significant vertical components of stepped faults along its flanks (Wishahi et al., 1999)

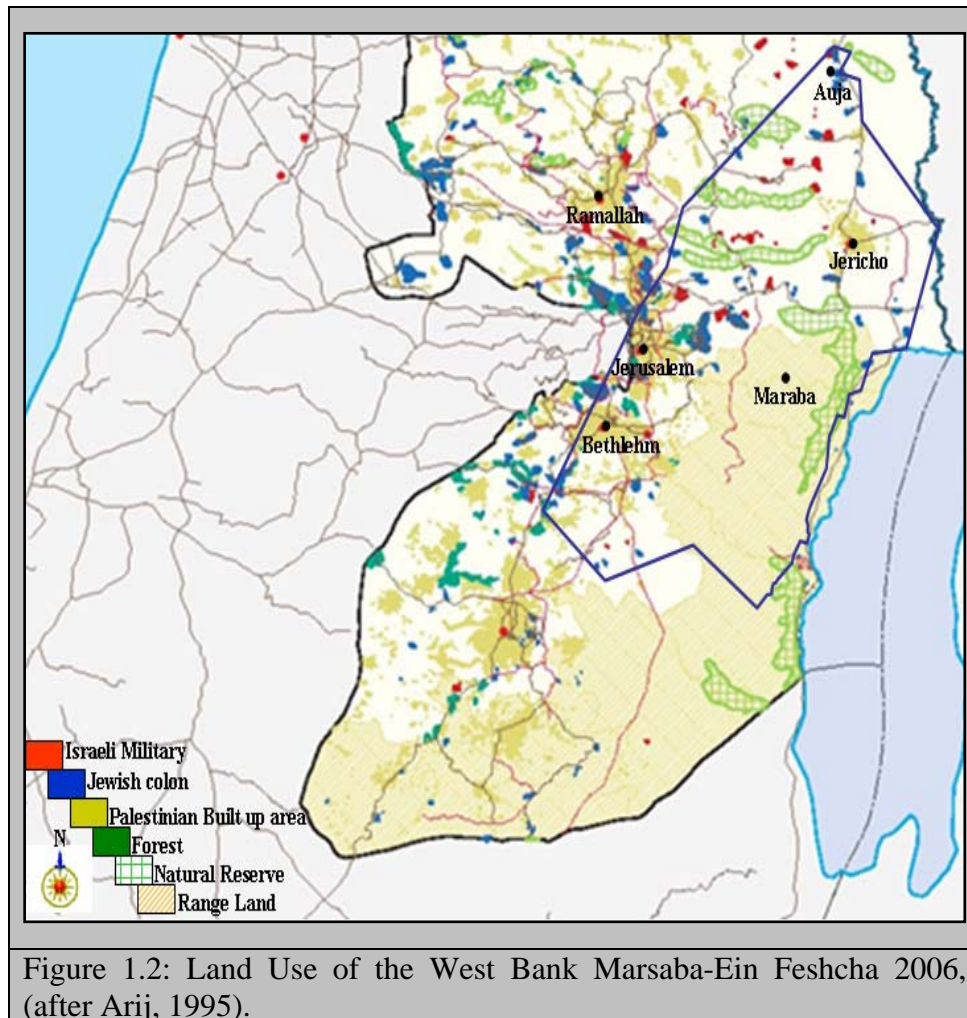


1.2 Land Use & Land Cover

Land and water are the two major natural resources that determine the feasibility of agriculture and patterns of agricultural production. In the Palestinian Territories, both they are limited therefore their proper use and efficient management must be accepted as the cornerstone for the development of Palestinian agriculture. In the study area there are two distinguished agro-ecological zones, the Eastern Slopes Zone and the Jordan Valley Zone.

- The Eastern Slopes Zone: is a transitional zone between the central high-land and the desert areas of the Jordan Valley. The steep mountain slopes with little rainfall that predominate in this region make it an almost semi-arid to desert zone. Agricultural production is of marginal importance and is limited to rainfed cereals such as wheat and barley. Olives are cultivated as well. Average annual rainfall is 650-300 mm, with altitudes varying from 800 meters above sea level until 400 m below sea level.
- Jordan Valley Zone: is a narrow strip between the Eastern Slopes and the River Jordan. It drops to about 400 m below sea level near the Dead Sea. Rainfall is low (100-200 mm), winters are mild and summers hot. Soils are sandy and calcareous. This zone is the most important irrigated area in the West Bank. The availability of both springs and ground water makes this area most suitable for off-season vegetables and for semi-tropical tree plantations, including bananas and citrus. All strains and varieties of dates palm trees are still in existence. Citrus orchards with special taste and early ripping season are remarkable in the Jordan Valley. However, without access to water this region would be a desert.

The study area covers about 800 km² and with an estimated population to be around 112,000 representing the two communities (Palestinians and Israel's). As shown in figure1.2, five major land use classes can be distinguished, these are Palestinian built-up areas and Israeli settlements (124.77 km²), nature reserves and forestry (117.65 km²), agricultural area (69.11 km²), roads and industrial area (56.14 km²), rang land and closed military areas (431.44 km²) (Arij, 1995). The area and the distribution of the main land use activities in the study area are subjected to change due to the continuous activity of opening new streets and population expansion.



1.3 Motivation and Problem

Water is considered to be one of the most important resources, so its presence is essential for achieving the overall economic and social development in the country. This area is water stressed country and lacks for enough water resources. This is because of the water demand in the country is much higher than the water supply from which emerge a real problem must be solved.

High and continually increasing demands for groundwater for domestic, industrial and agricultural and other needs due to high population growth rates (around 2.985%, PCBS, 2007), the continual upgrading in living standard and the existing degradation in groundwater quality because of pollution and salinization are putting more pressure on the groundwater resources of the country. Therefore the groundwater management and planning are required.

However the countries (Palestine, Jordan, Syria and Israel) controlling the fresh watershed of the Dead Sea. They began to consume these waters intensively. As well Israel and Jordan are using the Dead Sea water for potash and other minerals production, which contributes to the depletion of water (Gavrieli, 1997). Also the evaporation from the Dead Sea exceeded the rain and runoff into it. As a result, the inflow of fresh waters into the Dead Sea has diminished significantly. This drop of the Dead Sea level will have an effect on groundwater by increasing the head differences between the Dead Sea and the groundwater levels in the surrounding areas. Then the groundwater drainage is expected to increase toward the Dead Sea (Yechieli et al., 1996, Salameh and El-Nasir, 2000b). The area along the Dead Sea shore is already occupied by Dead Sea water. They become gradually flushed and occupied by freshwater. This freshwater become saline due to the residuals of the Dead Sea water in the aquifer matrix. Due to inflow of the fresh groundwater into the Dead Sea, several subsidence and sinkholes rose along the Dead Sea. These phenomena cause a serious danger to residence at these areas. It may be possible to reduce the scale of these subsidence by reduce the rate of dissolution of the layer by removing the waters undersaturated with respect to salt or by controlling the groundwater discharge into the Dead Sea.

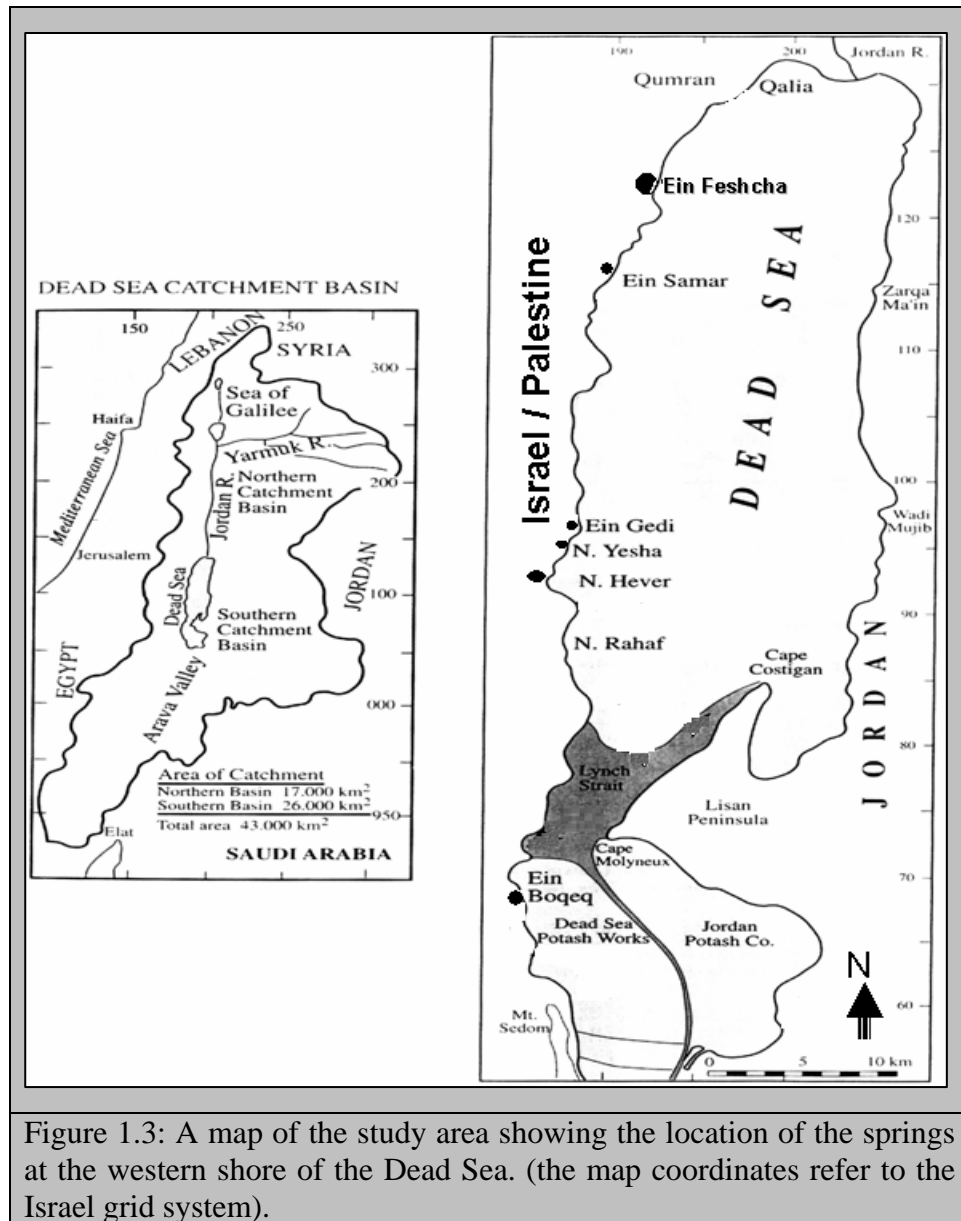
The difference in the elevation between the Dead Sea level and the highlands to the West is more than 1200 m.a.s.l over a horizontal distance of 25 km. These might be a reason for the submarine groundwater discharge into the Dead Sea. The quantity of freshwater input into the Dead Sea occurred due to surface water runoff in winter season and / or due to submarine groundwater discharge.

The drop of Dead Sea level is accompanied by a retreat of the shoreline and in reduction in the size of the surface area, accompanied by change in the location of existing springs, and in the appearance of new springs along shoreline.

Concluding that, the groundwater is a valuable and an important natural resource in the West Bank and the surrounding area. So the priority of all strategies is to preserve water quantity and quality to use clear fresh water. Groundwater is the major source of fresh water in the Dead Sea region which issuing from the surrounding highlands of the West Bank Then its need to understand the mixing water patterns at Ein Feshcha springs not only but also to evaluate the newly exposed western shoreline along the Dead Sea in respect of hydrogeology.

1.4 Importance of the Eastern Basin of the Mountain Aquifer

This basin lies almost entirely in the West Bank. The recharge area of this basin encompasses over 2200 km² and the storage area over 2000 km² (Gvirtzman, 1994). Estimates of the safe yield (or extraction potential) of this basin are not well determined; 100 MCM/Y (Gvirtzman, 1994 and Elmusa, 1996), 125 MCM/Y (Wolf, 1995) and 172 MCM/Y (Oslo II Accords, 1995). According to Oslo II Accords (1995), the 172 MCM/Y are shared as follows: 24 MCM/Y utilized by the Palestinians from wells, 30 MCM/Y utilized by the Palestinians from springs, 40 MCM/Y used by the Israelis and 78 MCM/Y to be developed in the future. The direction of the water flow of this basin is eastwards toward the Jordan River and the Dead Sea. Naturally this basin is drained by several groups of springs, whereas a fraction of its water discharges into the Jordan River and the Dead Sea. The springs emerge from the Judea Group layers and can be divided into two groups. The first group includes the springs located north of Jerusalem- Jericho road. The main springs are the Ein Al Sultan and Al Duok springs, Wadi Qielt springs and Auja springs. They are the outlet of the Upper Aquifer. The second group includes the Ein Feshcha springs, the Kane-Samar springs, Ein Shalem spring and Ein Gadi springs that are located along the Western Shore of the Dead Sea (figure 1.3). The springs of this basin were responsible for discharging about 42.2 MCM/Y with good water quality of which about 28.2 MCM/Y was used by the Palestinians and 14 MCM/Y was used by Israel (Israeli Hydrological Services and PWA, 2001). In addition to the good quality spring water, there is about 45-80 MCM/Y of brackish water discharged by the springs of the Eastern Basin on the western shore of the Dead Sea. The Dead Sea area contains a series of more than 17 closely located springs, collectively called the Ein Feshcha Springs. Ein Feshcha group is the remarkable discharge zone for large amounts of ground water (about 50-80 MCM/Y) through the alluvial deposits to the Dead Sea. So it is considered as one of the few places of the region where additional amounts of the ground water can be developed



1.5 Previous Studies

1.5.1 The Saline Water Formation

During several major phases of the geological history, brines were formed which endanger all groundwater reservoirs of the Dead Sea-Jordan Rift system. During the Late Proterozoic-Early Cambrian, a major evaporative phase occurred in the Middle East (Stoecklin, 1968). Later, the Triassic was characterized by large scale marine oscillations and due to alternations of normal shelf and intertidal hyper saline to brackish environments; thick layers of Upper Triassic

gypsum and halite were laid down both West and East of the present day Jordan River (Zak, 1963; Bandel and Khoury, 1981).

During the Mio-Pliocene, brines were mainly generated by the post-Messinian ingression of seawater which dissolved evaporates previously deposited on the dried up Mediterranean Sea bed and in the erosive channels incised into the adjoining coastal areas (Rosenthal et al., 1999). During the Pleistocene, fluvio-lacustrine conditions prevailed in the Jordan Valley and the fresh water Samra Lake developed. This lake became progressively saline, probably as the result of dissolution and flushing of salts from the previous hypersaline Sdom Sea (Picard, 1943) resulting in the saline Lisan Lake. From the Pleistocene onwards, the Lisan Lake became more and more saline by evaporation and by subsequent flushing of evaporites. At present, the remnant of this period is the Dead Sea. Thus, during four major periods, the rock sequences were flushed of previously formed brines and evaporites and were made ready for the following generations of liquids.

1.5.2 Previous Studies carried out in the Study Area

Understanding the hydrology, hydrogeology and hydro-stratigraphy, represents the key issues in groundwater research studies aimed at managing the groundwater resources. Climatic characteristics of the West Bank are strongly dependent on many physical features such as topography, geology and soil structure.

The first published water research studies in Historical Palestine were done by the Irrigation Service of the British Department of Land Settlement during the British Mandate of Palestine in 1947. That study was published in the form of three volumes which included the "Water Measurements" in Palestine for the periods "Prior 1944, 1944-1945 and 1945-1946. The most important and comprehensive groundwater study conducted during the Jordanian administration was executed by a British Consulting Company called Rofe & Raffety through a contract with the Central Water Authority of Jordan. That was a three year study (1963-1965) including geology and hydrogeology of the West Bank (Rofe & Raffety, 1963 & 1965). Herzalla (1973) published a report on the groundwater resources of the Jordan Valley which was mainly based on the Rofe & Raffety study mentioned earlier. That report made a comparison between the Jordan Valley on the East of the Jordan River and the Jordan Valley on the West. Among the main recommendations of that study was to set up a groundwater

management program to overcome the overdraft situation since most well fields were overexploited and saline. That program involved a ban on new extraction wells, exploration of new fresh water fields and controlling the surface water floods of the major side wadis.

The most important current groundwater study conducted in Palestine is the United States Agency for International Development (USAID) funded project initiated on July 1st, 1996. That project was a multi phase, multi task, multi disciplinary water resources project in the West Bank and Gaza Strip, aimed at implementing the water related aspects of the OSLO agreements (1993-1995) signed between the P.L.O. and Israel. The first phase of that project was conducted by the American companies Camp Dresser & McKee (CDM) and Morganti. CDM/Morganti (1996-1998) created a groundwater flow model to study the Sustainable Yield of the Eastern Aquifer Basin (EAB) in the West Bank and submitted their results in 1998 in the form of a final report. The main findings of that model were:

- a) The total estimated recharge was 197.3 MCM/Y.
- (b) Confined aquifers have a transmissivity ranging from $400\text{m}^2/\text{day}$ to $300,000\text{m}^2/\text{day}$, while storativity ranges from 0.1 to 1.
- (c) Unconfined aquifers have a specific yield ranging from 1 to 20%.
- (d) The flow pattern is very complex and structurally controlled.

The area has been investigated previously by other researchers with a number of regional hydrogeological publications that overlap the current study, including:

- ❖ Geological mapping was performed by Rofe & Raffety (1963), Begin (1974) and Arkin (1976).
- ❖ According to the geochemical model proposed by Starinsky (1974), the brines are the product of seawater that intruded into the rift in the Neogene and underwent evaporation and salt precipitation, particularly halite and gypsum.
- ❖ Rosenthal (1978) used uranium isotopes and found that the activity ratio ($^{234}\text{U}/^{238}\text{U}$) and ^{238}U concentration in Jericho 4 & 5 that penetrate the lower aquifer are similar to the values in Jericho 1 & 2 that are pumping from the upper aquifer. The main conclusion is that at the north of Jericho City there must be a hydraulic connection between the Lower Aquifer and the Upper Aquifer (probably a fault- but he didn't locate it). The mapping of Wadi Kelt region carried out by Wolfer (1998) provides indirect evidence of the existence of this assumed fault (at least its northern edge).

- ❖ Stiller and Chung (1984) measured the radium-226 in the meromictic Dead Sea during 1963-1978 for three profiles along the western shoreline of the Dead Sea for a depth of about 300 m. They found that the radium activities in the upper water mass for the depth between 0 and 160 m were higher than that in the lower water mass. On the other hand they mentioned that the radium inventory for the three profiles were similar. They tried also to find the geological origin of radium in the Dead Sea.
- ❖ The origin of Ca-Cl brines as a water type and particularly those in the Rift have been discussed for many years (Lerman, 1970; Starinski, 1974; Carpenter, 1978; Frapé and Fritz, 1987; Spencer, 1987; Herut et al., Nordstrom et al., 1987; 1990; Hardie, 1990; Rosenthal, 1997).
- ❖ Hydrogeology of the Eastern Aquifer in the Judea Hills and Jordan Valley (Guttman, 1997), it included a description of the geological and groundwater flow pattern of the regional aquifer (lower aquifer).
- ❖ Study of the salinization mechanism and water potential evaluation of the Mitspeh Jericho area (Guttman and Rosenthal, 1991).
- ❖ Issar, 1993 noted that there is mixing with water from confined deep aquifers containing brines, which ascend to the surface because of their own higher pressure and temperature. The saline springs that belong to this category tend to emerge along regional fault lines.
- ❖ Jiries and El-Alali (1996) studied the mechanism of salt Reef growth in the southern basin of the Dead Sea. They found that Reef growth at this area is due to common ion effect of chloride ions, from mixing of two different type of water, namely the artisan water issuing from groundwater flow, and the saltpan brine Dead Sea water.
- ❖ Yiechieli et al. (1996) studied the source and age of the groundwater brines in the Dead Sea area using Cl^{36} and Cl^{14} . They found that the groundwater brines in the Dead Sea area are the results of direct infiltration of brines from precursor Dead Sea Lake.
- ❖ Niemi and Ben-Avrahm (1997) analyzed the 3.5 kHz seismic reflection along the east to west trending of En Gadi fault which mapped by Neev and Hall (1976, 1979). They characterized a complex region of faults, channels and escarpments of uncertain origin. The date indicates a crosscutting relationship between the fault systems, with the northeast-trending faults. From the interpretation of these trends an interesting feature

was observed at the fault intersection of the Ein Gedi fault and the northeast-trending intrabasinal fault is an expected a site of hydrothermal activity, which possibly is a hot springs on the floor of the Dead Sea.

The source and the processes of salinization, mixing, interface movemint in Ein Feshcha area is not well known yet, and several scenarios of brine formation and of salinization, have been recently discussed:

- ❖ According to Ritter (2003), Ein Feshcha waters contain Dead Sea contributions while Stanislavsky and Gvirtzman (1999) noted that, the springs are a mixture of meteoric fresh water with a relatively small amount of ascending deep brine. Mazor and Molcho 1972 represent that the majority of the Feshcha waters belong to Tiberias-Noit water association group and up to 1954 had no Dead Sea contributions; they also noted that there are other springs are diluted with meteoric waters.
- ❖ Guttman (2004) noted that, substantial amounts of freshwater penetrate the aquifer in a relatively rainy replenishment zones on the west and flow eastward to the Dead Sea were become saline by mixing with the brines that are present there.
- ❖ Gavrieli and Oren (2004) studied the stratification of the Dead Sea. They observed that the stratification is maintained by a stabilizing thermocline (between 25 m and 30 m) during the summer months. They found that the surface water temperatures might reach 35-36°C, while the temperature of the water mass below the thermo-cline remains stable between 22-23°C. They mentioned that this stabilizing Thermo-cline is sufficient to balance the destabilizing halocline that is formed during the summer months as a result of increased evaporation. As well they found that the over turn occurs following the autumn cooling of the upper water column and the increase in its density. They found also that the Kinetic factors which dominant over thermodynamic considerations indicate that gypsum ($\text{CaSO}_4 \cdot 2\text{H}_2\text{O}$), rather than anhydrite is the actual Ca-sulphate mineral that precipitate from the Dead Sea brine. The Na/Cl ratio has slightly decreased over the years due to precipitation of halite from the Dead Sea brine.
- ❖ Study of Groundwater flow along and across structural folding: an example from the Judean Desert (Ben-Itzhak and Gvirtzman, 2005), this work attempted to explain groundwater outlet location of the Tsukim springs (Ein Feshcha) in the thick carbonate aquifer beneath the Judean Desert.

- ❖ The origin of Ca-Cl brines as a water type and particularly those in the Rift has been widely discussed and disputed in the literature Vengosh and Rosenthal (1994) and was recently summarized by Möller (2007).

1.6 The Main Objective of the Study

The general objective of this study is to understand the complex behaviour of mixing of saltwater and freshwater in Ein Feshcha springs area, in turn this study aims at identifying the main sources that affect the groundwater quality and the mechanisms of freshwater deterioration using natural stable isotopes, hydro-chemical tracers and electromagnetic measurements, thus to try to define the suitable sites and locations for water extraction before they become salty and flow outside at Ein Feshcha springs.

Since the springs discharge mechanism is not clear and need special investigation to identify the source of discharge and mixing, the following specific objectives and goals are required:

- a) Confirm the variety of origins and composition for each spring discharge in Ein Feshcha group leading to the identification of the salinisation sources and mechanisms at Ein Feshcha group.
- b) Obtain new insights about the fresh-saline water interface in the study area through the determination of the freshwater, brinewater and saltwater bodies and the estimation of their depth and thickness, since knowledge of its location is important for the utilization of the ground water.
- c) Detection of active structural features (flexures and faults) in the upper earth crust and determination of its role in mixing and salinization processes which may lead to the identification of flow patterns in the study area.

1.7 The Study Assumptions and Hypothesis

Several scenarios of brine formation and of salinization at Ein Feshcha springs area have repeatedly been discussed even though previous studies identified variable major sources of salinity but still the mechanism, source and salinization processes in this area not well identified yet. These questions need to be studied deeply: What is the origin of salt in the study area?, what are the patterns of hydraulic mixing mechanism of brines and freshwaters?, what is the depth of the fresh-saline water interface and its movement (freshwater saline-water flow

patterns)?, Explain the variation in water salinity at Ein Feshcha springs?, Is it possible to find freshwater and extract it before they become salty and flow outside at Ein Feshcha springs without disturbing the hydraulic system?.

Therefore several scenarios are suggested in order to give an answer to the previous questions, summarized as the following:

- 1) Dissolution of halite and of post-halite salts within the Lisan formation (Flexer et al., 2000),
- 2) Spring salinization due to up flowing from Kurnub deep aquifer through the faults, 3) Dead Sea water intrusions (Ritter et al. 2003), 4) Leaching of brine pockets trapped in the subsurface by freshly recharged pristine waters, (Kolodny et al., 1999) and 5) Formation of brines by ablation of a thick salt sequence and by leaching of its evaporitic sequences (Flexer et al., 2000).

Two proposed hypothesis are to be studied and followed in order to try to unsure the opened questions and some of the proposed scenarios. The first hypothesis indicates that: a hydraulic connection between the Lower Aquifer and the Upper Aquifer in which the freshwater apparently flows from the Lower Aquifer to the Upper Aquifer is somewhere west to the Mitspeh Jericho well field. However, it is difficult to find field evidence for this assumption. The whole region is covered by thick formations of the Belqa (Mt. Scopus) Group, so it is difficult to identify the nature of the tectonic element (a fault or and a flexure) that is responsible for the hydraulic connection between the lower and upper aquifer in Jericho-Mitspeh Jericho region. (Rosenthal 1978) (Wolfer 1998), (Flexer et al., 2001) and (Guttman et al., 2004). The second hypothesis indicates that: groundwater flow originating from the west shifts to the north towards the Mitspeh Jericho well field located within the saddle inside the Marsaba anticline, from where the flow is channeled south towards the Feshcha springs. (Flexer et al., 2001) and (Guttman et al., 2004)

This work attempted to combine different approaches of tracing the sources of salinization in order to explain the origin, water type in the lower aquifer and the nature of the freshwater flow patterns towards the Dead Sea. The examination of the chemical composition of the saline water in Ein Feshcha, may lead to the source and the distribution of the saline water and its mixing points with fresh water. Hence, this may allows use to capture the fresh water before its mixing with the brines. Isotopic studies for (springs and wells) are required in order to confirm the variety of origins of Ein Feshcha discharge leading to an identification of the

sources for Ein Feshcha water salinization. Using geophysical methods would give more information about the detection of brines, freshwater and saltwater bodies, the estimation of their depth and thickness as well as their interface with the brine-freshwater bodies.

The final expected output is to understand the sources and the mechanism of salinity and its mixing with fresh water, which may help in the future for developing aquifer management schemes, including pumping fresh groundwater and conservation of natural reserves.

1.8 Sources of Data

Files and Archives of the Palestinian Water Authority Hydrological Database:

- Palestinian Central Bureau of Statistics (PCBS).
- Palestinian Ministry of Agriculture.
- Palestinian Ministry of Transport, Meteorological Department.
- Rofe and Raffety Reports on Geology and Hydrogeology of the West Bank Research centers of the Palestinian Academic Universities.
- Israeli Sources such as the Hydrological Services, Meteorological Services, the Institute for Petroleum Research and Geophysics, the Geological Survey, Mekorot Co. reports and the Land Survey of Israel.
- Unpublished reports, published reports in Hebrew and Arabic language.

2. GEOLOGY AND TECTONIC SETTING

2.1 Overview on the Geology of the West Bank

By the end of the Precambrian era, an ancient ocean existed, the Paleo-Tethys, approximately in the present location of Mediterranean. It is believed that most of the detritus that resulted from erosion of Precambrian sediments were carried off into the Tethys. The Tethys invaded and flooded the area (Palestine, Israel, Jordan Lebanon and Syria) several times during the geologic history in the form of sea transgressions (Krenkel, 1924). Continental environment dominated the Arabian Shield during the Precambrian age and it was relatively stable from Precambrian to the early Cretaceous. Accordingly, both the Western and Northern sides of the shield received considerable amounts of clastic sediments (the Nubian Sandstone Formation). These sediments lay unconformably over the basement, which plunges Northwards and Eastwards (Rofe & Raffety, 1963).

In the Paleozoic era, Palestine was invaded by five major transgressions of the Tethys. At the end of this era, substantial sea regression occurred and desert conditions dominated in the country (Picard, 1937).

In the Mesozoic era, the major geologic formations in the study area were deposited in the form of sedimentary rocks. The largest sea transgression, both in duration and extent, was that of the Middle and Upper Cretaceous which resulted in the formation of the rocks outcropping on the hills of the West Bank of Palestine. In the Cenomanian and Turonian ages of the Upper Cretaceous, thick strata of limestone and dolomite with intercalations of marls were dominated (Goldschmidt, 1947).

In the Cenozoic era, particularly during the Eocene, the study area was characterized by the deposition of chalks and nummulitic limestone. The Lower Miocene, during which simple fold structures were created, is considered the principal stage of mountain building in the study area. At that time, the structural faults and folds (anticlines, synclines, and monoclines structures) began to appear, together with the uplifting forces producing the West Bank Mountains which are occupying the upstream and the recharge area of the West Bank and some parts of Israel.

Long time before the formation of the Dead Sea Rift, the movement of the African plate including the Arabian plate to the North caused the formation of the Syrian Arc Fold Belt. The Syrian Arc formed in two stages: the first in the Turonian-Maestrichtian and the second in the Oligocene (Krenkel, 1924 and Andrew, 2000). Two major tectonic events have shaped the area of the West Bank. The Syrian Arc System folded up the shelf deposits at the end of the Cretaceous Period and the Red Sea-Aqaba transform fault formed

the Dead Sea graben from the Miocene (Krenkel, 1924, Rofe & Raffety, 1963 and Andrew, 2000).

From the mid Miocene to Pliocene and recent times a lateral strike slip movement between the African and Arabian plates took place. This detached the Arabian Shield from the great African Shield thus initiating the opening of the Red Sea, facilitated by the left transform fault along the line Aqaba–Dead Sea Jordan Rift. Shallow environments, inland lakes and transitional continental conditions dominated throughout the Pliocene. In the Pleistocene, most of the present mantle rocks and soils of the West Bank were formed (Blake & Goldschmidt, 1947 and Rofe & Raffety, 1963-1965).

2.2 Regional Geological Setting

The West Bank located on the Northern edge of the Arabian Shield (figure 2.1). The Shield belongs to the Precambrian age and consists of a complex of crystalline plutonic and metamorphic rocks. The Shield's metamorphic rocks are mainly of a sedimentary origin (metasediments). The Arabian Shield is usually referred to as the basement complex and is a part of the Nubian-Arabian Shield (Yaghan, 1983).

The average geological displacement across the Arabian Plate and the African Plate is about 5-10mm/yr and the modern geodetic slip rate is 1-10mm/yr (Pe`eri et al., 2002). The Dead Sea basin is an actively subsiding two pull apart graben (Garfunkel & Ben-Avraham, 1996), in which the Western margin is characterized by sub parallel normal faults while the Eastern margin is characterized by more steeply dipping left lateral strike slip faults (Niemi & Ben-Avraham, 1997).

In fact Palestine is part of the Sinai sub plate and remains relatively static while the Arabian Plate on which the Kingdom of Jordan is located, slides Northwards along the Aqaba-Jordan Valley sinistral (twisting to the left-lateral) sheared transform fault. The Arabian Shield extends over an area that stretches from the Eastern and Southern edges of the Arabian Peninsula to the Southeastern shores of the Mediterranean. It constitutes the Eastern part of the great Afro-Arabian Shield. The Pan African Orogeny divided the Afro-Arabian Shield into two components: the African and the Arabian Shields (figure 2.1). The division takes the conformation of a triple junction. The first branch of the triple junction extended along the Red Sea to the South. The second extends through the Gulf of Aqaba, Wadi Araba, Dead Sea, Jordan Valley, Lebanon, Syria, to reach Turkey in the North. The third coincides with the extension of the Suez Gulf (Blake & Goldschmidt, 1947 and Yaghan, 1983).



Outcrops of the Arabian Shield occur in an area that extends from the Yamane-Saudi borders in the South to the Gulf of Aqaba in the North. The Arabian Shield outcrops also in Southern Sinai. In the West Bank, the basement complex is not outcropped. Sedimentary rocks overlaying the Shield are known as the shelf deposits. Two environments of sedimentation can be recognized within the shelf rocks: the stable (in the immediate surroundings of the shield) and the unstable environments. The stable environment is characterized by continental deposits interfingering with neritic, and littoral deposits. The unstable environment is characterized, in general, by carbonate sediments deposited in marine environment. Locally, the unstable shelf is divided into basins of Euxenic conditions and swells of continental conditions (Rofe & Raffety, 1963-1965). A zone of transition separates between the deposits of the stable and the unstable environments. This zone extends from Northeastern Sinai to Southeastern Saudi Arabia on the Arabian Gulf. The zone transcends through the Gulf of Aqaba, Wadi Araba depression, Southern Syria and Eastern coasts of the Arabian Peninsula on the Arabian Gulf.

Most of the West Bank is covered by carbonates of the Mesozoic and Cenozoic eras. The representation of the stable shelf environment in the West Bank is restricted to exposures

of a sequence of clastic sediments of the Lower Cretaceous overlying Jurassic carbonate rocks (figure 2.2), (Blake & Goldschmidt, 1947 and Rofe & Raffety, 1963-1965).

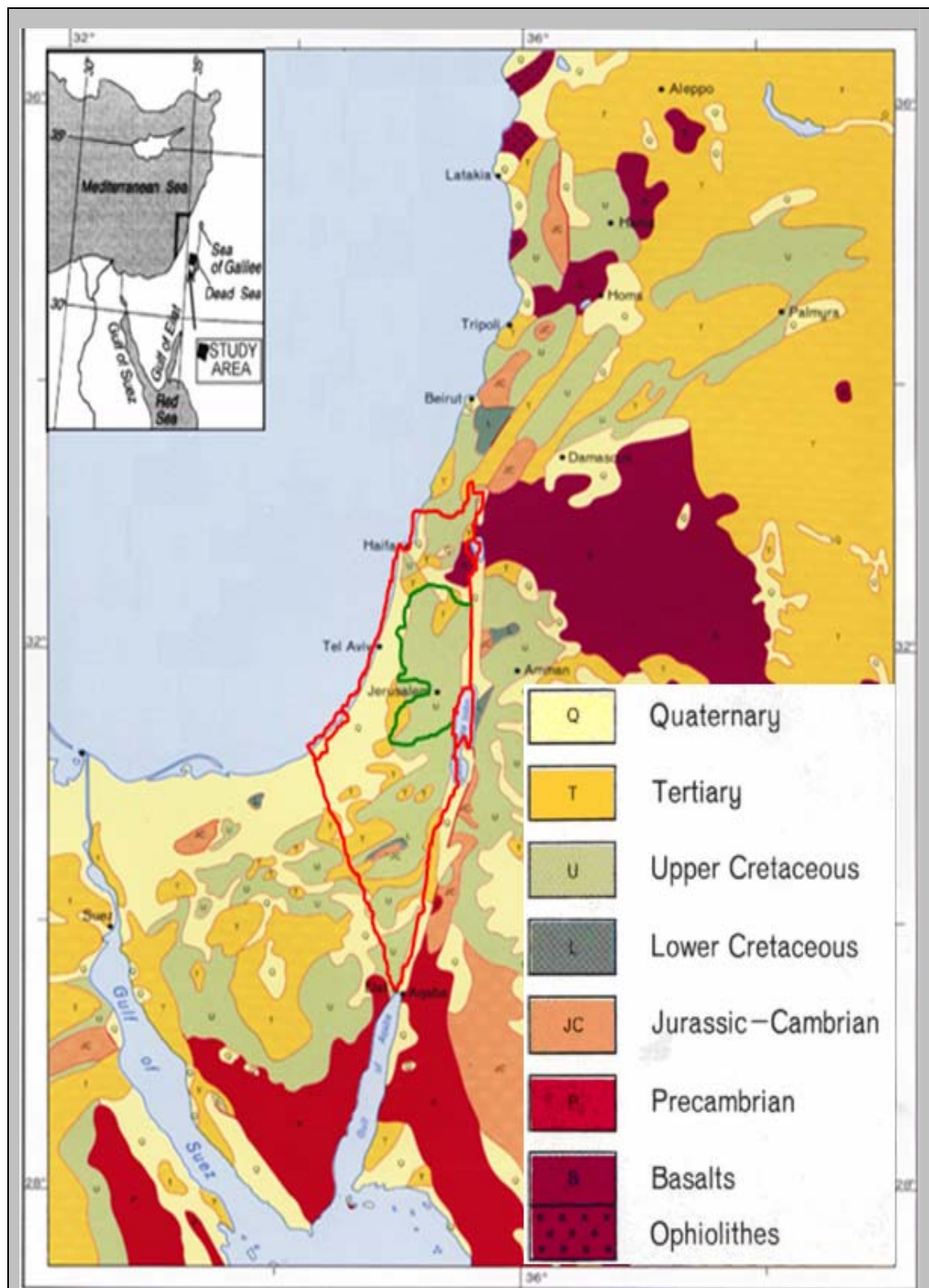


Figure 2.2: Geological overview of West Bank and adjacent areas (modified after: Bender, 1968 and Bayer, 1986).

2.3 General Structural Geology of the Study Area

The structural geology deals with the various structures which deform the earth crust. Two main structures are the most important in structural geology; these are the structural faults and folds. In some cases, a fault system occurs on two ends of a rock block to form a trench like structure called a graben which exists in several places of the West Bank.

The Dead Sea transform extends at a large angle from the Red Sea axis and is therefore quite close to the direction of plate motion. Small deviations in its trace lead to variations in its structure and physiography; at some places the two sides of the transform diverge, at others they converge (Quennel, 1959). The transform valley is generally delimited by narrow zones of normal faults with vertical throws ranging from 1 to 10km. The internal structure is dominated by left-stepping en-echelon strike-slip faults (Garfunkel and Ben-Avraham, 1996), which produced several rhomb-shaped pull-aparts, like the Dead Sea basin, Lake Tiberias or the Gulf of Aqaba. Figure 2.3 presents a schematic sketch for basic structural relations along the Dead Sea transform basin, part (a) presents the structural pattern in plain view along the part of the transform enclosing the Dead Sea basin. The main strike-slip faults trend at an angle to the transform valley whereas part (b) presents a schematic block diagram showing the architecture of the Dead Sea basin. As lateral motion continues the edges of the basin move apart and it becomes longer parallel to the transform.

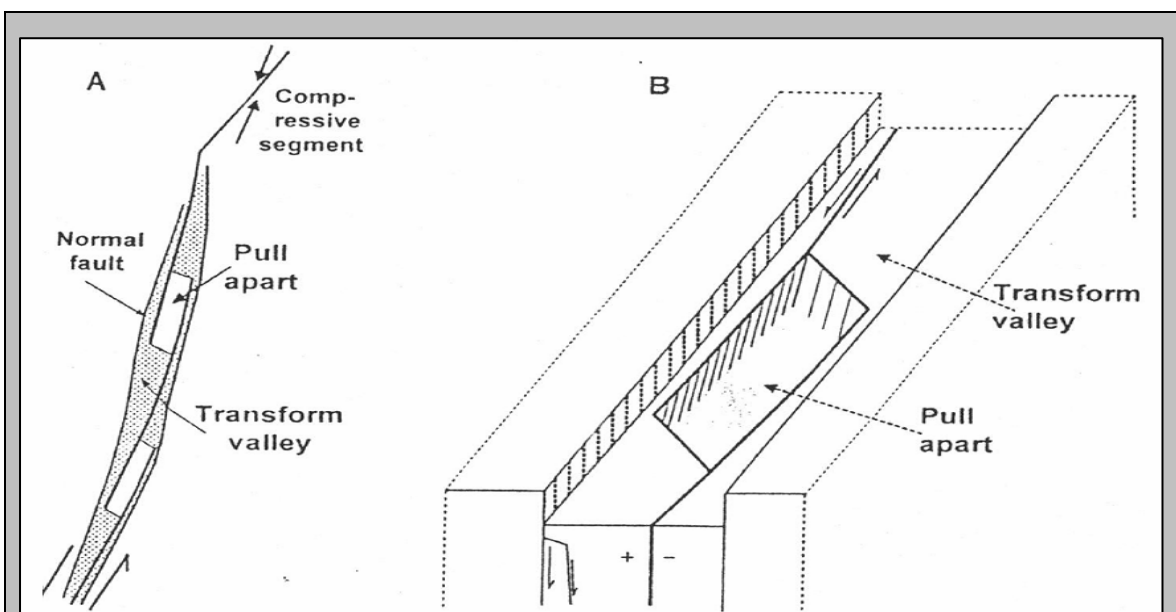


Figure 2.3: Schematic fault structure of the Dead Sea transform which forms a pull apart graben structure, (similar to the Dead Sea depression). (after: Garfunkel and Ben-Avraham, 1996).

As a result of major structures (Syrian Arc, Transverse Fault System and Dead Sea Rift) and the continuous Northward movement of the Arabian plate, faults of different trends and ages have been developed. The different trends are due to different stress fields resulting from the different tectonic movements in different ages. The main fault trends are North-South sinistral strike slip faults, East-West dextral strike slip faults, SE-NW tensional faults and SW-NE compressional faults. The tectonic structures found in the study area are connected to this sinistral transform movement, as well as to former tectonic stress tensors existent during the late Mesozoic.

The structural geology of the West Bank is dominated by a series of regional, parallel, SW-NE trending folds dissected by faults associated with the Jordan Rift Valley. The main structural elements are Hebron, Ramallah, Anabta, Faria, Al-Auja and Marsaba anticlines (figure 2.4).

The folds in the West Bank represent a period of uplifting and compression of the earth's crust during the late Turonian and early Eocene times. Some faults in West Bank act as conduits and some others represent barriers to groundwater flows.

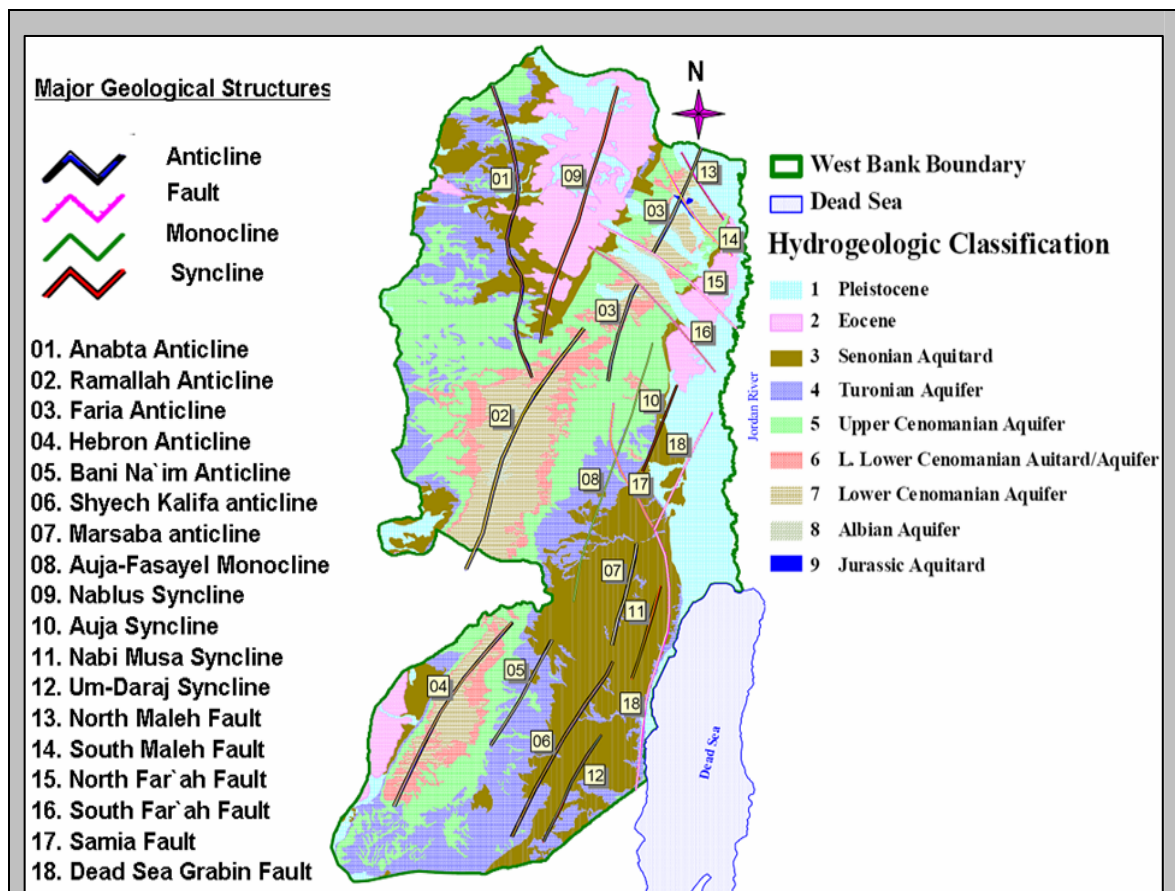


Figure 2.4: Major geological structures of the West Bank showing the main folds and faults. (after: Rofe & Raffety, 1965 and Fleischer, 1996).

According to the Continental Drift Hypothesis in geology, the West Bank in particular and Palestine / Israel in general was affected by the development of huge geologic structures since it is located within the great Afro-Arabian Shield which has drifted Northwards and narrowed the ancient Tethys Sea to the present Mediterranean (Blake & Goldschmidt, 1947 and Rofe & Raffety, 1963-1965). Two theories were used to explain the formation of the Dead Sea Rift: a vertical movement (Graben tectonics) and a horizontal movement (Plate tectonics). Detailed investigations have proved the horizontal movement theory, where the Arabian plate has been continuously moving to the North (Quennell, 1956 and Freund et al., 1970).

Freund and Garfunkel (1980) explained the relative horizontal motion of two tectonic plates on the East (Arabian Peninsula Plate) and West (Palestine Plate) of the Dead Sea as a result of a great structural fault where the Western plate moved to the South and the Eastern one moved to the North. Combined with the horizontal displacement, there was a vertical relative movement of the two tectonic plates due to a system of steeply dipping strike slip faults that formed what is known geologically as a graben. Also they submitted the regional structural map of Palestine with the main geologic transform plate boundary along the Gulf of Aqaba, the Tiberias Lake and the Dead Sea as shown in figure 2.5.

Freund and Garfunkel (1980) also submitted a geologic cross section across the Dead Sea depression which shows the formation of thick sediments in the depression and the graben geologic structure affected by structural faults as shown in figure 2.6.

The major structural element of the study area is the Jordan Rift Valley-Dead Sea system structure that was formed since the Miocene age. There are evidences of younger faulting of Pleistocene to present age. A number of faults cut across the Rift, resulting in the separation between the Southern and Northern basins. On both sides of the Rift, there are sets of faults facing away from the Rift to the Northwest and Northeast (figure 2.4 and 2.5). In the central Jordan Rift from the Dead Sea to Lake Tibereas, faults are discontinuous on the both sides. The Western side fault is normal and cuts some structures of the area such as Nabi Musa (Buqei'a) Syncline, Auja-Fasayel Monocline, K`an Al-Ahmar Syncline and the Auja Syncline. The beds of the Western side are dipping strongly towards the Rift. In upper crustal levels longitudinal strike slip and normal faults are the most prominent elements controlling the whole Dead Sea basin structure, but transverse faults that extend across the basin are also important. The principal fault structure in the study area is the Western fault of the Dead Sea-Jordan Valley graben. This fault runs along the Western shore of the Dead

Sea up to the Jericho City and its direction is S-N. Around Jericho the fault direction becomes N-W, continuing as the Ein Samiya fault strip (figure2.4) (Begin et al., 1974).

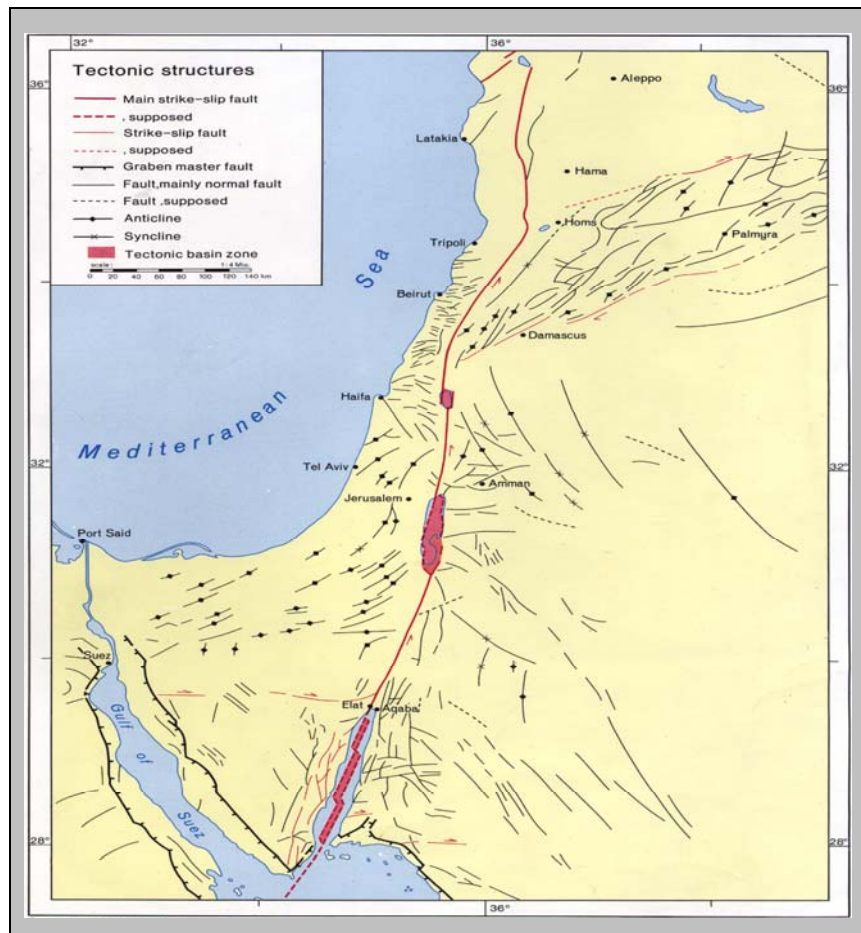


Figure 2.5: Regional Structural Map Of The West Bank/Palestine Within The Plate Tectonics Theory (modified after: Freund & Garfunkel, 1980 and Bayer, 1980).

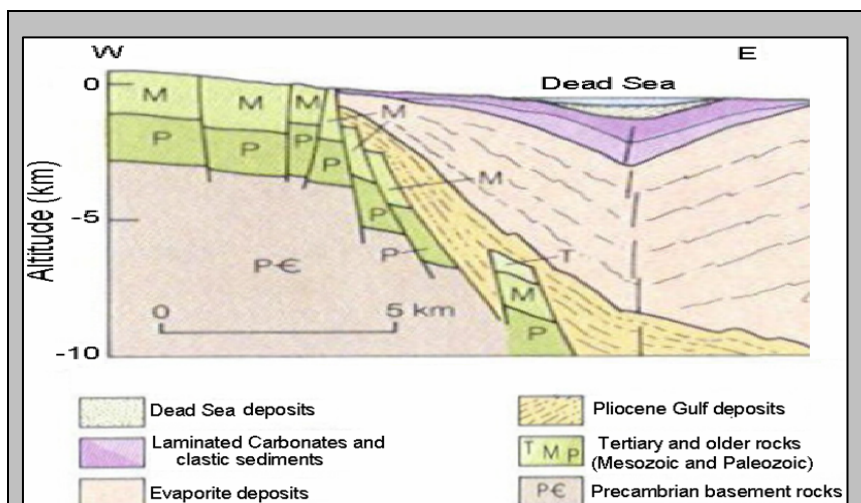


Figure 2.6: Geological cross section across the Dead Sea Depression (after: Freund & Garfunkel, 1980).

The dominant structures in the study area are of two types: folds and fractures; each is related to a different stress field (Eyal & Reches, 1983). The folds are the product of the Syrian Arc stress field, with dominating maximum horizontal compression trending W-NW, while most of the fractures are related to the Dead Sea stress field, with dominating horizontal extension trending E-NE. The folds are characterized by a series of asymmetric anticlines and synclines with axes plunging on the average to the NE. The two main structures of this type are the Hebron and the Ramallah Anticlines, in which the NW flanks are steeper than the SE flanks. The Hebron axis runs from the Hebron-Halhul area to Jerusalem in a general SW-NE direction and dips in the direction of Jerusalem. This anticlinal axis represents the maximum elevation in the area. To the East and West there are minor folds, representing the descent of the structures towards the plain in the West and the Dead Sea in the East. The anticlines descend in the direction of the Jordan Valley and the Dead Sea in a series of undulations, forming secondary structures. The anticlines and synclines are asymmetric, with steepest inclinations to the Eastern part of the anticlines (Flexer et al., 2001). The Dead Sea Basin is the largest fracture related structure in the region. It is a rhomb shaped pull apart basin and it is the deepest part of the Dead Sea transform (Garfunkel & Ben-Avraham, 1996). It is bounded to its North and South by two major strike slip faults and along its Western and Eastern margins there is a belt of sub parallel normal faults. The Western fault is the dominant morphological feature in the study area, creating a steep cliff near the Dead Sea shore. This fault places the Judea Group carbonates, which comprise the cliff, against the Dead Sea group in the East. Other smaller faults and joints do exist throughout the entire area. Two groups of fracture strike directions trend N-NW and N-NE, with fracture density increasing towards the Dead Sea (Sagy, 1999).

2.4 Lithostratigraphy of the West Bank

Concerning the geology and stratigraphy of the West Bank and Israel, there are variations and inconsistencies in the literature, because the study area is located in two political regions; Israel and the West Bank. Three sources of geological literature were used: Palestinian, Jordanian (Jordan administered the West Bank from 1949 to 1967), and Israeli. As a result, several terminologies were used as explained in table 2.1.

Table 2.1: Generalized stratigraphic column of the West Bank describing and illustrating the Israeli and the Palestinian names of the different geological formations in the West Bank as well as their lithology. (after: Guttman et al., 2000 and Geological Survey of Israel, 1990-2002).

Geological Time Scale			Group		Formation		Lithology	
Era	System	Epoch	Palestinian	Israeli	Palestinian	Israeli		
CENOZOIC	Quaternary	Holocene	Recent	Kurkar	Alluvium	Alluvium	Marl, alluvium, gravel	
		Pleistocene	Lisan	Dead Sea	Gravel	River gravel		
	Tertiary	Neogene	Pliocene-Miocene	Beida	Jenin Sub Series	Lisan	Lisan	Thinly laminated marl with gypsum bands
		Paleogene	Eocene	Belqa	Saqia	Beida	Bit Nir and Ziglag	conglomerate
			Paleocene			Avidat	Reef nummulitic limestone	Zor'a
			Senonian	Mastrichtian	Ajlun	Judea	Mount Scopus	Taqiya
Cretaceous	Campanian	Khan Al Ahmar and Zerqa	Ghareb	Yellowish chalk				
	Santonian	Amman and Abu Dis	Mishash	Chalk with back chert				
	Turonian	Jerusalem	Menuha	Chalk				
MESOZOIC	Cretaceous	Cenomanian	Ajlun	Judea	Bethlehem	Bina	Limestone and dolomite (karstic).	
		Albian			Hebron	Weradim	Hard gray porous dolomite	
					Yatta	Kfar Shaul	Kfar Shaul	Chalky limestone, chalk and marl
						Aminadav	Aminadav	Karstic limestone and dolomite
						Moza	Moza	Marl, clay and marly limestone
		Upper Beit Kahil			Beit Meir	Beit Meir	Limestone, chalky limestone and dolomite	
					Limestone inter-bedded with marl	Kesalon	Kesalon	Limestone inter-bedded with marl
								Soreq
		Lower Beit Kahil			Giva't Yearim	Giva't Yearim	Limestone, dolomite	
					Kefira	Kefira	Limestone, dolomite and marly limestone	
Kurnub	Aptian	Kurnub	Kurnub	Kurnub	Kobar	Qatana	Marl and clay	
					Ein Qinyia	Ein Qinyia	Marl and marly limestone	
					Tammun	Tammun	Caly and marl	
					Ein Al Asad	Ein Al Asad	Limestone	
Neocomian	Neocomian	Zerqa	'Arad	Kurnub	Nabi Said	Nabi Said	Limestone	
					Ramali	Hatira	Sandstone	
					Upper Malih	Upper Malih	Marl interbedded with chalky limestone	
Jurassic	Callovia-Bajocian	Zerqa	'Arad	Kurnub	Lower Malih	Lower Malih	Dolomitic limestone, jointed and karstic	

The following paragraphs give an introduction to the general lithostratigraphy of the West Bank formations that build up the aquifers in the study area. The lithostratigraphic succession outcrops within the West Bank are predominantly carbonate sediments and rocks of Tertiary and Cretaceous age. The Tertiary and the Cretaceous rocks in the West Bank are mainly made of limestone, dolomite, chalk and marl with bands of chert. These rocks built up the two main regional aquifers in the West Bank; the Cenomanian-Turonian aquifer (Upper) in the Jerusalem, Bethlehem and Hebron formations and the Albian aquifer (Lower) in the Upper and Lower Beit Kahil formations. The marls and clays of the Yatta formation, which represents the main aquiclude in the West Bank, separate the two aquifers. Older rocks cannot be found at the surface though they are known from the boreholes. The oldest exposed rocks belong to the Albian, overlain by younger strata of the Cenomanian, Turonian, Senonian and Eocene, exposed on both flanks of the anticlinal axis in the West Bank. The lithostratigraphic succession exposed on both sides of the Jordan Valley and along the shorelines of the Dead Sea as well in the wadis and the interior Valleys starts with top Precambrian sediments and volcanics, and terminates with young Pleistocene-Holocene Rift Valley (figure 2.7).

The exposed rocks of the West Bank are: The Lower Cretaceous formations (Albian) comprising the regional West Bank groundwater system (Beit Kahil, Yatta formations). The thickness of the groundwater system in this area ranges from 500-970 meters. The Upper Cretaceous formations comprising the regional West Bank groundwater system, (Hebron, Bethlehem and Jerusalem formations). The thickness of the groundwater system in this area ranges from 190-490m. The Senonian age rocks (Abu Dies formation) are composed mainly of chalks and marls. The thickness ranges between 0-450m. The Pleistocene to Eocene rocks overlay the Senonian rocks in the Northern and Northeastern area of the West Bank, the rocks are composed mainly of limestone, chalky limestone, chalks, marls, and siltstone, which are of limited extent and thickness. The Unconsolidated, Quaternary alluvial sediments overlie the major rock formations.

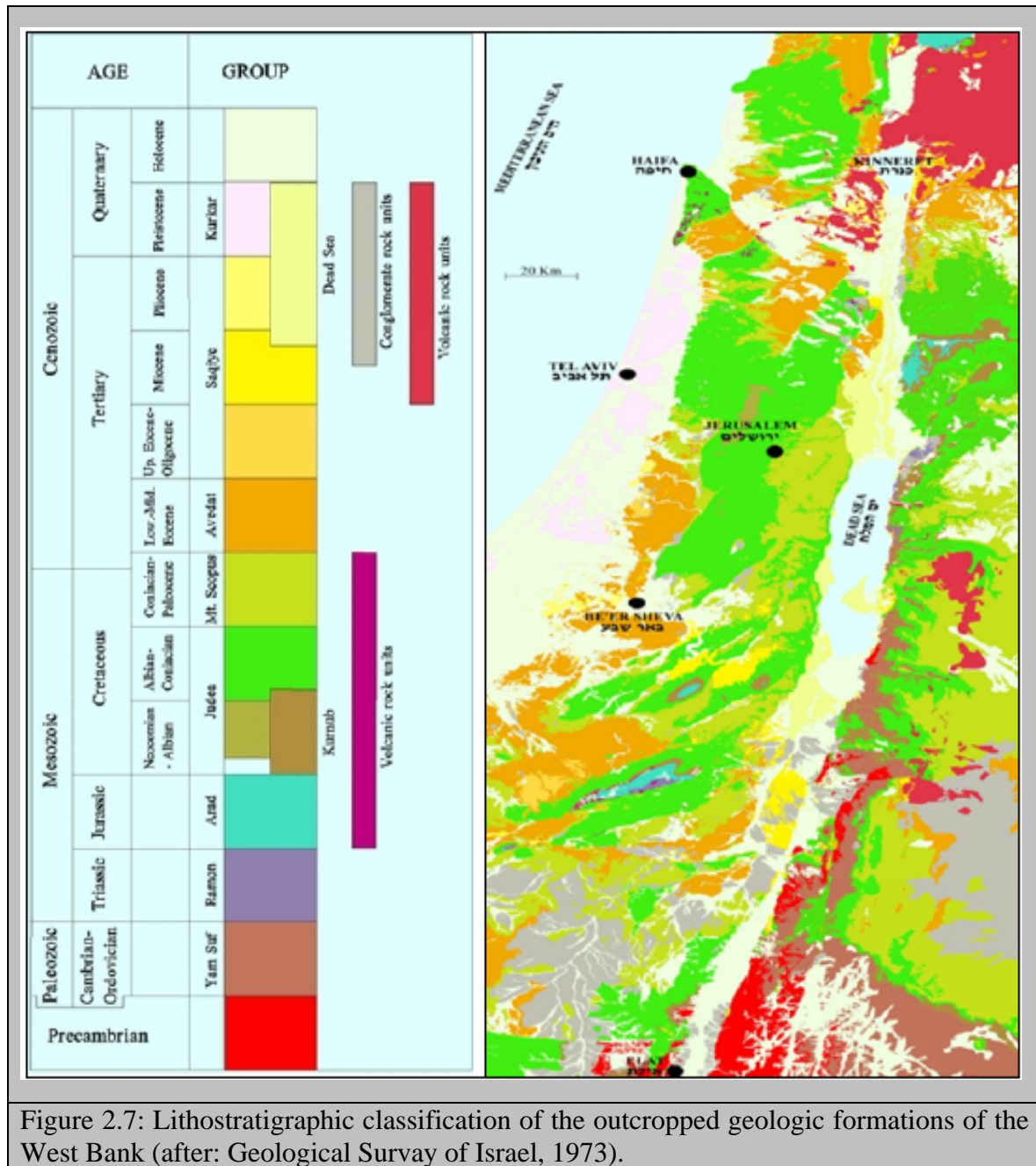


Figure 2.7: Lithostratigraphic classification of the outcropped geologic formations of the West Bank (after: Geological Survey of Israel, 1973).

2.5 Lithostratigraphy of Marsaba-Feshcha Driange Basin

The Rift Valley faults, the anticlines and synclines are the major geological structures that affect flow regime in the study area. The SE-NW geological cross section from 18000/12860 NW to 19225/12164 SE, illustrates these structural features as presented in figure 2.8.

The following discussion about the stratigraphy and the characteristics of the geological formations exposed in the study area is based on the findings of the wells drilled in the area as well as geological investigations carried out in the study area. Most of the drilled wells that provided geologists and hydrologists with the first detailed data concerning the

lithology are located in three clusters separated by large distances (Jerusalem Herodian area in the West, the Mizpe Jericho-Jericho Area in the East and the Ein Gadi Area in the South).

Three bore holes drilled by oil companies are particularly relevant; the Halhul 01 drilled by the MECOM oil company from an elevation of 930m at 159866/110677 to a depth of 3810m in 1964, the Marsaba 01(El Muntar well), also drilled by MECOM near the Marsaba monastery in the Wadi Nar Valley (Kidron), about half-way from Jerusalem to the Dead Sea at 181750/127129, to a depth of 1416m in 1965, and the Ein Gedi 02 on the shore of the Dead Sea East of Hebron (185820/089280) by Naphtha in 1957 to a depth of 2571m (Fleischer, 1996). The stratigraphy of the study area consists of carbonates, chert, chalk, gravel, sandstone and evaporates which ranges in age from the Triassic to Holocene age in the East near the rift. The ancient Jurassic and Lower Cretaceous formations are composed mainly of limestone, sandstone and marl layers (ARIJ, 1997). The stratigraphic profile of Marsaba-Feshcha drainage basin and its immediate surrounding exposed in the study area varies from the Lower Cenomanian age to a much younger formations of the Holocene age (table 2.2).

The thickness of the Judea Group is about 800-850m (Arkin et al., 1965 and Arkin & Hamaoui, 1967). The exposed layers are ancient formations of Cretaceous age, composed mainly of limestone layers, exposed along and at the vicinity of the Hebron anticline, in the West, formations of the Mt. Scopus Group (Belqa group) exposed near the Jordan Valley and throughout the Jerusalem Desert (Judea Desert), young formations of Pleistocene-Holocene age located in the Jordan Valley and along the shores of the Dead Sea as well as in inland wadis and valleys.

The following is a description of the stratigraphy and the characteristics of the geological formations exposed in the study area (table 2.2). It is based mainly on the studies of Braun & Hirsch 1994, Guttman et al., 2000, Millennium Engineering Group et al., 2000 and Guttman, 2006, as well as the generalized stratigraphic sequence of the West Bank. The geological formations exposed in the study area and a brief description of the stratigraphic column in the study area is presented in figure 2.9 and 2.10.

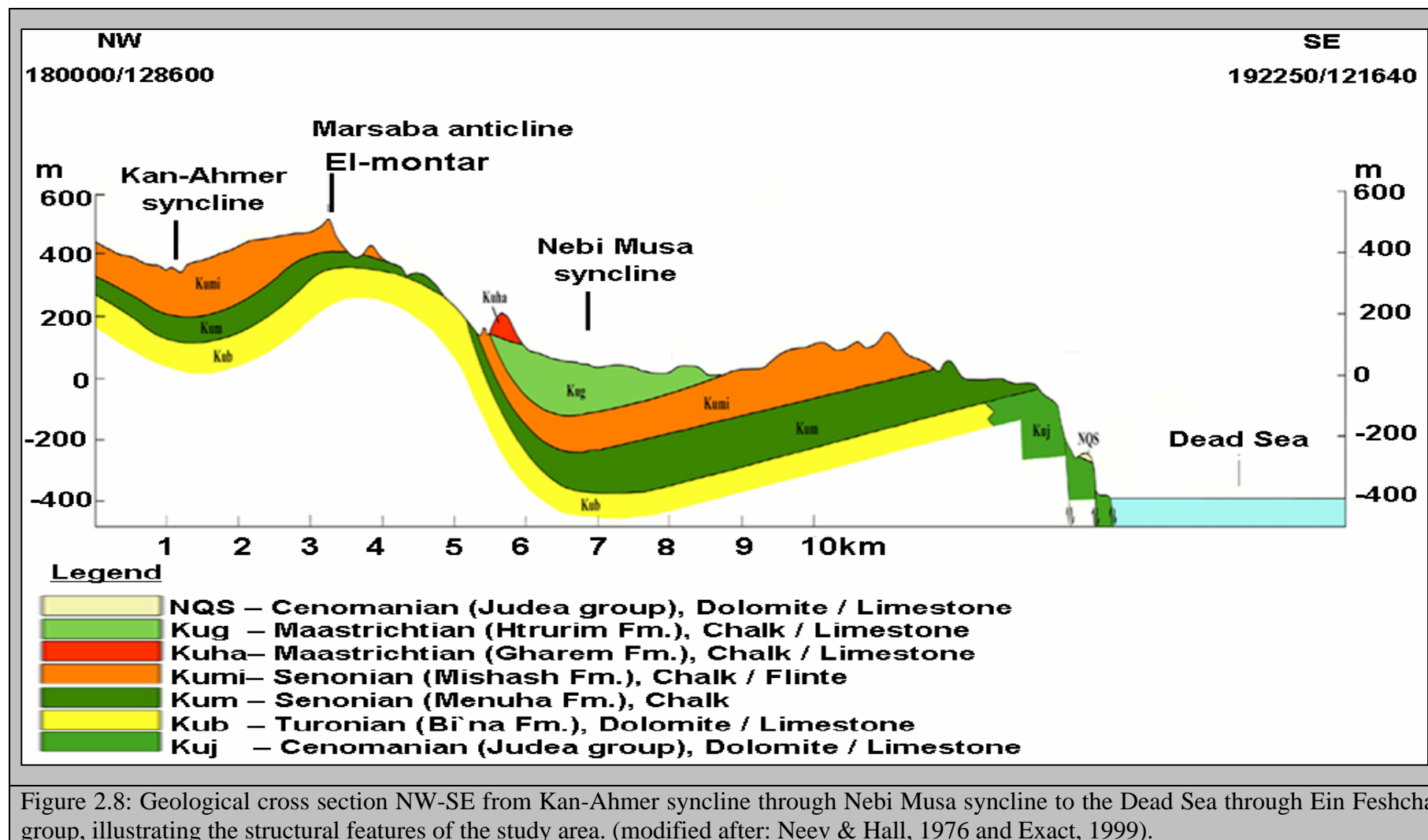


Figure 2.8: Geological cross section NW-SE from Kan-Ahmer syncline through Nebi Musa syncline to the Dead Sea through Ein Feshcha group, illustrating the structural features of the study area. (modified after: Neev & Hall, 1976 and Exact, 1999).

Table 2.2: Stratigraphic table of rock units at Marsaba-Feshcha drainage basin and its surrounding area (modified after: Millennium Engineering Group et al., 2000 and Guttman et al., 2000).

Age	Group		Formation		Lithological Composition	Thickness (m)	Hydrostratigraphy
	Palestine	Israel	Palestine	Israel			
Plio-Pleistocene	Lisan	Dead Sea	Lisan	Lisan	Clays, silt, conglomerate, gypsum, chalk	200+	
Paleocene			Nummulitic limestone	Taqiye	Marl, chalk, clay, limonite concentrations.		Aquiclude
Maastrichtian			Khan Al-Ahmar	Ghareb	Yellowish chalk		Aquiclude
Campanian	Belqa Group	Mt. Scopus	Abu Dies	Mishash	Chalk with black chert layers	100-400	Aquiclude
Santonian-Campanian			Abu Dies	Menuha	White chalk, some calcareous chalk		Aquiclude
Turonian	Ajlun Group	Judea Group	Jerusalem	Bina ⁽¹⁾	Fine grained limestone and dolomite	90-100	Aquifer
Upper Cenomanian			Bethlehem	Weradim	Hard gray dolomite, porous	90-100	Aquifer
			Kefar Shaul	Chalky limestone, chalk, marl	30-40	Aquitard	
Lower Cenomanian			Hebron	Aminadav	Hard gray dolomite, porous	110-140	Aquifer
			Yatta	Moza ⁽²⁾	Marl, clay	10	Aquiclude
Bet Meir ⁽²⁾				Chalky limestone, bluish clay, chert, dolomite in Bet Meir Lissan	120-140	Aquiclude	
Albian			Upper Beit Kahil	Kesalon	Limestone and dolomite rich in fossils	30	Aquifer
				Soreq	Limestone and marly dolomite, marl and some chert	110-170	Aquitard
			Lower Beit Kahil	Givat Yearim	Hard dolomite, at times also limestone	20-40	Aquifer
Aptian			Kurnub Group	Kurnub Group	Kobar	Qatana	Marl with some limestone
	Ein Qinya	Limestone				60-70	Aquifer
	Tammun	Limestone, marl and some sand				80-150	Aquitard

⁽¹⁾ The Bina Fm. divides into three formations in the eastern part of the study area, namely: Netzer, Shivta and Derorim Fms. (Begin, 1976).

⁽²⁾ The Moza and Bet Meir Fms. are referred to as the Ein Yorq'e'am Fm. in the eastern part of the study area (Begin, 1976).

2.5.1 Cretaceous Rocks

The Cenomanian-Turonian hard carbonates, such as dolomites and limestones, comprise the main aquifer of the region; the Lower Cretaceous shales and sandstones serve as source rocks and a reservoir for oil and water; a thick layer of oil shale was found in the Senonian. Materials from more than 250 boreholes are available for lithostratigraphic study. In addition, various aspects of the lithostratigraphy and biostratigraphy have been examined in detail (Flexer, 1968, Flexer & Honigstein, 1984 and Flexer et al., 1986).

2.5.1.1 The Kurnub Group

The Kurnub Group (Early Cretaceous) was deposited and accumulated while most of the area of Israel and Palestine was a landmass, covered by a considerable thickness of sedimentary sequence of eolian-fluviatile sands, silts and shale's inter bedded with an increasing Northward marine intercalations (Flexer et al., 2001). According to Palestinian terminology, the Kurnub Group is restricted to one unit formation known as Kobar formation. While according to Israeli terminology the Kurnub Group is subdivided into: a) the lower part of "Kobar" (Tammun formation) consists mainly of marl, marly limestone, and limestone. Its thickness is within a range of 50-120m. b) the middle part of "Kobar" (Ein Qinya formation) comprises mainly of limestone and intercalation of marl, which is highly fossiliferous. Its aquifer potentiality is larger than that of the upper and lower members due to its higher content of limestone. Thickness is within a range of 70-100m and c) the upper part of "Kobar" (Qatana formation): the formation consists mainly of marl and marly limestone. Its thickness is within a range of 40-60m.

2.5.1.2 The Ajlun Group

According to Palestinian terminology, Judea Group is known as Ajlun Group with two formations the Beit Kahil formation (Upper and Lower) and Yatta formation (Beit Meir and Moza formations in Israeli literature) (table 2.1 and 2.2). The total thickness of the Ajlun Group (Judea Group) in the research area is between 800-850m. The total thickness of the Ajlun Group penetrated in the Jericho-1 borehole is 700m. Most lithostratigraphic units have similar thicknesses in all the research area. The Jericho-1 borehole reaches the base of the Ajlun Group (Judea Group) at depth of 1020m (Begin, 1975).

2.5.1.2.1 Lower Beit Kahil Formation (Albian to Lower Cenomanian)

This formation represents the lower part of the upper Albian (Braun & Hirsch, 1994). The lower part of the Lower Beit Kahil (BK1) consists mainly of limestone, which is well bedded, fine crystalline and highly karstic, and sometimes dolomitic in the upper part. This formation has sometimes intermediate marl layers, and marl increases in downward direction. The lower part of this formation, is made up of limestone with thin layers of porous dolomite interchanging with marly limestone. Gray limestone layers alternating with layers of shale and marl, are typical for the lower part of the formation (Kefira) (Guttman & Gotlieb, 1996).

On the other hand the upper part of the Lower Beit Kahil formation (BK2) (Giv'at Yearim), has dark grey dolomite, massively bedded, fine crystalline and hard with clayey and marly limestone. It is highly fractured and karstic, though less than BK1. Generally, the Lower Beit Kahil is considered to be a moderate to good aquifer, forming the lower part of the Albian aquifer. Its vertical thickness ranges between 137m in PWA-1 and 215 in Hebron-1. (Qannam & Merkel, 2002).

2.5.1.2.2 Upper Beit Kahil Formation (Albian to Lower Cenomanian)

The lower part of Upper Beit Kahil (BK3), (Soreq) consists of porous dolomite, marly dolomite, marl and at times some chert. The occurrence of the marl in this formation reduces its water bearing capability. Its thickness ranges between 66m in Herodion-4 and 145m in PWA-I.

On the other hand, the upper part of Upper Beit Kahil formation (BK4) (Kesalon) is the lowest exposed unit in the area, mainly consists of brittle dolomite and brittle limestone rich in fossils. This formation usually appears as a cliff and some times as a rocky landscape. The age is Cenomanian and the base of the formation is not exposed (Arkin et al., 1965).

2.5.1.2.3 Yatta Formation (Lower Cenomanian)

The Lower Cenomanian Yatta formation (YL) (Beit Meir and/or Moza formations in Israeli literature) overlies the Upper Beit Kahil formation. The upper part of Yatta (Beit Meir), 50-110m thick, is composed of limestone, chalky limestone, dolomite, marl and greenish clay at the bottom. The lower part of Yatta (Moza), 10-20m thick, is composed of yellowish marly limestone with traces of greenish marl at the bottom. Yatta formation thickness varies between, 86m thick in Herodion-4 and 128m in Herodion-3, in general act

as an aquiclude and separate the Cenomanian aquifer from the Albian aquifer underlying it. The dolomite of the upper part of Yatta (Beit Meir) (YU) shows some water bearing nature (Guttman & Gotlieb, 1996). Sometimes the limestone near the top, officiates as a local perched aquifer, which explains why a few springs emerge 20m below the contact of the Yatta formation with the Hebron formation (Rofe & Raffety, 1963).

In the East of the West Bank and in the Naqab, Yatta formation consists mainly of dolomite with some chert nodules. The thickness is between 42-49m and the age of the tongue is Cenomanian. It occurs in the Jericho area as a tongue consists of limestone chalk and marl. Its thickness reaches between 40-72m in the exposed area. Its age is Cenomanian (Arkin et al., 1965).

2.5.1.2.4 Hebron Formation (Upper Cenomanian)

The Israeli use the term Amminadav for Hebron formation. It consists of brittle karstified gray dolomite, dolomitic limestone and gray limestone. At its base it is formed of hard dolomite and dolomitic limestone with some silicification. The lithology is uniform since dolomite and dolomitic limestone are found throughout the sequence of Hebron formation. The porosity of this formation is mainly secondary because the rocks are well jointed and karstified. The Hebron formation without doubt is the most important aquifer within the West Bank. Its Vertical thickness ranges between 70m in Herodion-4 and 120m in PWA-I (Qannam & Merkel, 2002). Hebron formation thickness is between 67-120m and the age of the formation is Upper Cenomanian (Arkin et al., 1965).

2.5.1.2.5 Bethlehem Formation (Upper Cenomanian to Turonian)

The Israeli divide Bethlehem into two formation units: The lower unit is referred to as Kfar Shaul. The upper part is called Weradim formation. The lower part of Bethlehem (Kfar Shaul) consists of limestone, chalky limestone, rich in faunal remains and marl that act as a confining aquiclude for the Hebron formation beneath. Its thickness ranges between 28-41m and its age considered to be Upper Cenomanian. The upper part of Bethlehem (Weradim formation) is built up of massive, coarse crystalline dolomite and well bedded limestone lenses. Bethlehem formation is frequently highly jointed and fractured making this formation a good aquifer. Its vertical thickness ranges between 88m in PWA-I and 260m in Herodion-4. The age of Weradim formation is considered to be Upper Cenomanian (Arkin et al., 1965).

2.5.1.2.6 Jerusalem Formation (Turonian)

Jerusalem formation is of Turonian age. It is restricted to one unit. The Israeli refer to it as Bi`na formation. Its lithology is characterized by karstified limestone and dolomite with marl and clay mainly near the bottom. Sometimes occurrence of chalk is evident on the top of this formation. The Jerusalem formation has a thickness of about 90-100m as in Herodion-3 and 4. Due to fractures and joints of this formation turns out to be a good aquifer. Three sub formations can be differentiated in the Eastern parts of the district down slope towards the Jordan valley:

The lower part of Jerusalem (Derorim formation): consists mainly of limestone, soft thin bedded, dolomitic, chalky and marly limestone. Its thickness ranges between 8-25m and the age of the formation is Lower Turonian (Bentor & Vroman, 1963).

The middle part of Jerusalem (Shivta formation): consists mainly of limestone, hard and massive and forms typical cliff morphology with many caves. It can be missing or its thickness can reach up to 40m. Its age considered to be Lower Turonian. The formation is correlative to the detrital limestone member of the Jerusalem formation in the Jerusalem area (Arkin et al., 1965).

The upper part of Jerusalem (Nezer formation): consists mainly of hard limestone, dolomitic limestone, marl and some chert. Two faces are discerned in the formation: A 70m thick limestone faces and a dolomite and limestone faces of 16-65m. In both cases in their lower parts appears a marl bed of 2-4m thick. The age of the upper part of Jerusalem formation is Turonian-Cenomanian.

2.5.1.3 Senonian Group (Belqa Group)

The Senonian Group is called Mount Scopus Group by the Israeli but Belqa Group in the Palestinian terminology and the formation is known as Abu Dies formatio. Abu Dies formatio is equivalent to Menuha and Lower Mishash in Israel terminology, while Amman stands for Upper Mishash. Zarqa is referred to as Ghareb, and Khan El-Ahmar as Taqiye.

Abu Dies (Mishash) formation is mainly exposed in the Western part of the Jericho district, near the Sultan area. It consists of chalk and chert with some limestone and phosphorite, the chalk usually white but in some areas dark colored due to the presence of bituminous materials. The thickness of Abu Dies (Mishash) formation ranges from 20-115m and the age of the formation is Santonian-Campanian (Flexer, 1968).

Abu Dies (Menuha and Lower Mishash) consists of white chalk with a prominent twin band of chert. The thickness varies from 40-70m in most of the district to about 200m,

mainly near the Jordan Valley. The upper contact with the formation is defined by the first appearance of chert beds. The age of the formation is Santonian.

Amman (Upper Mishash formation) contain chert, marl and chalky limestone. The thickness of the formation ranges from 26-50m and its age is Campanian. The top of the formation is missing due to erosion. Khan El-Ahmar formation (Taqiye formation) contains chalk and chert. The thickness of the formation ranges from 0-90m.

The Zarqa (Ghareb) formation consists of alternating bituminous marl, chert and phosphatic chalk. It is rich in fossils (Foraminifers) and reaches a thickness of up to 35m. In general chalk often appears to be a fracture flow aquifer but because of its clayey nature it is considered as an aquiclude. The formation is structurally cut by minor faults.

2.5.2 Neogene and Quaternary

The study area is mainly composed of continental sediments of quaternary age. These constitute clastic (clay, sand and gravel) deposited in fan deltas with some intercalations of lacustrine sediments (clay, gypsum and aragonite) of the Lisan formation and younger Holocene sediments (Begin et al., 1974 and Sneh et al., 1998). The area occupied by quaternary sediments varies greatly (the distance from the Dead Sea to the rift margins is about 5km at Wadi Ze`elim but less than 1km at Ein Feshcha area).

The Neogene and Quaternary successions are built mainly of marine and continental clastic formations, marine and limnic chalk, evaporates and magmatic rocks (Schulman, 1959). Alluvial formations are of Pleistocene, Holocene to Recent age. During the Neogene-Quaternary, several water bodies occupied the tectonic depressions along the Jordan-Arava Valley. These depressions are associated with the tectonic movements along the Red-Dead Sea transform fault (Freund & Garfunkel, 1980). The sediments that accumulated in the rift depressions comprise the Dead Sea Group and they include evaporites, carbonates and terrigenous material. The marine and continental clastic formations are limited mostly to the Jordan Rift Valley itself. The thickness varies between a few hundreds of meters on the rift shoulders to a few thousands in the deep centers. The sequence is divided into two Groups: the Tiberias Group of Neogene age at the base and the Dead Sea Group (or the Jordan Valley Group) of Plio-Pleistocene-Holocene age, at the top (Khayat, 2005). The study area as a part of lower Jordan Valley is belonging to the second group.

2.5.2.1 Plio-Pleistocene Formation

The topographic sill at Wadi Malih separated the Southern Lake Lisan (occupying mainly the Dead Sea basin) from the Northern Lake Tabariyya (Kinneret) (occupying the Tabariyya and Beesan basins) during most of the past 70,000 yr (Begin et al., 1974 and Bartov et al., 2002). The Quaternary sediments filling the depressions to the South of the Wadi Malih sill (at ~280 m.b.s.l) form the Samra (Amora), Lisan, and Ze'elim formations and the late Pleistocene–Holocene sediments deposited North of the Wadi Malih sill form the Kinneret formation. The three major lacustrine water bodies that occupied the Dead Sea basin during the late Pleistocene-Holocene are Lake Samra (Amora), Lake Lisan and the Dead Sea (Stein, 2001). Samra (Amora) formation: crops out along the Western part of the Jordan Valley floor, at the base of the marly cliffs lining the Jordan River. It was deposited as marginal sediments along the Jordan Valley. The formation consists of conglomerates, sandstones and silts. It is subdivided into two members:

a) Coarse Clastic member: which is formed as a result of wadis fan deposits and dominated in the Western part of the study area, it consists of gravel and conglomerate with a thickness that reach 35m and b) Silt member: this member exists further to East of the coarse clastic member, it covers a large part of the study area. It consists of finer particles of silt and clay with a thickness that reaches 20m. The two members show interfingering relationships and both interfinger with the Lisan formation.

The Lisan formation is exposed in the Eastern part of the study area as well as the whole Jordan valley rift and the wadis. The Lisan formation, which was deposited from the lake and its surrounding fan deltas, consists mainly of authigenic aragonite and gypsum and clastic material transported by floods. The aragonite appears in thin (~0.5–1mm thick) laminae alternating with detrital laminae of similar thickness. The detrital laminae consist mainly of quartz and calcite grains, probably of wind blown origin, and dolomite, calcite, and clay minerals derived from the surrounding basin shoulders. The Lisan formation acts as an aquiclude and it hosts the hypersaline and brackish fauna.

The Ze'elim formation consists of different lacustrine to fluvial facies. The lacustrine sedimentary section of the Ze'elim formation, consists of alternating aragonite laminae (~1-2mm thick) and detritus layers (1mm to >10cm thick), similar to the Lisan formation laminae. The detritus layers consist of clay and silt size grains of Cretaceous rocks exposed in the catchment area (Stein, 2001).

2.5.2.2 Holocene formation

After the retreat of Lake Lisan, the Dead Sea lake level stabilized at ~ 400 m.b.s.l. The sediments deposited in this post Lisan water body (paleo-Dead Sea) compose the Ze'elim formation (Yecheili, 1993). The Ze'elim formation is exposed along the periphery of the Dead Sea and was recovered in several boreholes along the Western shore of the lake. In addition, several boreholes were drilled in the Ze'elim plain next to the exposed section and in several other shore locations (Ein Gedi, Nahal Hever and Ein Feshcha). These cores provide an unprecedented inventory of the Holocene history of the Dead Sea region (Migowski et al., 1999).

The thickness of the Holocene deposits reaches about 20 to 30m at the Western shore of the lake's Northern basin, and about 80m in the Southern basin (Yecheili et al., 1993 and Migowski et al., 1999). Beneath it lies a halite sequence, which is probably correlated to the salt layer in the drill hole of Dead Sea interface (Yecheili et al., 1993). These formations comprise recent alluvial deposits in the wadis and associated flood plains of ephemeral streams. These sediments found in the Eastern part of the study area lining and surrounding the Jordan River. In the study area this formation have five members that varied in its lithology from one location to another (figure 10), these members are consist of: conglomerate, Gravel, Stream soil and Sabha soil.

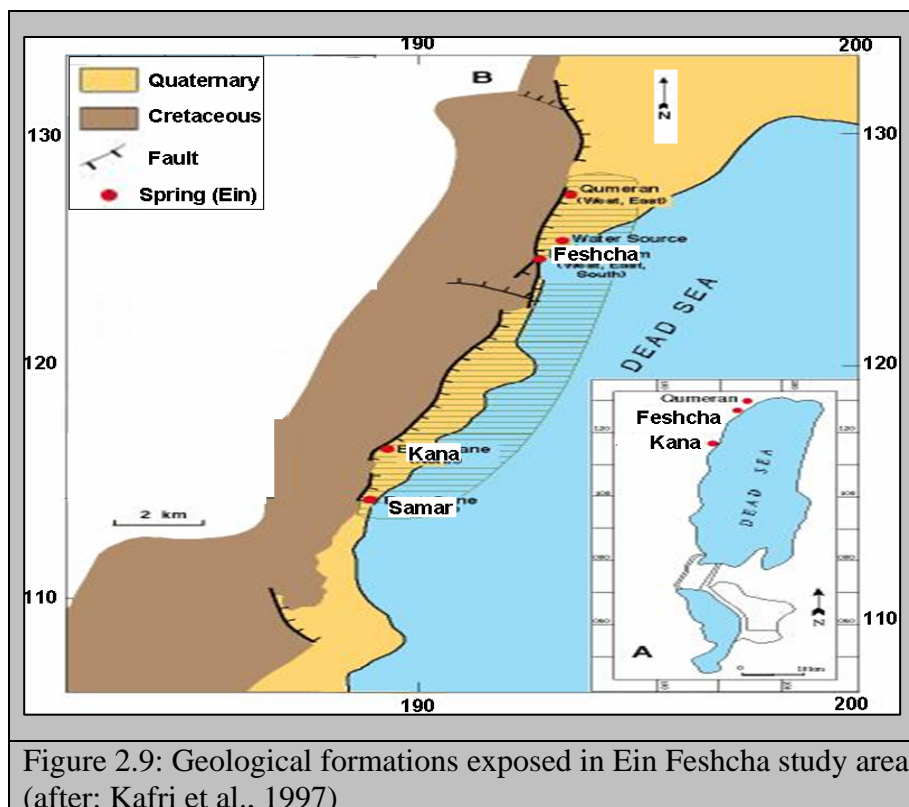


Figure 2.9: Geological formations exposed in Ein Feshcha study area (after: Kafri et al., 1997)

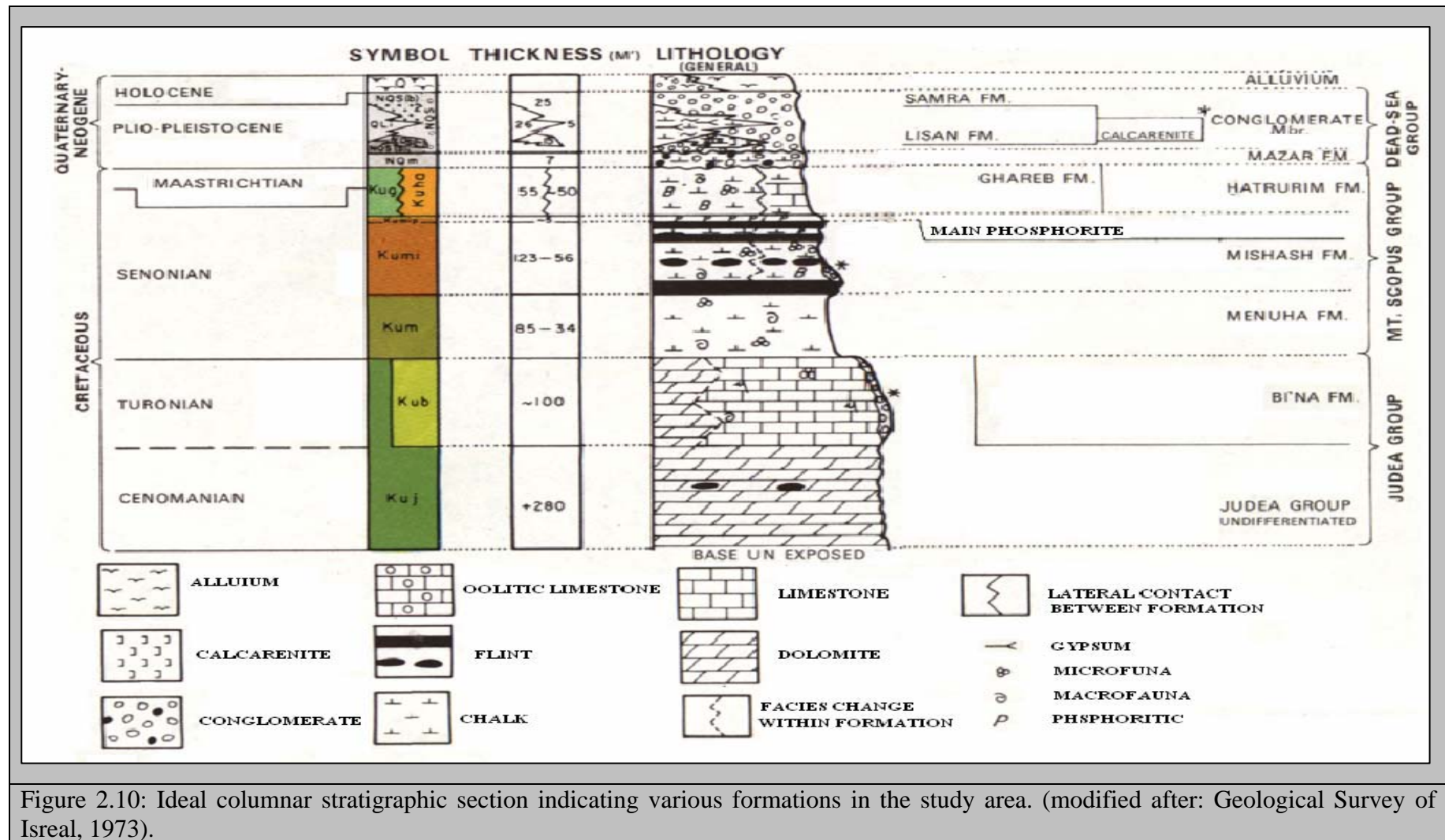


Figure 2.10: Ideal columnar stratigraphic section indicating various formations in the study area. (modified after: Geological Survey of Isreal, 1973).

3 HYDROGEOLOGY & GROUNDWATER AQUIFERS

3.1 Climate Conditions of the West Bank

The West Bank has a typical Mediterranean climate with two distinct seasons: dry hot season from June to October and cold wet season from November to May. The predominantly low pressure area of the Mediterranean is centered between two air masses: the North Atlantic high pressure of North Africa and the Euro-Asian winter high pressure located over Russia. This is the primary cause of winter weather in the West Bank and the Eastern Mediterranean in general (Husary et al. 1996).

The majority of the West Bank area has the climatic characteristics of the Mediterranean climate zone. This type of climate prevails along the highlands with precipitation amounts of 450-800mm/yr, and potential evapo-transpiration rates of about 1600-1900mm/yr. Between the Mediterranean zone along the highlands and the arid zone of the Jordan Valley floor a transitional climatic zone is found (Semi arid to Mediterranean Zone) prevails along the slopes from the highlands to the Jordan Valley. This zone receives average precipitation rates ranging between 200-300mm/yr, with average potential evapo-transpiration rates of 1900-2400mm/yr. The arid climate zone (Lower Jordan Valley) has a different transitional climate with dry and extremely desert conditions in the Dead Sea region. This type of climate prevails in the Jordan Valley. Precipitation ranges from <100 to 150mm/yr and the potential evapo-transpiration rates reach 2400-2600mm/yr. The average annual precipitation rate and the potential evapo-transpiration rate of the West Bank are presented in figures 3.1 and 3.2.

3.1.1 Climate Conditions of Marsaba-Feshcha Study Area

In general the climate of the whole Jordan Valley is characterized by a hot dry summer and warm low rain winter. Marsaba-Feshcha area can be classified as Semi arid to arid area, its location along the feet of the mountains accompanying the Jordan Valley in the West protect it from the cooler North Western Mediterranean wind. The temperature of the area varies from high temperature in the South that slightly decreases further to the North. Typically, the temperature reaches its maximum in August with an average of 38C°, while January considered as the coldest month in the year with an average of 19C°. The study area is characterized by sharp fluctuations in precipitation. On the high mountains in the West, the average rainfall ranges from 500-700mm/yr (Jerusalem-630mm/yr). Towards the East and Southeast there is a sharp drop in precipitation over a relatively short distance. In the Jordan Valley, the average rainfall is less than 200mm/yr (Jericho-160mm/yr).

Precipitation decreases to less than 100mm/yr on the Dead Sea shore (69mm/yr), (figure 3.1) (EXACT, 1999).

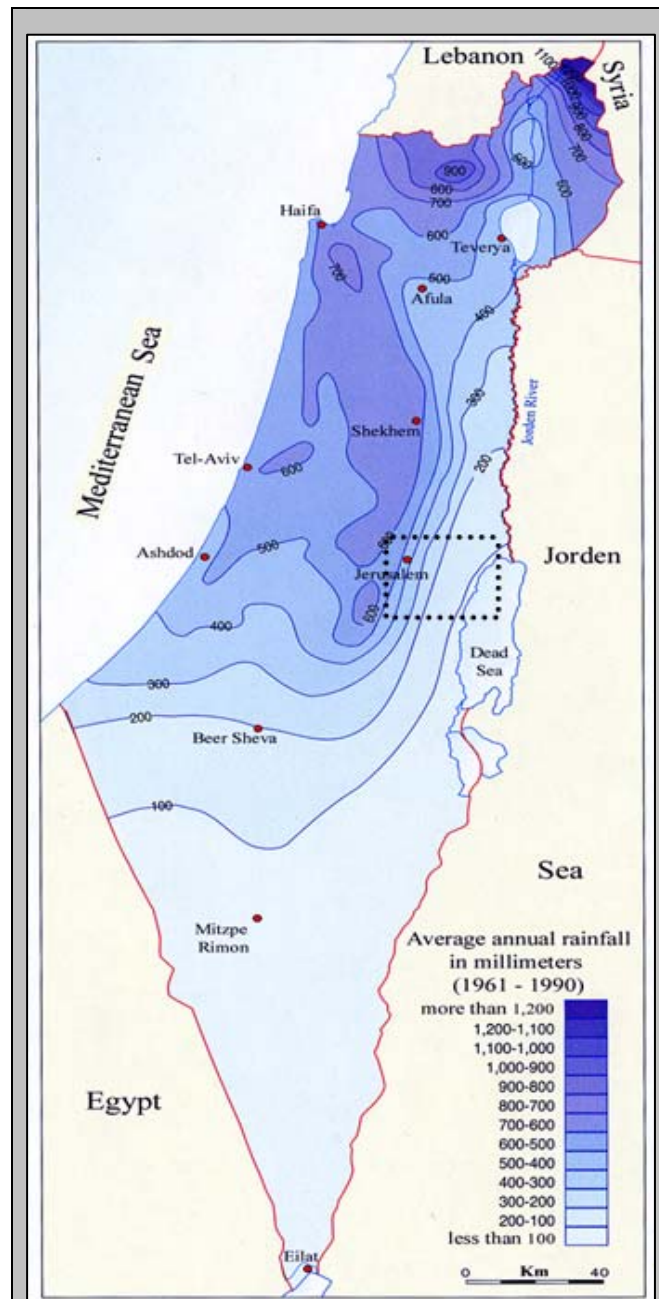
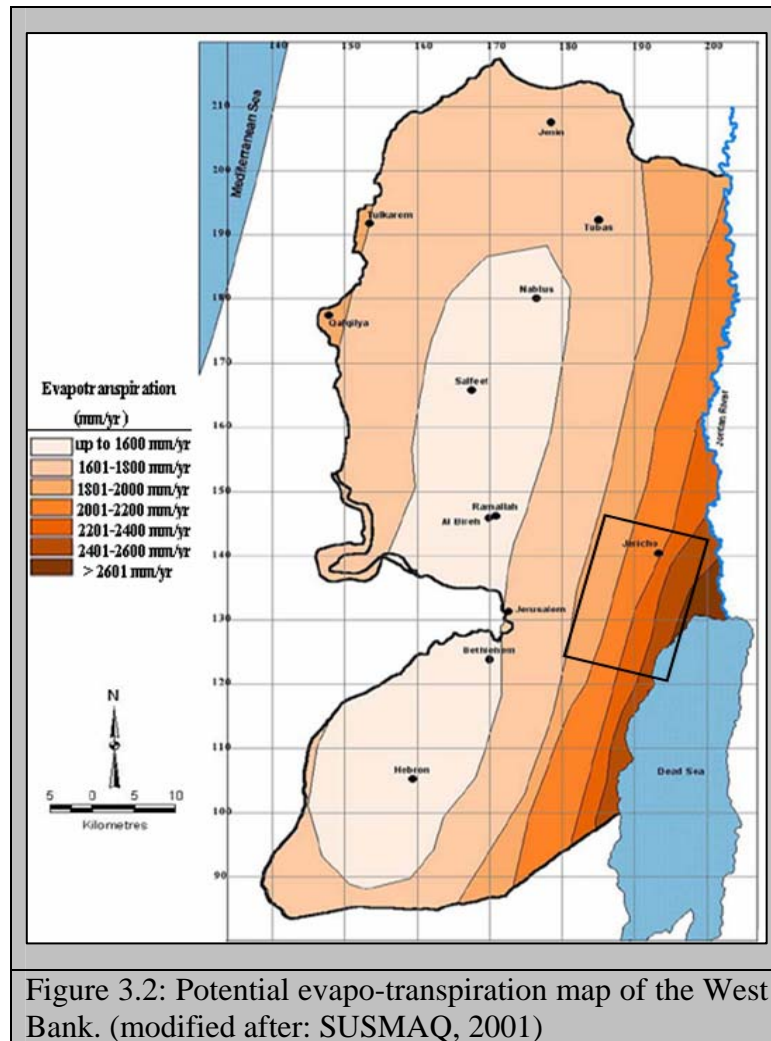


Figure 3.1: Average annual precipitation rate in mm in the Jordan Valley Area (EXACT, 1999).



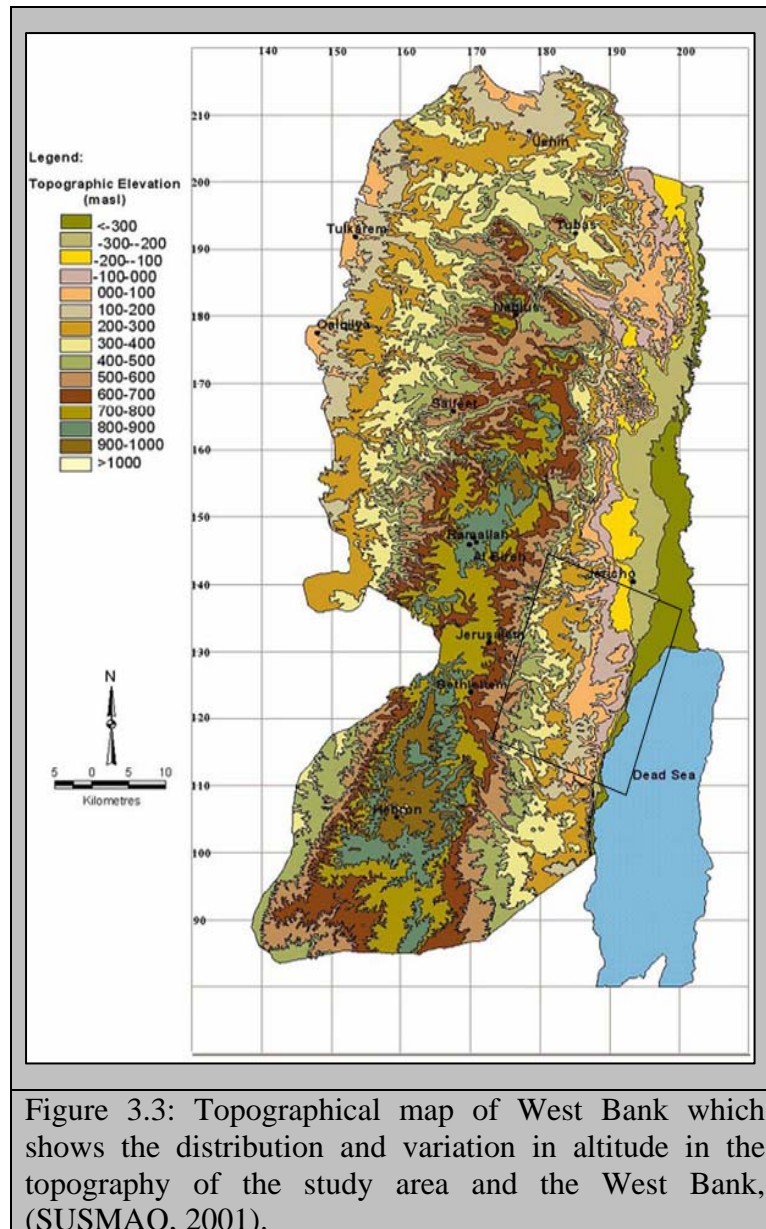
3.2 Drainage System

The understanding of the flow pattern from the regional aquifers into the Rift Valley is important in building a conceptual model and in understanding the salinization processes. From practical point of view, the understanding of the flow mechanism is an important tool for the sustainable exploitation of the groundwater resources to the population in the region. The drainage system of the West Bank is mainly controlled by tectonics. It was initiated by the uplift of mountains through the folding of the Syrian Arc system and rejuvenated through the formation of the Jordan Rift Valley. Between the mid Miocene and Pliocene recent phases a lateral strike slip movement of the African and Arabian plates took place. This movement placed the West Bank in the Sinai sub-plate and led to the development of the rhomb-graben left lateral shear fault system along the line of the Dead Sea. This fault system had a vertical, stepped component, which led to the lowering of the base level for both the surface and phreatic ground water drainage (Rofe & Raffety, 1963

and Andrew, 2000). This new base level of erosion deflected the drainage system from flowing to the Mediterranean Sea to flow towards the Dead Sea. This deflection divided the West Bank into two major basins, Mediterranean basin and Dead Sea basin, divided by the ridge on the Mountain Plateau. This process as a whole leads to the formation of the Jordan River basin. The West Bank area is affected by intensive structural patterns (anticlines and synclines) on which extensive secondary structures of different ages were formed, where the major folds are accompanied by a great number of faults, joints and fractures.

From the hydro-geological point of view, such extensive structural patterns affecting the study area controls the groundwater and surface water flow patterns and makes the West Bank a very good recharge area of the various aquifer systems. Also the highly faulted rock formations, which may reach several kilometers in some areas, increase the possibility of hydraulic connection between the various aquifer formations. For example, most springs of the West Bank formed within structural fault zones where the fault acts as a water barrier which transfers water from the affected aquifer formation to the ground surface. On the other hand, some drilling experiments in the West Bank showed that the groundwater wells have higher yield potential in areas with highly structural fault intersections (Sabbah & Isaac, 1996).

Combined with the topography of the area, the land forms and drainage patterns are highly determined by the geological structures. The predominant feature in the West Bank is the considerable contrast in elevation between the uplands (West Bank Mountains), with an altitude of up to 1200 m.a.s.l, and the great depth of the Jordan Rift Valley, with a depth of ~400 m.b.s.l. This distribution and variation in altitude can be seen in the topographical map of West Bank in figure 3.3. The crest axial line extending from the mountains of Hebron, Jerusalem, Ramallah, and Nablus is parallel to the Jordan Rift Valley in the East of the West Bank. The horizontal distance between the axial line and Jordan River is about 25-30km. This indicates a steep overall topographic gradient of about 1:20 to the East of the West Bank Mountains and at some locations the gradient is much steeper. For example, the gradient is about 1:90 in Jericho area.



3.2.1 Surface Water Flow Direction of Marsaba-Feshcha Study Area

The flow direction of the surface water in the main streams of Marsaba-Feshcha drainage basin is at most towards the Northeast and to less extent towards the East and Southeast, while in the secondary creeks it is mainly Eastwards. Marsaba-Feshcha, the main wadi discharging this catchment, is a tributary of Wadi Qilt, Wadi Muqalek (Og), Wadi Qumeran and Wadi Al-Nar (Kidron), that flows Northeast, East and Southeast towards the Dead Sea (figure 3.4).

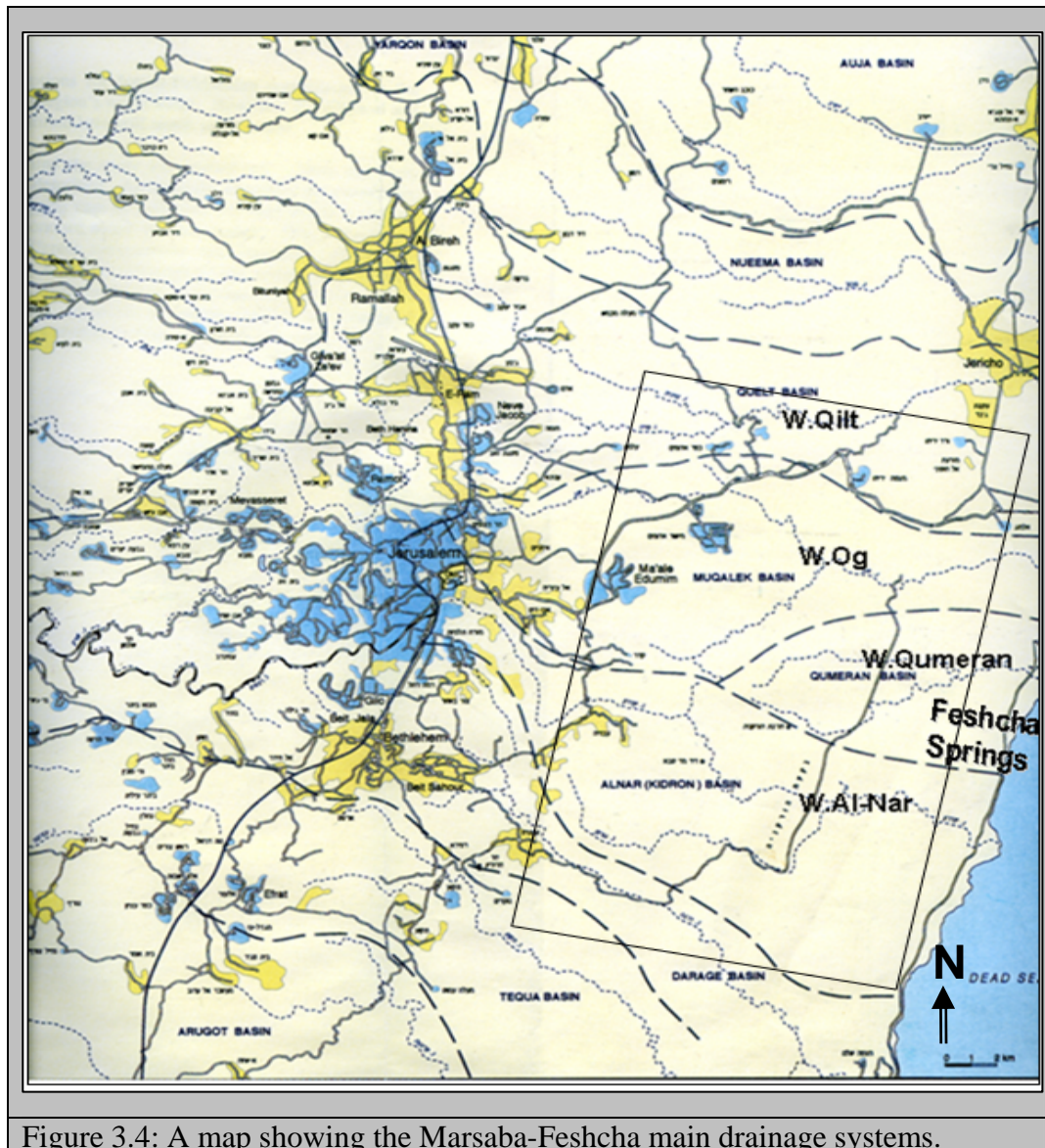


Figure 3.4: A map showing the Marsaba-Feshcha main drainage systems.

3.2.2 Ground Water Flow Patterns of Marsaba-Feshcha Study Area

Most of the natural replenishment in the study area is from precipitation on the outcrops in the Western part of the basin. Accordingly groundwater flow direction is mainly from the West to the East. Groundwater head varies from +450m level along the Hebron and Ramallah anticlinal axes to -300m in the Jordan Valley and -400m in the Dead Sea. This groundwater head drop of 850m occurs over a distance of approximately 25-30km. However, this flow pattern is far from being uniform. There are zones with a relatively low groundwater head gradients (Herodion, Ma'ale Edumim and Mizpe Jericho wells) while there are others in which the gradient is rather steep (Jerusalem-5 and Azriya-1 wells). This

variability in the hydraulic gradient is indicative of either a strong heterogeneity of the aquifer or steep changes in the layer geometry (Flexer et al., 2001).

Groundwater flow is governed by the geological structure of the area, uplifting of the secondary anticlinal axes, as well as flexures and fault systems (Rofe & Raffety, 1963; Bensabat et al., 2004). The Marsaba Anticline in the East is the most dominant tectonic element, which acts as the Eastern model boundary and influences the groundwater flow path and the outlet in the Ein Feshcha Springs (Flexer et al 2001, Ben-Itzhak and Gvirtzman, 2005).

Several studies have focused on the groundwater flow field through the carbonate aquifer beneath the Jerusalem Desert. Arad and Michaeli, (1964) suggested a uniform West to East flow, parallel to the hydraulic gradient, because no contradicted observations were available. Subsequent studies have suggested a non-uniform groundwater hydraulic gradient, where the flow pattern is influenced by the geological structure (Burstein, 1970; Fink, 1973). Guttman et al (2004), suggested that the groundwater flow bypasses the low conductivity zones, as shown by the fact that groundwater flow from Herodion and Shdema wells is mainly in the direction of Northeast parallel to the Bet Sahur (Beesan) Syncline axis and subsequently East. Ben-Itzhak and Gvirtzman (2005) noted that the groundwater flow is diverted Northward due to the geological folding structure but also they added the drainage basins are not completely separated; meaning that the structural barriers do not block the eastward flow everywhere throughout the area.

Therefore it is questionable why the groundwater flow changes its path from West-East direction to Northeast and/or Southeast direction, while the groundwater drains through the Feshcha springs a few km southern, instead of flowing the direct and short path to the East into the Rift Valley fill.

3.3 Surface Water Resources

Surface water is that water which flows in the form of rivers and streams or the water which is captured by seasonal reservoirs. Surface water flowing in streams may include flood flow water and base flow water. The base flow is the contribution of groundwater in feeding surface drainage basins through springs. Surface runoff depends mainly on the quantity and duration of rainfall during the wet seasons. The water resources of the West Bank come mainly from natural rainfall. The water resources in the region comprise of both, surface and subsurface waters. The surface water mainly flows in the Jordan River, in addition to many intermittent wadis. The amount of the groundwater recharge into the

aquifer and surface runoff depends on: rainfall amount, intensity, duration, evapo-transpiration, soil cover, surface slopes, sizes and rock types of the catchments areas.

3.3.1 The Jordan River

The Jordan River is the only river which can be used as a source of surface water in the West Bank. The Jordan River is 360km long with a surface catchment area of about 18300km² of which 2833km² lie upstream of Lake Tiberias outlet.

The Eastern catchment area downstream of Lake Tiberias is about 13027km², while the Western catchment is about 2344km². The riparian countries of the Jordan River are Lebanon, Syria, Israel, Palestine and Jordan. The average annual precipitation in the Upper Jordan and Lake Tiberias is around 1600mm/yr and 800mm/yr, respectively. The Jordan River becomes progressively more saline and the water is less usable towards the Dead Sea. In the 1950's and before the diversion of the Jordan River by the various riparian countries, the Jordan River was draining 1287 MCM/Y into the Dead Sea (Johnston Plan, 1955). Recent studies estimate that the average flow in the Upper Jordan River is currently about 1300 MCM/Y, which is very close to its flow in the 1950's reported by Johnston Plan but of which only 13% (169 MCM/Y) reaches the Dead Sea. The other 87% is being consumed by the upstream riparian countries as follows: 47% (611 MCM/Y) by Israel, 22% by Jordan (286 MCM/Y), 16% by Syria (208 MCM/Y), and 2% (26 MCM/Y) by Lebanon (Al-Weshah, 2000).

3.3.2 The Dead Sea

The Dead Sea is a closed lake which represents the sink for the whole Jordan River drainage basin. The Dead Sea can be divided into two basins; the deep wide Northern basin and the Southern shallow basin which are separated by a peninsula called the Lisan. In 1982, the level of the Dead Sea water was 400 m.b.s.l and its total surface area was about 800km² (the northern basin's area is about 740km² and the southern basin's area is about 60km²), (Abed, 1985). The shrinkage of the Dead Sea is due to the diversion of the Jordan River water and related West and East streams by upstream riparian users as well as due to the industrial activities of the potash mining by Israel on the Western shore and by Jordan on the Eastern shore of the Dead Sea.

In order to stop the deterioration of the ecosystem and to restore the water level of the Dead Sea as it was in the 1950s (~395 m.b.s.l), several scenarios were suggested such as the Med-Dead and the Red-Dead canals to convey water from the Mediterranean or the Red Sea to the Dead Sea, respectively.

3.3.3 Flood Water Runoff

The measurements of the runoff in the West Bank are very rare and the majority of the available data is only estimations which are around 7-14% of the annual rainfall (Rofe and Raffety, 1963), and 5% (Gvirtzman, 1994). Surface flood runoff in the West Bank is mostly intermittent and probably only occurs when the rainfall exceeds 50mm in one day or 70mm in two consecutive days. The surface runoff in the West Bank, which occurs on the dry riverbeds in winter after heavy rainfall, is sporadic. The rainfall intensity, duration of the rainfall storm, land use, soils; elevation, surface slope and the shape of the catchment are the deciding factors. High priority must be given to the construction of small and large scale dams to collect flood water to be used for various purposes.

3.4 Ground Water Resources

Groundwater resources in the West Bank are derived from three aquifer basins through wells and natural springs. The total water use from the West Bank aquifers is about 134.3 MCM/Y of which 89 MCM/Y was extracted from wells and 45.3 MCM/Y was used from the major springs. Another 36 MCM/Y of water is usually purchased from external sources (such as Mekorot) or from public springs or from private irrigation wells (PWA, 2003).

3.4.1 Groundwater Wells

Currently there are about 550 groundwater wells in the West Bank, the current number of working wells is about 370, of which 53 wells are being used for drinking purposes and 323 wells are being used for irrigation (PWA, 2003). In addition to the Palestinian wells, there are 36 wells owned by the Israeli settlements established in the West Bank after 1967 which produce about 50 MCM/Y (PWA, 2003).

Tens of wells (observation, production and a few oil wells) have been drilled in the Jerusalem Desert (eastern slopes), 16 in the Upper Cenomanian and 22 in the Lower Cenomanian. Most of the production wells are located in three pumping fields: Herodion, Jerusalem and Mizpe Jericho. [Figure 3.5](#) show the springs and wells location which has been sampled and investigated through out this study. Most of the water is extracted from

the lower aquifer of the Ajlun Group (Judea Group). The depths of the wells range from 350 to 900m, depending on their geological location and the depth of the lower aquifer. Pumping has begun in the early 1970s. Since then, it has been steadily increasing, owing to the addition of new wells. A few new Palestinian production wells have been added in recent years, mostly in the Herodion area.

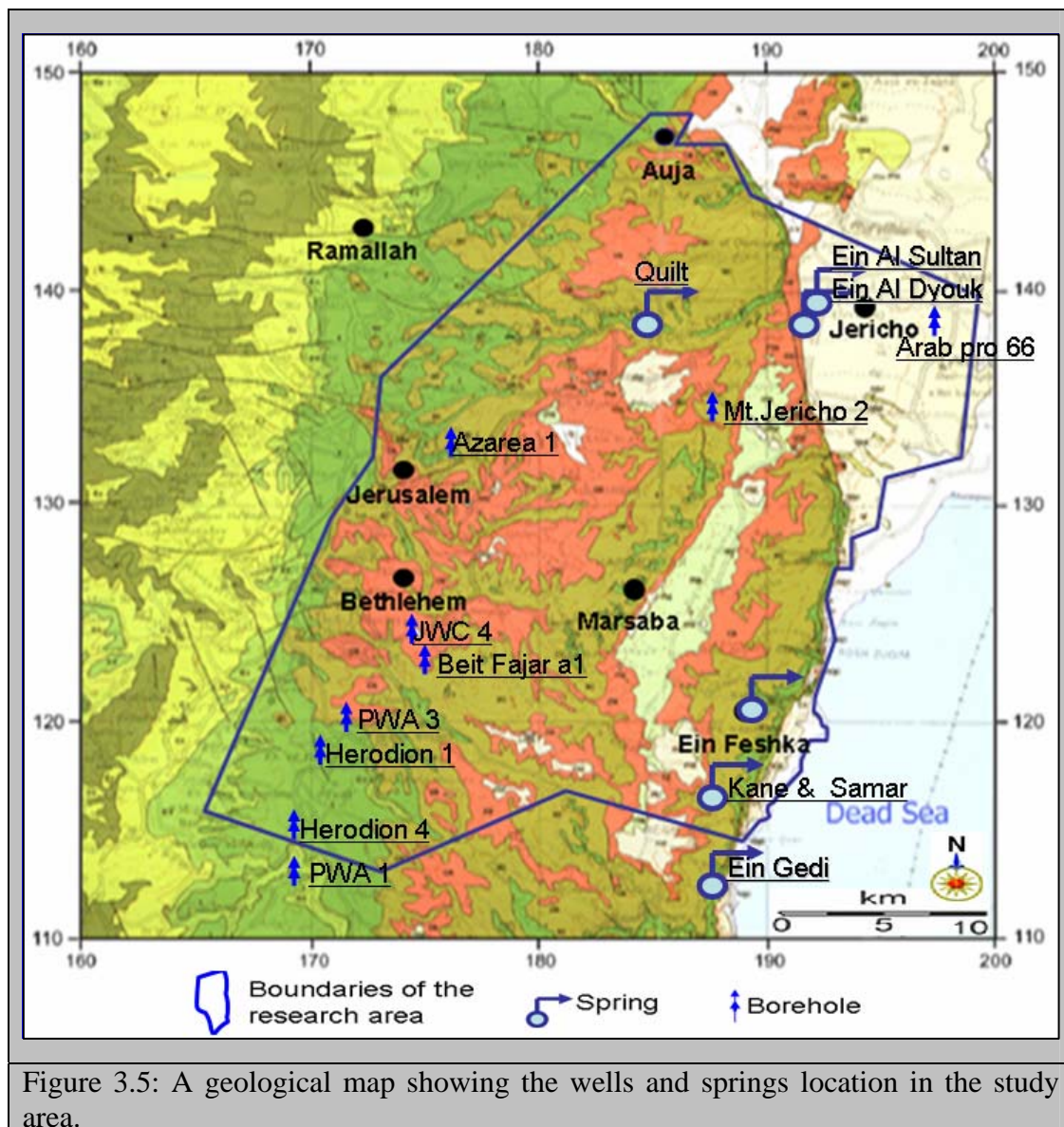


Figure 3.5: A geological map showing the wells and springs location in the study area.

3.4.2 Springs

Springs are the second important source for groundwater exploitation throughout the West Bank and the study area. It is used for drinking and irrigation use such as in Auja area and Jericho which depend on spring water to a much greater extent. There are more than 500 springs and seeps in the West Bank. The number of springs which are subjected

to flow measurements on a regular basis by the Palestinian Water Authority is 114. These springs have a minimum flow discharge of 0.1l/s. These springs discharge flow in two general directions, East and West. These 114 springs are distributed through 10 spring systems based on their watersheds; each system is subdivided into several groups. Six spring systems with 79 springs discharge their flow to the East towards the Jordan Valley and the Dead Sea and to the Northeast towards Bet Sha`n area in Israel, while another 4 spring systems with 35 springs discharge their flow to the West (Isaac & Sabbah, 1998). The fluctuations in the springs discharge pattern depend on the precipitation rate in the recharge zone (Wolfer, 1998).

According to the geographical distribution and discharge behavior, the springs in the study area can be divided into three groups:

a) Wadi Qilt Spring Group: this group of springs (Ein Qilt, Ein Fawwar and Ein Fara springs) is located in wadi Qilt and its tributaries. These wadis are deeply incised canyons and only here the Turonian aquifer is exposed where the spring outflow occurs. The springs discharging in this area are characterized by an immediate response to precipitation and a highly fluctuating discharge pattern.

b) Jericho-Auja Spring Group: this group of springs is located in the Lower Jordan Valley to the North of the study area and is related to the Samia fault (Ein Sultan, Ein Duyuk and Nuwe'meh springs). Due to various step faults close to the Jordan Valley the base of the uppermost aquifer is exposed. These springs discharge at a constant rate. The main springs of this group are described as follows:

Ein Sultan: Sultan is located 2km NW of Jericho and discharges at an elevation of 215 m.b.s.l. The outflow of the spring is structurally controlled by a large SW-NE trending normal fault and the spring can be classified as a fault spring (Wolfer, 1998).

Ein Duyuk and Nuwe'meh Spring: these springs discharge at the margin of the Eastern slopes 3.7km NW of Ein Sultan. The system consists of three springs emerging at 110 m.b.s.l.

Auja-Fazael Springs: They are the outlet of the upper sub-aquifer. The springs are characterized by a quick response to climate changes. Guttman (2004) investigated the behavior of the Auja spring as an example of a typical karstic spring in the study area. The maximum discharge appears a little after the rainiest month. It can be seen that the discharge dies out towards the end of the winter season.

The Jericho springs discharges are more stable and constant and do not show high response to climate change like in Auja spring. The reason is that the recharge area of the spring is

far from the spring outlet and the storage is much greater than the storage of the other springs like in Auja and in Ein Samiya.

c) Feshcha Spring Group (the regional spring group): this group of springs which is located along the Western shore of the Dead Sea. These springs are the outlet of the regional aquifer. The average annual discharge is about 50-80 MCM/Y (Guttman & Simon, 1984). The recharge area is far from the springs outlets. The springs have large storage and are characterized by stable discharge with only small annual fluctuations. The main springs of this group are described as follow:

Ein Feshcha: The Feshcha springs are located along the Dead Sea shore, looking toward the Dead Sea to the East, a large area with vegetation can be seen. Ein Feshcha springs spread over a relatively large area of 3-4km along the Dead Sea shore. This is the discharge zone for large amounts of groundwater from alluvial aquifer to the Dead Sea. They represent the outlet of the Judea Group aquifer (Upper and Lower aquifers). There are large variation in salinities and chemical composition among the numerous springs of this area.

Kane-Samar: The Kane-Samar springs are located few hundred meters to the South of Ein Feshcha. This is the discharge zone of groundwater from alluvial aquifer to the Dead Sea. To the West of Kane-Samar springs were large discharge of groundwater occurs, several wells were drilled in the area. In this area there is evidence for at least two distinct sub-aquifer in the alluvial aquifer. This is best demonstrated in Turieb-4 well where higher salinity, higher temperature and higher water level is found in the lower sub-aquifer.

3.5 The Eastern Aquifer Basin (EAB)

The Eastern Aquifer Basin (EAB) is of great tectonic complexity and the major movement is Eastwards with a Southerly component near the River Jordan. The recharge and discharge areas of this basin are completely located within the West Bank boundary and predominantly in the mountain outcrop regions of the Albian-Turonian formations. The Eastward dip of the Eastern flank of the major anticline structure allows most of the percolating water into the subsurface to pass down dip towards the Jordan Valley and Dead Sea by gravity. Part of the groundwater emerges as springs. The EAB extends from the crests of the West Bank Mountains on the West to the Jordan River and the Dead Sea on the East. Some Palestinian and Israeli hydro-geologists are sub-dividing the Eastern Aquifer Basin (EAB) into three smaller sub-basins which are; the Eastern Aquifer Sub-Basin (less in area than the overall Eastern Aquifer Basin), the Jordan Valley Floor Aquifer

Sub-Basin (JV FAB), and the Dead Sea Aquifer Sub-Basin (DSAB). The direction of the water flow of this basin is Eastwards toward the Jordan River and the Dead Sea. Naturally this basin is drained by several groups of springs in the West Bank, whereas a small fraction of its water discharges into the Jordan River and the Dead Sea and a negligible amount leaks to Israel. The EAB drain from Neogene, Pleistocene, Lower and Upper Cenomanian sub-aquifers. The Cenomanian-Turonian aquifer system in the eastern basin can be divided into two sub units: the shallow and relatively thin Upper Cenomanian-Turonian sub-aquifers and the deep Lower Cenomanian sub-aquifer. The recharge area of this basin encompasses over 2200km² and the storage area over 2000km² (Gvirtzman, 1994). The aquifer sustainable yield (ASY) of the EAB was estimated to be about 202 MCM/Y. Estimates of the extraction potential of this basin are not well determined; 100 MCM/Y (Elmusa, 1993 and Gvirtzman, 1994), 125 MCM/Y (Wolf, 1995) and 172 MCM/Y (Oslo 2 Accords, 1995). According to Oslo 2 Accords (1995), the 172 MCM/Y is shared as follows: 24 MCM/Y utilized by the Palestinians from wells, 30 MCM/Y utilized by the Palestinians from springs, 40 MCM/Y used by the Israelis and 78 MCM/Y to be developed in the future. In addition to the good quality spring water, there is about 45-80 MCM/Y of saline water discharged by the EAB on the Western shore of the Dead Sea. According to the surface and subsurface hydrological divisions of the West Bank, Marsaba-Feshcha area is part of the Jerusalem Desert; accordingly it is related to the Dead Sea Aquifer Sub-Basin (DSAB) which is part of the Eastern Aquifer Basin.

3.6 Groundwater Aquifers in the West Bank

The main aquifer system in the West Bank is of the Albian-Turonian geologic time (Cretaceous age). That aquifer is mainly composed of karstic and permeable limestone and dolomite inter bedded with argillaceous formations of lower permeability which separate the upper and lower parts of the Judea Group creating two sub-aquifers.

Groundwater, derived from the shallow and deep water bearing formations of the Mountain Aquifer represents the main source of domestic water in the entire West Bank. The aquifer basins are recharged directly from the natural rainfall on the outcropped geologic formations in the West Bank Mountains forming the phreatic portion, while the major storage areas are in the confined portions which either flows to the West towards the Israeli underground and the Mediterranean, or flows to the East towards the Jordan Valley and the Dead Sea. The aquifer unites in the West Bank are variable, some aquifer units may not exist in one basin and may do in other one, or it may do exist in more than one

basin. This is could be related to the following: the basin location with respect to the direction of groundwater movement, the thickness of that basin, the lithology and the hydraulic properties of that basin. The quantity of cross boundary fluxes between the basins and of inter aquifer flow within the basins are not well understood, making it difficult to accurately quantify the total groundwater storage and yield in each aquifer system.

3.6.1 The Shallow Aquifer

The Pleistocene, Neogene (Pliocene-Miocene) and Eocene represent what so called, the Shallow Aquifer and are utilized on the local level only.

3.6.1.1 Pleistocene Aquifer

This aquifer extends from Jericho in the South to Marj Na'jeh and lower wadi Fari'a in the North. The aquifer consists mainly of unconsolidated beds of sands, gravel, separated by impermeable layers of saline lacustrine marl deposits. The aquifer deposits are bound to alluvial fans that have formed at the outlets of major wadis. The thickness ranges from 0 to 120m. The water quality is variable with Chloride levels from 100 mg/l to more than 2000 mg/l. The groundwater occurring in the alluvial fans differs quantitatively and qualitatively according to its location within the fan. Fresh water occurs around the apex of the fan, whereas saline water occurs at the fringes. Very steep deep faults in the Jordan Rift Valley may cause deep circulation of the groundwater bringing it into contact with salty formations which appears as brackish springs near the river. This aquifer is composed of lisan, alluvium and gravel fan formations. Lisan formation (Pleistocene sub-aquifer) as well as alluvial and gravel fans (Holocene) extends along the Jordan Valley. The alluvium is unconsolidated in the Rift Valley, where it is formed of laminated marls with occasional sands. However, the Pleistocene sub-aquifer is composed of basalt in some places.

3.6.1.2 Neogene (Miocene-Pliocene) Aquifer

The Neogene aquifer is of local importance at the Northeastern boundary of the West Bank in the Jordan Valley and wadi Al Fari'a especially near the Bardala and Ein Beida areas. It consists of well cemented conglomerates with a high permeability (contains a small amount of fresh water). Its water quality is good with a Chloride concentration of about 70 mg/l. However, the aquifer is of limited lateral extent and thickness (around 100m).

3.6.1.3 Eocene Aquifer

The Eocene aquifer is underlain and overlain by impermeable sediments (chalk and marl). In addition to the underlying Eocene chalk, the aquifer is separated from the Cenomanian-Turonian Upper Aquifer by a 200-500m thick Senonian sequence of chalk and marl. It is of limited thickness and comprises a nummulitic limestone sequence with intercalations of chalk, chert and marl that reduce the aquifer potential. Therefore, the aquifer has limited storage and water transmitting properties. The aquifer is mainly found in the Fari'a and Jenin areas. Its water table normally occurs within a depth of 100m below ground surface.

3.6.2 The Upper Aquifer

The Upper Aquifer formations comprise of Cenomanian age (Bethlehem and Hebron formations) and Turonian age (Jerusalem formation).

3.6.2.1 Cenomanian Aquifer

The formations of this aquifer are Bethlehem and Hebron. They consist mainly of interbedded dolomites and chalky limestone. It is heavily exploited in the areas near Tulkarem and Qalqilya. However, the aquifer is at an intermediate depth in the Bethlehem and Hebron areas. Its water table normally occurs within a depth more than 200m below ground surface.

3.6.2.2 Turonian Aquifer

The formation of this aquifer is Jerusalem, which consists of massive and thick limestone and dolomitic limestone with well developed karst features. The Turonian aquifer is part of the Upper Aquifer but can represent a local aquifer by its own if the formation beneath it acts as an aquitard as it is the case in some areas in the Eastern and Southern parts of the West Bank. The aquifer thickness is approximately 130m thick, and extends in the Tulkarem area.

3.6.3 The Lower Aquifer

Part of the Lower Cenomanian Yatta formation hydraulically separates the Upper and Lower Aquifers across most of the West Bank, although to the North, the presence of the Yatta limestone gives rise to minor springs and seepage. Water levels (heads) in the Upper Aquifer are generally higher than in the Lower Aquifer. The Lower Beit Kahil and Upper Beit Kahil formations and at places also the lower part of Yatta formation form the Lower Aquifer, which across most of the West Bank is a deep seated, strongly confined aquifer. The

aquifer thickness ranges between 300-400m. The high water bearing capacity and productivity is owed to the great thickness of the carbonates, mainly dolomitic limestone and limestone.

3.6.4 The Deep Aquifer

The Neocomian and Lower Aptian formations form the Deep Aquifer. This aquifer is not yet understood and it seems there is a great change in the characteristics of these formations from the middle to the North of the West Bank. In general, the aquifer seems to be of low potential. Of minor significance is Ein Qinya formation that builds a local aquifer at its outcrop area.

3.7 The Aquifers and Aquicludes of Marsaba-Feshcha Study Area

The aquifer potentiality of the geological formations of the Southern part of the Eastern Basin of the Mountain Aquifer part of which is Marsaba-Feshcha drainage basin is represented in table 3.1. The formations thickness and lithology presented in table 3.1 are based on the geological log of the wells of Hebron 1 and 2, Arroub 1B, Herodion 3 and 4, PWA I and II.

Table 3.1: The stratigraphic table of rock units in the study area. Jerusalem formations divides into three formations in the eastern part of the study area (Begin, 1974).

Period	Epoch	Group (Israeli terminology)	Formation (Israeli terminology)		Formation (Palestinian terminology)	Hydrogeological Unit		Thickness [m]		
Quaternary	Holocene	Dead Sea	Alluvium		Q	Lisan		Base unexposed		
	Pleistocene		Lisan		Qli					
			Samra		Qs(a)					
Teritary	Pliocene									
Upper Cretaceous	Campanian	Mt. Scopus	Mishash		Kumi	Abu Dis	Aquiclude	100- 400		
	Santonian-Campanian		Menuha		Kum					
	Turonian	Judea	Bina	Nezer Shivta Derorim	Kub	Jerusalem	Aquifer	Aquifer Aquifer Aquiclude	90-100	
	Upper Cenomanian		Weradim		Kuw	Upper Bethlehem	Aquifer		90-100	
			Kefar Shaul		Kuks	Lower Bethlehem	Aquitard		30-40	
			Aminadav		Kua	Hebron	Aquifer		110-140	
	Lower Cenomanian		Moza	Ein Yorqe'am	Beit Meir	Kuey	Yatta	Aquiclude	Aquitard	10
								Aquitard		120-140
	Lower Cretaceous		Albian	Kesalon		Kuke	Upper Beit Kahil	Aquifer		30
				Soreq		Kus		Aquitard		110-170
Givat Yearim		Kugy		Lower Beit Kahil	Aquifer		20-40			
Kefira		Kk			Aquifer		160-180			

Lower Aquifer
 Upper Aquifer
 Uppermost Aquifer (part of the upper aquifer)

3.7.1 Regional Aquifers in Marsaba-Feshcha Area

There are three main aquifers in the area surrounding the Dead Sea (Naor et al., 1987), the deepest is built of sandstone layers of Kurnub Group of lower cretaceous age, the aquifer above it is built of limestone and dolomite layers of Ajlun Group (Judea Group) of upper cretaceous age, and the third aquifer is alluvial aquifer of Quaternary rocks. The alluvial aquifer is generally separated from the other aquifers by faults of the Western margin of the Dead Sea Rift (figure 3.6).

The whole sub-basin is mainly feed by inflows of excess water from the surface runoff across the wadis and the neighboring aquifers, namely the Lower Cretaceous Kurnub sandstone aquifer and the Albian to Turonian limestone and dolomite aquifer, also known as the lower and upper aquifer.

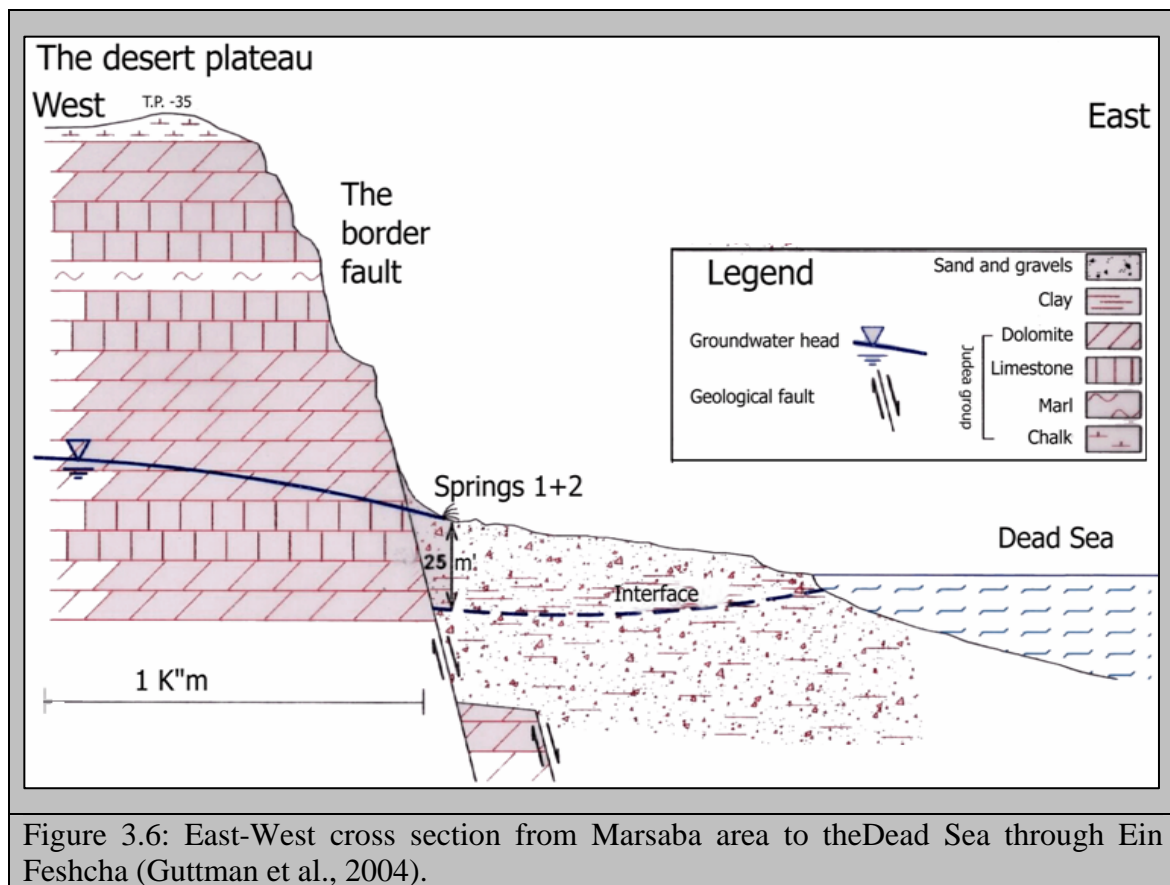


Figure 3.6: East-West cross section from Marsaba area to the Dead Sea through Ein Feshcha (Guttman et al., 2004).

3.7.1.1 The Upper Cretaceous Carbonate Aquifer

The main source of the fresh water into the quaternary aquifer is lateral flow from the Ajlun Group (Judea Group) aquifer, which is replenished in the mountain area (about 25-30km) to the West. The Ajlun Group aquifer is the main aquifer in the study area (Rofe

and Raferty, 1965) with a thickness of 800 to 850m and comprises several sub-aquifers (Guttman & Rosenthal, 1991).

Two sub-aquifers are present in most of the study area, refer to table 3.1:

- a) The Upper aquifer generally includes: Upper Bethlehem (Weradim), Hebron (Aminadav) and Jerusalem (Bina) formations. Its total thickness varies between 350-370m.
- b) The Lower aquifer includes: the Lower Beit Kahil formation (Givat Yearim and Kefira formations) and parts of aquiferous horizons in the Upper Beit Kahil (Soreq) formation. Its total thickness varies between 300-320m.
- c) A third local freshwater sub-aquifer (an uppermost horizon) exists in the Turonian layers in the Jerusalem (Bina) sub-formations (Netzer and Shivta), only in a Northern part of the research area in the wadi Qilt region. It is characterized by fast flowing groundwater within a well developed karstic system and it is discharged at the Jericho and wadi Qilt springs (north of the study area). This aquifer is perched on impermeable layers of the Derorim formation. This aquifer is phreatic in most parts, with the exception of a small part in the synclinal section of Nabi Mousa Syncline (Boqea). This aquifer is separated hydraulically from the upper aquifer and has no influence on the flow regime to Ein Feshcha springs group (Guttman et al., 2000 and Guttman, 2006).

3.7.1.2 Hydraulic Separation between the Two Aquifers

The separation between the upper and lower sub-aquifers (aquitard) occurs within the Yatta formation (Moza and Bet-Me'ir formations), composed of bluish-greenish clay, marl and chalk. The total thickness of this aquitard varies between 150-200m. The separation is manifested in the difference in water levels in the two sub-aquifers. The groundwater levels in the upper aquifer are higher than those in the lower aquifer throughout most of the area (Guttman & Zuckerman, 1995 and Guttman et al., 2000). Figure 3.7 shows a hydrogeological cross section of the regional aquifers and aquicludes, the dip of the strata as well as the elevation of regional water tables in the study area and its surrounding.

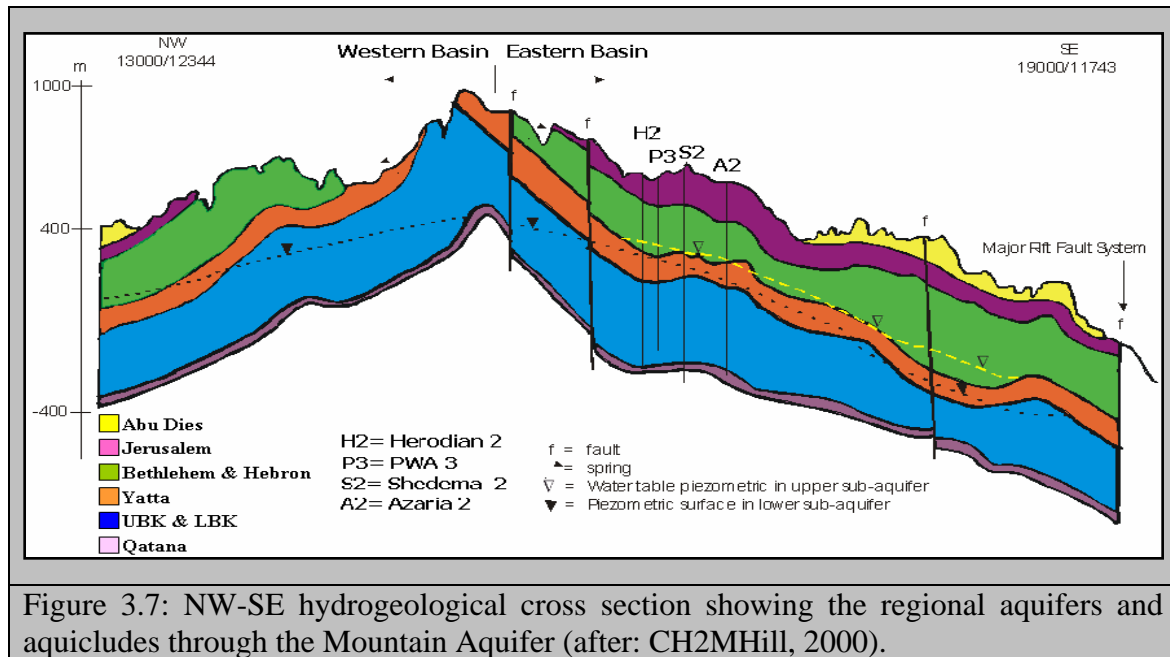


Figure 3.7: NW-SE hydrogeological cross section showing the regional aquifers and aquicludes through the Mountain Aquifer (after: CH2MHill, 2000).

3.7.1.3 The Jordan Valley Deposits [Dead Sea Group]

Two Dead Sea group aquifers are located in the study area and its surrounding, these are:

a) The Holocene or sub-recent alluvial aquifer: distributed mainly in the Jordan Valley and neighboring areas. It is built up of sub-recent terrigenous deposits formed along the outlets of major wadis. These alluvial fans are still under accumulation after large floods and consist of debris from all neighboring lithologies. The alluvial aquifer often directly overlies the Pleistocene gravel aquifer and by that is hydraulically interconnected with this aquifer.

b) Pleistocene Lisan-Samra aquifer: it reflects the Pleistocene depositional conditions of the Lisan Lake. Lisan, marl, gypsum and silt lacustrine unit is generally considered as an aquiclude, void of exploitable water. It is distributed mainly towards the middle of the graben. Samra formation consists of two members: A silt member underlying or interfingering with Lisan and a coarse clastic member that predominantly consists of gravel, interbedded with clay, sand and marl horizons.

The natural recharge by rain is almost negligible. Therefore, the aquifer is mainly feed by inflows of excess water from neighboring aquifers, namely the Lower Cretaceous Kurnub sandstone aquifer and the Albian to Turonian limestone and dolomite aquifer, also known as the lower and upper aquifer and from runoff in the wadis on the Eastern slopes of the West Bank.

3.7.2 Wells Abstraction and Groundwater Levels

Since the 1950's, the sources and the processes of salination of groundwater in the lower Jordan Valley was a major topic of investigation. The Salinity values in the replenishment zones (up hills-Herodion field) ranges from 30 to 50 mg/l and remained constant throughout the years. In wells located along the eastern foothill, a wide range of salinity values are observed ranging from 30-40 mg/l to about 700.

In the wells located along the foothills, two types of salinity behavior were observed. In certain wells such as Fazael 2, the salinity is constant over time. In other wells such as Mtzpe-Jericho and Jericho well field, salinity fluctuates seasonally by tens to hundreds mg/l.

In the Western part the groundwater in both aquifers contain freshwater. The salinity remains low up to Mizpe-Jericho well field. In the Mizpe-Jericho and Jericho well field the lower aquifer contains saline water (up to 13,000 mg/l in Jericho 2). The possible explanation is that the fresh water in the lower aquifer in the West flows vertically into the upper aquifer in the Jericho-Mizpe-Jericho region (Guttman et al., 2000). The upper aquifer in Mizpe-Jericho contains fresh water that has the same chemical and isotopic composition as the fresh water in the lower aquifer in the western part of the aquifer (for example Jerusalem and Azaria wells).

The transition zone in which the freshwater apparently flows from the Lower Aquifer to the Upper Aquifer is somewhere West of the Mizpe-Jericho well field. However, it is difficult to find field evidence for this assumption. The whole region is covered by thick formations of the Mt. Scopus Group. It is difficult to identify the nature of the tectonic element (a fault and/or a flexure) responsible for the hydraulic connection between the lower and upper aquifer in Jericho- Mizpe-Jericho region. The assumption in this case is that the lower aquifer is blocked towards the Dead Sea. Otherwise during a relatively short period of time the salty water of the lower aquifer would have been flushed out and replaced by fresh water. In that case, freshwater should have been found in the lower aquifer, similar to the upper aquifer (Guttman et al. 2004). In our case the lower aquifer contains only salty water. Geochemical and isotope studies support this assumption. Rosenthal (1978) used uranium isotopes and found that the activity ratio ($^{234}\text{U}/^{238}\text{U}$) and ^{238}U concentration in Jericho 4 & 5 that penetrate the lower aquifer are similar to the values in Jericho 1 & 2 that abstract from the Upper Aquifer.

4 METHODOLOGIES

This work attempted to combine different approaches for tracing the sources of salinization in order to explain: the origin, water type and the nature of the flow patterns.

In order to achieve the proposed objectives the following methodologies were implemented:

1. Hydrogeological and hydrochemical mapping of the spring area and adjacent areas through using analytical instruments (IC and ICP) and computer software. The examination of the chemical composition of the saline water in Ein Feshcha may lead to the source and the distribution of the saline water and its mixing points with fresh water. Hence, this may allow use to capture the fresh water before its mixing with the brines.
2. Determine and study the chemical and isotopic compositions of Ein Feshcha spring waters in order to track their origin and composition through using analytical instruments (IRMS, RAD 7 and DCC). Isotopic studies are required in order to confirm the variety of origins of Ein Feshcha discharge leading to an identification of the sources for Ein Feshcha water salinization
3. Identification of flow patterns by geoelectrical surveying, using the Vertical Electric Soundings (VES) method. Determination and studying the fresh-saline water interface in the study area by geoelectrical surveying, since knowledge of its location is important for utilization of ground water. Detection of active structural features (flexures and faults) in the upper earth crust using the Natural Pulsed Electromagnetic Field of the Earth (NPEMFE) and determination of its role in mixing and salinization processes in the study area. Using geophysical methods would give more information about: brines detection, freshwater and saltwater bodies, the estimation of their depth and thickness as well as their interface with the brine-freshwater bodies.

4.1 Sampling Sites and Collection Time

During the course of this study several campaigns have been carried out for sampling and analyzing the waters of the springs and groundwater wells of the catchment Marsaba-Ein Feshcha Dead Sea area.

In many samples the chemical composition has been determined. The abundance of the isotopes of the elements Rn, Ra, H and O has been measured. Vertical Geo-electrical

soundings method has been carried out systematically to map the salinity distribution points. Also, the Natural Pulse Electromagnetic Field of the Earth (NPEMFE) method was used to identify the underground active faults and fractured zone along the borders of the closed reserve in Ein Feshcha study area.

A total of 65 samples were collected and analyzed during the course of this study. Table 4.1 presents the sample name, description and coordination of the samples collected during the courses of this study from the springs and wells of the catchment area.

Several sampling campaigns took place the first was through the hydrological year, 2005/2006, the second was through the hydrological year 2006/2007 and the last one was in the hydrological year 2007/2008 as explained below:

a) the first campaign included the collection of the water samples from the springs and wells of the catchment area. A total of 15 springs and boreholes were sampled for chemical and isotopic analyses. The sampling time started at the end of October 2005 (dry season) up to the end of April 2006 (wet season). Sample name, description and coordination are summarized in appendix table 4.2. For location on map see figure 4.1 and 4.2.

b) the second sampling collection campaign started at the end of October 2006 (dry season) up to the end of April 2007 (wet season) with a total of 32 springs and boreholes were sampled for chemical and isotopic analyses. Sample name, description and coordination are summarized in appendix table 4.3. For location on map see figure 4.1 and 4.2.

c) a total of 18 water samples were collected from the springs and boreholes during the third sampling campaign through the year 2007/2008. These samples were used for the analysis of Cl, Br, Rn and Ra. Sample name, description and coordination are summarized in appendix table 4.4. For location on map see figure 4.1 and 4.2.

All the samples were analyzed in AQU labs for the major cations and anions as well as the trace elements. Among these samples, 37 samples were analyzed for the isotopes (^2H and ^{18}O) in the labs of Umweltforschungszentrum (UFZ) Leipzig-Halle Germany and other 17 samples were analyzed for the isotope (Rn and Ra) at AQU labs. The basic field measurements ($T^{\circ}\text{C}$, pH, TDS and EC) were also carried out during the sampling time.

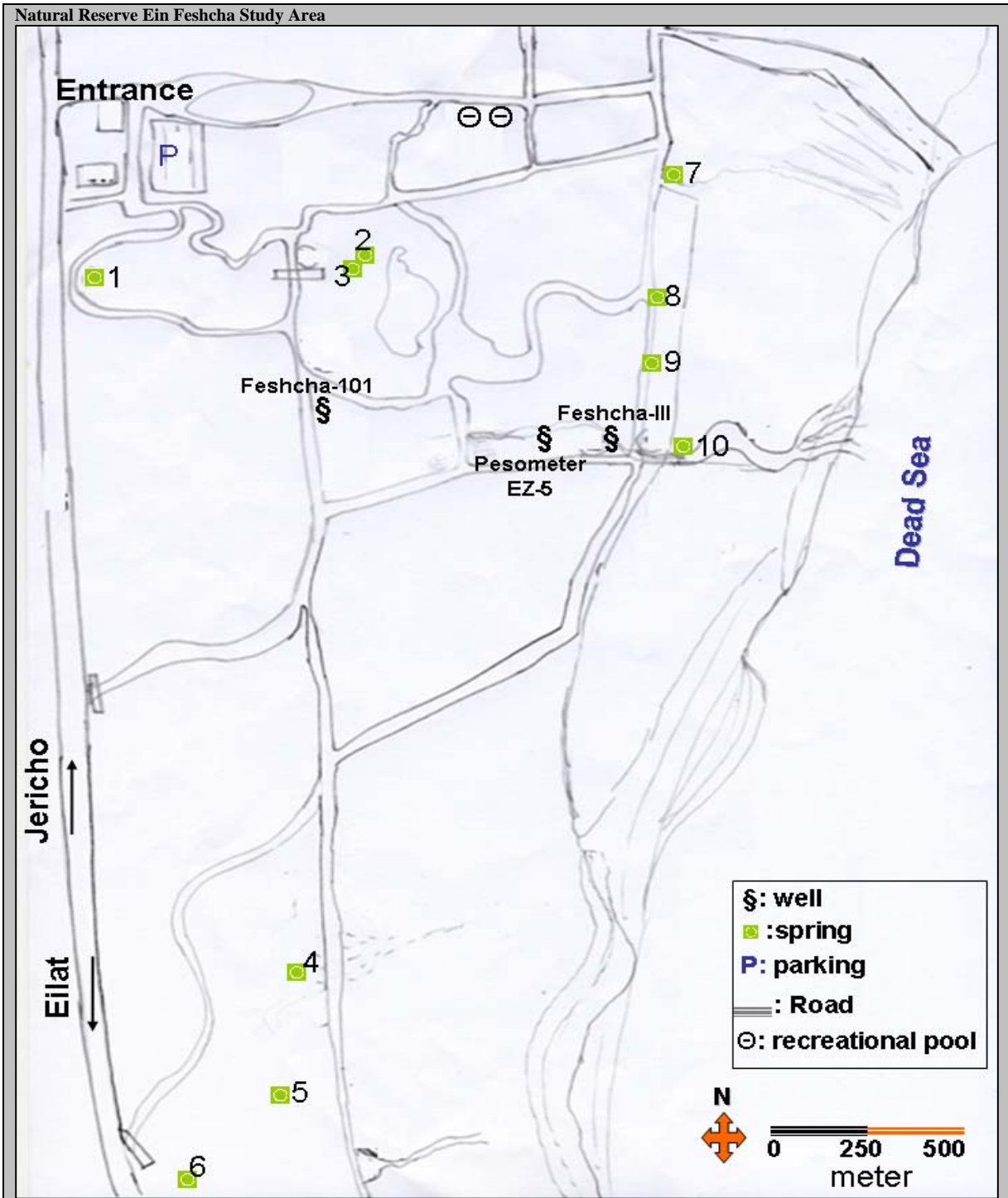


Figure 4.1: Sample location map presenting the locations of the sampled springs and wells at Ein Feshcha study area.

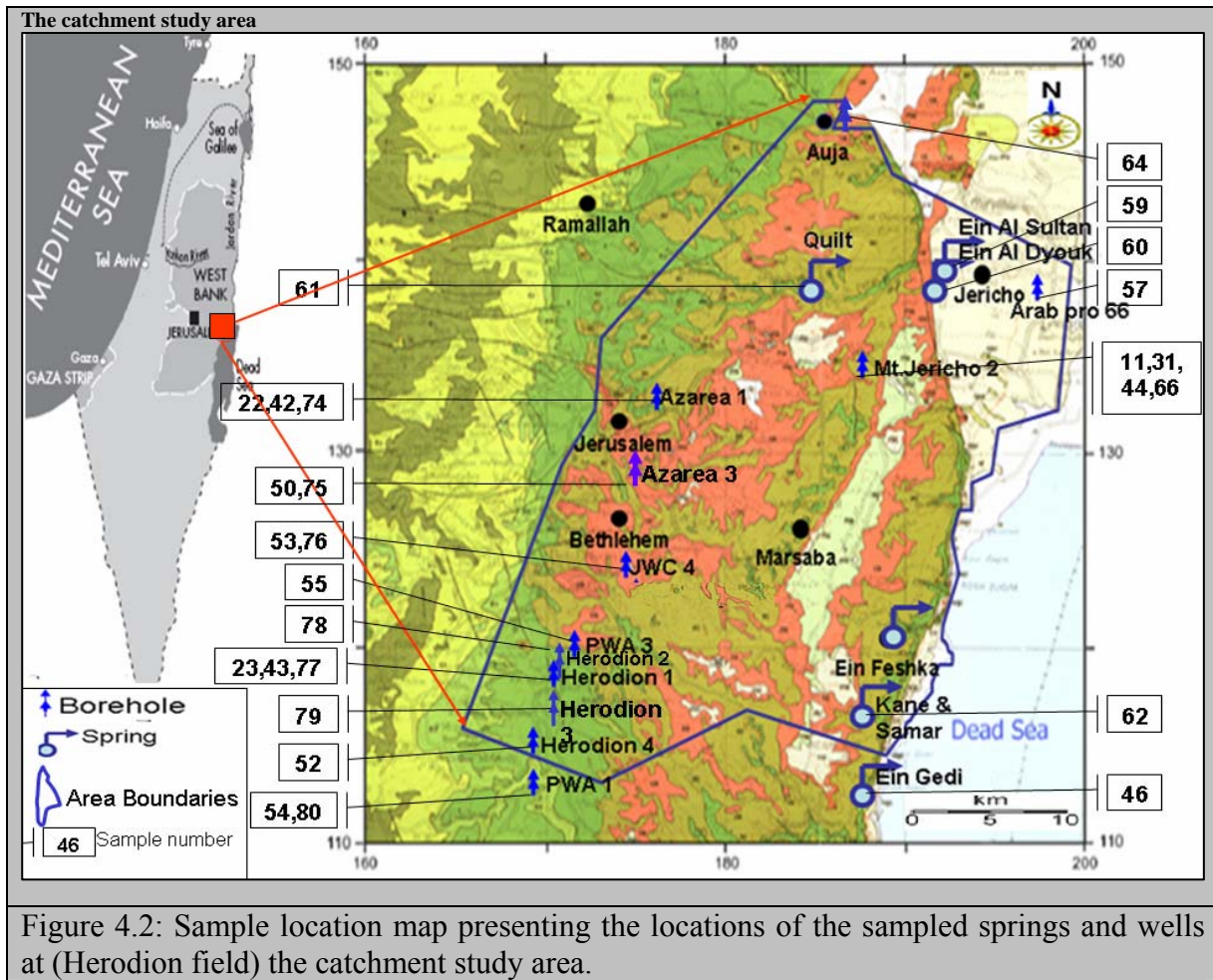


Figure 4.2: Sample location map presenting the locations of the sampled springs and wells at (Herodion field) the catchment study area.

Table 4.1: Sample name, description and coordination of the samples collected during the courses of this study from the springs and wells of the catchment area.

	Sampling #:	Coordination	Description
Spring (1)	10	192805/124691	(Spring 1+2), the main spring at the old entrance of the reserve.
	30		
	65		
Spring (2)	12	192908/124518	North east, spring branching in between a group of trees and boshes. Under small bridge.
	32		
	67		
Spring (3)	39	192911/124520	North east, spring branching in between a group of trees and boshes.
	68		
Spring (4)	19	192764/123395	a pool rich with vegetation at the spring exit. Water passing underneath the street.
	40		
	71		

Spring (5)	20	192725/122848	Water passing underneath the street through a rock canal.
	41		
	72		
Spring (6)	21	192560/122135	At the southern part of the closed reserve, merging beneath the main street.
	82		
Spring (7)	13	193061/124396	Strong stream of water hading to the Dead Sea
	33		
Spring (8)	14	193121/124066	Strong stream of water hading to the Dead Sea, (beneath a bridge 2m).
	34		
Spring (9)	15	193335/123977	A group of variable paths joined together forming stream passing through formations of marlstone.
	35		
Spring (10)	16	193143/124095	A small path getting stronger after joining to it a big canyon.
	36		
Spring Gadi	46	164968/128741	Ein Gadi spring at the natural reserve.
Spring Samia	58	181950/154567	Ein Samia spring
Spring Sultan	59	192155/141952	Ein Al-Sultan spring – Jericho city
Spring Dyuk	60	190110/144645	Ein Al-Dyuk spring – Jericho city
Spring Quilt	61	185622/138165	Ein Al-Quit spring
Spring Knia	62	169799/130011	Ein Kane and Samar group springs
Well Feshcha-III	17	193112/124086	Feshcha-III, 60m in depth with artesian preacher.
	37		
	69		
Well EZ-5	70	193143/124095	Pesometer EZ-5, 6 m in depth.
Well Feshcha-101	73	192900/124327	Feshcha well 101, 11 m in depth.
Well Auja-2	64	186760/151431	Al-Auja-2 to the north
Well Arab-66	57	197030/141050	Arab project well-66 Jericho city
Well Mt.Jericho-2	11	188257/134390	Mt.Jericho Well field.
	31		
	44		
Well Azarea-1	22	176610/132018	
	42		
	74		

Well Azarea-3	50 75	173830/112878	
Well JWC-4	53 76	170871/121879	JWC-4, 788 m in depth.
Well PWA-1	54 80	167367/112394	PWA-1, 601 m in depth.
Well PWA-3	55	171255/120265	
Well PWA-11	81	169161/116310	PWA-11, 851 m in depth.
Well Herodion-1	23 43 77	170930/118325	Herodion-1, 350 m in depth
Well Herodion-2	78	170901/119301	Herodion-2, 770 m in depth.
Well Herodion-3	79	170902/117551	Herodion-3, 743 min depth.
Well Herodion-4	52	169460/114087	
Well Beit Fajar-1a	51	169607/115110	
Well Fasaal-2	63	183059/130210	
Well Abu Dies	56	174313/124109	
D.S lake	25 47	192830/122698	At the southern part of the closed reserve.
Spring al-malh	24 45	195010/192617	Wade ein al-malh spring

4.2 Sample Collection Methodology

The selection of the sampling time and site for the springs and the groundwater wells based on the accessibility to the location sites (well sites in Herodion area and the Ein Feshcha closed reserve).

Three polyethylene bottles for collecting samples for water isotopes, chemical and heavy metal analysis were prepared in the laboratory of the Center for Chemical & Biological Analysis AQU, for each sampling site. The preparation of the bottles included washing with distilled water followed by acid soaking and then final washing with distilled water before left for air drying. The bottles were filled by direct flow of the spring water into the bottle. Before sampling the deep wells the water was allowed to flow for few minutes before the samples were taken.

As a general rule all the bottles were first rinsed with the water intended for sampling and then filled completely. All the collected and filtered samples were placed in a cold box until analysis in the laboratory.

Samples of 50 ml were filtered using 0.2 μm pore-sized filters and acidified by 1 ml concentrated analytical nitric acid to be analyzed for the heavy metals.

The water samples to be analyzed for 18O and 2H were collected in 250 ml dark glass bottles and 500 ml polyethylene bottles for 3H determination. A polyethylene plastic container was used for water sampling for Radium (^{223}Ra , ^{224}Ra and ^{226}Ra) analysis, volume of 50 L of the sampled water was pumped into two acid-washed plastic containers each with volume of 25 L, using a bilge pump as presented in figure 4.3 (Moore and Reid, 1973). Water samples for

Radon (^{222}Rn) analysis were collected in 40 ml and 250 ml evacuated gas bubbler bottles.

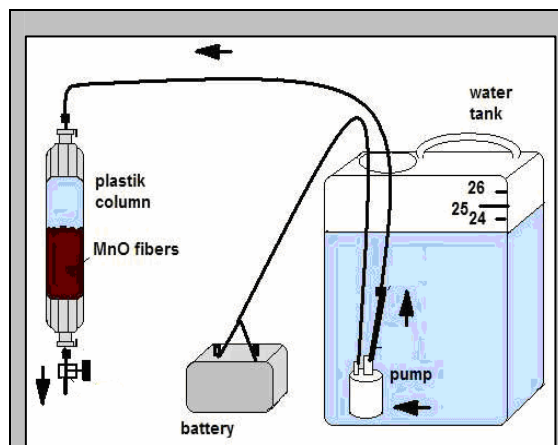


Figure 4.3: Sample filtration methodology used for Radium pre-concentration (^{223}Ra , ^{224}Ra and ^{226}Ra).

4.3 Determination of Chemical Parameters

Parameters that were measured and recorded at the time of sampling were alkalinity, electrical conductivity (EC), pH, temperature, dissolved oxygen (DO) and redox potential (Eh). The EC, pH, temperature and Eh was measured using portable Orion EC and pH meters. The collected samples then were kept and cooled until measurement. The concentration of cations and anions were measured using deferent analytical methods depending on the chemical composition and ion concentration of each sample. A list of the analytical methods used for determining the various parameters is listed in table 4.5.

The saturation indices (SI) of the collected samples were calculated for the major mineral phases using the Geochemical modelling software package (PHREEQC for windows version 4.0.278) (Parkurst and Appelo 2001).

Table 4.5: An illustration for the used analytical methods in the determination of the various chemical parameters.

Parameter	Method of analysis	Detection limit (mg/l)
Temperature, pH-value, DO and EC	Field portable multi-electrode Orion meter.	—
TDS	Gravimetric (evaporation) and total ionic counts	
Na ⁺ and K ⁺	Flame Photometer	0.50
	IC ¹	0.06
Total Hardness (Ca ²⁺ and Mg ²⁺)	Na ₂ -EDTA-Titration using Eriochrome black-T indicator.	0.50
	AAS ²	0.05
(CO ₃ ²⁻ /HCO ₃ ⁻)	Acidimetric neutralization	5.00
Cl ⁻	IC	0.07
	Mohar titrametric: titration with AgNO ₃ using potassium chromate indicator	1.00
SO ₄ ²⁻ , NO ₃ ⁻ and F ⁻	IC	0.05
Havey mettals	ICP-AES ³	0.01

1. IC: Ion chromatography.

2. AAS: Atomic absorption spectrophotometer.

3. ICP-AES: Inductively coupled plasma atomic emission spectroscopy.

4.4 Graphical Classification Methodology

The classification of water chemistry data based on the use of AquaChem 4.0.278 waterloo hydrogeologic software computer program, in which graphical and statistical methodologies were used to classify the water samples into homogeneous groups. These methodologies

include the diagrams of Piper, Durov, Schoeller, Giggenbach Triangular plot. Other classifications based on correlation matrices and SI as well as the total hardness, were performed and compared.

The AquaChem 4.0.278 waterloo hydrogeologic software computer program was used to perform all statistical analysis. The accuracy of the analysis was tested based on the error in the electrical balance, which was calculated as:

$$\text{Error \%} = [(\text{total cations} - \text{total anions}) / (\text{total cations} + \text{total anions})] * 100$$

Applying this equation on the results leads to errors of less than 5 %.

4.5 Isotopic Analysis

4.5.1 Tritium, Deuterium and Oxygen Isotopes

The ^{18}O and ^2H isotope content ratios of collected spring and groundwater samples were determined using Gas Source Isotope Ratio Mass Spectrometry (IRMS) with detection limits of 0.15 ‰ for ^{18}O and 1.5 ‰ for ^2H . Oxygen isotope ratios were measured by the Carbon Dioxide Equilibration Syringe method proposed by Matsui (1980), in which carbon dioxide is equilibrated with CO_2 and then isolated from water vapour and other trace gases prior to injection into the mass spectrometer. Gehre et al. (1996) method was used to prepare samples for deuterium analysis in the mass spectrometer. This method involves reducing sample water into elemental hydrogen through use of a Heated Chromium Furnace packed with oxidizable material at 850°C . The resulted H was measured in Isotope Ratio Mass Spectrometer (IRMS) of delta S type (Fa. Finnigan MAT, USA). Data quality was checked through an internal laboratory calibration of standards (Coplen et al., 1991).

The ^3H was analyzed using the electrolytic enrichment with a detection limit of 0.2 TU. Distillation of samples under N_2 -atmosphere, then NaO_2 in electrolysis cells was added as batch process electrolytically decomposes (Taylor, 1982; Rozanski & Groening, 2004). PbCl_2 was added on the produced NaOH. A distillation process was adopted until drying, water after addition of Ultima gold radiometric detection over 1000 minute in liquid scintillation spectrometer Quantulus 1220 Canberra luggage pool of broadcasting corporations 2770 TR/SL (EG&G Wallac, Finland). By this method, Tritium emits beta decay electrons, which excites the solvent. The solvent transfers its energy to the solute, which emits light photon pulses which are detected and counted.

4.5.2 Radium Isotopes (Rn222, Ra223, Ra224 and 226Ra)

4.5.2.1 DURRIDGE RAD 7 (Rn 222, Ra226)

Radon-222 gas was extracted and counted using RAD 7 device manufactured by (Durrige Co. Inc) (figure 4.4). The sample was purged by air pumped in by the RAD 7 internal pump. The out flowing gas was dried with a drier before entering the RAD 7 device in order to keep the humidity into the device always less than 10 %, which is required to obtain an optimum Rn-222 concentration result, then the radon start for counting.

The starting counting time was written down for each sample. This time was used latter for the decay-corrected back to the time of sampling. Each sample was purging for about 40 minutes to account all the radon gas in the samples.

Then the reading of Rn-222, obtained from the Device and the volume of water in the radon bubbler were written down. The Rn-222 concentration values were decay corrected back to the time of sampling in order to assess the in situ radon concentrations. They were calculated for all the samples by using the following formula:

$$F = 1/\exp(-2.097 \times 10^{-6} \times \Delta t).$$

Where F is the radon decay corrected-back factor, Δt is the difference of time between the analysis time and sampling time (in second).

The factor of volume was calculated for each sample by using the formula:

$$VF = 900/VI.$$

Where VF is the volume correction factor, VI (in ml) is the initial volume of the sample in the gas bubbler (between 30 and 35 ml), and 900 ml is the constant number storage in the RAD7 device.

The actual radon concentration for each sample was calculated by using the following equation:

$$Rn\ 222 = (Rn\ (\mathbf{RAD7}) * F * VF)/1000.$$

Where Rn (**RAD7**) is the radon reading got direct from RAD7 device.

The ²²²Rn concentrations were measured and calculated for each sample taken using the same procedures and equations that mentioned above.

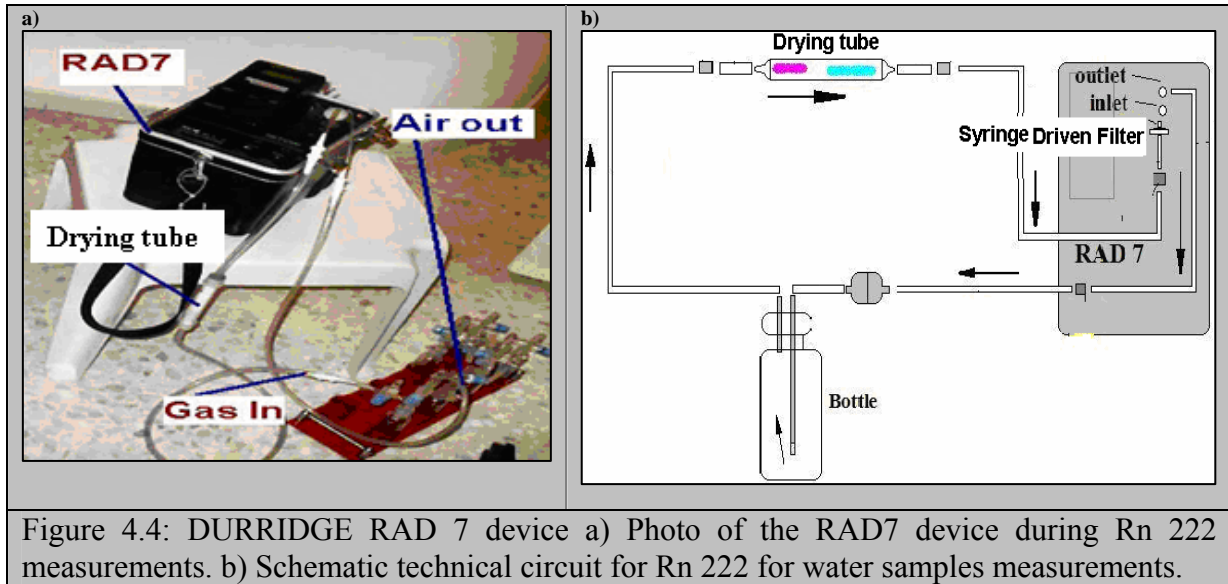


Figure 4.4: DurrIDGE RAD 7 device a) Photo of the RAD7 device during Rn 222 measurements. b) Schematic technical circuit for Rn 222 for water samples measurements.

For Radium (^{226}Ra) sampling and analysis, polyethylene containers of 25 L were used. Radium was extracted by passing the water sample through a 5 cm diameter, 30 cm long exchange column packed with 10 grams of MnO_2 -coated acrylic fiber (Moore and Reid, 1973) at a flow rate of 5-10 ml/minute for radium pre-concentration as described in figure 4.3. The MnO_2 fibers after the radium pre-concentration transferred to glass tube and barged for 2-3 minutes using He gas, then these tubes were incubated for 30 days for the equilibration of radium daughters. The recovery of Radium-226 activity (dpm/L) on the MnO_2 fiber was determined by the radon emanation technique analyzed on a DurrIDGE RAD7 electronic radon monitor (figure 4.5); activities were decay-corrected to the time of collection.

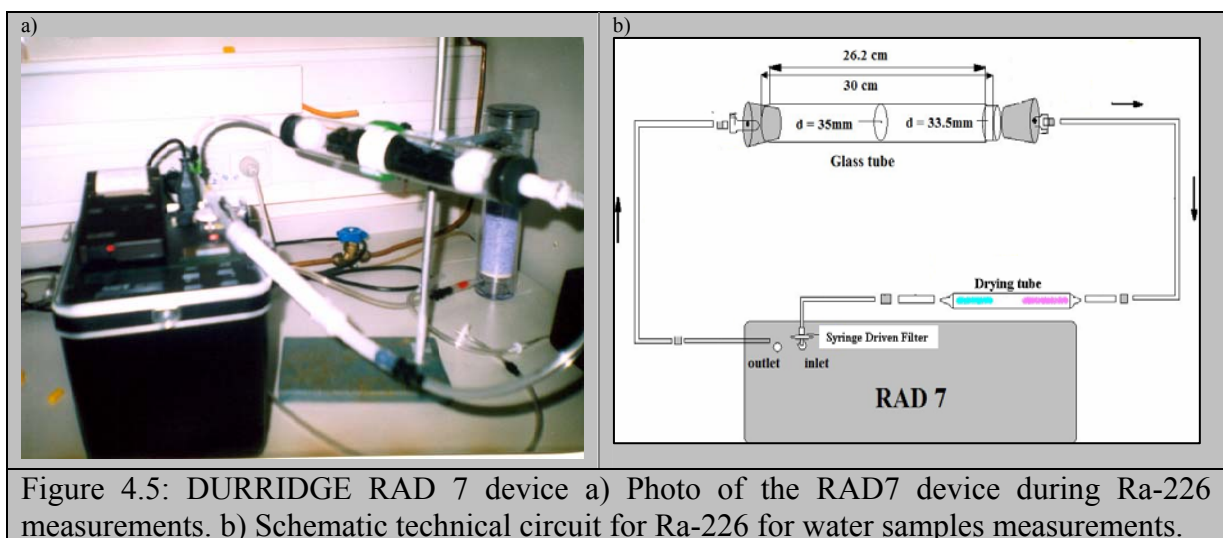


Figure 4.5: DurrIDGE RAD 7 device a) Photo of the RAD7 device during Ra-226 measurements. b) Schematic technical circuit for Ra-226 for water samples measurements.

4.5.2.2 Delayed Coincidence Counter (Ra223, Ra224)

The same sampling and filtration procedures were applied for Ra-223 and Ra-224 collection as described in figure 4.3. The measurement procedure is based on the observation that radon ejected from the MnO₂ fiber (Rama et. al., 1987). The partially dried MnO₂ fibers were analyzed for total dissolved ²²³Ra and ²²⁴Ra activity using a delayed coincidence counter system (Moore and Arnold, 1996) with RaDeCC version 1.15 software (Scientific Computer Instruments). The average detector efficiencies (average of 2 to 4 detectors used for each isotope), for ²²³Ra and ²²⁴Ra were 0.4 and 0.5, respectively, with a typical precision of ±2–5% for each individual detector. Each sample was counted from three to six times with an average statistical counting error of ±16% for ²²³Ra and ±5% for ²²⁴Ra. All the measurement procedures for analyzing ²²³Ra and ²²⁴Ra using the Delayed Coincidence Counter were passed on the methodologies adapted from Moore and Arnold (1996), while the calculations and corrections between the initial and final counts were based on Giffin calculations and studies (Giffin et al., 1963).

4.6 Geophysical Methods

4.6.1 Principle of Vertical Electric Sounding (VES)

By this geoelectric method, the variation of the resistivity with depth is measured, depending on the electric properties of the geologic sequences in the subsurface. This method, known also as Schlumberger sounding, is mainly applied in groundwater exploration, but also for structural geological investigation. Through two electrodes named current electrodes, A and B, a pulse like with high voltage current is injected in the ground (figure 4.6). At two electrodes named receiving electrodes, M and N, placed symmetrically at the center of AB and the origin O, the response of the soil, as current and voltage are measured and transformed in an apparent specific resistivity value. By increasing the length of the AB transmission line and keeping the center and the receiving electrodes MN fixed, the information obtained from the VES will be performing the sounding from greater depths.

For VES, at Ein Fashcha a high performance field instrument was used, a SYSCAL R2 from IRIS-Instruments, France (figure 4.7). SYSCAL R2 is a high power fully automatic resistivity meter designed for DC electrical exploration surveys. A converter, powered by a 12V car battery, transforms the DC current in a pulse-like signal of high voltage (100-800V) and high

intensity (maximum 2A). The receiver part of SYSCAL works fully automatically through the control of a microprocessor. On the display the voltage and the intensity between the receiving electrodes and finally the apparent resistivity value are shown. To get information from 100m depth, at Ein Fashcha the AB-line was extended until 300m from each sides of the center of MN. For each sounding 34 measurements were performed in order to get the complete sounding curve. The results were obtained by using Zhody software; finally resistivity values for different depths were obtained and presented in the form shown in figure 4.8.

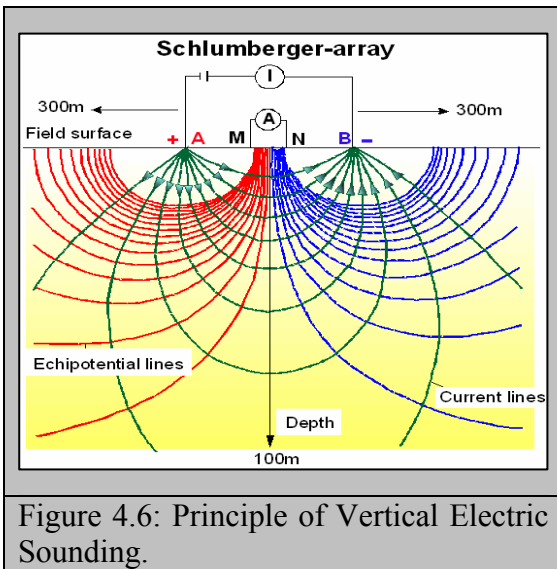


Figure 4.6: Principle of Vertical Electric Sounding.

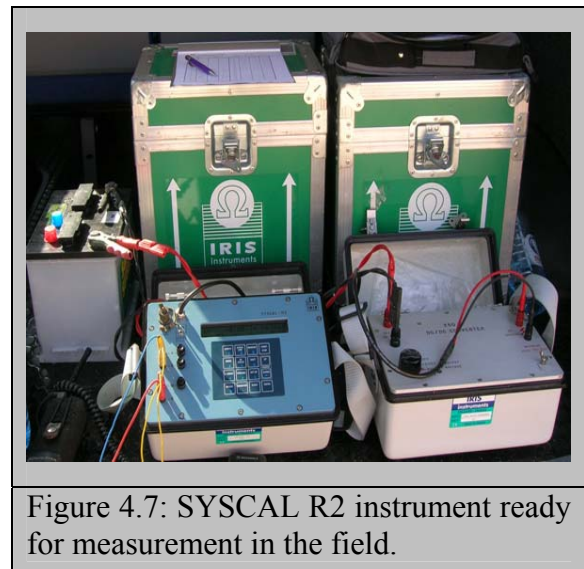


Figure 4.7: SYSCAL R2 instrument ready for measurement in the field.

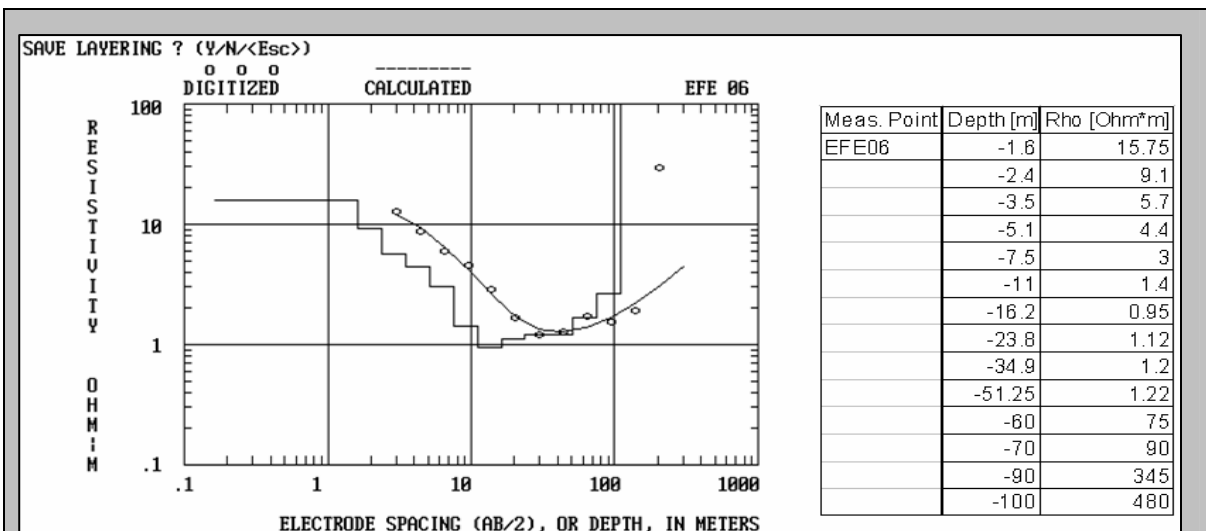


Figure 4.8: An example for data processing of the measured resistivity values and final results from Ein Feshcha study area (sounding point EFE06).

4.6.2 Principle of the Natural Pulse Electromagnetic Field of the Earth (NPEMFE)

The orientations of active crustal stresses in the uppermost lithosphere are reflected by electromagnetic wave directions. Electric and magnetic fields in the earth crust are generated by mechanical disturbances known as seismoelectromagnetic phenomena (Moser and Reuther, 2006). The electromagnetic wave emission from rocks can be related to the formation of microcracks or to piezoelectric, piezomagnetic, or to electrokinetic effects in the earth crust experiencing recent tectonic stresses and / or topographic loading and gravitational stresses. The direction of the emitted waves is directly controlled by the orientation of the affecting stresses (Moser and Reuther, 2006).

The NPEMFE method is depending on the measurement of natural pulsed low frequency electromagnetic radiation (EMR) signals. Generally in geosciences the detection and analysis of these signals can assist to conceive and understand deformation processes. This method (the NPEMFE measurements with the CERESKOP instrument) – detects peak values in the geogenic electromagnetic field clearly exceeding the background noise and registers the orientation of the corresponding electromagnetic waves (Hanns Obermeyer, personal communication). The CERESKOP (figure 4.9) is a scientific instrument for detection and registration of transient pulses of electromagnetic radiation (EMR), which produced by nanofractures, and by piezoelectric, turboelectric or pyroelectric effects (Bahat et al. 2005).

Through the Natural Pulsed Electromagnetic Field of the Earth method (NPEMFE), the emission of electromagnetic waves/pulses from rocks in the earth crust related to recent tectonic stresses, topographic loading and gravitational stresses are measured. Thus, the main application of this method is for the detection of active fractures or faults in the upper earth crust. In the field the measured signal is obtained as a graph with peaks above the fracture or fault. Figure 4.9 shows an example of such a registered signal. This method was used to identify the underground active faults and fractured zone along the Ein Feshcha study area. These faults and joints consider as a zones of weakness for the groundwater discharge along the shoreline.

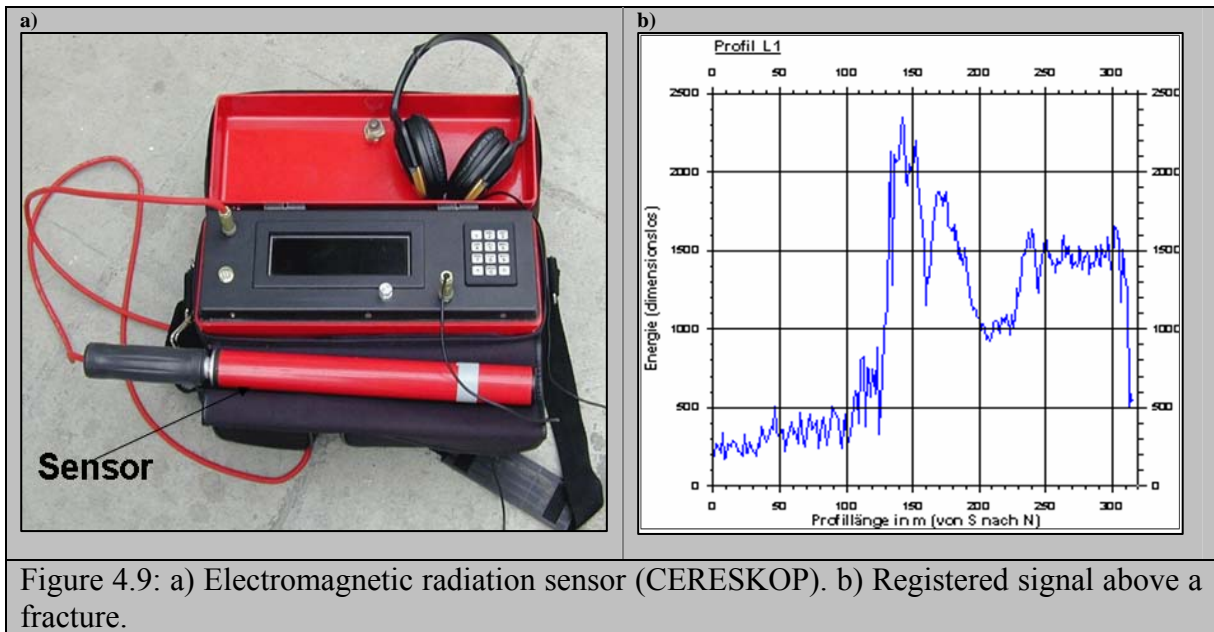


Figure 4.9: a) Electromagnetic radiation sensor (CERESKOP). b) Registered signal above a fracture.

5 HYDROCHEMISTRY

5.1 Hydrochemical Data

A total of 65 samples were collected and analyzed during the course of this study. Sampling coordination and description can be found in chapter four in table 4.1 and in the appendices table 4.2, 4.3 and 4.4. These samples cover the study area from NS and EW. The samples were analyzed in the Center for Chemical and Biological Analysis and in the Water and Environmental Research Lab, AQU. The basic field measurements (Temp., pH, TDS, HCO₃,...) were also carried out and the results are presented in table 5.1

Table 5.1: Basic field measurements, representing the basic field analyzed data carried out during the course of this study.

Sample #	Temp. (°C)	TDS (g/l)	EC (mS/cm)	pH	DO (mg/l)	Cl- (mg/l)	HCO ₃ (mg/l)	Eh (mV)
10	27	2.05	4.39	7.61	1.88	1411	183	-3
11	31.3	0.31	0.647	6.31	5.9	137	100	-19
12	27.3	2.41	5.28	6.73	6.18	1870	170.8	-18
13	28.4	3.05	6.58	6.82	7	2461	207.4	-32
14	28.4	3.11	6.72	6.85	5.9	3280	207.4	-21
15	28.5	2.93	6.29	7.05	7.84	2037	183	-30
16	29	2.82	6.24	7.37	7.71	2063	476	-17
17	26.5	8.1	16.28	8.11	*ND	11048	195.2	-15
18	ND	2.78	5.41	7.61	ND	1947	170.8	-46
19	24.7	7.24	14.48	7.30	12.7	4898	215	-28.5
20	27.4	3.12	6.25	7.10	2.6	1824	246	-43.6
21	27.6	3.61	7.23	7.20	4	2196	276	ND
22	ND	0.29	0.6	7.50	ND	42.6	320	ND
23	ND	0.24	0.51	7.60	ND	22.7	305	ND
24	35.6	3.649	6.01	7.12	ND	1730	265	ND
25	40.9	338.3	183	6.43	ND	219872	180	390
30	26.1	1.75	4.1	7.01	5.03	1469	186.2	-49.6
31	25.4	0.36	0.72	7.41	5.66	320	183.5	-53.5
32	24.5	2.2	4.5	7.40	5.77	1720	198.4	-37.5
33	23	2.8	5.7	6.80	5.5	2024	183.5	-43.9
34	23.7	2.7	5.4	6.60	5.07	2061	195.6	-49.5
35	24.7	2.8	5.5	6.80	4.3	1976	186.2	-47.3
36	23.5	3.5	7	6.90	5	1959	192.3	-44.3
37	25	9.1	18.3	6.60	5.08	6469	238.9	-19.9
39	26	3.1	6.5	6.90	6.03	1588	195.6	ND
40	25	5.8	11.7	6.90	4.65	3823	200.8	-29
41	25.2	2.2	4.5	6.50	5.13	1723	220.4	-43.5
42	ND	0.394	0.55	7.40	ND	23.4	311.2	ND
43	ND	0.303	0.55	7.30	ND	21.7	317	ND
44	24.71	0.591	0.783	7.31	ND	75	253	441
45	34.5	3.533	5.9	7.01	ND	1688	254	ND
46	28	0.496	0.71	7.41	ND	82.3	211	370
47	25.3	321	181.12	6.23	ND	120050	167	295
50	ND	0.291	0.59	7.50	ND	43	190	ND

51	ND	0.49	0.59	7.81	ND	32	318	ND
52	ND	0.295	0.61	7.22	ND	21	300	ND
53	ND	0.328	0.51	7.45	ND	22.6	336	ND
54	ND	0.328	0.56	7.41	ND	23.8	315	ND
55	ND	0.253	0.481	7.71	ND	24.1	267	ND
56	23.4	0.438	0.794	7.01	ND	56	269	ND
57	25.9	2.978	5.36	7.41	ND	1451	411	ND
58	15	0.252	0.457	7.94	ND	23	291	ND
59	24	0.186	0.678	7.39	ND	52.6	266	ND
60	24.7	0.189	0.678	7.35	ND	46	293	ND
61	16	0.273	0.495	6.73	ND	25	261	ND
62	25.6	1.093	1.94	7.58	ND	400	311	ND
63	25.11	0.441	0.613	7.34	ND	49	267	ND
64	20.1	0.263	0.475	7.21	ND	38	315	ND
65	26.4	1.98	4.16	7.10	0.89	1154	188	ND
66	26	0.21	0.46	7.43	5.66	99	184	ND
67	24.8	2.29	4.97	6.70	2.6	1507	176	ND
68	26.8	2.19	4.82	6.93	2.31	1493	179	ND
69	26.1	10.71	21.2	7.72	4.53	7445	210	ND
70	27.7	3.42	6.13	7.33	1.59	1985	196	ND
71	25.5	6.42	13.11	7.56	4.41	4821	221	ND
72	23.3	6.35	13.12	7.46	4.93	4721	214	ND
73	26.3	2.25	4.36	7.73	ND	2659	179	ND
74	25.7	0.29	0.61	7.39	4.01	42.6	327	ND
75	24.09	0.27	0.57	7.54	4.02	43	296	ND
76	24.13	0.33	0.53	7.38	3.93	22.9	332	ND
77	24.1	0.24	0.51	7.60	5.13	32	300	ND
78	22.4	0.20	0.53	7.34	4.04	28.3	154	ND
79	23.7	0.28	0.61	7.27	3.1	36	257	ND
80	25.5	0.327	0.55	7.41	4.09	24.8	314	ND
81	24.3	0.29	0.59	7.36	5.07	27	296	ND
82	24.02	2.4	5.04	7.17	4.71	4821	270	ND

*ND: Not Determined

5.2 General Water Quality Variations

The chemical analysis and the field measurements of the springs and borehole samples comprise a wide range of water qualities. In which there are varies water types Na-Mg-Ca-Cl, Na-Ca-Mg-Cl-HCO₃, Na-Ca-Cl, Na-Mg-Cl and Mg-Ca-HCO₃ with pH ranging between 6.2 and 8.2. The chloride content ranges from 137 up to >11048 mg/l and the sodium content from 60 up to >3541 mg/l. The electrical conductivity ranges from 0.20 up to 18.3mS/cm, increasing from NW towards the SE parts of the study area to a point and again the salinity trend changes either decreasing or increasing, (figure 5.1). This is generally could be attributed to salinisation due to mixing with old seated waters and/or due to dissolution.

Figure 5.1 shows that the sit at Ein Feshcha reserve can be subdivided into three or four salinization zones depending on the Cl distribution along the spring’s line. The first zone with Cl concentrations ranging between 1400 – 1999 mg/l the second zone Cl concentration ranges between 1999 – 2500 and the third one the Cl concentration ranges between 3000 – 5000 mg/l. In some springs the concentration of the Cl doesn’t change much as in spring number 15 in which the Cl concentration remained almost with slight changes. Cl concentration for the spring 15 (resembled on the map figure 5.1 with number 7) was 2200, 2236 and 2037 through the years 1984, 2000 and 2007 respectively, which means a constant and continues flow of water source with out any intrusions from other sources. Other spring shows different trend, spring number 18 (this spring was resembled on the map figure 5.1 with number 12) showed Cl concentrations of 2475, 3042 and 1974 through the years 1984, 2000 and 2007 respectively, this means that different mechanism is tacking place. Therefore these notes will be studded in more details in this chapter and in the following chapters in which more detailed chemical analysis will be taken in consideration for each spring.

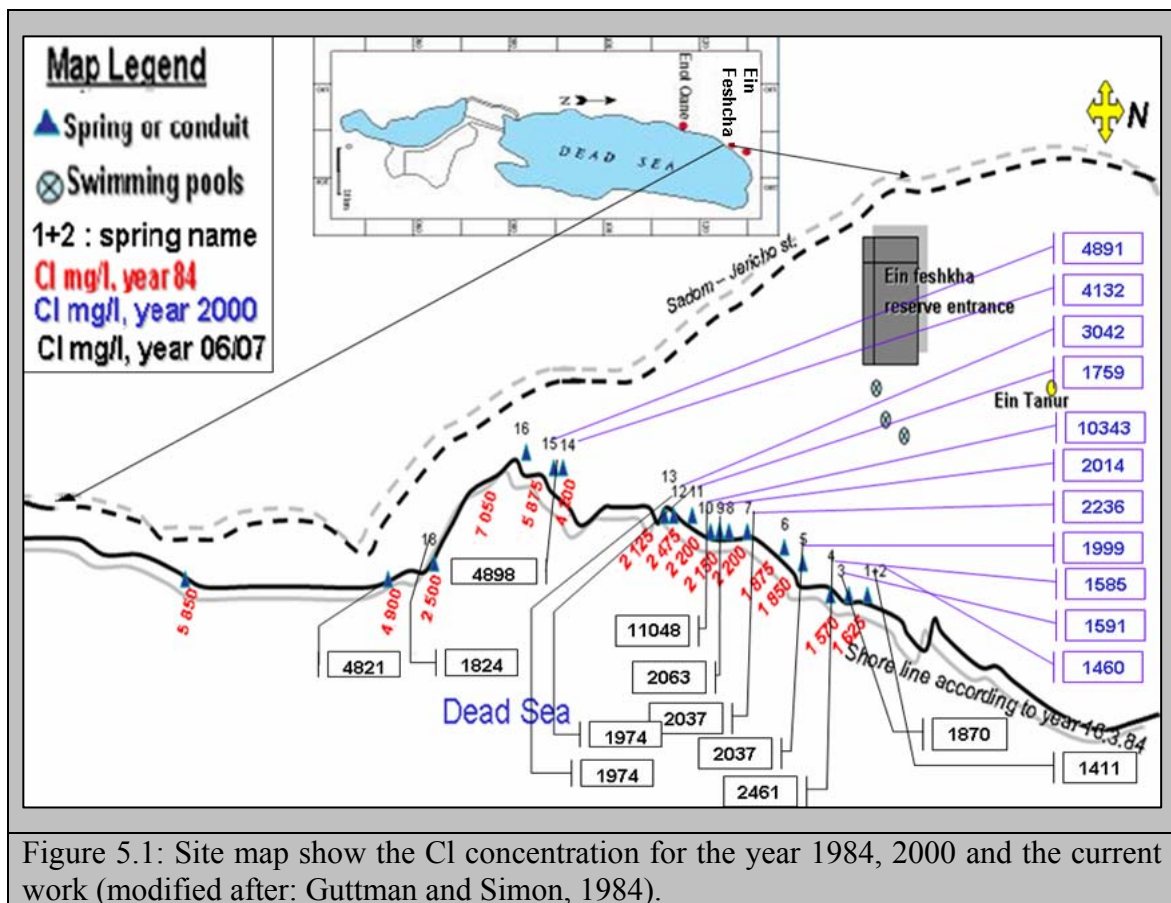


Figure 5.1: Site map show the Cl concentration for the year 1984, 2000 and the current work (modified after: Guttman and Simon, 1984).

5.3 Groundwater Chemistry

For chemical classification the analyzed water samples were divided in groups with similar chemistry. The redox-potential was not used for further interpretation, because a defect in one of the electrodes therefore there was not always time for the stabilization of the Eh value in the field and thus the measured results do not agree with literature values. For detailed data analysis for cations and anions, refer to the appendix table 5.2.

Groundwater from Jerusalem desert (Judea desert) and Jordan Valley has higher Cl contents and a concomitant increase of TDS. Factors other than residence times and evaporation, thus, also affect groundwater salinity and chemical composition. Rapid recharge through preferential pathways where faults and fractures might be exposed to the surface could be a possibility. The Dead Sea transform fault, which is still active today, may be a preferential pathway for groundwater flow. The sediments filling the inner part of the basin consist mainly of low permeability ($3 \cdot 10^{-13}$ to $3 \cdot 10^{-19}$) of evaporate and clay (Guttman et al., 2000). Therefore, most groundwater flow out of the springs and under the Dead Sea is expected to occur via fractures and fault.

The chemical analyses were plotted on different classification diagrams (Giggenbach Triangular, Schoeller Graph, Durov and Piper Diagram...) using AquaChem 4.0.278 waterloo hydrogeologic software.

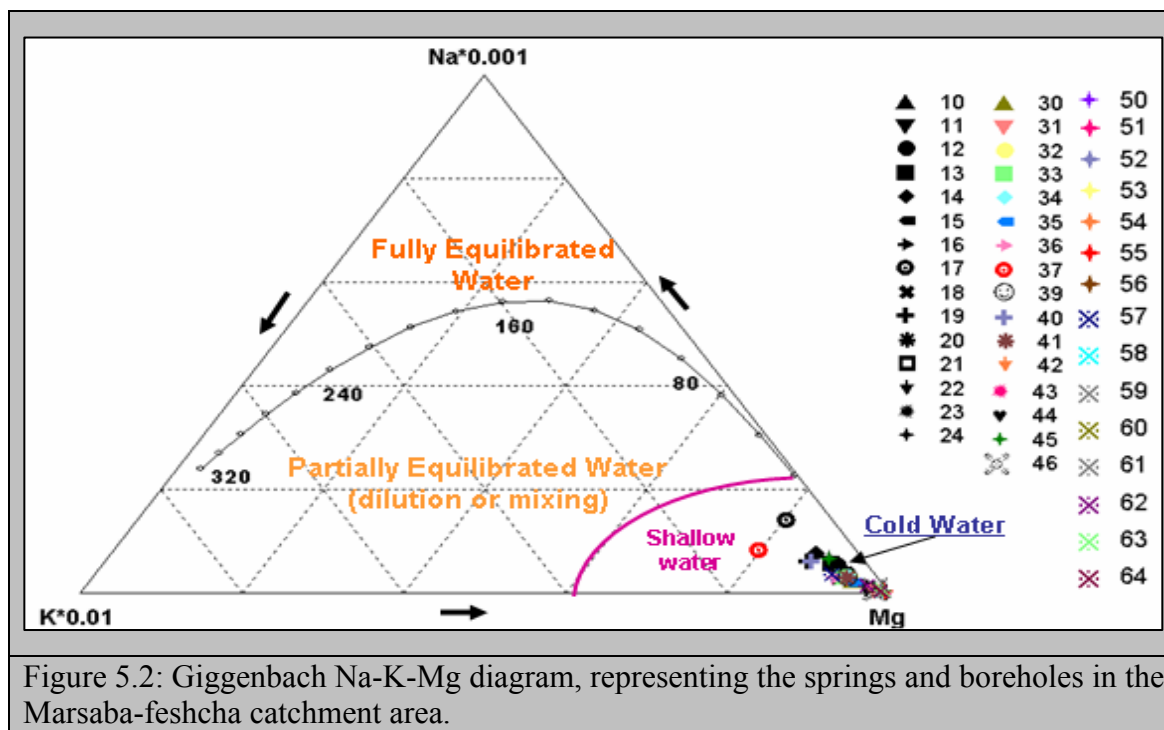
5.3.1 Giggenbach Triangular Plot

The Giggenbach Na-K-Mg Triangular plot was obtained in order to classify the water samples according to the dominant ions and to estimate reservoir temperatures (Segovia et al., 2005). The Giggenbach Triangle provides a visual aid to determine the water rock equilibrium, thermal water classification and may give an initial indication of mixing relationships or geographic grouping and trends. The Giggenbach (Na-K-Mg Triangle) representation allows use to verify the extent to which water rock equilibrium has been attained (Giggenbach, 1988). The triangle is comprised of three zones:

- Immature waters (at the base);
- Partially equilibrated waters (in the middle); and
- Fully equilibrated waters (along the upper curve).

The Na-K-Mg diagram shows the equilibrium state of the water from the springs and boreholes, not only but also it shows the relative Na-K-Mg content for the samples. The diagram constructed using Giggenbach's equation. Figure 5.2 shows that the water samples fall in the area of immature water (shallow water), very close to the Mg corner indicating

that the water is in partial equilibrium with reservoir rock, either as a result of mixing or water rock reaction during up flow, the temperature of 26-30 °C, the water springs are slightly thermal.



5.3.2 Schoeller Graph

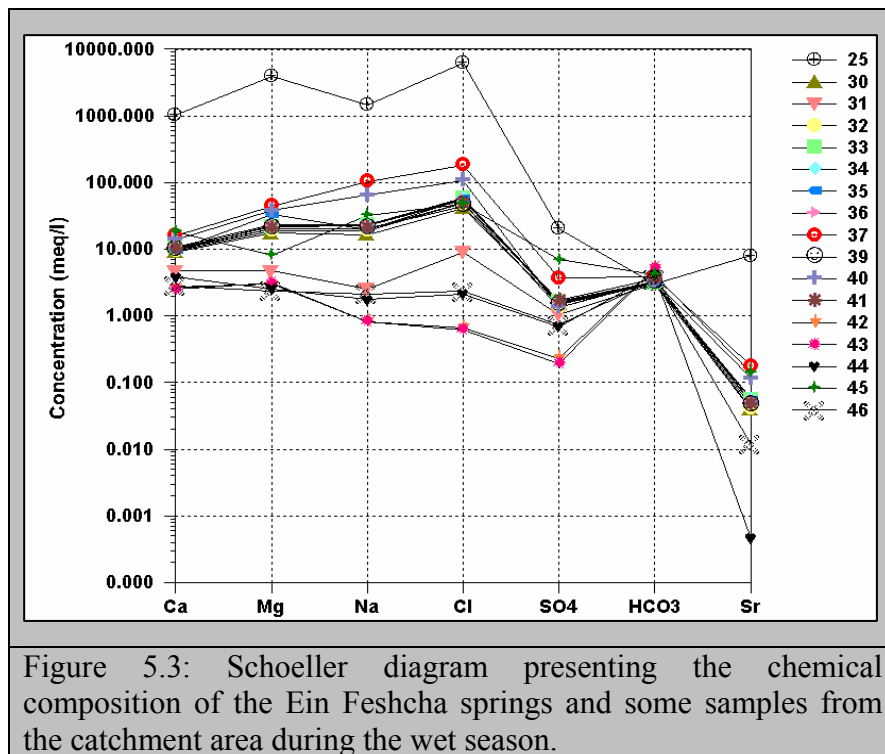
Schoeller (1962) developed semi-logarithmic plots to represent major ion analyses in milliequivalents per liter and to demonstrate different hydrochemical water types on the same plot. Schoeller diagram is used to classify the type of water. It may be also used to show the changes over time of the different water types.

According to Schoeller diagram figure 5.3, indicates that water samples contain the same dissolved salt assemblage but in various concentrations except for HCO_3 content, which is almost the same in all samples indicating that separate mechanisms governs its concentration.

The results show that the water samples of the Azarea-1 (42), Herodion-1 (43), Mt.Jericho-2 (44) wells and Ein Gadi spring (46) in figure 5.3 are similar in origin. Flexer (2001) noted that the upper aquifer in Mt.Jericho well contains fresh water that has the same chemical and isotopic composition as the fresh water in the lower aquifer in the western part of the aquifer (Jerusalem and Azarea wells).

This suggests that the groundwater comes from the same aquifer and has passed through similar rock types. This suggests that the groundwaters are mixed with isolated trapped

water pockets formed in the geologically recent past, but with separate mechanisms and/or possible up flowing water through the fault system. This leads to mixing between these water types, as a result brackish water appear as an end member at the vicinity of the Ein Feshcha springs area, this can be seen in the Sr composition.



5.3.3 Durov and Piper Diagram

Durov diagram is based on the percentage of the major ions in meq/l. The advantage of this diagram is that it displays some possible geochemical processes that could affect the water genesis. This diagram is composed of two triangles and one square. The values of the cations and anions are plotted in the appropriate triangular and projected into the square of the main field (figure 5.4). According to Lloyd and Heathcoat (1985), the square is subdivided into 9 zones; each zone indicates a different water type and conditions. The zones and lines on the diagram show the classifications of Lloyd and Heathcoat (1985) as stated below:

Zone (1): HCO_3 and Ca dominant, frequently indicates recharging waters in limestone, sandstone, and many other aquifers. **Zone (2):** This water type is dominated by Ca and HCO_3 ions. Association with dolomite is presumed if Mg is significant. However, those samples in which Na is significant, an important ion exchange is presumed. **Zone (3):**

HCO_3 and Na are dominant, indicates ion exchanged water, although the generation of CO_2 at depth can produce HCO_3 where Na is dominant under certain circumstances.

Zone (4): SO_4 dominate, or anion discriminate and Ca dominant, Ca and SO_4 dominant, frequently indicates recharge water in lava and gypsiferous deposits, otherwise mixed water or water exhibiting simple dissolution may be indicated. **Zone (5):** No dominant anion or cation, indicates water exhibiting simple dissolution or mixing. **Zone (6):** SO_4 dominant or anion discriminate, and Na dominant; is a water type that is not frequently encountered and indicates probable mixing influences. **Zone (7):** Cl and Na dominant are frequently encountered unless cement pollution is present. Otherwise the water may result from reverse ion exchange of Na-Cl waters. **Zone (8):** Cl dominant anion and Na dominant cation, indicate that the groundwater be related to reverse ion exchange of Na-Cl waters. **Zone (9):** Cl and Na dominant frequently indicate end-point waters.

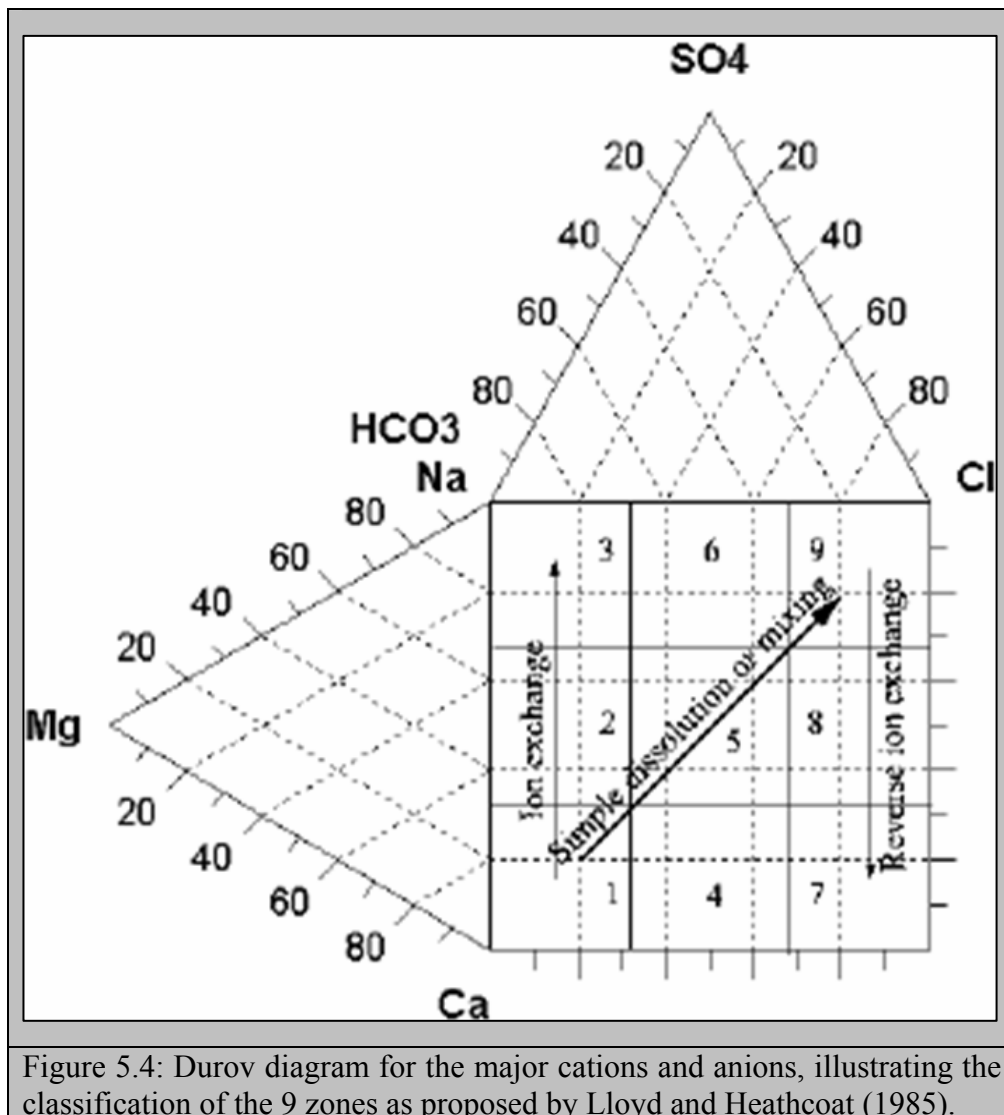


Figure 5.4: Durov diagram for the major cations and anions, illustrating the classification of the 9 zones as proposed by Lloyd and Heathcoat (1985).

The major cation and anion concentrations of the groundwater from springs and wells in the region are plotted on Durov diagram, figure 5.5. The figure shows that sample 23 (Herodion-1) in the dry season and samples from the wet season 53 (JWC-4), 54 (PWA-1), 55 (PWA-3), 59 (Ein Sultan), 60 (Dyook), and 64 (Auja) fall in the recharge water zone with a dominant Ca-HCO₃, indicates recharging waters in limestone formation, while the samples 22 (Azarea-1), 42 (Azarea-1), 43 (Herodion-1), 50 (Azarea-3), 51 (Beit Fajar-1), 52 (Herodion-4), 56 (Abu Dies), 58 (Ein Samia), 61 (Quilt) and 63 (Fasael), this water type is dominated by Ca and HCO₃ with significant Mg ions, indicates recharging waters in limestone and dolomite aquifers (figure 5.5)

The samples 11 (Mt.Jericho-2), 62 (Knia) and 46 (Ein Gadi) show no dominant anion or cation, indicates water exhibiting simple dissolution or mixing. These samples fall in the mixing zone as shown in figure 5.5.

Samples of Ein Feshcha springs of the dry season (14, 16 and 19) and the samples of the wet season (37 and 40) are characterized with Cl and Na dominant ions, frequently indicate end-point waters.

The rest of samples of dry season (10, 13,15,17, 18, 20, 21 and 24) and wet season (30, 31, 32, 33,34, 35, 36,39, 41 and 45) fall in the zone of Cl dominant anion and Na dominant cation, indicating that the groundwater's be related to reverse ion exchange of Na-Cl waters, (figure 5.5).

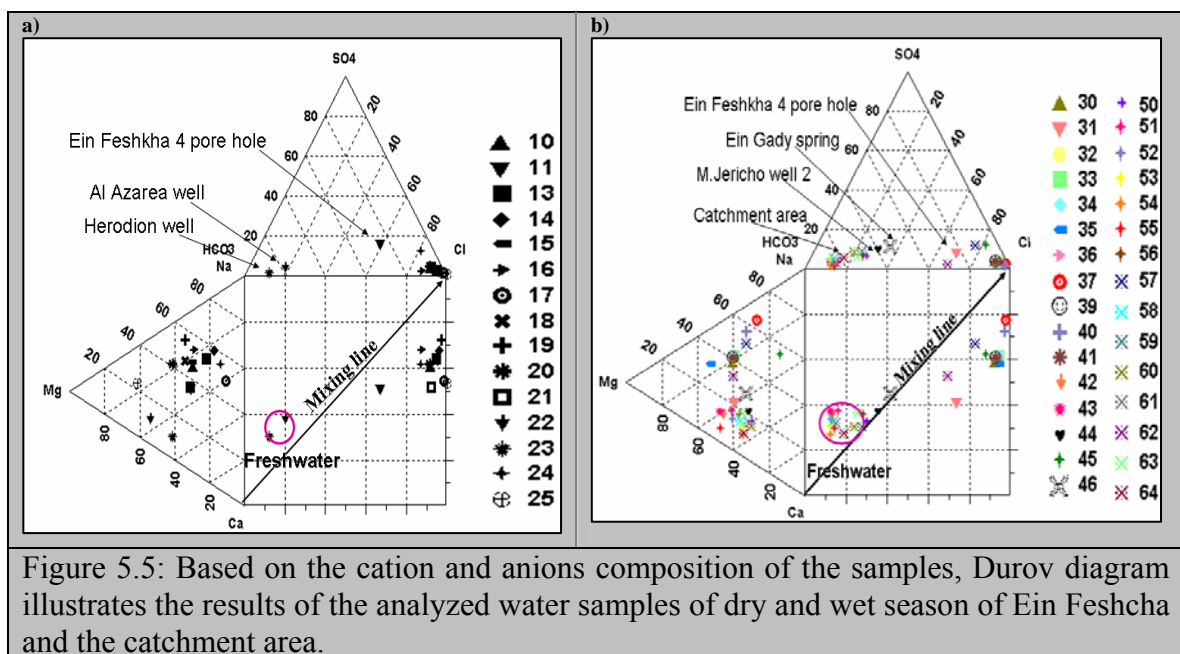


Figure 5.5: Based on the cation and anions composition of the samples, Durov diagram illustrates the results of the analyzed water samples of dry and wet season of Ein Feshcha and the catchment area.

The piper diagram (figure 5.6) plotting the proportions in meq/l of the major cations and anions, it shows the main hydrogeochemical features as well as their temporal evolution.

Based on piper plot the water composition of the samples in the study area can be divided into several groups based on their chemical composition. Samples of the dry season (figure 5.6) divided into three groups:

- a) samples 22 (Azarea-1) and 23 (Herodion-1) represents the normal earth alkaline water with prevailing bicarbonate, Ca-Mg-HCO₃ and Mg-Ca-HCO₃ water type,
- b) the samples 10 (main spring), 11 (Mt.Jericho-2), 13, 15, 17 (Feshcha-III), 20 and 21, represents the earth alkaline water with increased portions of alkalis, Na-Ca-Cl water type.
- c) the samples 14, 16, 18, 19 and 24 (Malh spring) represents the alkaline water with prevailing sulfate-chloride.

While the chemical composition plot of the samples during the wet season (figure 5.6) is divided into:

- a) the samples of the Herodion and Jericho fields, 42 (Azarea-1), 43 (Herodion-1), 50 (Azarea-3), 51 (Beit Fajar-1), 52 (Herodion-4), 53 (JWC-4), 54 (PWA-1), 55 (PWA-3), 56 (Abu Dies), 58 (Ein Samia), 59 (Ein Sultan), 60 (Dyouk), 61 (Quilt), 63 (Fasael) and 64 (Auja) represents the normal earth alkaline water with prevailing bicarbonate, Ca-Mg-HCO₃ and Mg-Ca-HCO₃ water type,
- b) the samples 44 (Mt.Jericho-2) and 46 (Ein Gadi) represents the earth alkaline water with increased portions of alkalis with prevailing bicarbonate, , Ca-Mg-Na-HCO₃-Cl water type
- c) Ein Feshcha springs 30, 32, 33, 34, 35, 36, 39, 41 and 62 (Knia) represents the earth alkaline water with increased portions of alkalis with prevailing sulfate and chloride, Na-Mg-Cl and Mg-Na-Cl water type, and
- d) the samples 37 (Feshcha-III) and Feshcha Spring (4) , represents the alkaline water with prevailing sulfate-chloride, Na-Ca-Cl water type.

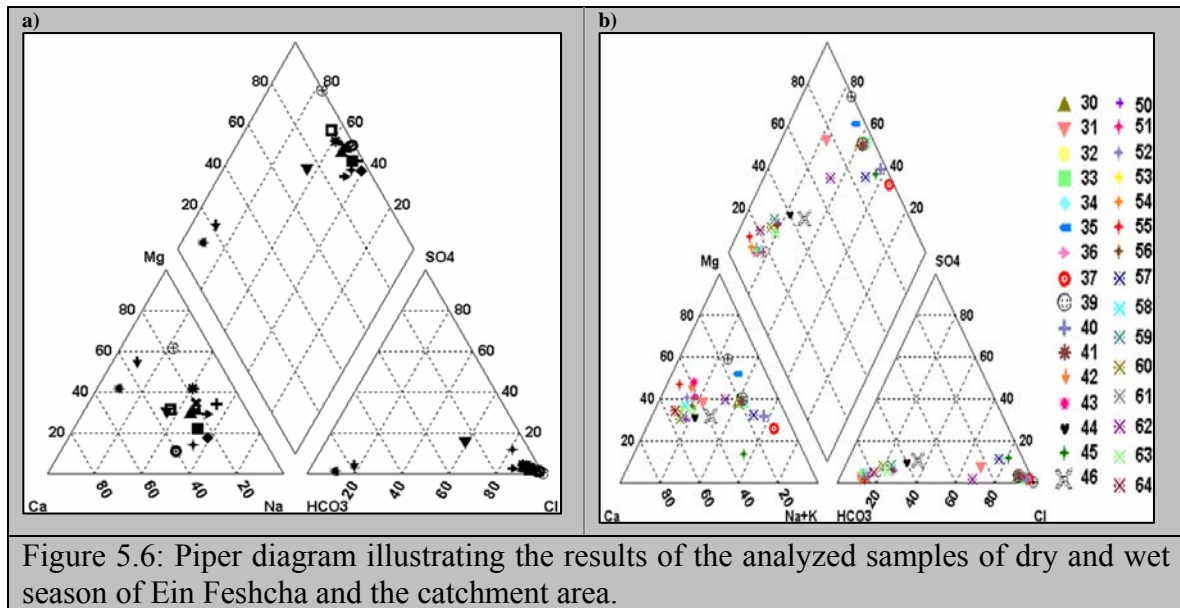


Figure 5.6: Piper diagram illustrating the results of the analyzed samples of dry and wet season of Ein Feshcha and the catchment area.

5.3.4 Geochemical Behavior of Selected Minerals

The distribution trends of trace elements over all the study area were examined in relation to fresh, brackish and saline water zonations. The concentration of the inorganic chemicals in different boreholes and springs of the study area are given in table 5.3. The following trace elements (Cd, Co, Cr, Cu, Ga and Ni) all are below the detection limits of the instrument, these elements didn't show any response during the wet season.

Linearity of ions to chloride reflects mixing of a specific saline brine end member, with meteoric water of low salinity (Moise et al., 2000). Depending on the linear conservative Cl-ion relationship with the major and trace constituents dissolved in the waters, the following selected ions: Na, Ca, Mg and Ba were plotted versus Cl ion in figure 5.7 representing the dry season and figure 5.8 representing the wet season. In figure 5.7 it is clear that the samples representing Na plot are strongly related to Cl-ion indicating mixing of a brine end member, with meteoric water of low salinity. With respect to Ca some samples are strongly related to Cl-ion but other samples (11, 17, 19) are weakly related to Cl-ion, could be due to ion exchange and/or dissolution of phreatic carbonate aquifer most likely since, most outcrops in the study area belong to the late Cretaceous Judea Group comprising predominantly carbonate rocks (Arkin et al., 1965 and Sneh et al., 1998).

Whereas Mg ion is weakly related to Cl-ion, possibly due to saturation condition since all the samples in the dry season are over saturated except samples 11 (Mt.Jarecho-2) and Spring-12 are under saturation. The geochemical behavior of Ba in the saline brines is

sharply deviates. This element varies little with chloride concentration (figure 5.7 and 5.8) and remains rather constant within each group.

Table 5.3: Trace element composition of the analyzed water samples from Marsaba-Feshcha study area.

Sample #	Al (ppb)	B (ppb)	Ba (ppb)	Fe (ppb)	Mn (ppb)	Pb (ppb)	Sr (ppb)	Zn (ppb)	Li (ppb)
10	1622	521	173	886	28	<25	1475	211	96.1
11	208	212	101	102	<3	<25	460	42	57.7
12	121	642	152	23	<3	<25	1739	18.5	123
13	172	791	173	64	<3	<25	2154	57.2	169
14	143	796	176	44	5.1	<25	2249	45	167
15	165	752	165	63	<3	<25	2070	44	154
16	189	710	165	46	<3	<25	1977	57	147
17	54	4268	206	<15	61	<25	7847	822	890
18	58	820	108	<15	<3	<25	1970	49	155
19	79.5	1177	106	<15	<3	570	4700	<9	296
20	73	499	98	<15	<3	312	2000	15	83
21	76	570	113	<15	<3	351	2400	<9	108
24	*ND	727	62	<15	<3	<25	6210	<9	<10
25	*<30	28371	2254	ND	2600	ND	350000	ND	12355
30	75.3	431	185	<15	<3	183	1700	16	70
31	83	62	36	<15	<3	129	<10	57	19
32	77	464	106	<15	<3	249	1800	<9	90
33	73	657	121	<15	<3	358	2400	<9	130
34	80.6	659	128	<15	<3	235	2500	57	123
35	77	613	113	<15	<3	252	2300	16	116
36	74	630	111	<15	<3	336	2300	17	117
37	72	2569	162	<15	40	655	7670	58	799
39	73	570	106	<15	<3	196	2000	<9	97
40	75	1159	141	<15	<3	604	5020	11	476
41	76	534	109	<15	<3	140	2100	9	99
44	<30	39	97	<15	<3	<25	17	11	<10
45	ND	723	56	<15	<3	<25	6100	<9	<10
46	<30	87	81	<15	<3	<25	524	<9	<10
47	<30	24360	510	ND	ND	ND	185000	ND	4821

*ND: Not Determined

*<30: below the detection limits of the instrument.

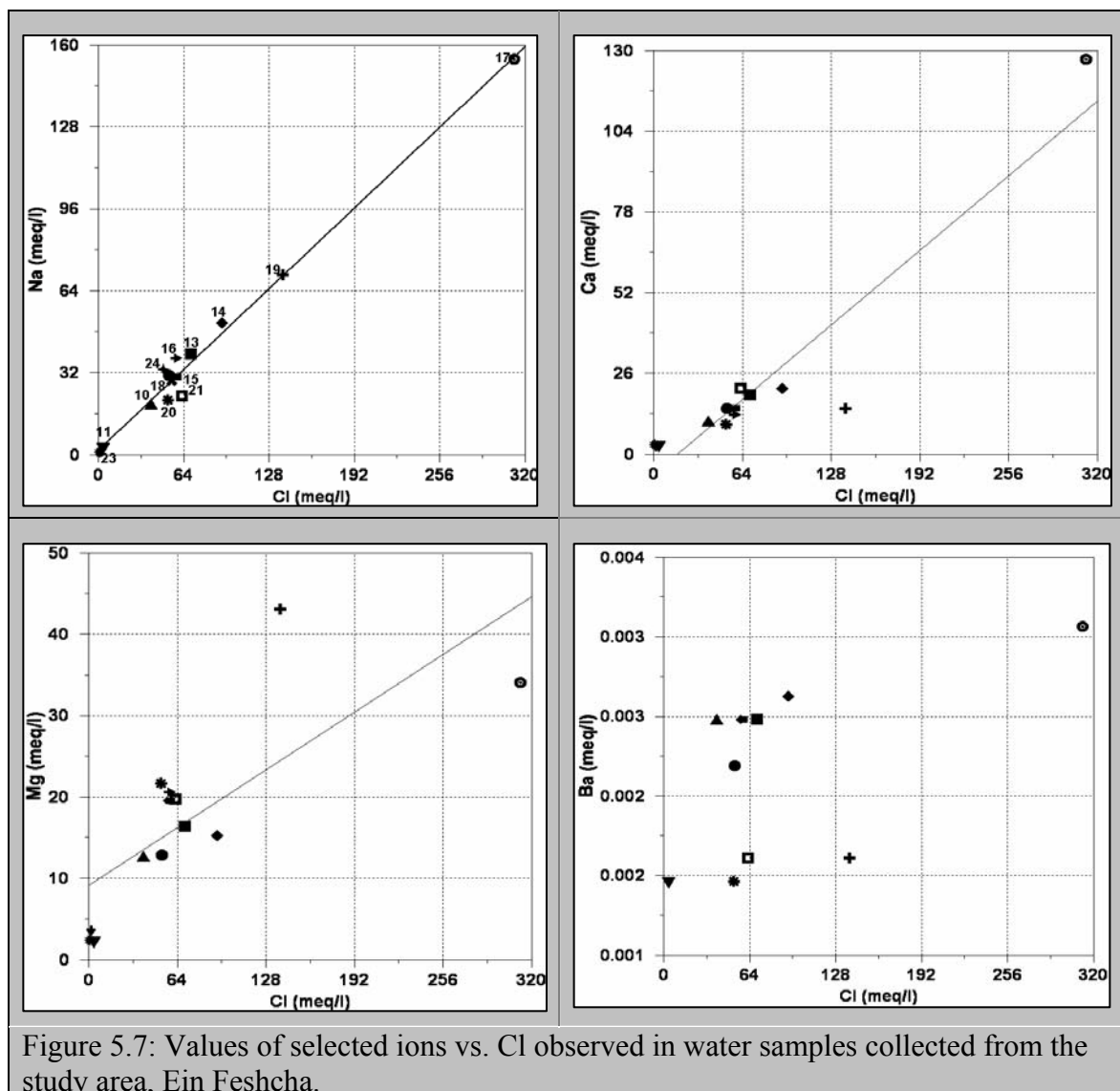
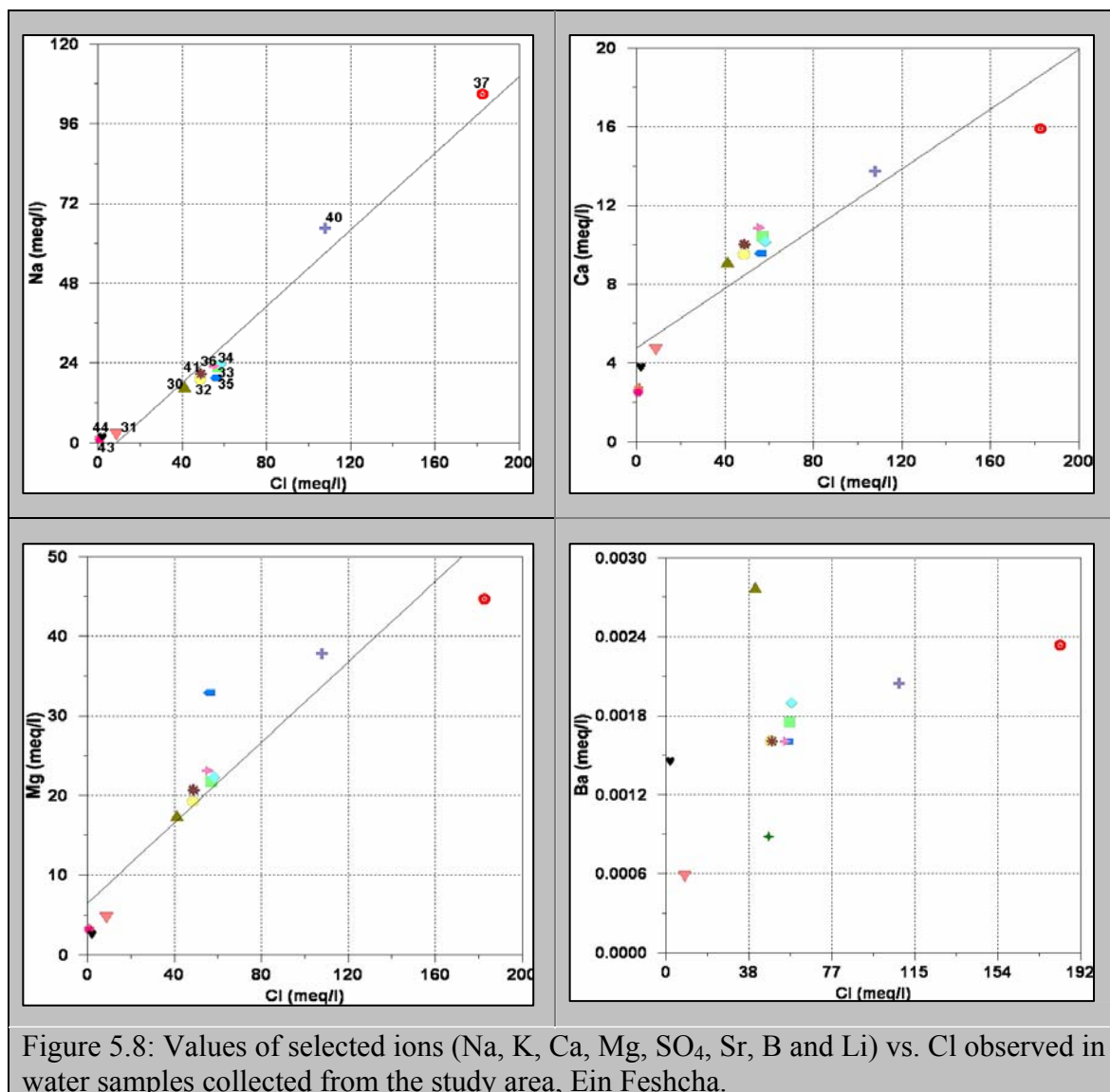


Figure 5.8 presents the linear conservative Cl-ion relationship with Na, Ca, Mg and Ba in the wet season. The Feshcha springs during wet season shows different trend than that during the dry season in which Na is strongly related to Cl. During the wet season Mg ion in most springs shows linearity to Cl-ion, while samples show deviation with respect to Ca, this is could be related to ion exchange as indicated in Durov diagram.

With respect to Ba samples are weakly related to Cl, could be due to precipitation (sample 30) or dissolution (37) of Barite. Saturation of the brines with respect to BaSO₄ controls the behavior of Ba.



Hydrothermal barite-calcite veins have been noted in the Senonian strata of the Southern Judean Desert (Gilat et al., 1978). In the Dead Sea area secondary barite in veins and joint fillings is common (Gilat, 1986). The geological section in the vicinity of the barite mineralization consists of bedded chert and chalk of the Senonian Mishash Fm, Sr is strongly enriched in barite relative to calcite, the barite and iron oxide may have formed later than the particular generation of calcite in which they occur. (Bogoch and Schwartz, 1978). Barite commonly occurs in lead-zinc veins in limestones, in hot spring deposits, and with hematite ore (Fe₂O₃). It is often associated with the minerals anglesite (PbSO₄) and celestine (SrSO₄).

The analyzed trace elements (B, Ba, Pb, Sr, Zn and Li), show that these elements are enriched in different rock units of the study area and support the suggestion that these elements originated from different sources. The occurrence of waters saturated with respect

to BaSO_4 in the Dead Sea Rift Valley suggests the presence of barite at depth. Lead (Pb) is expected to be leached from rock-forming minerals containing high amounts of Pb (Cerussite- PbCO_3 or Galena- PbS), or from earlier formed ore deposits. It is clear that the composition of the trace elements is altered during the wet season indicating mixing of different water types.

The Pb content in the dry season samples is below the detection limit of the instrument (< 25 ppb) except for the samples 19, 20 and 21 which shows high Pb content (table 5.3). It was observed that the concentration of Pb during the wet season increased remarkably except for the sample 19, Pb content did not change during the wet season but accompanied with increase in Ba content, while the Pb concentration in sample 20 depleted from $312\mu\text{g/l}$ to $140\mu\text{g/l}$ (sample 41) during the wet season, this decrease accompanied with decrease in EC from 6.25 mS/cm to 4.5 mS/cm .

The salt composition and temperature of the hydrothermal fluids responsible for Barite and Galena precipitation also show different characteristics in which the behavior of Ba with respect to temperature showed a trend that the concentration of Ba decreases with decreasing solution temperatures in some samples due to mixing with cold waters (figure 5.9a). Sample 19-40 of dry-wet season show no change in spring temperature and in Pb content accompanied with increase in Ba content from 106 ppb to 141 ppb indicating separate mechanism water flow from the depth (no mixing) regarding this spring.

Figure 5.9b presents the relation between Ba and pH. Ba content decrease with decrease in pH in most samples, leading to precipitation of Ba as BaSO_4 and dissolution of Galena which explains the high content of Pb in Ein Feshcha springs (figure 5.9b). Salinity, salt composition, and temperature of the hydrothermal fluids is responsible for barite and galena precipitation

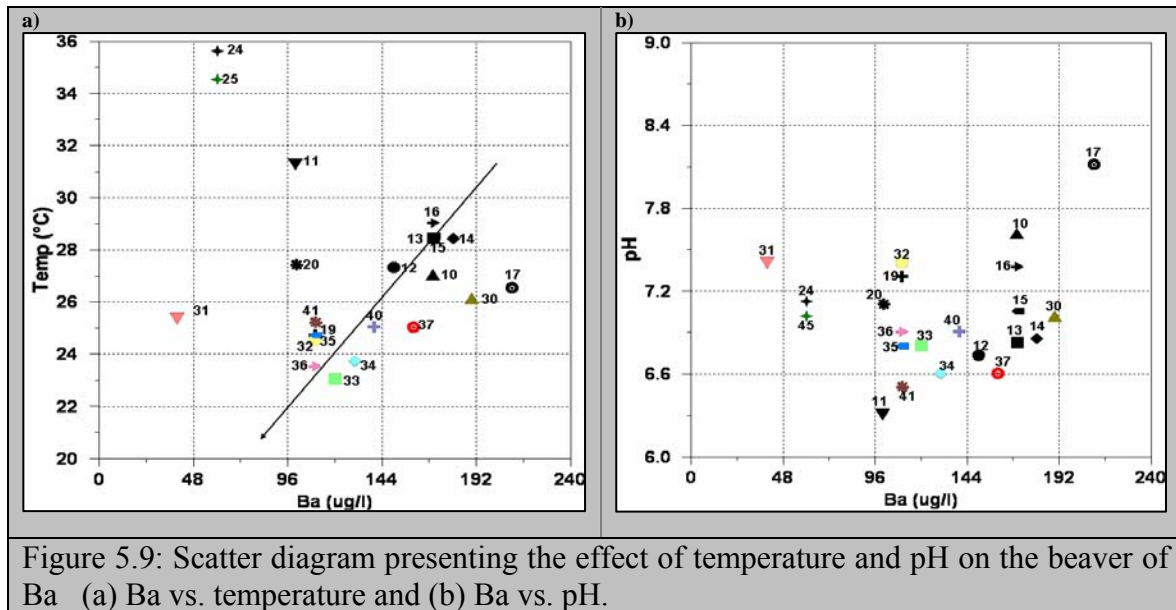


Figure 5.9: Scatter diagram presenting the effect of temperature and pH on the beaver of Ba (a) Ba vs. temperature and (b) Ba vs. pH.

The cation exchange pool at any location along a flow path reflects contributions from both mineral weathering reactions and atmospheric inputs to the watershed. Presumably, mobile elements such as Sr are efficiently exchanged at mineral surfaces, and the ratio of a cation such as Sr to other exchangeable cations (Sr/Ca, Sr/Mg, Sr/Na) in the exchange pool remains relatively constant for given clay mineralogy, water pH and water chemistry (Davis, J. and Kent, B., 1990).

Strontium and boron have shown significant variations in fresh-, brackish- and saline-water environment. Barium, Boron, Strontium and Lithium are the most dominating metallic trace elements in these groundwater samples (table 5.3). On synthesizing the chemical data as reported in figure 5.10, good correlations have been found between TDS versus strontium and between TDS versus Boron. Only one spring 17-37 (fishcha-III) deviates with respect to B concentration in which B decrease with increasing TDS. Sr and B concentration remains relatively constant despite the change in TDS concentration during the dry-wet season indicating linear conservative Sr ionic relationship to the major exchangeable ions Sr–Ca, Sr–Mg, Sr–Na, Sr–K, Sr–Cl and Sr–B all correlate positively, whereas B show a positive correlation to B–Na, B–Ca and B–Cl.

In general, Strontium and Boron were found to be less in fresh groundwater, but more in brackish and saline waters (table 5.3). Freshwater zones identified by strontium and boron were compared with TDS (table 5.4). This indicated the applicability of strontium and boron as useful parameters for the delineation/identification of fresh groundwater resources (Saxena et al., 2004).

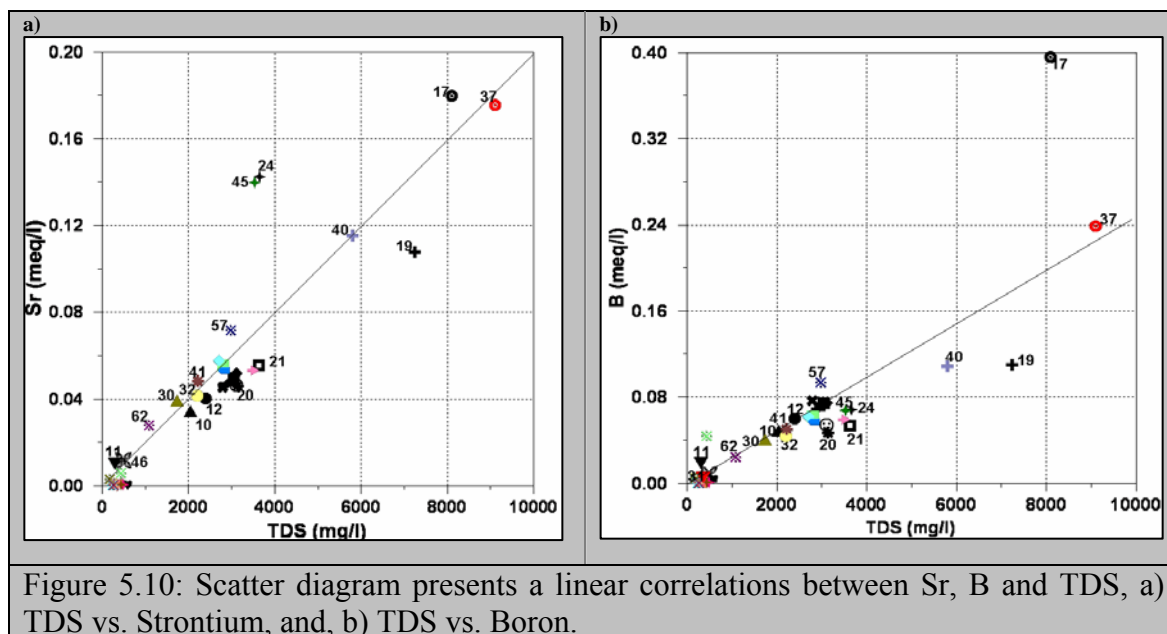


Table 5.4: Water salinity classification based on TDS, Strontium and Boron (Saxena et al., 2004).

Parameter	Fresh water			Brackish water			Saline water		
TDS (mg/l)	<1500			1500 – 3000			>3000		
Sr (µg/l)	<1600			1600 – 5000			>5000		
B (µg/l)	<200			200 – 500			>500		
Sample #	TDS	Sr	B	Sample #	TDS	Sr	B		
10	*B	*F	*S	11	F	B	B		
12	B	B	S	13	S	B	S		
14	S	B	S	15	B	B	S		
16	B	B	S	17	S	S	S		
18	B	B	S	19	S	B	S		
20	S	B	B	21	S	B	S		
22	F	*n.a	n.a	23	F	n.a	n.a		
24	S	S	S	25	S	S	S		
30	B	B	B	31	F	F	F		
32	B	B	B	33	B	B	S		
34	B	B	S	35	B	B	S		
36	S	B	S	37	S	S	S		
40	S	S	S	39	S	B	S		
42	F	n.a	n.a	41	B	B	S		
44	F	F	F	43	F	n.a	n.a		
46	F	F	F	45	S	S	S		
50	F	n.a	n.a	47	S	S	S		
52	F	n.a	n.a	51	F	n.a	n.a		
54	F	n.a	n.a	53	F	n.a	n.a		
56	F	n.a	n.a	55	F	n.a	n.a		
58	F	n.a	n.a	57	B	B	S		
60	F	F	F	59	F	F	F		
62	F	B	F	61	F	n.a	n.a		
64	F	n.a	n.a	63	F	F	B		
* F: Fresh water		*S: Saline water		* B: Brackish water		* n.a: not analyzed			

5.3.5 Chemical Composition Ratios

The hydrogeochemical parameters are useful for comparing different water bodies and for tracing the geochemical evolution of groundwater. The evolution of chemical composition of waters may be observed by following changes in ionic ratios. Rosenthal (1987) noted, in general no rule of thumb regarding ionic ratios can be specified. For each particular situation, the selection of the more significant ratios to be studied should be made according to the possible sources of ions and the expected chemical processes along groundwater flow paths.

Sulin (1946) assumed that the Mg-rich waters were of marine origin therefore classified saline groundwaters into two main groups: (1) Groundwater with ionic ratio of $\text{Na/Cl} > 1$ and (2) Groundwater with ionic ratio of $\text{Na/Cl} < 1$. The latter group was further subdivided into the following equations: (1) $(\text{Cl-Na})/\text{Mg} < 1$, representing Mg-chloride waters and (2) $(\text{Cl-Na})/\text{Mg} > 1$, representing Ca-chloride waters.

According to Lerman (1970) and Levy (1972), Ca-chloride waters are defined by $\text{Na/Cl} < 1$ and by $\text{Ca}/(\text{HCO}_3 + \text{SO}_4) > 1$. Starinsky (1974) demonstrated that in brines in which $\text{Na/Cl} < 1$ (with low concentrations of K and Br), the relationship of $(\text{Cl-Na})/\text{Mg} > 1$ leads necessarily to $\text{Ca}/(\text{HCO}_3 + \text{SO}_4) > 1$.

Alekin (1970) and Starinsky (1974), Ca-chloride brines are always characterized by the decrease of Na/Cl and Cl/Br ratios to values below those characterizing sea water ($\text{Na/Cl} = 0.86 \text{ meq/l}$ and $\text{Cl/Br} = 286 \text{ mg/l}$).

Rosenthal (1997), Ca-chloride waters are defined as those in which:

- (1) $Q = \text{Ca}/(\text{HCO}_3 + \text{SO}_4) > 1 \text{ meq/l}$;
- (2) $\text{Na/Cl} < 0.80 \text{ meq/l}$;
- (3) $\text{Mg/Ca} < 0.5 \text{ meq/l}$; and
- (4) $\text{Cl/Br} \leq 286 \text{ mg/l}$.

Möller (2007), the brines are characterized by their chemical composition and by their Cl-excess ($\text{Cl excess} = \text{Cl} - \text{Na} - \text{K}$, meq/l) and Q value ($Q = \text{Ca}/(\text{HCO}_3 + \text{SO}_4)$, meq/l) which yield a qualitative information about the presence of Ca–Mg–Cl brines when exceeding 1.

Meybeck (1984) and Abdesselam (2000) stated, the use of the Sr/Ca ratio (‰) enables us to distinguish among aquifers completely developed in limestones, others related to Triassic sandstones and/or if it is related to salty layers. Abdesselam (2000) demonstrated that:

- (1) if the water samples have a low Sr/Ca ratio $< 1\%$, then the water samples would be related to limestone Triassic formations,

(2) if Sr/Ca ratio ranges between 1 to 1.5 ‰, then the water samples would be related to sandstones and dolomite Triassic formations, and

(3) if the water samples have high Sr/Ca ratio > 5‰ then classifies this water into the category of waters originating from Triassic evaporates.

Regarding Sr/Ca ionic ratios springs of Ein Feshcha display similar hydrochemical responses. Along the western margins of the transform, particularly around Lake Kinneret, the Jordan Valley, the western shore of the Dead Sea and the Arava Valley, fresh groundwaters become saline owing to intermixing with Ca-Chloride brines (Rosenthal, 1987; Vengosh and Rosenthal, 1994).

Ein Feshcha water acquires a characteristic chemical composition dominated not only by high Cl-Excess (19 – 154) and Ca-Mg-Excess (18 – 154) concentrations but also by low equivalent ratios of Na/Cl <0.7 and high Q Value >1. The groundwaters from the Ein Feshcha springs can be identified by their average meq ionic ratios of Sr/Ca (2.4 and 11.3), Mg/Ca (0.27 and 3.0) and Na/Cl (0.37 and 0.65).

The chemical classification of all water bodies involved in the system in question was investigated, with special emphasis given to ionic ratios computed from ionic concentrations. The ionic ratios of Na/Cl, B/Cl, Ca/Cl, Mg/Cl and Ca/(HCO₃+SO₄) are resembled in table 5.5, for more detailed chemical composition ratios refer to the appendix table 5.6.

The Sr/Ca Ratio

High Strontium (Sr) content in waters associated with high content of Pb and Ba can only be explained by its relevance to Aragonite group dissolution (Cerussite-PbCO₃, Strontionite-SrCO₃ and Witherite-BaCO₃). Strontium (Sr) is thus a good tracer of the existence of evaporates.

Analyses of Sr in Ein Feshcha waters demonstrate that most of the springs have high Sr contents (1.3 up to 8.1 mg/l). While water samples 11-31 (Mt.Jarechi-2) of the dry-wet season have a lower Sr content (0.46 - <0.01 mg/l) respectively. Ein Feshcha springs are characterized by waters which have transited generally outcrop through the evaporitic Triassic formations since Sr/Ca ratios are > 1.5‰. The Sr/Ca spring ratios range between (2.4 up to 11.3 ‰).

An exception is the samples (11) Mt.Jericho-2 well and (17) Feshcha-III well, in which sample number 11 during the dry season show Sr/Ca ratio > 1.5‰ while during the flood period the water sample 31 have a low Sr/Ca ratio < 1‰, indicating that the water sample

would be transited through limestone Triassic formations. While sample 17 has Sr/Ca ratio ranges between 1 to 1.5 ‰ which means that the water samples would be related to sandstones Triassic formations, this situation is changed during the flood period, this can be seen in sample number 37 (Feshcha-III), in which the Sr/Ca ratio exceeds the 5‰ ratio reaching to a value of 11.34‰, classifying this water into the category of waters originating from Triassic evaporates taking place in the vicinity of the borehole.

During the dry season Ein Feshcha springs show dolomitization of aragonite, during the wet season Ein Feshcha springs show an increase in Sr/Ca ratio accompanied with increase in Mg/Ca ratio indicating partial solution reprecipitation of calcite (calcite recrystallization).

The scatter diagram of Sr/Ca vs TDS (figure 5.11), shows that the samples of the dry season when mixed with other end member an increase in Sr/Ca ratio takes place shifting to the left and approaching to the trend of Knia-Feshcha-III water, indicating the possibility of mixing between fresh groundwater with evaporates representing the origin of the end member waters.

The waters of Ein Feshcha spring have high concentrations of evaporitic tracers: chlorides (137 – 11048 mg/l), sodium (60 – 3541 mg/l), sulphate (50 – 170 mg/l) and potassium (10 – 344 mg/l), for detailed analysis refer to table 5.5 and in the appendix table 5.6.

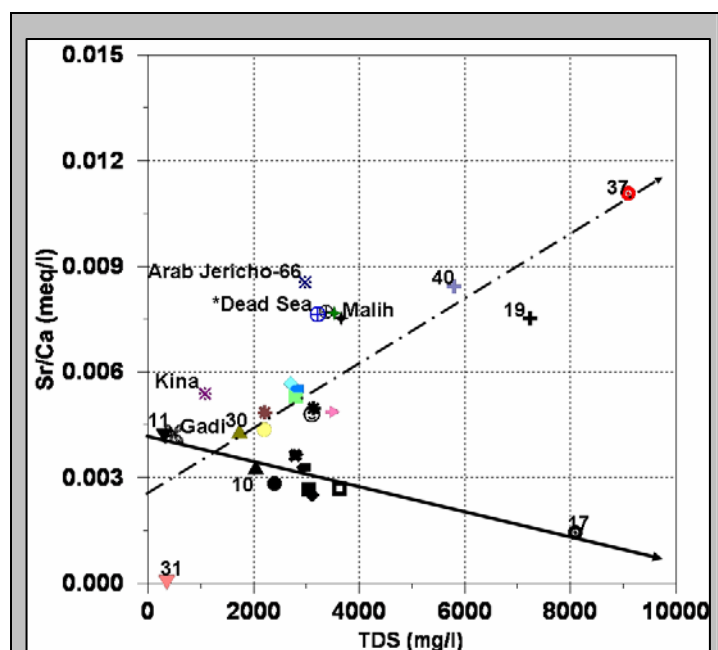


Figure 5.11: Sr/Ca vs TDS scatter diagram of water groups presents the correlation between the TDS and Sr/Ca ionic ratios. *D.S samples for TDS divided by 100.

The Mg/Ca Ratio

Samples of Ein Feshcha springs during the dry season show variable Mg/Ca ratios ranging between 0.27 in well Feshcha-III and 3.00 in spring-19. The samples (12, 13 and 14) of the dry season fail in the Mg/Ca ratio rang of 0.7-0.9 which might resembles association with dolomite or dolomitic aquifers. This is in agreement with the results of Sr/Ca ratios. While the samples of the wet season (32, 33 and 34) fails in the Mg/Ca ratio rang of > 0.9 indicting removal of Ca by precipitation of CaCO_3 and CaSO_4 , aragonite precipitation also is favoured, whereas the Mg/Ca ratio rises due to Dolomite dissolution.

Sample 17 (Feshcha-III) fails in the Mg/Ca ratio rang of < 0.5 indicative for dolimitization in which Ca is released leading to an increase in Ca ions in the solution. During the wet season the (Feshcha-III) sample 37 fails in the Mg/Ca ratio rang of > 0.9 , in which Ca concentration decreased from 127 to 16 meq/l and Mg increases from 34 to 45 meq/l. This decrease in Ca concentration could be attributed to mixing with meteoric waters (ion exchange)

The rest of the Ein Feshcha samples of the dry season (10, 15, 16, 18 and 21) and wet season (30, 35, 36, 39), fail in the Mg/Ca ratio rang of > 0.9 indicting mixing with meteoric waters leading to dissolution precipitation processes associated with evaporaites with respect to aragonite, calcite and dolomite.

The spring-19-40 and spring 20-41 of the dry-wet season, fail in the Mg/Ca ratio rang of > 0.9 , show no deference in the Ca-Mg ion balance during the dry-wet season indicting possible Mg-rich brines, no meteoric water mixing.

The samples (11-31) Mt.Jericho-2 during the dry-wet season, fail in the Mg/Ca ratio rang of 0.7-0.9 indicting dissolution-precipitation conditions are in equilibrium stat.

The samples (24-45) Malih during the dry-wet season, fail in the Mg/Ca ratio rang < 0.5 , show no deference in the Ca-Mg ion balance during the dry-wet season indicting Ca-rich brines, no meteoric water mixing.

The samples 22-42 (Azarea-1) and 23-43 (Herodion-1) during the dry-wet season, fail in the Mg/Ca ratio rang of > 0.9 , associated with dolomite or dolomitic aquifers and usually accompanied with additional sources of Mg ions. The samples of the catchment area fail in the Mg/Ca ratio rang of 0.5 – 0.7, water flowing through chalky or limestone aquifers.

The Na/Cl Ratio

All samples resembling dry-wet season of Ein Feshcha springs fail in the Na/Cl ratio range of < 0.8 meq/l. The Na/Cl ionic ratio values are ranging between 0.37 and 0.64, while the Na/Cl ionic ratio of Dead Sea water is lower 0.32 meq/l. The HCO_3/Cl ratio is very low in Ein Feshcha samples, ranging between 0.01 up to 0.43 which shows low aquifer contribution with CO_2 but strong dissolution of evaporite minerals. The low Na/Cl ionic ratios less than 0.7 indicate loss of Na through precipitation of evaporite salts.

Samples from the catchment area 23 (Herodion-1), 46 (Gadi), 54 (PWA-1), 60 (Dyouk) and 63 (Fasael) are characterized by ratios in the range of 0.86-1.0, representing water in the normal hydrological cycle.

The samples 24-45 (Malih), 19-40 (Feshcha spring) and 20-41 (Feshcha spring) of the dry-wet season respectively fail in the Na/Cl ionic ratio range of < 0.8 with $\text{Br}/\text{Cl} < 286$ (mg/l), $\text{Ca}/(\text{SO}_4 + \text{HCO}_3) > 1$, $(\text{Cl}-\text{Na})/\text{Mg} > 1$ and $\text{Mg}/\text{Ca} < 0.5$, these ionic ratios indicate an inflow of Ca-chloride brines, whereas the $\text{Mg}/\text{Ca} > 1$ ratio for the samples 24-45 (Malih), 19-40 (Feshcha spring) may be caused by changes in the solubility's of CaCO_3 or CaSO_4 in water as the result of ion exchange for Na and K.

The rest of the samples representing the catchment area (Herodion field) show different ionic ratio responses. The ionic ratios of Na/Cl (0.44 – 0.75), Mg/Ca (0.55- 0.69), K/Cl (< 0.07), and $\text{Ca}/(\text{SO}_4 + \text{HCO}_3) < 0.8$ of Herodion field samples resemble those of precipitation water in which high values of Ca/Cl ratio (1.7 – 6.5) and Mg/Cl ratio (1.5 – 4.2) considered as indication of carbonate dissolution. The HCO_3/Cl ratio is very high (3.2 – 8.5) which shows the CO_2 contributions of the soil and aquifer and the stronger dissolution of carbonates relative to chlorides.

The samples which are characterized with Na/Cl ratios exceeding 1.0 is a characteristic of groundwater flowing through crystalline or volcanic rocks, others with Mg/Ca ratio ranging between 0.6 and 0.9 associated with dolomitic aquifers and $\text{Ca}/(\text{SO}_4 + \text{HCO}_3)$ with the range of (0.5 – 0.62), indicate groundwaters flowing in calcareous aquifers.

This means that the water samples of the catchment area indicate recharging waters in chalky limestone and dolomite aquifers (Upper and lower Cretaceous aquifers).

Mg/Ca verses Na/Cl

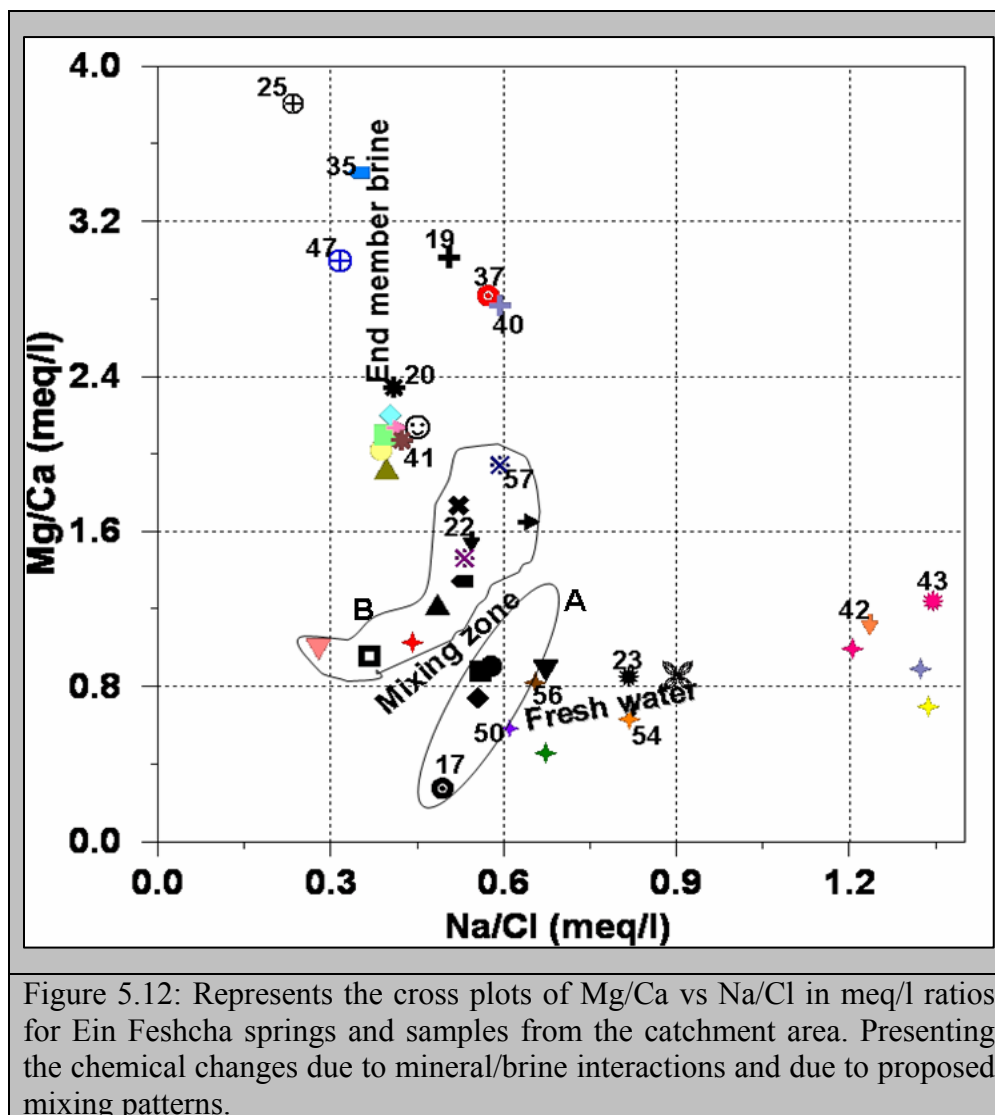
The Dead Sea water show the highest Mg/Ca ionic ratio (3.0 – 3.8) representing the end member brine of the study area, they are plotted at the outmost point of Mg/Ca ratios trend (figure 5.12). The Mg/Ca vs. Na/Cl ratios yields a complex distribution of data points,

which may reflect different water origins and different mixing mechanisms. The first trend of Mg/Ca ratios increases with decreasing Na/Cl ratios. These low ratios can be explained by sodium deficiency relative to chloride, which is usually the result of positive ion exchange in which sodium is replaced by alkaline earths (Schoeller, 1956).

Dissolution of MgCl_2 salts such as bischofite ($\text{MgCl}_2 \cdot 6\text{H}_2\text{O}$) and carnallite ($\text{KMgCl}_3 \cdot 6\text{H}_2\text{O}$) decreases Na/Cl and Br/Cl ratios (Molar et al, 2007).

The second trend presented in figure 5.12 shows a slight decrease in Mg/Ca ratios represented by the springs (19-40 and 20-41) of the dry-wet season, this can be explained by Mg–Ca exchange process such as dolomitization which will lead to a shift of brine water towards low Mg/Ca ratios, which would explain the slight increase in Na/Cl ratios which is a result of brine/rock interaction.

Figure 5.12 presents two possible zones of water mixing in the vicinity of the Ein Feshcha area with different end members. Mixing zone (A): pointing to a suggested meteoric water sources sample 50 (Azarea-3), 54 (PAW-1) and 56 (Abu Diea) wells, characterized with low Mg/Ca ratios indicating water reaction with limestone aquifer. Mixing Zone (B), shows two water types of different origins, one of them is a meteoric water source 55 (PWA-3) and 22 (Azarea-1) the other source is a brine water source, ascending brines from the depth. The mixing between these two components leads to the saline end member waters at Ein Feshcha springs which is characterized with an increase in Mg/Ca ratios accompanied with decrease in Na/Cl ratio indicating removal of Ca by precipitation of CaCO_3 and CaSO_4 , the Mg/Ca ratio rises due to Dolomite dissolution as a result of mixing with meteoric waters. In dolomite and anhydrite Sr typically replaces Ca, which could be considered as another factor responsible for the increases in Mg/Ca ratio (development of brines by Mg-Ca exchange during dolomitization). However, Sr structural position in halite and K-Mg chloride minerals is not exactly known.



The Ein Feshcha waters show $\text{Ca}/(\text{Ca}+\text{SO}_4)$ ionic ratios ranges between 0.8 and 0.97, suggesting surplus calcium from the Ca-Chloride brine, moreover, the increase in ion content, mainly Mg from a suggested brine source, favored a process of dolomitization of the calcite (calcite recrystallization) and aragonite that dominating the entire sequence. The $\text{Ca}/(\text{Ca}+\text{SO}_4)$ results indicate that Calcium source other than gypsum.

The Ein Feshcha waters show $\text{Mg}/(\text{Ca}+\text{Mg})$ ratios with the range of (0.46 – 0.78) during the dry-wet season indicating a source of Mg rich leachate by wadi fans from the dolomitic limestone's formation accompanied with calcite precipitation.

The catchment area samples shows an increase in the ionic ratios due to the seasonal variation in which the ratios of: Ca/Cl varied from 1.86 to 5.41, the Mg/Cl ratio increases from 1.07 to 4.17 and SO_4/Cl value increases from 0.09 to 0.42 as an indication of carbonate dissolution.. These ratios show higher values than those of Ein Feshcha springs.

The ionic ratio of Ein Feshcha springs for Ca/Cl, Mg/Cl and SO₄/Cl are very low ranging between 0.01 to 0.41, 0.11 to 0.42 and 0.01 to 0.05 respectively.

Anaerobic reduction of sulfate and dolomitization ($2\text{CaCO}_3 + \text{Mg}^{2+} \rightarrow \text{CaMg}(\text{CO}_3)_2 + \text{Ca}^{2+}$), followed by gypsum anhydrite precipitation has been suggested as the cause of the low Mg/Ca and SO₄/Cl ratios (Starinsky, 1974).

Na/K ratio in the wells of the Herodion field and Mt.Jericho-2 field fall in the range of < 10-28, resembling the characteristics of the recharge area waters. Whereas the Ein Feshcha waters are characterized by their low ionic ratio for Na/K ranging between 12 to 43 meq/l during the dry season. These springs shows a decrease in the Na/K ionic ratio during the wet season to <15 meq/l. This decrease in concentration could be attributed to depletion in Na ion caused by a considerable exchange with Ca ion and not to mixing with Ca-chloride waters. This can be seen in the ionic ratio of Ca/Na. Some spring behave differently, sample 17-37 (Fshcha-III) of the dry-wet saeson showed a decrease in Na/K, Ca/Na, Ca-excess, Ca-Mg-excess, Cl-excess ratios which support the idea of meteoric water mixing with brine water leading to dissolution of MgCl₂ salts, proposed by Moler (2007). Springs number 19-40 and 20-41 of the dry-wet season shows a conservative condition, no change in the ionic ratio of Na/K indicting continues flow of same source and same aquifer.

Table 5.5: Chemical Composition Ratios for water samples of the study area. The ionic ratios are in meq/l.

Sample #	Na/Cl	B/Cl	Ca/Cl	Mg/Cl	SO ₄ /Cl	Ca/(Ca+SO ₄)
10	0.49	796.00	0.26	0.32	0.04	0.87
11	0.67	193.00	0.65	0.55	0.26	0.71
12	0.58	879.00	0.27	0.24	0.03	0.91
13	0.56	991.71	0.27	0.23	0.02	0.92
14	0.55	1321.71	0.22	0.16	0.02	0.92
15	0.52	820.86	0.25	0.34	0.03	0.90
16	0.64	831.29	0.21	0.35	0.03	0.89
17	0.49	799.05	0.41	0.11	0.01	0.97
18	0.52	686.50	0.23	0.39	0.03	0.89
19	0.50	1256.00	0.10	0.31	0.01	0.91
20	0.41	1029.00	0.18	0.42	0.05	0.80
21	0.37	1238.80	0.34	0.32	0.03	0.91
22	0.54	120.00	1.83	2.81	0.21	0.90
23	0.81	64.00	4.20	3.53	0.09	0.98
24	0.67	697.14	0.39	0.17	0.15	0.73
25	0.24	2367.11	0.17	0.64	*ND	0.98
30	0.40	1036.25	0.22	0.42	0.04	0.86
31	0.28	903.00	0.52	0.52	0.12	0.82
32	0.39	1213.00	0.20	0.39	0.03	0.88
33	0.39	951.50	0.18	0.38	0.03	0.87
34	0.40	968.83	0.17	0.38	0.03	0.86

35	0.35	929.00	0.17	0.59	0.03	0.86
36	0.41	921.00	0.20	0.42	0.03	0.87
37	0.57	760.29	0.09	0.24	0.02	0.81
39	0.46	895.80	0.22	0.46	0.03	0.87
40	0.59	980.27	0.13	0.35	0.01	0.91
41	0.42	972.00	0.21	0.42	0.03	0.86
42	1.23	66.00	4.05	4.47	0.35	0.92
43	1.34	61.00	4.10	5.05	0.31	0.93
44	0.82	53.00	1.79	1.20	0.33	0.85
45	0.67	680.14	0.38	0.17	0.15	0.72
46	0.91	232.00	1.20	1.03	0.31	0.79
47	0.32	1504.98	0.16	0.49	0.00	1.00
50	0.61	ND	1.86	1.07	0.21	0.90
51	1.21	ND	3.07	3.02	0.20	0.94
52	1.32	ND	4.71	4.17	0.36	0.93
53	1.33	ND	5.39	3.72	0.42	0.93
54	0.82	ND	4.85	3.03	0.10	0.98
55	0.44	ND	3.54	3.59	0.09	0.98
56	0.66	ND	1.73	1.41	0.26	0.87
57	0.60	454.78	0.20	0.40	0.14	0.59
58	1.14	ND	3.98	2.97	0.37	0.92
59	0.76	ND	2.83	1.55	0.34	0.89
60	0.88	ND	3.30	1.81	0.38	0.90
61	1.15	ND	3.86	2.32	0.17	0.96
62	0.53	564.00	0.46	0.66	0.02	0.96
63	0.82	34.50	2.06	1.55	0.22	0.90
64	0.68	ND	3.87	2.38	0.29	93

*ND: Not Determined

5.3.6 Mineral Saturation Levels

The quality of the recharge water and its interactions with soil and rocks during its percolation and its storage in the aquifers are key factors in the chemistry of groundwater. These interactions involve mainly dissolution and precipitation processes, which are controlled by the solubility products of the different involved mineral phases. Generally, the saturation indices (SI) are used to express the tendency of water towards precipitation or dissolution. The saturation indices (SI) of the samples collected in this study were calculated for the major mineral phases using the Geochemical modelling software package (PHREEQC for windows version 2.8) (Parkurst and Appelo 2001).

It is postulated that mineral phases that are under saturation ($SI \leq -0.1$) will tend to dissolve and mineral phases that are over saturation ($SI \geq 0.1$) will precipitate these mineral phases out of solution. Equilibrium is taken to be between $SI = -0.1$ to 0.1 . An error of ± 0.05 pH units leads to an uncertainty of ± 0.05 units in the SI of minerals and in view of the uncertainties in the Ca, Mg and HCO_3 analyses, the total uncertainties are of the order of

± 0.01 units of SI (Langmuir, 1971). The dissolution of minerals and the subsequent exchange between cations leads to the precipitation of minerals.

The average saturation indices of the samples of the study area show different trends for each mineral, these SI are summarized in table 5.7, for more detailed results refer to appendix table 5.8.

All the samples of the study area during the dry and wet season are under saturation with respect to the minerals (Anhydrite, Gypsum, Halite and Siderite) and this can be seen in appendix table 5.8. Thus the waters have the potential to dissolve evaporates and calcium sulphate minerals. For Barite which is associated with metal sulfides, solubility of this mineral is variable and in most cases, the minerals are either consistently saturated or consistently under saturated. With respect to barite the water samples of the study area vary from under saturation to saturation.

The minerals (aragonite, calcite and dolomite) which represents the major sediments that built-up the geology of the study area, saturation indices are variable and affected by seasonal variation which means mixing with meteoric waters. The patterns are as follows:

- 1) Aragonite and calcite (CaCO_3): they show SI close to saturation in some samples and over saturated for other samples. Thus, some of the waters may have calcium carbonate solubility controls while most others have the potential to precipitate aragonite and calcite.
- 2) Dolomite ($\text{CaMg}(\text{CO}_3)_2$): The water samples show a variable saturation with respect to dolomite. Some waters, particularly those high in magnesium are over saturated, some are approximately saturated others are saturated to under saturated. Thus, for the different water types, affected by seasonal variation there is potential for mineral dissolution and/or precipitation depending on the water source and on the aquifer composition.

The summarized results presented in table 5.7 describe the predictions of dissolution / precipitation of mineral phases depending on mineral saturation indices (SI). The water sample Mt.Jericho-2 well was under saturation during the dry season and changed to slightly saturated in the wet season with respect to the mineral aragonite, but with respect to calcite and dolomite the SI changed from under saturation in the dry season to over saturated in the wet season which means that the water composition of the well is altered increasing the tendency of the water to precipitate. Feshcha-III well during the dry season was over saturated with respect to the minerals aragonite, calcite and dolomite but during the wet season the SI changes from over saturation to under saturation for the three minerals

Table 5.7: Interpretation or predictions of dissolution / precipitation of mineral phases depending on mineral saturation indices (SI), evaluation output from appendix table 5.8.

Sample Name :		Aragonite	Barite	Calcite	Dolomite
Spring (1)	D10	Precipitation	Precipitation	Precipitation	Precipitation
	W30	Dissolution	Precipitation	Dissolution	Precipitation
Mt. Jericho	D11	Dissolution	Precipitation	Dissolution	Dissolution
	W31	Precipitation	Dissolution	Precipitation	Precipitation
Spring (2)	D12	Dissolution	Dissolution	Dissolution	Dissolution
	W32	Precipitation	Dissolution	Precipitation	Precipitation
Spring (7)	D13	Dissolution	Dissolution	Precipitation	Precipitation
	W33	Dissolution	Dissolution	Dissolution	Dissolution
Spring (8)	D14	Dissolution	Dissolution	Precipitation	Precipitation
	W34	Dissolution	Dissolution	Dissolution	Dissolution
Spring (9)	D15	Precipitation	Dissolution	Precipitation	Precipitation
	W35	Dissolution	Precipitation	Dissolution	Dissolution
Spring (10)	D16	Precipitation	Dissolution	Precipitation	Precipitation
	W36	Dissolution	Dissolution	Dissolution	Precipitation
Feshcha-III	D17	Precipitation	Dissolution	Precipitation	Precipitation
	W37	Dissolution	Precipitation	Dissolution	Dissolution
Spring (4)	D19	Precipitation	Dissolution	Precipitation	Precipitation
	W40	Dissolution	Dissolution	Dissolution	Precipitation
Spring (5)	D20	Dissolution	Dissolution	Precipitation	Precipitation
	W41	Dissolution	Dissolution	Dissolution	Dissolution
Azarea-1	D22	Precipitation	ND	Precipitation	Precipitation
	W42	Dissolution	ND	Precipitation	Precipitation
Herodion-1	D23	Precipitation	ND	Precipitation	Precipitation
	W43	Dissolution	ND	Precipitation	Precipitation
Dead Sea Lake	D25	Precipitation	Dissolution	Precipitation	Precipitation
	W47	Precipitation	Dissolution	Precipitation	Precipitation

*W: Wet Season

*D: Dry Season

*ND: Not Determined

5.3.7 Correlation Matrices

Pearson's correlation matrices (Swan and Sandilands, 1995) were used to find relationships between two or more variables. Only correlations with ($r > 0.4$) are shown (table 5.9). Samples showing ($r > 0.7$) are considered to be strongly correlated whereas ($r > 0.5-0.7$) shows moderate correlation at a significance level (p) of (< 0.05).

Strong correlations exist among the major elements, Na, Mg, Ca, K and Cl, and EC ($r > 0.7$) (table 5.9). These relationships clearly identify the main elements contributing to the groundwater salinity and their tendency to follow a similar trend (could be due to concentration by evaporation). Moderate correlations ($r > 0.5-0.7$) between SO_4 , Sr and B with EC indicate that these ions tend to increase in concentration as the salinity of the water increases. The salinisation of the groundwater would be expected to result from the ionic concentrations increasing due to both evaporation of recharge water and to the effects of interactions between the groundwater and the geological formations.

5.4 Summary of Results

The groundwater of the Judea desert and Jordan Valley show a gradual increase of the Cl content in groundwaters and a concomitant change in the values in the composition of the ionic ratios in either positive or negative dependence of the Cl content. These changes in salinity and ionic ratios occur systematically from the recharge areas to the West through the karstic formation exposed in study area towards Mt.Jericho well field and Ein Feshcha springs to the East, this can be seen in the Cl-excess result of Mt.Jericho-2 well in which the concentration of the ionic ratio of Cl-excess increased from <0.08 in the recharge areas (Herodion field) to the values of $(1.01 - >6.26 \text{ meq/l})$ in Mt.Jericho field.

Whereas at the vicinity of Ein Feshcha springs area three or four salinization zones can be observed depending on the Cl distribution along the springs line. The first zone with Cl concentrations ranging between 1400–1999 mg/l the second zone Cl concentration ranges between 1999 – 2500 and the third one the Cl concentration ranges between 3000 – 5000 mg/l (figure 5.1).

The dominant anion of the groundwater changes from bicarbonate, to sulphate to chloride with a corresponding increase in TDS. The waters exhibit a wide range of major cations; major anions and trace element concentrations (table 5.2 and 5.3). This is generally related to the length of the groundwater flow paths, host rock and to the relative waters age. Rapid recharge through preferential pathways where faults and fractures might be exposed to the surface could be a possibility. Therefore, most groundwater flow out of the springs and under the Dead Sea is expected to occur via fractures and fault.

The Na-K-Mg diagram of Giggenbach, figure 5.2 shows that the water samples fall in the area of immature water very close to the Mg corner indicating that the water is in partial equilibrium with reservoir rock, the figure suggest that there is mixing between meteoric water with old seated brines, the water springs are slightly thermal.

Based on the results of the chemical analysis for the selected water samples and on the information gained from Durov and Piper Diagram in figures 5.5 and 5.6, the following classifications could be considered. The hydrochemical water types of the study area were distinguished and grouped depending on their distributions on a Piper and Durov diagrams (figure 5.13). Broadly, they fit into three hydrochemical water types with some sub-groupings:

Type I: Sodium-Chloride:

Na-enriched waters with either Cl-HCO₃ or Cl as balancing anions, for this group Sodium (Na) are the predominant cation and the Chloride (Cl) is the predominant anion. This water type can be subdivided into five subgroups:

- **Na-Mg-Ca-Cl:1a:** For this subgroup, over 20% of the cation charge is from Na followed by Mg and Ca, and as balancing anions a similar proportion of the anion charge is associated with chloride. The pH is in the range of 6.8 to 7.16 and their temperatures vary between 24.7 to 28.4°C. Three springs represent this subgroup, 10-30, 15-35 and 18.
- **Na-Ca-Mg-Cl-HCO₃:1b:** This subgroup is similar to 1a but the balancing anions is Cl-HCO₃ although the waters are considered as fresh water with low TDS ranging between 310 to 360 mg/l, the pH is in the range of 6.3 to 7.41 and their temperatures vary between 25.4 to 31.3°C. This subgroup represented by Mt.Jericho-2 well.
- **Na-Ca-Mg-Cl :1c:** This category still has Na and Cl as the dominant ions in solution and with higher concentrations than the subgroups 1a and 1b, although Mg concentration in this subgroup is lower than Ca concentration. The pH is in the range of 6.8 to 7.4 and their temperatures vary between 23 to 28°C. This subgroup represented by three springs, 12-32, 13-33 and 21.
- **Na-Ca-Cl :1d:** For this group Na concentrations range from 51 to 154 meq/l, depletion of Mg and enrichment of Ca with concentration ranging between 20 to 126 meq/l, the balancing anion Cl ranges with concentration between 92 to 311 meq/l. the pH is in the range of 6.6 to 6.8 and their temperatures vary between 23.7 to 28°C. This subgroup is represented by one springs (14-34) and one well Feshcha-III well. The Malih spring show a similar water composition in which an enrichment in Ca, K, SO₄ ions and slight depletion in Mg ion due to water rock interaction and equilibration.
- **Na-Mg-Cl :1e:** This group is similar to 1d but with depletion of Ca and enrichment of Mg and still Na control the cations concentration as prevailing cation over Ca and Mg. the pH is in the range of 6.5 to 7.37 and their temperatures vary between 24.7 to 29°C. This subgroup represented by two springs, 16-36 and 19-40.

Type II: Magnesium-Chloride

This water type (Mg-Na-Cl), classified as Mg-enriched waters with Cl as balancing anion. The enrichment of Mg and depletion of Ca characterizes this water type but still Na

considered a limiting factor in this grope. This group with respect to its chemical concentration is similar to subgroup 1c in water type 1. The pH is in the range of 6.5 to 7.1 and their temperatures vary between 25 to 27°C. This water type is represented by two springs, 20-41 and 39.

Type III: Magnesium-Bicarbonate

Mg/HCO₃ water type, where Magnesium (Mg) is the predominant cation and the Bicarbonate (HCO₃) is the predominant anion. The major controlling cation is Mg-Ca enriched waters with either HCO₃ or Cl-HCO₃ as balancing anions. The water samples of this group represent waters of the catchment area. This water type is attributed to dolomite which is one of the main constituents of the West Bank which contains several hundred meters of Upper Cretaceous carbonate rocks. This group is subdivided into three subgroups:

- ▲ **Mg-Na-Ca-Cl-HCO₃ :3a:** In this subgroup Magnesium (Mg) and Chloride (Cl) are considered as the dominant ions in solution. One sample represents this subgroup characterized with similarities with water type 2. The pH is in the range of 7.5 to 7.6 and its temperature varies between 25 to 26°C. This subgroup represented by Knia spring located to the south of Ein Feshcha reserve.
- ▲ **Mg-Ca-HCO₃ :3b:** In this subgroup, Magnesium (Mg) is the predominant cation and the Bicarbonate (HCO₃) is the predominant anion. The pH is in the range of 7.4 to 7.7 but their temperatures were not determined. This water type is represented by two water samples Azarea-1 well and PWA-3 well. This water type is attributed to dolomite aquifer exposed in the western flanks of the study area.
- ▲ **Ca-Mg-HCO₃ :3c:** Ca/HCO₃ water type where Calcium (Ca) is the predominant cation and the Bicarbonate (HCO₃) is the predominant anion. This water type is attributed to the Calcite which is one of the main constituents of the West Bank carbonate aquifers. The pH is in the range of 6.7 to 7.8 and their temperatures vary between 15 to 27°C. This water type is represented by samples number Herodion-1, Ein Gadi spring, Azarea-3, Beit Fajar-1a, Herodion-4, JWC-4, PWA-1, Abu Dies, Al-Sultan spring, Al-Dyook spring, Al-Quilt spring and Al-Auja-2 well.

Figure 5.13 shows that water type III (3b and 3c), fall in the recharge water zone with a dominant Ca-HCO₃, indicates recharging waters in limestone formation and water type is dominated by Ca and HCO₃ with significant Mg ions, indicates recharging waters in

limestone and dolomite aquifers. Whereas water types (1b, 3a, 3c) show no dominant anion or cation, indicates, water exhibiting simple dissolution or mixing. These samples fall in the mixing zone. Water types (1a, 1c, 1d, 1e and water type 2) fall in the zone of Cl dominant anion and Na dominant cation, indicating that the groundwaters be related to reverse ion exchange of Na-Cl, end-point waters.

From figure 5.13 it can be concluded that springs salination differences are due to evaporation and/or dissolution-precipitation reactions of host rock filing (aragonite, calcite, dolomite and $MgCl_2$ salts and minor gypsum) which takes place along the water flow path and in the vicinity of the springs. Not only but also due to mixing with variable amounts of originally deep-seated Ca-Mg-Cl brines with meteoric waters through the fractures and the fault system in the vicinity of the study area. In order to trace the geochemical evolution of different water bodies evolved in the study area, changes in trace elements and ionic ratios (table 5.10), were followed and studied.

High Strontium (Sr) content in waters associated with high content of Pb and Ba can only be explained by its relevance to Aragonite group dissolution., Strontium (Sr) is thus a good tracer of the existence of evaporates. Ein Feshcha springs are characterized by waters which have transited generally outcrop through the evaporitic Triassic formations since Sr/Ca ratios are $> 1.5\%$, as presented in table 5.10.

The scatter diagram of Sr/Ca vs TDS (figure 5.11), shows that the samples of the dry season when mixed with other end member, an increase in Sr/Ca ratio takes place shifting to the left and approaching to the trend of Kina-Jericho-Malih line indicating the possibility of same origin of end member.

Depending on the ionic ratios in figure 5.12, presents two possible zones of water mixing in the vicinity of the Ein Feshcha area with different end members. Mixing zone (A): pointing to a suggested meteoric water type 3c (Azarea-3, PWA-1 and 56 Abu Diea wells). Mixing Zone (B), show two water types of different origins, one of them is meteoric water type 3b (PWA-3 and Azarea-1) the other source is a brine water type 1e (Arab project-66), mixing of these components leads to the saline end member waters at Ein Feshcha springs. Based on the hydrochemical analysis and on the available literature, Ein Feshcha water quality varies even over short distances and this implies a fracture flow system that is heterogeneous with respect to both hydrogeology and mineral reactivity. In order to study the relation between the proposed fractures and its relation with water flow and mixing mechanism, a geophysical test and water isotopic analyses were implemented and will be discussed in the next chapters.

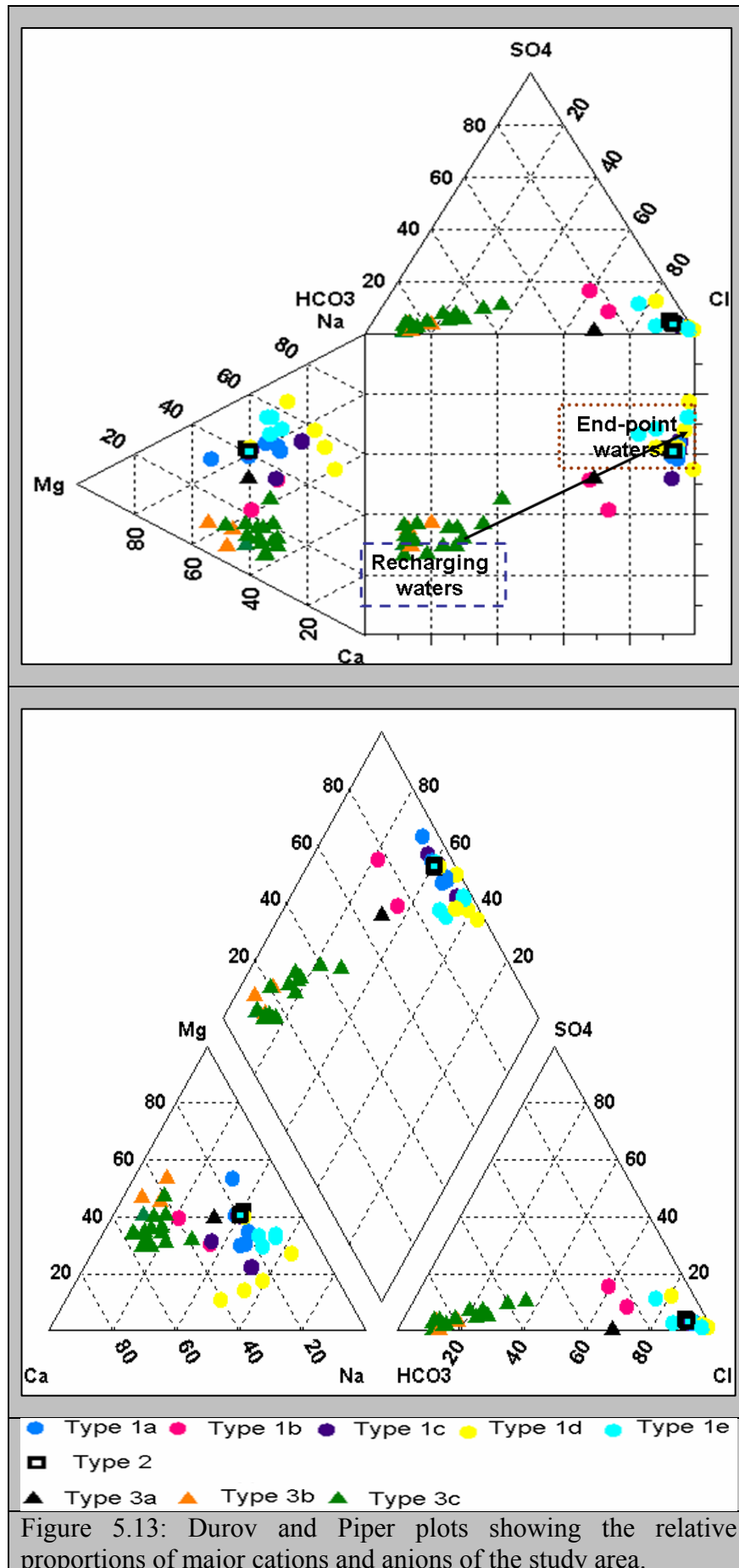


Figure 5.13: Durov and Piper plots showing the relative proportions of major cations and anions of the study area.

Table 5.10: Average ionic ratios in groundwaters in source aquifers and in the investigated springs.

Ionic ratio	Type1					Type2	Type3		
	1a	1b	1c	1d	1e		3a	3b	3c
Sr/Ca	2.88-5.25	0.21-4.0	2.41-4.82	1.42-11.34	4.01-8.35	5.01-5.42	5.84	-----	-----
Cl-excess	19.29-34.62	1.01-6.26	21-37	14.8-68	14.57-64	22.8 -28.9	4.83	-0.19-0.49	-0.26-0.49
(Ca+Mg)/(Na+K)	1.07-2.01	1.63-3.39	0.85-1.65	0.53-1.3	0.75-1.35	1.37-1.39	1.96	6.6-13.8	4.22-8.95
HCO₃/Cl	0.052-0.075	0.33-0.42	0.049-0.073	0.01-0.09	0.03-0.16	0.07-0.08	0.45	4.37-7.73	1.49-8.52
Cl/Br	49-142	386-451	73-155	54-210	90-124	45-131	-----	-----	-----
Mg/Ca	1.21-3.44	0.86-1.0	0.87-2.08	0.27-2.81	1.64-3.0	2.06-2.34	1.46	1.01-1.53	0.55-0.99
Na/Cl	0.35-0.49	0.28-0.67	0.37-0.58	0.40-0.67	0.41-0.64	0.41-0.46	0.53	0.44-1.23	0.61-1.34
Ca/(SO₄+HCO₃)	2.0-2.84	0.94-1.16	2.07-3.72	1.65-19.58	0.67-2.95	1.45-2.06	0.97	0.41-0.54	0.51-0.86
Na/K	10.79-20.74	9.5-11	12.43-24.79	11.9-43.9	9.8-23.9	13.1-13.73	13.33	6-20.25	8.11-27.25
SO₄/HCO₃	0.48-0.57	0.35-0.62	0.42-0.53	0.51-1.65	0.20-0.86	0.45-0.58	0.04	0.01-0.05	0.01-0.11
SO₄/Cl	0.03-0.04	0.12-0.26	0.02-0.03	0.11-0.38	0.01-0.14	0.03-0.05	0.02	0.09-0.35	0.09-0.42

6 ISOTOPIC ANALYSIS

6.1 Water Isotopic Composition

Water isotopes, Oxygen ($\delta^{18}\text{O}$) and hydrogen ($\delta^2\text{H}$) are commonly used tools for determining water sources in catchments. Isotope ratios especially $^2\text{H}/^1\text{H}$, usually reported as $\delta^2\text{H}$ tend to be conservative and good indicators of the origin of flow, mixing and evaporation. Water stable isotopes are useful tools in revealing mechanisms of recharge, differentiation of modern meteoric water and fossil water (paleo-recharge), aquifer interactions and groundwater salinisation mechanisms (Sklash et al., 1976; Sklash and Farvolden, 1979; Bishop, 1991). The water isotopes are such effective tracers for water sources because oxygen and hydrogen are the constituents of, and thus move with water molecules (Sklash et al., 1976). Understanding the relationship between the variation of oxygen-18 ($\delta^{18}\text{O}$) and deuterium ($\delta^2\text{H}$) content of precipitation during its evolution through primary evaporation, condensation, re-evaporation and infiltration is essential for studying groundwater origin.

Under favourable circumstances, waters flowing along a particular flow path may have distinctive O- and/or H-isotopic compositions; hence, the water isotopes can sometimes be viewed as tracers of water flow paths.

The general relationship between oxygen-18 and deuterium for natural waters in the Eastern Mediterranean was found to be linear and represented by a line called Eastern Meteoric Water Line (EMWL), (Gat and Carmi, 1970); this relationship is expressed in equation number (1):

$$\text{EMWL: } \delta^2\text{H} = 8 * \delta^{18}\text{O} + 22\text{‰} \text{-----} \quad (1)$$

Dansgaard (1964) noted that the deviation from the (EMWL) is called Local Meteoric Water Line (LMWL) and can be expressed through the deuterium excess parameter (d-excess). The d-excess parameter is defined in equation number (2):

$$\text{d-excess} = \delta^2\text{H} - 8 * \delta^{18}\text{O} \text{-----} \quad (2)$$

The local meteoric water line, based on analyses of surface water samples from the recharge area of Jerusalem and Ramallah mountains (Abu Dies meteorological station at AQU) is represented by equation number (3):

$$\text{LMWL: } \delta^2\text{H} = 8 * \delta^{18}\text{O} + 19.5\text{‰} \text{-----} \quad (3)$$

Craigs (1961) observations only has been applied globally because it represents an average of many local and regional meteoric water lines, which are individually affected by varying climatic and geographic factors, therefore his equation was represented by a line called the Global Meteoric Water Line (GMWL), equation number (4):

$$\text{GMWL: } \delta^2\text{H} = 8 * \delta^{18}\text{O} + 10\text{‰} \text{-----} \quad (4)$$

The analyzed isotopic water compositions ($\delta^{18}\text{O}$ and $\delta^2\text{H}$) for the groundwater samples collected during the dry-wet season from the Marsab-Feshcha catchment area are presented in tables 6.1. Depending on the above equations and on the presented data in table 6.1, the stable isotopic data of the springs and groundwater wells tapping various aquifers (Marsab-Feshcha catchment), were plotted on the $\delta^{18}\text{O} - \delta^2\text{H}$ diagram, figure 6.1, showing the distribution of the water isotopes in the dry-wet season with respect to EMWL and LMWL. The samples deviate far away from the GMWL toward the EMWL and LMWL signifies a climatic recharge origin dominating the rift graben. The data points fall between the EMWL and the LMWL, some samples fall on, or even above the EMWL, other samples fall on or even below the LMWL (figure 6.1).

Figure 6.1 shows that the springs and groundwater samples reveals a wide variation in $\delta^{18}\text{O}$ and $\delta^2\text{H}$ content. The water samples 22 (Azarea-1), 23-43 (Herodion-1), 52 (Herodion-4), 54 (PWA-1), 55 (PWA-3), 56 (Abu Dies) and 62 (Knia spring) plotted on figure 6.1 are all distributed to the left of the EMWL, indicating that these fresh waters are originating from the local mountain aquifer and could be tapping the lower cenomanian aquifer, the differences in the isotopic compositions ($\delta^2\text{H}$ and $\delta^{18}\text{O}$) between these samples are not so large.

The samples, 58 (Ein Samia), 59 (Sultan), 60 (Dyouk) and 64 (Auja) are plotted along the EMWL and were observed to be significantly lighter (more negative), these samples are effectively recharged by meteoric waters. These samples are originating from shallow modern groundwater; this can be seen in the isotopic tritium composition clustering around 3.9 to 4.1 TU.

Some of the groundwater samples 11-31 (Mt.Jericho-2), 46 (Gadi), and 57 (Arab project-66), plotted on figure 6.1 fall along the LMWL, indicating secondary processes tacking place, such

as evaporation prior infiltration or isotope exchange with aquifer rocks, while other group of samples representing the wet season 42 (Azarea-1), 50 (Azarea-3), 51 (Beit Fajar-1a) and 53 (JWC-4), show values lie below the LMWL in which these samples are reflecting secondary fractionation by evaporation prior to infiltration.

Sample number 22-42 (Azarea-1) shows depletion in $\delta^2\text{H}$ accompanied with staple $\delta^{18}\text{O}$, moving from the left side of the EMWL to the right side of the LMWL. The depletion in $\delta^2\text{H}$ content in the sample 22-42 (Azarea-1) during the dry-wet season could be attributed to silicate hydrolysis producing hydrated minerals leading to deuterium depletion.

Sample 23-43 (Herodion-1) shows a slight depletion in $\delta^{18}\text{O}$ with almost no change in $\delta^2\text{H}$ content. These two wells (Azarea-1 and Herodion-1) proves that there waters are originating from meteoric water but each of them originating from different recharging area with different altitudes.

In the $\delta^{18}\text{O} - \delta^2\text{H}$ cross plot in figure 6.2, the water samples during the dry-wet season are clustered near the LMWL, during the wet season several changes took place, showing a possible evidence of mixture of different aged water bodies. Sample 17 (Feshcha-III), 18, 20 and 39 lie below the LMWL, could be due to intensive evaporation loses forming a local evaporation line.

The deviation of the springs and wells from the LMWL indicates that either the water has experienced some degree of evaporation relative to the local rain, and/or that it contains some isotopically enriched water from the Dead Sea evaporates and/or mixing with old brines.

The dashed line presented in figure 6.2 represents the evaporation line in which sample 17-37 (Feshcha-III) fail on the path of evaporation, during the wet season this well shows depletion in $\delta^2\text{H}$ and $\delta^{18}\text{O}$, representing mixing mechanism with other source of lighter waters causing isotopic depletion due to dilution.

It is observed that several springs (10-30, 13-33, 14-34 and 20-41) during the dry-wet season, shows a slight enrichment of both $\delta^2\text{H}$ and $\delta^{18}\text{O}$ in the residual brine accompanied with a preferential increase of Ca and Mg relative to Na, this enrichment in the water isotopes could be attributed to ultra filtration caused by the high clay content found in the area as proposed by Coplen and Hanshaw (1973). Due to the flow of water through the clay layers a decrease in TDS tack place accompanied with an increase in the Ca/Na and Mg/Na ratios which may lead to forming CaCl_2 and MgCl_2 water types.

White (1973); have claimed that in the presence of clays $\delta^2\text{H}$ exchange can occur, resulting in a slight decrease of the $\delta^2\text{H}$ values. This can be seen in sample 12-32 during the dry-wet season, this spring shows slight depletion in $\delta^2\text{H}$ value accompanied with no change in $\delta^{18}\text{O}$ value.

The springs (15-35, 16-36 and 19-40) representing the dry-wet season are all fall along the LMWL shows no significant changes in the isotopic composition, could be attributed to dissolution of anhydrous evaporate deposits.

Table 6.1: The $\delta^{18}\text{O}$ and $\delta^2\text{H}$ composition of the samples collected during the dry and wet season from the study area.

Sample #	$\delta^2\text{H}$	$\delta^{18}\text{O}$	d-excess	Sample #	$\delta^2\text{H}$	$\delta^{18}\text{O}$	d-excess
10	-23.9	-5.39	19.22	40	-23.1	-5.32	19.49
11	-23.9	-5.52	20.26	41	-24.3	-5.43	19.14
12	-22.9	-5.38	20.13	42	-27.9	-5.87	19.06
13	-23.3	-5.41	19.97	43	-23.9	-5.87	23.06
14	-23.3	-5.39	19.84	44	-24.1	-5.55	20.30
15	-23.6	-5.42	19.78	45	-23.1	-5.48	20.74
16	-23.7	-5.41	19.60	46	-23	-5.48	20.84
17	-21.1	-4.73	16.72	47	23	4.33	-11.64
18	-22.5	-5.15	18.62	50	-26.9	-5.61	19.22
19	-22.9	-5.30	19.46	51	-28.7	-5.83	20.26
20	-25.2	-5.47	18.55	52	-24.4	-5.91	20.13
21	-24.4	-5.45	19.21	53	-27.4	-5.81	19.97
22	-23.2	-5.83	23.44	54	-24.4	-5.86	19.84
23	-24.1	-5.8	22.30	55	-24.2	-5.8	19.78
24	-22.12	-4.93	17.32	56	-22.6	-5.58	19.60
25	-3.41	0.96	-11.09	57	-23.5	-5.41	16.72
30	-22.5	-5.22	19.27	58	-25.31	-5.86	18.62
31	-23.8	-5.49	20.12	59	-26.2	-5.95	19.46
32	-23.8	-5.36	19.08	60	-26	-5.94	18.55
33	-23.0	-5.38	20.04	61	-23.7	-5.77	19.21
34	-22.9	-5.36	20.03	62	-22.4	-5.66	23.44
35	-23.5	-5.37	19.49	63	-24.32	-5.53	22.30
36	-23.5	-5.43	19.90	64	-21.12	-5.33	17.32
37	-23.8	-5.42	19.49				
39	-23.2	-5.28	19.01				

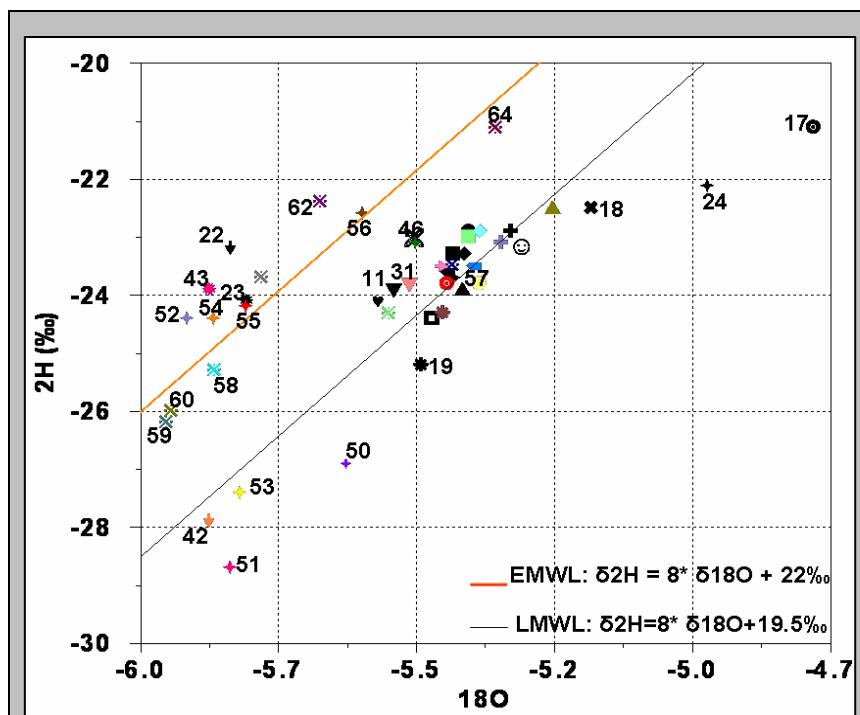


Figure 6.1: The stable $\delta^2\text{H}$ and $\delta^{18}\text{O}$ composition relation of all samples collected from the study area plotted and compared with respect to the EMWL and to the LMWL.

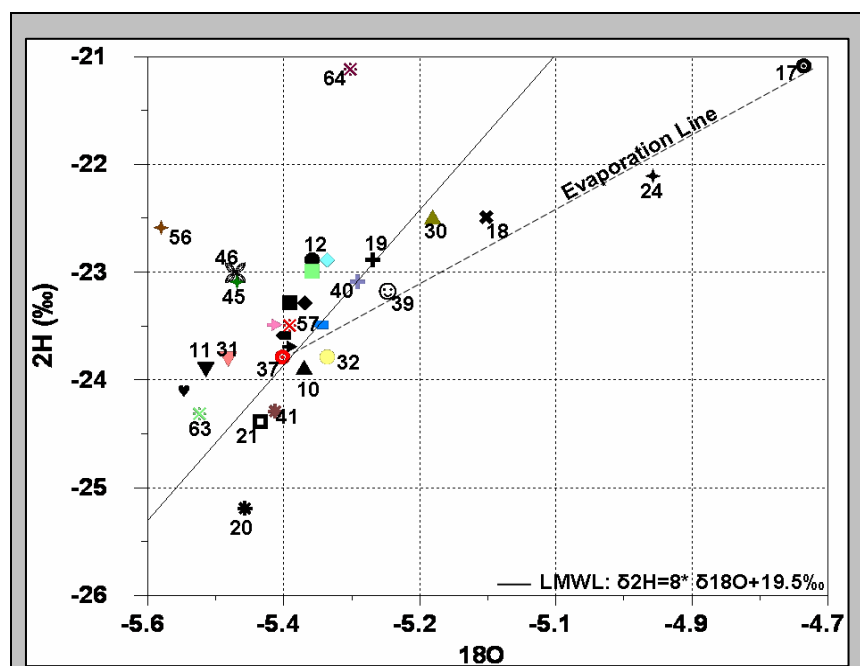


Figure 6.2: The isotopic compositions ($\delta^2\text{H}$ & $\delta^{18}\text{O}$) of selected water samples, representing a possible evaporation trend and mixing trend with other source of lighter water

6.2 $\delta^{18}\text{O}$ and $\delta^2\text{H}$ vs. Cl and TDS

The solid line in figures 6.3 and 6.4, represents a possible mixing line between meteoric groundwaters and evaporated waters enriched in $\delta^{18}\text{O}$ due to prolonged water–rock interaction and/or water mixing with variable amounts of deep seated CaCl_2 and MgCl_2 water types trapped in the clay formations found in the study area, whereas the dashed lines represents the evaporation-dissolution path.

The plot of $\delta^{18}\text{O}$ and $\delta^2\text{H}$ vs. Cl concentrations (figure 6.3) shows that the relationship between Cl and $\delta^{18}\text{O}$ is not simple. The water samples lie within a mixing trend between freshwater samples of the catchment area from the West, saline waters from North of Jericho and some deep seated waters in Ein Feshcha study area. Moreover, Ein Feshcha samples can be related to a freshwater – brine water mixing trend if Cl values are compared with those of $\delta^{18}\text{O}$, while they fall largely outside the mixing trend deviating toward the evaporation trend when $\delta^2\text{H}$ values are taken into account (figure 6.3), this could be attributed to different and independent processes: evaporation, water rock interaction and mixing with isotopically modified waters (cropping out of the liesan formation enriched in $\delta^{18}\text{O}$). The $\delta^{18}\text{O}$ -Cl ratios of the selected water samples rule out any processes to explain the observed heavy isotopic compositions, while $\delta^2\text{H}$ -Cl ratios of the selected samples fit with the groundwater / evaporation line.

Evaporation can be a major factor since these samples do fit with the expected evaporation line when $\delta^2\text{H}$ and $\delta^{18}\text{O}$ are plotted vs. Cl concentration. An evaporation process should have shifted both $\delta^2\text{H}$ and $\delta^{18}\text{O}$ along the reported evaporation line. Since water/rock isotopic re-equilibration should affect only $\delta^{18}\text{O}$, hence the observed trends must be related to evaporation instead of water–rock interaction.

The plot of $\delta^{18}\text{O}$ - $\delta^2\text{H}$ vs. TDS (figure 6.4) showing mixing between meteoric waters (isotopically lighter) and salty waters (isotopically heavier). The samples in the study area are clustering along the mixing line in which the salinity (TDS) is related to $\delta^{18}\text{O}$ – $\delta^2\text{H}$, which confirm the presence of common seated brine that mixes with groundwater in variable amounts.

Sample 17-37 (Feshcha-III) during dry-wet season shows an increase in TDS content accompanied with an enrichment in $\delta^{18}\text{O}$ – $\delta^2\text{H}$ value, this enrichment could be due to evaporative water loss and fluid exchange with minerals found in the formation during the dry

season, while in the wet season, Feshcha-III water follow the dissolution-leaching path leading to depletion in $\delta^{18}\text{O} - \delta^2\text{H}$ value due to mixing with meteoric waters.

Sample number 10-30 (main Feshcha spring) during the wet season shows an increase in the $\delta^{18}\text{O} - \delta^2\text{H}$ value, this enrichment in $\delta^{18}\text{O} - \delta^2\text{H}$ value is accompanied with no significant change in salinity values, this is could be attributed to ultra filtration by clays found in the aquifer working lick a clay membranes and accompanied with ionic exchange, this exchange can be seen in the results of the ionic ratios in table 5.6 in the appendices in which an increase in the exchangeable ions (Ca/Na and Mg/Na) is clear.

Sample number 12-32 during the dry-wet season shows no significant change in salinity and $\delta^{18}\text{O}$ value, while during the wet season this spring shows depletion in $\delta^2\text{H}$ value. This depletion could be attributed to both exchange with clays and mixing with meteoric waters.

The groundwater samples representing the aquifer systems in the catchment area is more depleted than Ein Feshcha water springs in the study area. These groundwater samples also show variation among each other. This is a substantial indication that the groundwater can not be recharged locally from rain originating from similar altitudes. This means that the rain infiltration to the groundwater of various aquifers took place at different altitudes. The isotopic data are scattered widely along the evaporation line, which indicates that the infiltrated water down gradient is subject to different degrees of evaporation before infiltration.

With stable isotopes no clear evidence show that an evaporation brine play an important role for salinisation of groundwater within the rift graben. There is more evidence for dissolution of salts.

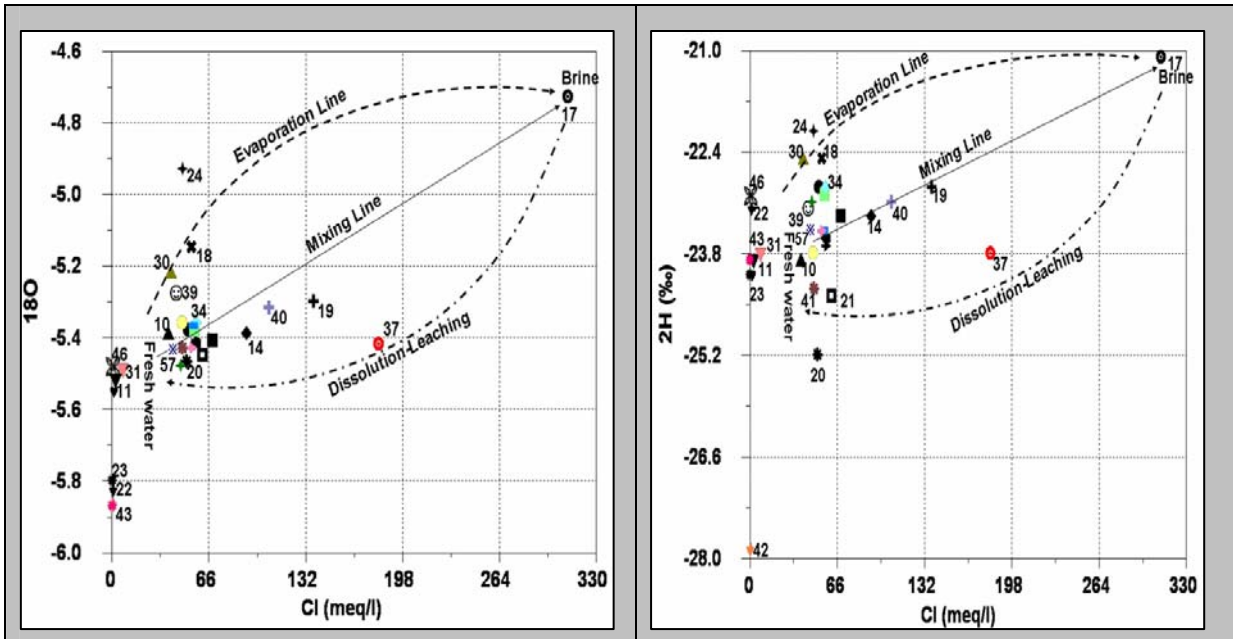


Figure 6.3: 18O and 2H vs. Cl, the two lines represent the expected variations due to mixing of present groundwaters with brine waters and due to evaporation.

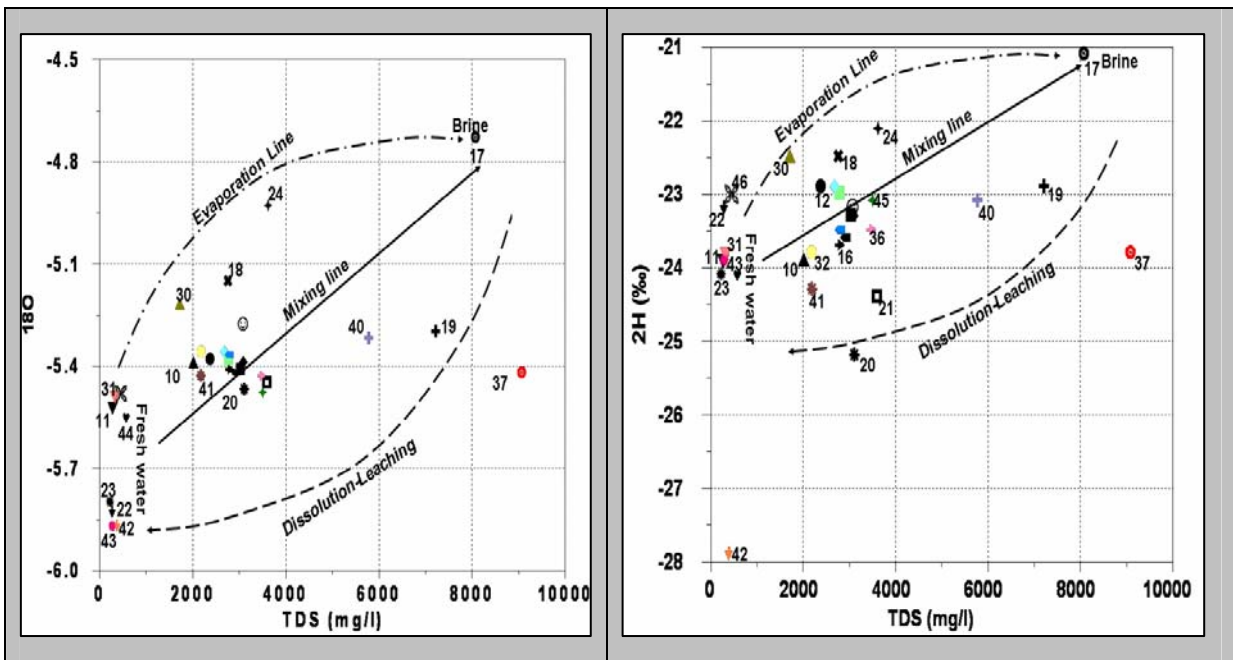


Figure 6.4: 18O and 2H vs.TDS, the two lines represent the expected variations due to mixing of present groundwaters with brine waters and due to evaporation.

6.3 The Radioactive Isotope Tritium

The radioactive isotope Tritium ($\delta^3\text{H}$) is a short-lived isotope of hydrogen with a half-life of 12.32 years. Tritium concentrations are represented in tritium units (TU). One tritium unit is equal to one molecule of $\delta^3\text{H}$ per 10^{18} molecules of ^1H and has an activity of 0.118 Bq/kg (3.19pCi/kg). The large pulse of tritium, that entered the hydrologic cycle from the middle of 1950's to early 1960's during atomic bomb test in the atmosphere, could be used to establish the age of groundwater recharge. Tritium concentration in ground water provides an indication for the mean residence time of water. Accurate dating of water based on tritium is not possible, because of the spatial and temporal variation in the tritium composition of the precipitation and the complicated mixing-processes that take place in each aquifer.

High levels of tritium (≥ 30 TU) indicate water that was recharged during the late 1950's or early 1960's; moderate concentrations indicate modern recharge; levels close to (~ 1 TU) are likely sub-modern or paleo-groundwaters that have mixed with shallow modern groundwaters. Clark and Fritz (1997) estimated the following rough general guidelines for tritium:

- <0.5 TU, sub-modern age (pre-1952),
- 0.5 - 5 TU, sub-modern and modern age (pre-1952 and post-1952),
- 5 - 15 TU modern age (<5 to 10 years age),
- 15 - 30 TU some bomb tritium,
- 30 - 50 TU recharge in the 1960's to 1970's,
- >50 TU recharge in the 1960's (Bomb Tritium).

According to Carmi and Gat (1973), the tritium concentration in the precipitation is similar for the whole West Bank and Israel. During the 1950's the tritium concentration in the precipitation of these areas was about 5 TU (Kaufman and Libby 1954). After 1953 the testing of nuclear weapons had increased the tritium level in the rainfall and consequently, ground water. This $\delta^3\text{H}$ content of the atmosphere were peaking in 1963, after that the surface nuclear tests stopped and the tritium concentrations in precipitation decreased in general.

Carmi and Gat (1973 and 1978) stated that the tritium concentration in Israel was 30 TU in 1960, 522 TU in 1962, and 26, 24, 30 and 27 TU from 1975 to 1978. Tritium reaches the Dead Sea from the atmosphere by direct and delayed surface runoff, by molecular exchange through the surface of the lake, and from springs. The surface layers of the Dead Sea were first analyzed for tritium in 1960, when they contained 8.5 TU. A maximal value of 200 TU was

measured in 1964, and not more than 50 TU were measured in 1975; this further decreased to 30 TU in 1977 and 12 in 1979 (figure 6.5). During the course of this study (2007) one sample from the surface layer of the Dead Sea was analyzed for tritium, the tritium value was 3.6 TU. The deeper waters contained 1.8 TU in 1960 and up to 7 in 1975-1977, but these measurements are less reliable than later ones (Ilana Steinhorn 1985). Ein Feshcha springs near the Dead Sea shore contained up to 36 TU (Mazor and Molcho, 1972), while during this study the maximum value was 1.2 TU. The tritium content of the samples collected from the study area during the course of this study presented in table 6.2.

Based on table 6.2, water samples have tritium concentrations around 0.4 TU dates back to the early 1950's. An example of this water in the study area is that of the Azarea wells, which discharges the lower confined aquifer. Water that has tritium concentrations $0.4 \text{ TU} < \delta^3\text{H} < 3.5 \text{ TU}$ dates back to the late 1950's to 1960; an example of this group is the Herodion-1 with $\delta^3\text{H}$ value of 1.5, which discharges the upper aquifer, Herodion-4 with $\delta^3\text{H}$ content of 0.3 TU, tapping the Albian aquifer which discharges the lower confined aquifer, dates its water back to the early 1950's, while 1.0 TU in the water of Beit Fajar-1a tapping the Turonian-Cenomanian aquifer dates it back to the late 1950's. Tritium values greater than 4 is expected to have contact with the atmosphere after 1963, three springs in Jericho area (Wadi Qilt, Ein-Sultan and Ein-Dyouk) represents this group, the $\delta^3\text{H}$ concentration of these springs indicate that their water discharge is out of the upper aquifer, suggests recent recharge and tritium of meteoric origin.

Depending on $\delta^3\text{H}$ values for the groundwater in the Marsaba-Feshcha study area presented in table 6.2 and figure 6.6, it can be concluded that Ein Feshcha waters are originated from deferent aquifers in which some springs show water that has tritium concentrations $< 0.4 \text{ TU}$, dates back to the early 1950's, this water is considered sub-modern or paleo-groundwater, spring number 13 and 19 representing this group, and those with tritium values $> 0.4 \text{ TU}$ indicating mixing of old seated waters with shallow modern groundwaters (figure 6.6). Kina spring and Ein Gadi spring shows tritium value of 0.7 TU, indicating possible mixing of sub-modern to modern age waters (pre-1952 and post-1952), representing fresh water discharge from the upper and lower aquifer. These values could reflect a mixing process between two waters of different age, were the tritium units differentiate two different age end members of old to modern and sub-modern recharged water that represent this mixing.

The Ein Feshcha water samples has tritium values <0.5 TU dates back to the early 1950's. The Ein Feshcha springs discharge from the mixture of the fresh water coming from upper and lower aquifer and mixes with saline water of the regional aquifer.

The low tritium concentration from the Ein Feshcha wells and springs emphasizes the presence of such mixing process. The lower tritium units ranging between 0 - 1.2 TU might reflect a mixing of recent age water infiltrated from wadis runoff through the alluvium fan with deep old water characterized by high salinity. The low $\delta^3\text{H}$ values indicate that transport time from the recharge zone in the mountain areas is more than 40 years.

According to the figures 6.3, 6.4 and 6.6 a mixing process between freshwaters of meteoric origin and significantly evaporated and isotopically modified brines ($\delta^{18}\text{O} - \delta^2\text{H}$) because of salts dissolution, seems to better explain the observed $\delta^3\text{H}$, $\delta^2\text{H}$ vs. $\delta^{18}\text{O}$ trend for the water samples.

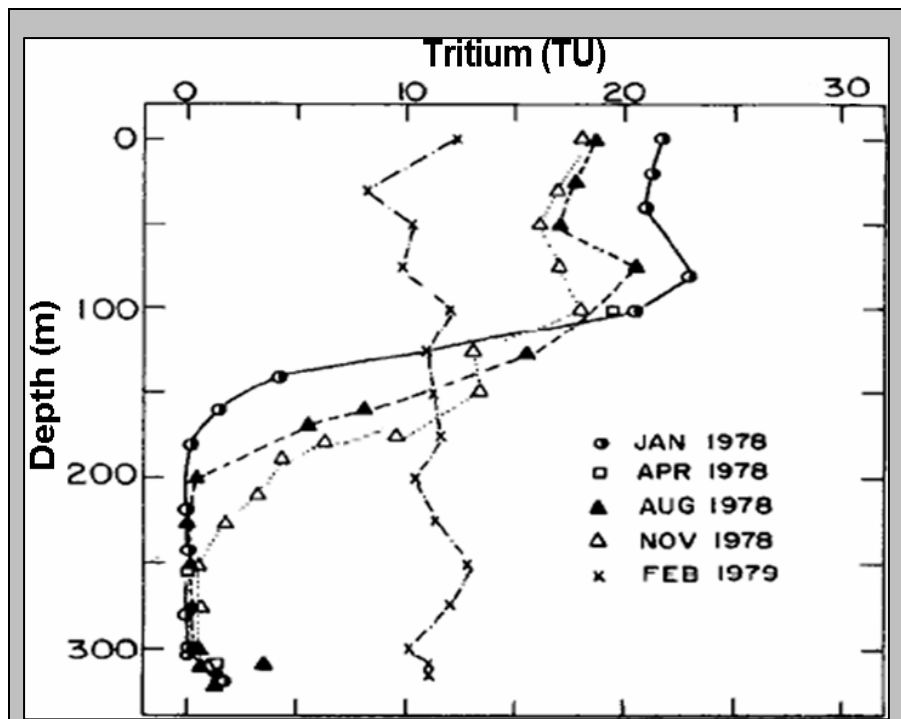


Figure 6.5: Results of the tritium measurements at the Dead Sea (after Ilana Steinhorn 1985).

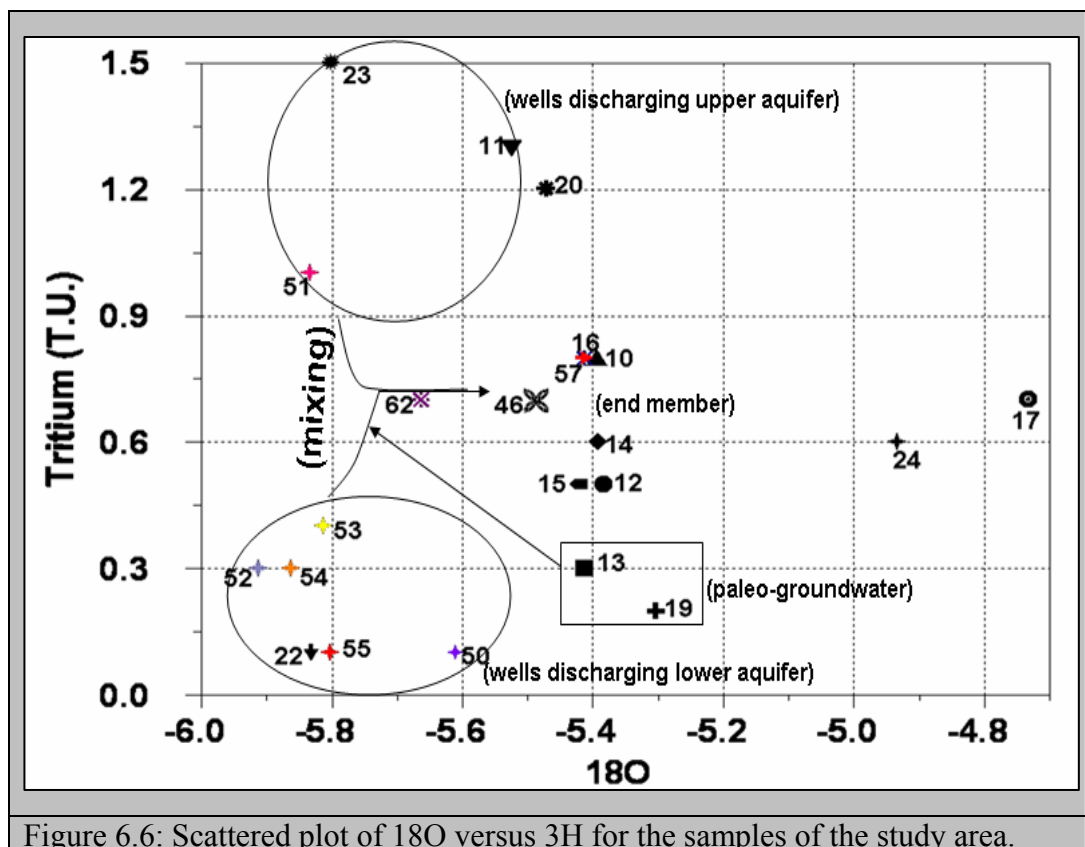


Table 6.2: The tritium ($\delta^3\text{H}$) concentration in the groundwater and springs of the samples collected during the courses of this study.

Borehole, Spring	Sample#	Description	Coordination	$\delta^3\text{H}$ (TU)
Spring	10	(spring 1+2), the main spring at the old entrance of the reserve.	192805/124691	0.8
Borehole	11	Mt.Jericho well 2.	188257/134390	1.3
Spring	12	North east, spring branching in between a group of trees and boshes. Under small bridge.	192908/124518	0.5
Spring	13	Strong stream of water hading to the Dead Sea.	193061/124396	0.3
Spring	14	Strong stream of water hading to the Dead Sea, (beneath a bridge 2m).	193121/124066	0.6
Spring	15	A group of variable paths joined together forming stream passing through formations of marlstone.	193335/123977	0.5
Spring	16	A small path getting stronger after joining to it a big canyon.	193143/124095	0.8
Borehole	17	(feshkha III),60m in depth with artesian preacher.	193112/124086	0.7

Spring	19	a pool rich with vegetation at the spring exit. Water passing underneath the street	192764/123395	0.2
Spring	20	Water passing underneath the street through a rock canal	192725/122848	1.2
Borehole	22	Azarea-1	176610/132018	0.1
Borehole	23	Herodion-1.	170930/118325	1.5
Spring	24	Wade ein al-malh spring	195010/192617	0.6
D.S lake	25	At the southern part of the closed reserve.	192830/122698	3.6
Spring	46	Ein Gadi spring at the natural reserve	164968/128741	0.7
Borehole	50	Azarea-3	173830/112878	0.1
Borehole	51	Beit Fajar-1A.	169607/115110	1.0
Borehole	52	Herodion-4.	169460/114087	0.3
Borehole	53	JWC-4.	170871/121879	0.4
Borehole	54	PWA-1.	167367/112394	0.3
Borehole	55	PWA-3.	171255/120265	0.1
Borehole	57	Arab project-66, Jericho.	197030/141050	0.8
Spring	59	Ein Al-Sultan spring, Jericho.	192155/141952	3.9
Spring	60	Ein Al-Dyouk spring, Jericho.	190110/144645	4.1
Spring	61	Wade Al-Quilt spring.	185622/138165	3.5
Spring	62	Kina spring.	169799/130011	0.7
Borehole	63	Fasael-2.	183059/130210	1.3

6.4 The Radioactive Isotopes Radium and Radon

The radioactivity of groundwater and brines in the area was first measured by Rosenberg almost 50 years ago, (Mazor, 1962). Chan and Chung (1987) noted that, the most important radium flux into the Dead Sea is from springs around the Dead Sea and submerged seepages, though the primary source of the radium is not known. Some additional measurements were made again in the late 1980s (Kronfeld et al., 1991). Unusual concentrations of uranium are found in extensive sedimentary phosphorites and bituminous shales of upper cretaceous age flanking the Dead Sea depression. Ein Feshcha springs are associated sedimentary carbonate rocks [limestone], which form calcareous crusts and cement the graben fill gravels. These crusts also contain secondary accumulations of hydrous manganese oxides and iron oxides as thin black layers (laminae) (figure 6.7). The black laminae, which alternate with aragonite layers, vary in thickness from 0.1 to 5 mm and consist predominantly of MnO_2 , (Nishri, 1982).

The deposits of the sedimentary phosphorites and bituminous shales are considered as a probable source of dissolved U, Ra and Rn to the springs and to the Dead Sea, which conceded as a large reservoir for dissolved Ra (Mazor, 1962 and Kronfeld, 1991).

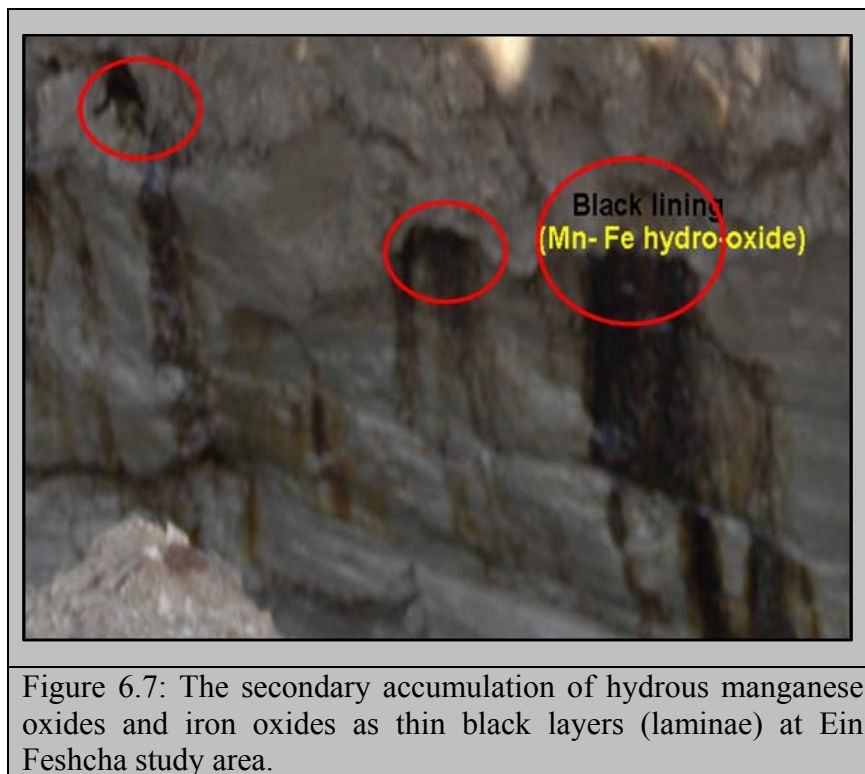


Figure 6.7: The secondary accumulation of hydrous manganese oxides and iron oxides as thin black layers (laminae) at Ein Feshcha study area.

6.4.1 Radium (Ra) and Radon (Rn)

The isotopes ^{223}Ra , ^{224}Ra , ^{226}Ra and ^{222}Rn , belong to both the uranium and thorium series and having different half-lives (11.4 d, 3.66 d, 1,602 yr and 3.83 d respectively).

Radon (^{222}Rn) is a useful geochemical tracer for analyzing groundwater discharge due to facts that are ^{222}Rn is greatly enriched in groundwater relatively to seawater by three or four orders and it can be measured at very low concentration (Cable, 1996, Lambert and Burnett, 2003.). Because ^{222}Rn is a noble gas, its distribution throughout the aquifer should be uniform, and not affected by changes in salinity. The ^{222}Rn content at Ein Feshcha area was first measured by Rosenberg (unpublished reports cited by Mazor, 1972). His data include four repeated measurements together with the corresponding discharges. It was shown that the total ^{222}Rn discharge was constant, although the water discharge varied seasonally. This indicates that the waters he investigated are a mixture of brine waters and seasonally varying amounts of meteoric groundwaters.

^{222}Rn activities in the groundwater obtained from springs located around the Dead Sea (Ein Feshcha springs) shows big variation. Two samples represent ^{222}Rn enriched and ^{222}Rn poor waters flow in what appears to be lithologically identical fill at a depth difference of 5 to 60 m. Its activities ranged from 4560 Bq.m^{-3} to 786250 Bq.m^{-3} . The maximum value was 786250 Bq.m^{-3} in the main spring (65) with EC 4.16 mS/cm and the minimum measured value was 4560 Bq.m^{-3} in sample number (69) with EC 21.2 mS/cm which represents Feshcha-III well, whereas the samples of the catchment area shows variation in ^{222}Rn activities ranged from 2450 Bq.m^{-3} as a minimum value representing PWA-1 well, while the maximum value was 11720 Bq.m^{-3} tapping Azarea-1 well, (table 6.3). ^{222}Rn being the daughter product of ^{226}Ra and both nuclei are formed in the ^{238}U decay series.

Radium (^{226}Ra) concentrations in the groundwaters of the Rift Valley are a reflection of ^{226}Ra enrichment in the brines at depth. The ^{226}Ra activity for the analyzed samples during the course of this study ranges from a low values of 0.003 Bq/l in Mt.Jericho-2 well to high value of 0.779 Bq/l in Feshcha-III well (table 6.3), this means ^{226}Ra -rich sources are located at Ein Feshcha study area, on the shore of the Dead Sea and not from the meteoric waters. Fresh water samples from the catchment area with low chloridity show low ^{226}Ra and hence low ^{222}Rn content, (figure 6.8). The water samples plotted on figure 6.8 show two trends, some samples show a positive correlation between ^{226}Ra when plotted versus Cl, whereas inverse relation tacking place as the Cl concentration increases to $>5000 \text{ mg/l}$, ^{226}Ra decreases leading to a decrease in ^{222}Rn value, two samples represent this situation sample number 69 (Feshcha-III) and sample number 82. Thus it can be expected that very recent mixing between the saline brine and a meteoric freshwater component is tacking place at Ein Feshcha area.

All water samples contain high activity values of ^{222}Rn over dissolved ^{226}Ra , all waters show disequilibrium between the parent and daughter nuclide, the $^{222}\text{Rn}/^{226}\text{Ra}$ ratio being $\gg 1$. Obviously, the radioactive elements found in these solutions cannot be as ancient as the salts, because they would have decayed long ago to background values, this mean that ^{226}Ra isotopes are continuously being replenished in the saline brine end members.

The $^{222}\text{Rn}/^{226}\text{Ra}$ value is between 418 and 668.75 in fresh waters with Cl content below 100 mg/l, whereas the $^{222}\text{Rn}/^{226}\text{Ra}$ value is below 100 in waters with Cl content above 4,000 mg/l except spring number 82, which shows $^{222}\text{Rn}/^{226}\text{Ra}$ value of 1361 with Cl content 4821 mg/l, another group of springs can be distinguished with $^{222}\text{Rn}/^{226}\text{Ra}$ value ranging between 1126 to

1695 with Cl content ranging between 1154 to 2659 mg/l (table 6.3). This variation in distribution over a small area indicates different and separate mechanisms controlling the spring system in the area.

The $^{222}\text{Rn}/^{226}\text{Ra}$ activity ratio increases with the decreasing chloridity after mixing of brines with fresh waters. In some springs at Ein Feshcha group, as their salinity decreases, the $^{222}\text{Rn}/^{226}\text{Ra}$ activity ratio increases (figure 6.9). The highest $^{222}\text{Rn}/^{226}\text{Ra}$ activity ratio 1695 is observed in the low salinity main spring (spring number 65) compared to the more saline deeper waters Feshcha-III well which have a $^{222}\text{Rn}/^{226}\text{Ra}$ activity ratio of only 54. Obviously, since the $^{222}\text{Rn}/^{226}\text{Ra}$ activity ratio in the diluted waters is much higher than in the concentrated brines, the former cannot be a dilution product of the latter. The high ratios are expected to be the result of dominant adsorption of ^{226}Ra from the up flowing brine waters to the lining of the water bath which contains hydrous manganese oxides and iron oxides.

The highest ^{222}Rn activity is measured in the southern Rift Valley at Ein Feshcha at surface averages 47,160 Dpm/l, whereas at depth the activity is about 274 Dpm/l at Feshcha-III well. Hence, in contrast to ^{226}Ra that is transported from the deeper water to the surface, ^{222}Rn is derived locally, close to the surface. The conclusion that ^{222}Rn is enriched very close to the emergence of the waters has been reached by several researchers before, (Steinitz et al., 1995). The variability in the ^{222}Rn activity is at least in part explained by variance of the tectonic activity along the Dead Sea transform (Steinitz et al., 1995).

This study suggests that the ^{222}Rn enriched and ^{222}Rn poor waters found at very small distances at Ein Feshcha group can be explained by assuming an inhomogeneously high ^{226}Ra activity accumulation probably due to adsorption of ^{226}Ra to the surface laminae (surface bound Ra, whether it is bound to an organic coating the bituminous shales or to inorganic surface siliceous oxide or Mn-Fe hydro-oxide) which coats the surfaces of the water conduits and cracks.

Sample number 69 (Feshcha-III well) represents an artesian well characterized with minimal $^{222}\text{Rn}/^{226}\text{Ra}$ activity ratio of 54, this sample could represent the nearby submarine brines mixed with meteoric waters having low ionic strength and thus the ^{226}Ra mobility (and hence activity) in the water decreases, ^{226}Ra is scavenged and coprecipitates, so it is fixed in the sediments by Mn oxides, whereas sample number 70 (pesometer EZ-5) characterized with high $^{222}\text{Rn}/^{226}\text{Ra}$ activity ratio of 1312, can be explained by the adsorption of the ^{226}Ra to the

lamina Mn-Fe layers lining the water path. And those samples rich with ^{222}Rn are to be considered as a result of mixing with fresh waters that are deficient in ^{226}Ra , Mn and Fe, which is characteristic of the waters of the Judea Group carbonate aquifer, in which ^{226}Ra and ^{222}Rn value is low (table 6.3). This means that the ^{226}Ra is derived from other sources than that of fresh water.

Two springs 71 and 72 represent the saline brines with EC of 13.12 mS/cm, these samples have the highest ^{226}Ra value compared to the other samples. These two samples could represent the saline brines that might desorb ^{226}Ra from the lining of the water bath. The high ^{226}Ra content appears to be fault controlled for transferring water from the depth. Water mixing is not likely, this result is in agreement with the hydrochemistry results and since Ra and Rn value is almost the same this suggest same water source for these two samples.

The two naturally occurring, short-lived radium isotopes (^{223}Ra and ^{224}Ra) were analyzed in attempt to identify wither the source of Ra and Rn in groundwater is from ^{235}U and/or from ^{232}Th . ^{223}Ra is a member of the uranium (^{235}U) decay chain while ^{224}Ra , is a member of the thorium (^{232}Th) decay chain.

The measured activity ratios of $^{222}\text{Rn}/^{223}\text{Ra}$ and $^{222}\text{Rn}/^{224}\text{Ra}$ in groundwater may reflect the U/Th ratios in the analyzed water samples. The very high activity ratio of $^{222}\text{Rn}/^{223}\text{Ra}$ and $^{222}\text{Rn}/^{224}\text{Ra}$ (table 6.3) indicates that the main source of ^{222}Rn and ^{226}Ra in the study area is ^{238}U and the contribution from ^{232}Th and ^{235}U is very small.

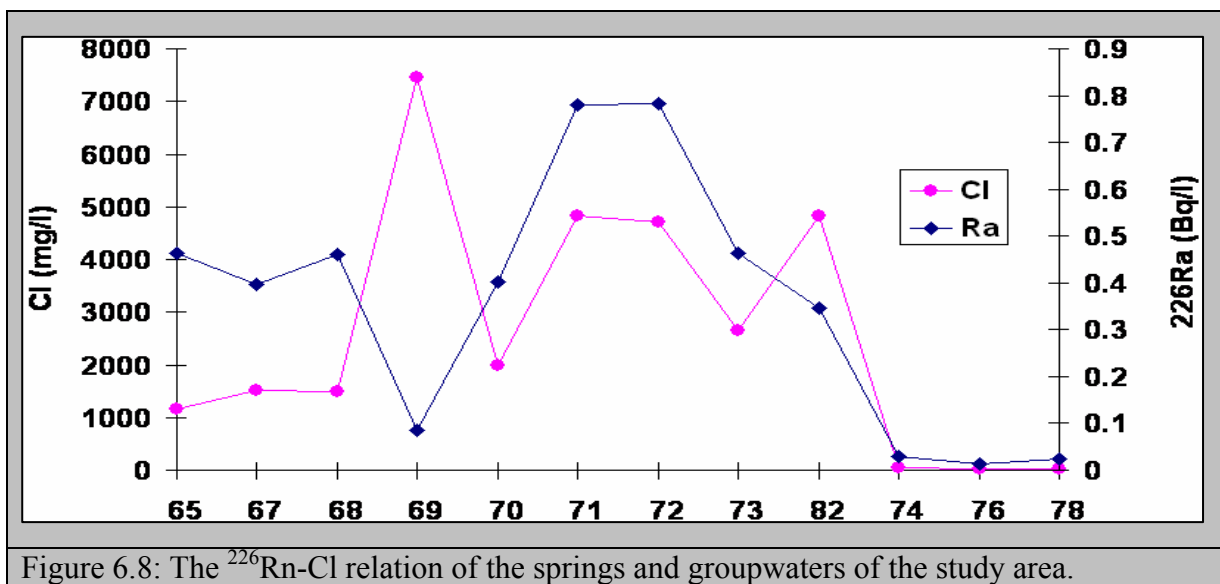


Figure 6.8: The ^{226}Rn -Cl relation of the springs and groupwaters of the study area.

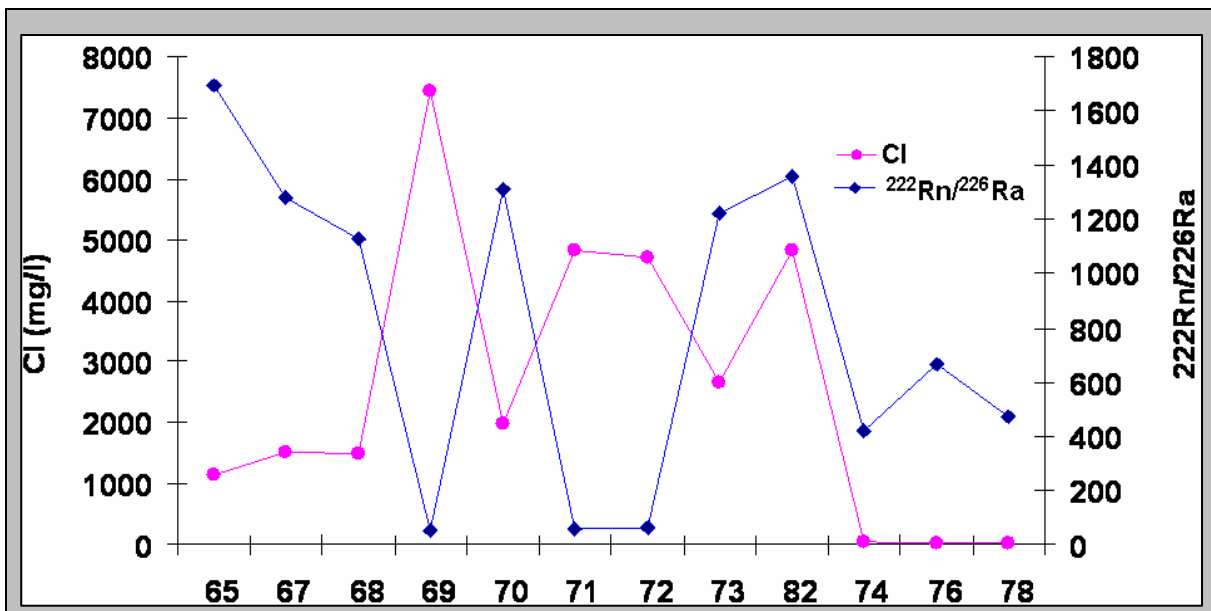


Figure 6.9: $^{222}\text{Rn}/^{226}\text{Ra}$ activity ratios vs. Cl of the springs and groupwaters of the study area.

Table 6.3: shows the ^{222}Rn concentrations and electrical conductivity for Ein Feshcha springs and the catchment area wells.

Sample ID	Cl	EC	^{222}Rn	^{226}Ra	^{223}Ra	^{224}Ra	$^{222}\text{Rn}/^{226}\text{Ra}$	$^{222}\text{Rn}/^{223}\text{Ra}$	$^{222}\text{Rn}/^{224}\text{Ra}$
	mg/l	mS/cm	Bq/l	Bq/l	Bq/l	Bq/l			
65	1154	4.16	786.25	0.464	0.00098	0.0026	1694.5	802296	302404
66	99	0.46	ND	0.003	0.00093	0.0031	ND	*ND	ND
67	1507	4.97	509	0.398	0.00098	0.0035	1278.89	519388	145429
68	1493	4.82	518.02	0.46	ND	ND	1126.13	ND	ND
69	7445	21.2	4.56	0.085	ND	ND	53.65	ND	ND
70	1985	6.13	526.28	0.401	ND	ND	1312.42	ND	ND
71	4821	13.11	46	0.779	ND	ND	59.05	ND	ND
72	4721	13.12	48.05	0.782	ND	ND	61.45	ND	ND
73	2659	4.36	566.54	0.463	ND	ND	1223.63	ND	ND
74	42.6	0.61	11.72	0.028	ND	ND	418.57	ND	ND
75	43	0.57	10.79	0.025	0.00232	0.0075	431.6	4651	1439
76	22.9	0.53	8.56	0.0128	ND	ND	668.75	ND	ND
77	32	0.51	6.75	0.059	0.00199	0.0016	114.41	3392	4219
78	28.3	0.53	11.39	0.024	0.0011	0.0033	474.58	10355	3452
79	36	0.61	9.7	ND	0.00162	0.004	ND	5988	2425
80	24.8	0.55	2.45	0.006	0.00047	0.0012	408.33	5213	2042
81	27	0.59	7.46	0.007	0.00052	0.0021	1065.71	14346	3552
82	4821	5.04	471	0.346	ND	ND	1361.27	ND	ND

*ND: Not Determined

6.5 Summary of Results

6.5.1 Water Isotopes Composition in Selected Water Samples (^2H , ^{18}O , ^3H , Rn and Ra)

The stable isotopic data of the springs and groundwater wells tapping various aquifers (Marsab-Feshcha catchment), were plotted on the $\delta^{18}\text{O}$ – $\delta^2\text{H}$ diagram, figure 6.1, showing that the water samples distributed to the left of the EMWL, indicating that these fresh waters are originating from the local mountain aquifer and could be tapping the lower cenomanian aquifer, the differences in the isotopic compositions ($\delta^2\text{H}$ and $\delta^{18}\text{O}$) between these samples are not so large. Some of the groundwater samples plotted on figure 6.1 fall along the LMWL, indicating secondary processes taking place, such as evaporation prior infiltration or isotope exchange with aquifer rocks, while other group of samples representing the wet season, show values lie below the LMWL in which these samples are reflecting secondary fractionation by evaporation prior to infiltration.

In the $\delta^{18}\text{O}$ – $\delta^2\text{H}$ cross plot in figure 6.2, the water samples during the dry-wet season are clustered near the LMWL, during the wet season several changes took place, showing a possible evidence of mixture of different aged water bodies. The deviation of the springs and wells from the LMWL indicates that either the water has experienced some degree of evaporation relative to the local rain, and/or that it contains some isotopically enriched water from the Dead Sea evaporates and/or mixing with old brines. The dashed line presented in figure 6.2 represents the evaporation line in which sample 17-37 (Feshcha-III) fall on the path of evaporation, during the wet season this well shows depletion in $\delta^2\text{H}$ and $\delta^{18}\text{O}$, representing mixing mechanism with other source of lighter waters causing isotopic depletion due to dilution.

Ein Feshcha samples can be related to a freshwater – brine water mixing trend if Cl values are compared with those of $\delta^{18}\text{O}$, while they fall largely outside the mixing trend deviating toward the evaporation trend when $\delta^2\text{H}$ values are taken into account (figure 6.3), this could be attributed to different and independent processes: evaporation, water rock interaction and mixing with isotopically modified waters. The $\delta^{18}\text{O}$ -Cl ratios of the selected water samples rule out any processes to explain the observed heavy isotopic compositions, while $\delta^2\text{H}$ -Cl ratios of the selected samples fit with the groundwater/evaporation line.

The plot of $\delta^{18}\text{O}$ - $\delta^2\text{H}$ vs. TDS (figure 6.4) showing mixing between meteoric waters (isotopically lighter) and salty waters (isotopically heavier). The samples in the study area are

clustering along the mixing line in which the salinity (TDS) is related to $\delta^{18}\text{O} - \delta^2\text{H}$, which confirm the presence of common seated brine that mixes with groundwater in variable amounts.

Ultra filtration caused by the high clay content found in the area lead to slight enrichment of both $\delta^2\text{H}$ and $\delta^{18}\text{O}$ accompanied with an increase in Ca and Mg concentrations in the water samples and hence it may explain the CaCl_2 and MgCl_2 water types in the area.

With stable isotopes no clear evidence show that evaporation brine play an important role for salinisation of groundwater within the rift graben, there is more evidence for dissolution of salts.

Depending on $\delta^3\text{H}$ values for the groundwater in the Marsaba-Feshcha study area presented in table 6.2 and figure 6.6 it can be concluded that Ein Feshcha waters are originated from deferent aquifers. Kina spring and Ein Gadi spring shows tritium value of 0.7 TU, indicating possible mixing of sub-modern to modern age waters representing fresh water discharge from the upper and lower aquifer.

Tritium units ranging between 0 - 1.2 TU might reflect a mixing of recent age water infiltrated from wadis runoff through the alluvium fane with deep old water characterized by high salinity. The low $\delta^3\text{H}$ values indicate that transport time from the recharge zone in the mountain areas is more than 40 years.

According to the figures 6.3, 6.4 and 6.6 a mixing process between freshwaters of meteoric origin and significantly evaporated and isotopically modified brines ($\delta^{18}\text{O} - \delta^2\text{H}$) because of salts dissolution, seems to better explain the observed $\delta^3\text{H}$, $\delta^2\text{H}$ vs. $\delta^{18}\text{O}$ trend for the water samples.

All water samples contain high activity values of ^{222}Rn over dissolved ^{226}Ra , all waters show disequilibrium between the parent and daughter nuclide, the $^{222}\text{Rn}/^{226}\text{Ra}$ ratio being $\gg 1$. Obviously, the radioactive elements found in these solutions cannot be as ancient as the salts, because they would have decayed long ago to background values, this mean that ^{226}Ra isotopes are continuously being replenished in the saline brine end members.

The ^{226}Ra activity for the analyzed samples during the course of this study ranges from a low values of 0.003 Bq/l in Mt.Jericho-2 well to high value of 0.779 Bq/l in Feshcha-III well (table 6.3), this means ^{226}Ra -rich sources are located at Ein Feshcha study area, on the shore of the Dead Sea and not from the meteoric waters.

The water samples plotted on figure 6.8 show two trends, some samples show a positive correlation between ^{226}Ra when plotted versus Cl, whereas inverse relation taking place as the Cl concentration increases to >5000 mg/l

The $^{222}\text{Rn}/^{226}\text{Ra}$ activity ratio increases with the decreasing chloridity after mixing of brines with fresh waters. In some springs at Ein Feshcha group, as their salinity decreases, the $^{222}\text{Rn}/^{226}\text{Ra}$ activity ratio increases (figure 6.9). The highest $^{222}\text{Rn}/^{226}\text{Ra}$ activity ratio 1695 is observed in the low salinity main spring (spring number 65) compared to the more saline deeper waters Feshcha-III well which have a $^{222}\text{Rn}/^{226}\text{Ra}$ activity ratio of only 54. Obviously, since the $^{222}\text{Rn}/^{226}\text{Ra}$ activity ratio in the diluted waters is higher than in the concentrated brines, the former cannot be a dilution product of the latter. The high ratios are expected to be the result of dominant adsorption of Ra from the up flowing brine waters to the lining of the water bath which contains hydrous manganese oxides and iron oxides.

This study suggest that the ^{222}Rn enriched and ^{222}Rn poor waters distributed over small distances at Ein Feshcha group can be explained by assuming an inhomogeneously high ^{226}Ra activity accumulation probably due to adsorption of ^{226}Ra to the surface lamina which coats the surfaces of the water conduits and cracks as presented in figure 6.10.

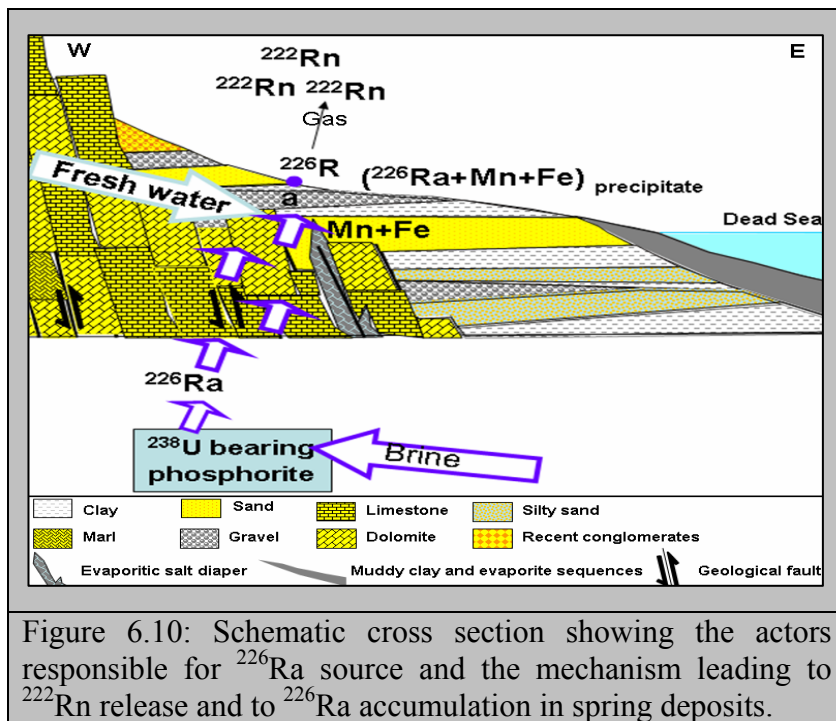


Figure 6.10: Schematic cross section showing the actors responsible for ^{226}Ra source and the mechanism leading to ^{222}Rn release and to ^{226}Ra accumulation in spring deposits.

7 GEOPHYSICAL RESISTIVITY ANALYSES

Geophysical resistivity techniques are based on the response of the earth to the flow of electrical current. In the shallow subsurface, the presence of water controls much of the conductivity variation. Measurement of the resistivity is a measure of the amount of water saturation and connectivity of pore space. Increasing water content and increasing salinity of the underground water will decrease the measured resistivity. So, increasing porosity of rock and increasing number of fractures will tend to decrease measured resistivity if the voids are water filled.

In the past, in 1997, Time Domain Electromagnetic Sounding (TDEM) was executed in the whole area along the western coast of the Dead Sea, to outline the interface limits between freshwater and brackish or saline water bodies (Kafri et al., 1997).

The present study was carried out due to the scarcity of boreholes, which could provide information about the main groundwater flow paths, the fresh-saline water interface, the freshwater bodies, the saline water bodies and the depth of these bodies. Therefore geophysical methods were applied to get information about these topics. Vertical Electric Soundings (VES) and the method of measurement of the Natural Pulsed Electromagnetic Field of the Earth (NPEMFE) were applied. The electric soundings had to bring information about fresh, brackish or saline water bodies in the underground, but also information about the geological structure until 100m depth. The special electromagnetic measurements were applied to bring direct information about fractures and rupture zones in the underground.

7.1 Vertical Electric Sounding

In the Vertical electric sounding (VES) method, an electrical current passed through the ground and two potential electrodes allow us to record the resultant potential difference between them, giving a direct measure of the electrical impedance of the subsurface material. Since the resistivity of a water-bearing formation decreases with increasing salinity of the groundwater, this method is suitable for detecting variations in the salinity of the groundwater to a depth of 100m compared to common geoelectrical methods. Difficulties for the interpretation of the data occur since a varying resistivity of a formation may result from changes in lithology and/or changes in water salinity. The source of the salinity at Ein Feshcha

area is assumed to be either highly saline sediments or underlying brines. These sources can be distinguished by their resistivity.

The electric properties are influenced by the lithology, the saturation degree and the salinity of the fluids involved, salt water can be easily distinguished from almost any lithological combination, having a resistivity below 1 Ohm/m. It was found that resistivities below 1 Ohm/m and mostly below 0.6 Ohm/m are typical of the concentrated brines in the Dead Sea region which might be partly diluted (Kafri et al., 1997). Yechieli et al., (1993) noted that the resistivity of the Dead Sea brine in the subsurface along the Dead Sea shore was found to be 0.25 Ohm/m. Resistivities below 2 Ohm/m are entirely indicative of water salinity in the range of normal seawater, and cannot be a result of any lithological combination. Generally resistivities above 3 Ohm/m are considered for fresh water (Palacky, 1987). Values between 1 - 3 Ohm/m are attributed to brackish water, as indicated in figure 7.1 which presents the resistivity value range for different lithologies and different water types. In the year 1997 in unpublished report Goldman proposed guidelines for comparing water quality (TDS) by resistivities in this specific area:

Resistivity [Ohm/m]	Label	TDS [mg/l]
> 3	Fresh	1000 – 2000 mg/l TDS,
3 to 2	Brackish	2000 – 10000 mg/l TDS ,
< 2	Saline	> 10000 mg/l TDS,
< 1	Brines	Dead Sea saltwater intrusion.

The sounding measurements at Ein Feshcha site was performed by using a high performance field-instrument, the VES-SYSCAL R2 from IRIS-Instruments, France. To get information from 100m depth, the AB-line was extended until 300m long on both sides of the center of MN (for more details refer to chapter four). For each sounding point 34 measurements were performed in order to get a complete sounding curve. At Ein Feshcha study area three profiles were modeled and studied. The site map, figure 7.2 presents the three modeled profiles using VES-SYSCAL R2 instrument. Along the three profiles a total of 19 sounding points were carried out. By using the Zhody software the final resistivity values for different depths were obtained in order to look for anomalous regions.

The 19 sounding points are plotted on Google satellite map figure 7.3; were the three profiles can be seen. Along these three profiles, vertical sections are elaborated, showing the distribution of the apparent resistivity in the depth.

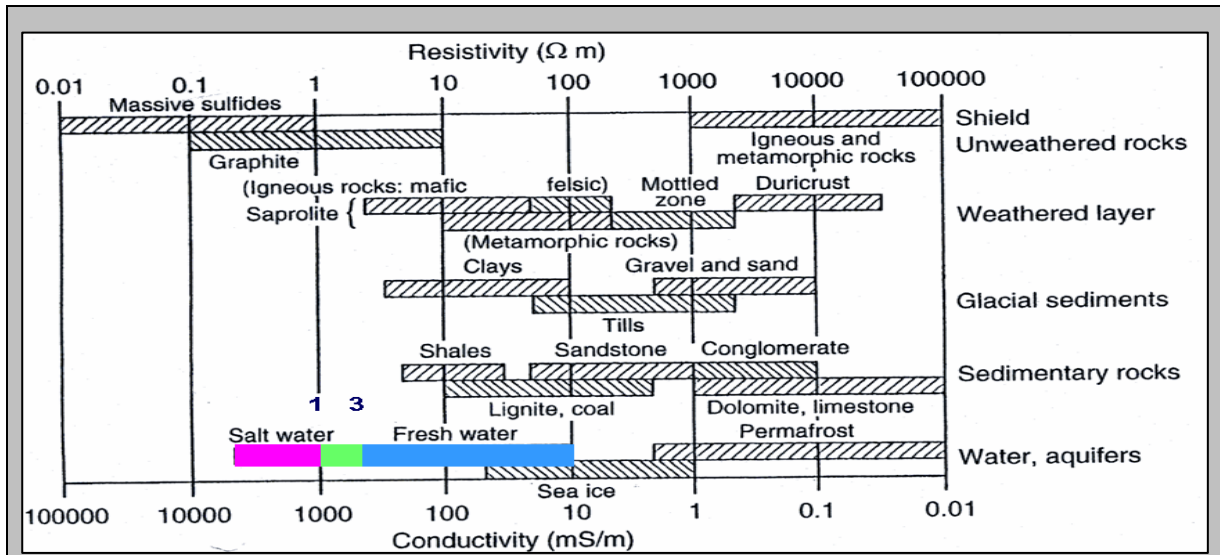


Figure 7.1 : Electric resistivities of different lithologies and waters with different salinities (after Palacky, 1987)

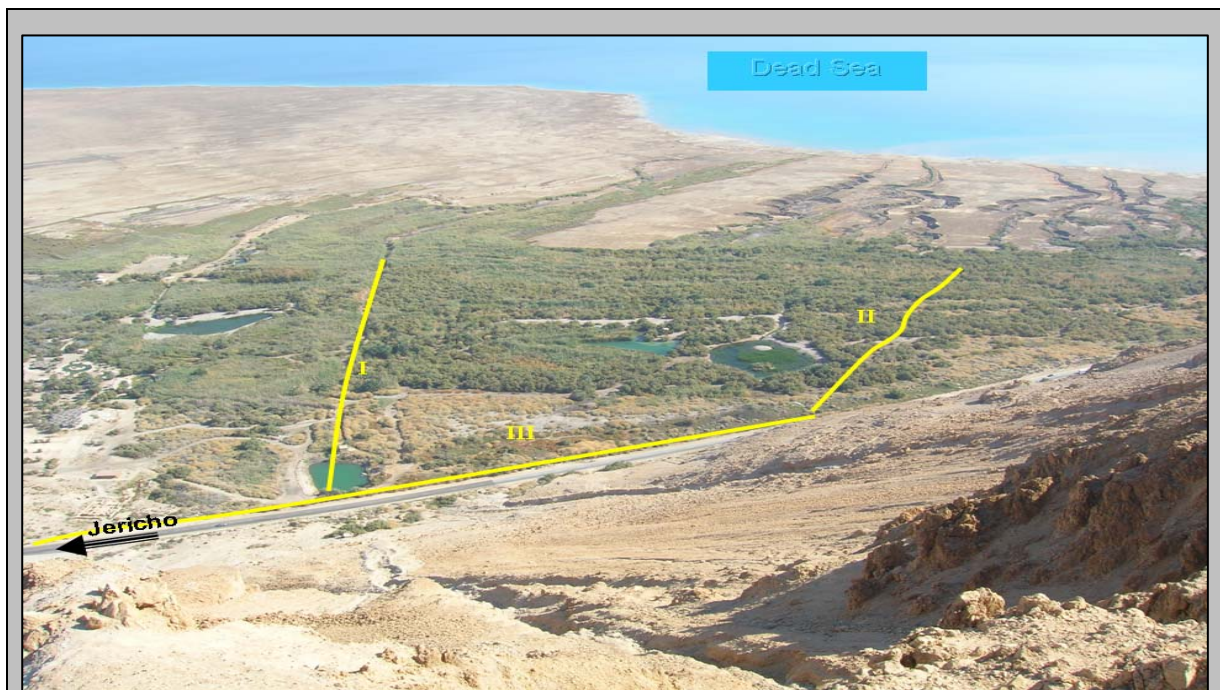


Figure 7.2: Photograph presenting the location site at Ein Feshcha natural reserve. It shows the location of the three profiles and the main topography of the area.

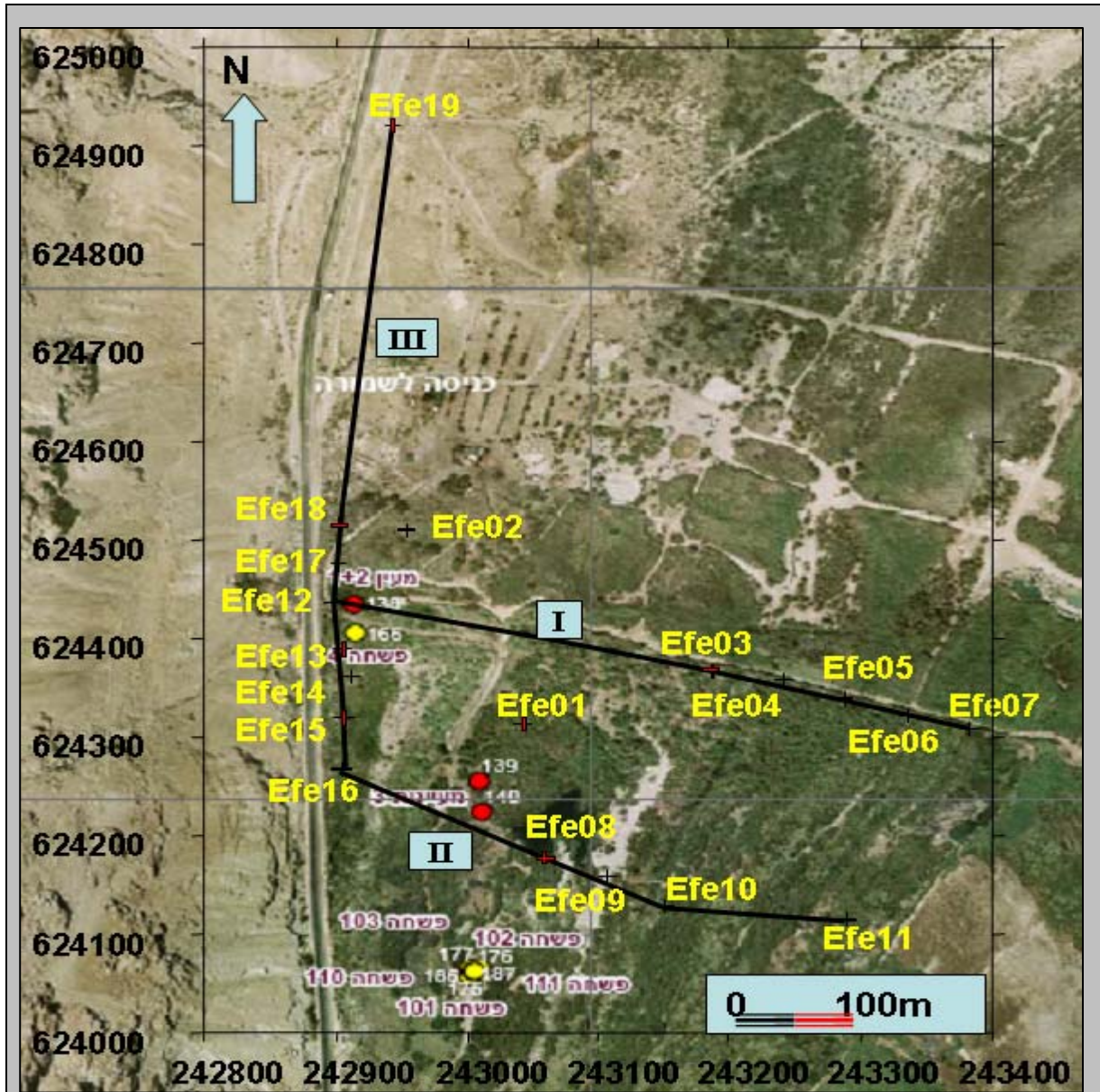


Figure 7.3: Satellite map with the localization of the 19 VES-soundings on three profiles.

7.1.1 Profile I

The vertical section along profile-I, figure 7.4, extend from the West with the coordination of (624435/242900) to the East with the coordination of (624312/243385), starting from the main spring (1+2) and extending toward the Dead Sea to the East. This profile composed of 8 sounding points, in the Western part of this section a large development of resistivity values ranges between 3 – 15 Ohm/m can be seen, suggesting the existence of fresh water over the

whole investigated depth interval of 100m. This domain corresponds to the area around Ein Feshcha main spring (1+2). This fresh water is being mixed with trapped saline waters leading to dilution of these saline pockets. Mixing tacks place at the vicinity of the spring at least at two points, this can be seen from the chemistry of the borehole loge Feshcha-4. The chemical analysis and the lithology of borehole Feshcha-4 is presented in figure 7.5 which shows that the salinity increases with increasing depth up to the depth of 37.5m in which the maximum salinity values were EC: 26.5mS/cm, Br: 166mg/l and TDS: 16147mg/l, afterwards the salinity decreases with increasing depth in which the values were lowered to EC: 11.4mS/cm, Br: 57mg/l and TDS: 6378mg/l at the maximum depth of the borehole 49.5 m. This separation in mixing points could be attributed to the oily greenish clay layer found at the depth (32m) with thickness around 4m. This layer separates the upper layers from the lower layers. Several meters to the East two springs are exposed having the same chemical characteristics of the main spring (1+2) which could explain the source of water drainage from the lower layers.

In the Eastern part of the section, between the sounding points 5-7 at distance of 350 to 490 meter along profile-I, starting from the depth of 60m downward, high resistivity values up to 500Ohm/m were measured, suggesting a sedimentary rocks overlaid with sedimentary block from the late Pleistocene epoch. The borehole Feshcha-10 at figure 7.5, presents the Eastern lethology of profile-I, it shows that late Pleistocene - Holocene sediments are dominating the area up to the depth of 38m and more. The sedimentary rocks are probably a block of limestone. Figure 7.6 presents field evidence for these sedimentary rocks which is exposed at the field site several meters to the East from the main street orienting South-North direction. This block acts as a barrier in the advancing of saline water intrusion from the Dead Sea to the West not only but also it prevent the trapped water to retreat to the East, evidenced by low resistivity values, <1 Ohm/m. At sounding point 4, at distance of 300 to 350 meter on profile-I, local low resistivity values suggest possible trapped saline/brackish water, behind the assumed clay-limestone block.

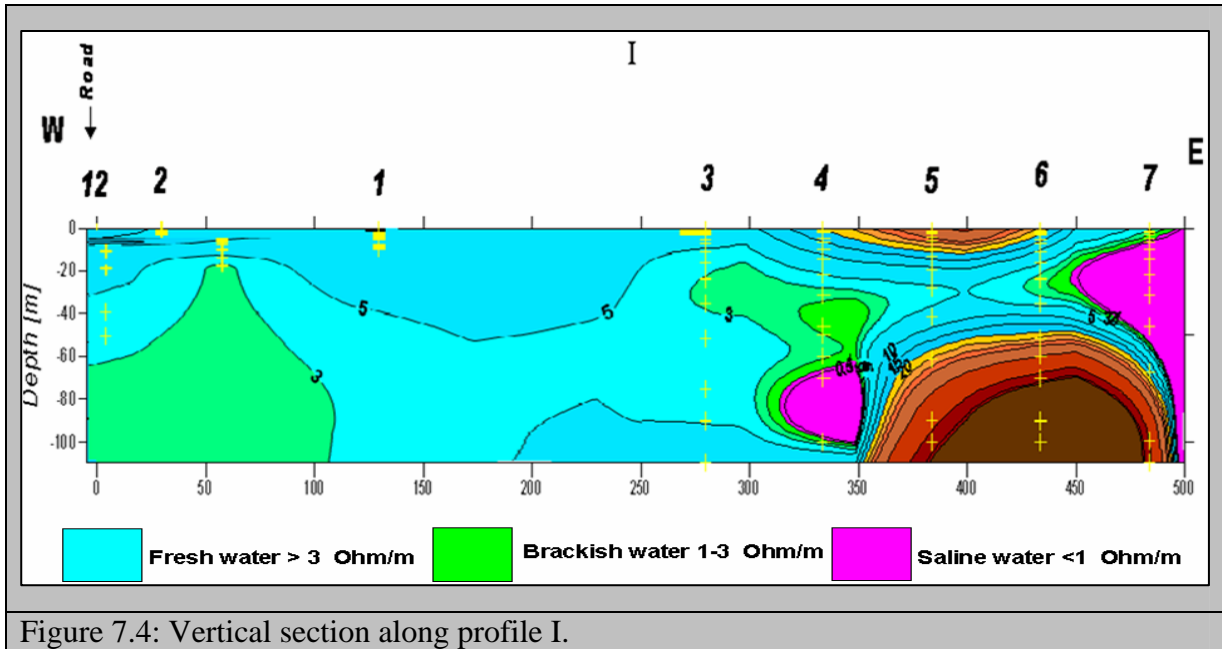


Figure 7.4: Vertical section along profile I.

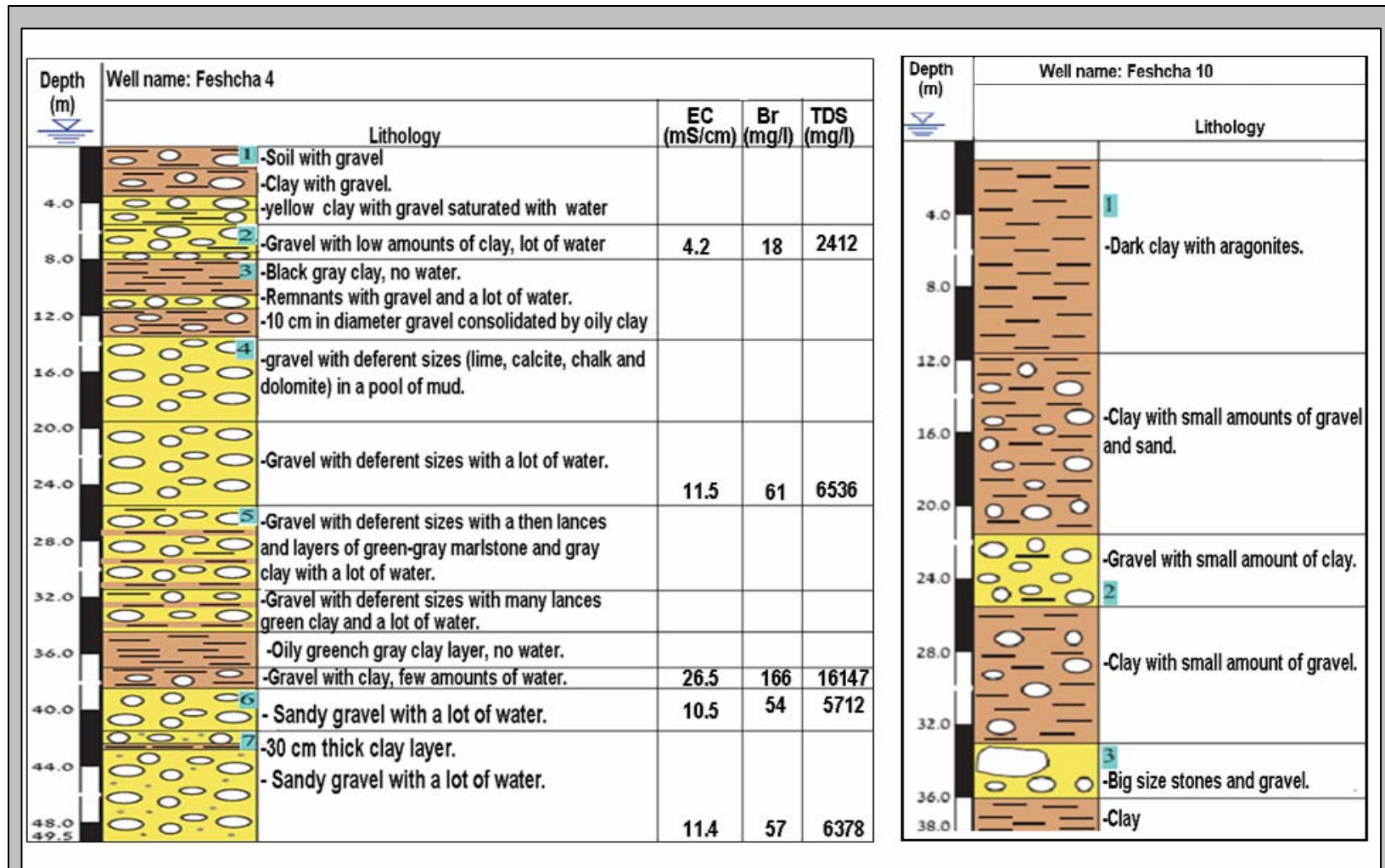


Figure 7.5: Lithological section presenting the lethological setting of borehole Feshcha-4 and Feshcha-10 (modified after GSI, 2006).

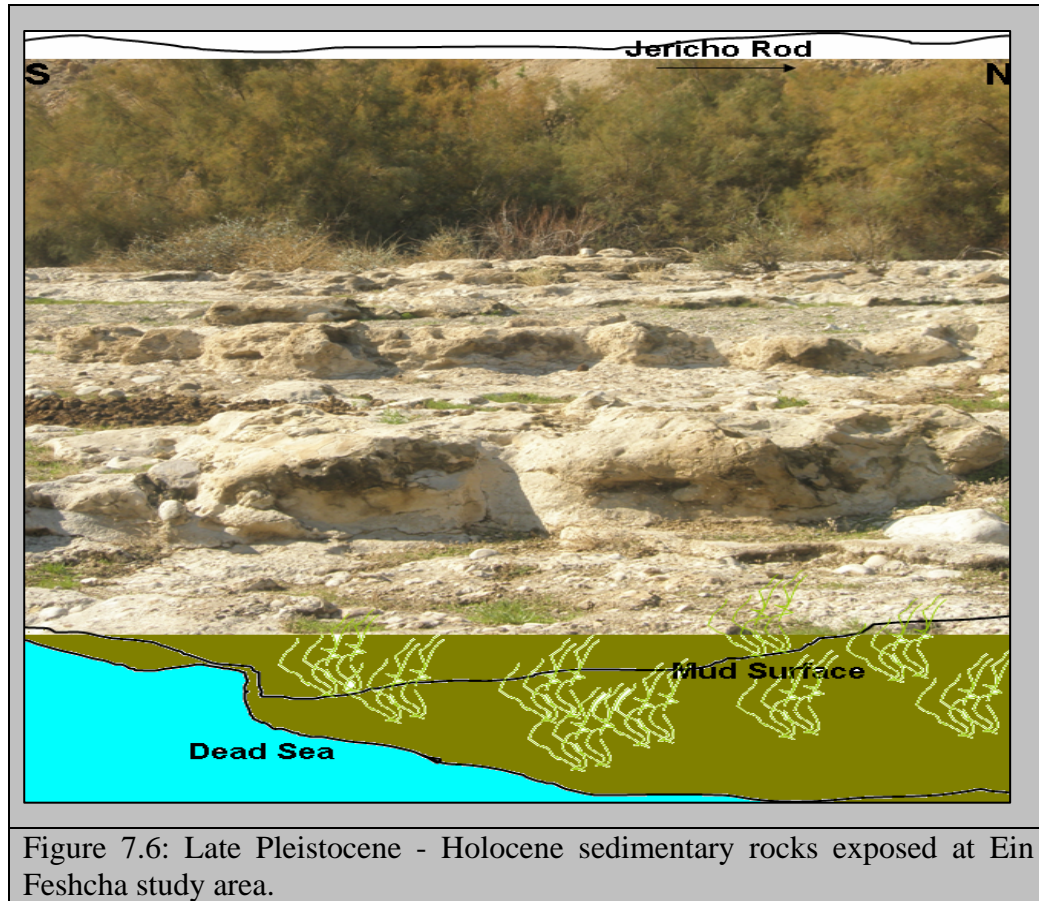


Figure 7.6: Late Pleistocene - Holocene sedimentary rocks exposed at Ein Feshcha study area.

7.1.2 Profile II

Profile-II extends also from the West (624263/242910) to the East (624114/243290), from the road toward the Dead Sea (figure 7.3). This profile composed of 5 sounding points. The vertical section elaborated along this profile (figure 7.7), shows that through the distribution of resistivities of the measured sounding points, at the depth interval 30-100m at sounding point 11 resistivity values ranges between 0.35 –0.8Ohm/m at distance of 350 to 400 meter on profile-II.

According to Goldman guidelines, these low resistivity values $\ll 10\text{Ohm/m}$ are considered as brine waters and there source could be attributed to precursors of trapped Dead Sea saltwater or a retreat of Dead Sea saline waters.

These low resistivities extend toward the East through sounding point 10 until sounding point 9 in the West at distance of 200m; this saline water is surrounded by a zone of brackish water. Near the surface, until the depth of 20m the measured resistivity values suggest the existence

of fresh water. In the Western part of the section the values suggest the existence of fresh water, but over a smaller depth interval than of profile-I.

At the Western side of profile-II at the depth of 60m and more a mass of late Pleistocene - Holocene sediments (clay, gravel and shales) is identified working like an aquiclude.

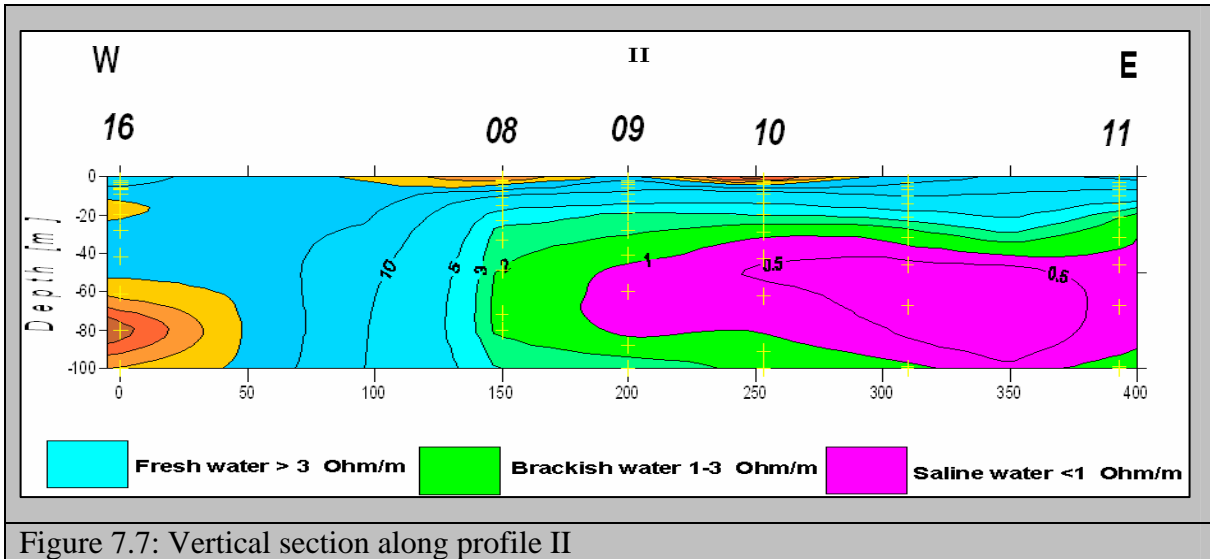


Figure 7.7: Vertical section along profile II

7.1.3 Profile III

Profile-III is located along the road, in the North-South direction as presented in figure 7.3. The coordination points of the beginning of this profile are, (624920/242944) while the end of the profile was at the coordinate of (624263/242910). This profile composed of 8 sounding points. On the vertical section along this profile (figure 7.8), can be seen values of resistivities greater than 3Ohm/m around the main spring suggesting the existence of fresh water until a depth of 100m. To the South of the main spring, on sounding points 14, 15 and 16, higher resistivity values were measured, suggesting the existence of sedimentary rocks overlaid with late Pleistocene - Holocene sediments (tills and clays) block, forming a barrier in the fresh groundwater flow along the North-South oriented main fault system. In the Northern part of this section, at sounding point 19, the measured resistivity values suggest fresh water at greater depth, below 80m and rising up in the Southern direction toward the main spring. Between the sounding points 18 and 19, at distance of 25 to 325 meters on profile-III, the soil was very dry may be due to the existence of tills filling the main fault system, the 34 resistivity measurements were not possible, therefore with the help of the available data and Zhody

software the expected missing part is presented in figure 7.8b. The simulated results at this section suggests the existence of tills and limestone blocks, forming a barrier in the fresh groundwater flow along the North-South oriented main fault system. Exposed sedimentary rocks at the field site can be seen (figure 7.6). At sounding point 18 low resistivity values were identified ranging between 1-3 Ohm/m indicating existence of localized brackish water zone at the depth of 30 up to 60 m. Very close to the main spring between sounding points 12 and 13 a mass of brackish water was identified with resistivity value ranging between 1-3 Ohm/m indicating existence of localized brackish water zone at the depth of 30 up to 100 m finding its way out in the main spring.

Since these two localized zones are surrounded with fresh water then it can only be explained by a salt dissolution from the surrounding rocks (salt diaper) and/or conduction of saline waters through associated fractures.

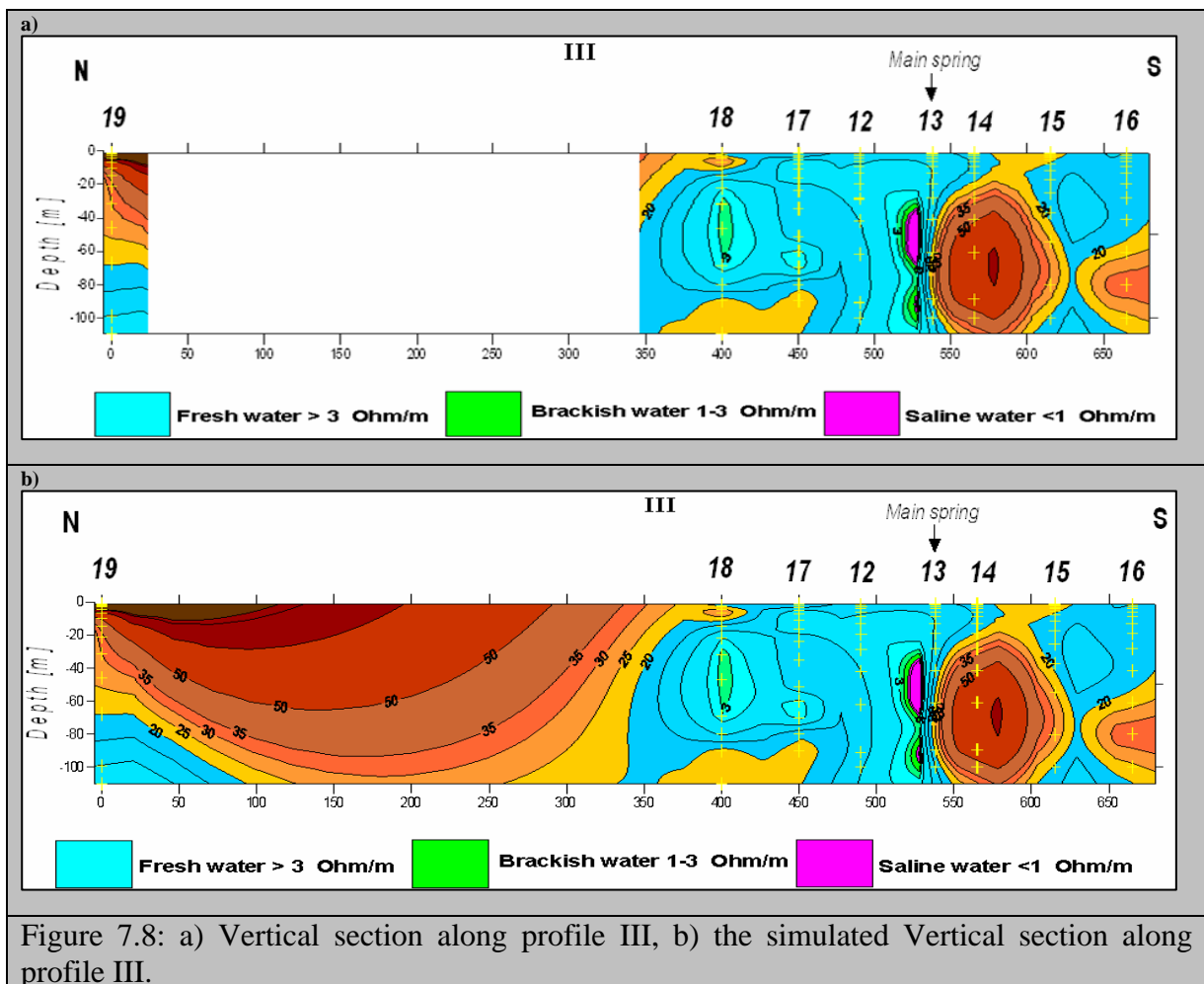


Figure 7.8: a) Vertical section along profile III, b) the simulated Vertical section along profile III.

7.2 Electromagnetic Radiation (EMR)

Along Ein Feshcha natural reserve borders in a North-South direction along the main fault system a profile was constructed in order to localize the fractures and rupture zones in the underground. This profile was explored using the Electromagnetic Radiation (EMR) reflecting the orientations of active crustal stresses in the uppermost lithosphere. The beginning of the explored profile was at the coordinate (625000/242800) and the end of it was at the coordinate (624000/242800).

Along this profile several scans East-West direction was carried out using the high-sensitive geophysical electromagnetic instrument CERESKOP depending on the NPEMFE-method (Natural Pulsed Electro Magnetic Field of the Earth).

Through the NPEMFE-method a lot of fractures were identified, mainly along the main fault system of the Dead Sea Rift, but also two transversal faults perpendicular with the main fault, one of them crossing the main fault at the main spring (1+2). The first transversally fault can be seen in the field, extending in an East-West direction heading to the Dead Sea cliffs (figure 7.9a) instrumentally this fault has been detected using the CERESKOP and it is plotted on figure 7.10. The other one is located at Ras Feshcha farther to the South figure 7.9b. This fault needs to be studied in more details. Figure 7.11 presents field evidence regarding the East-West direction of the transversally faults and cracks. These cracks could explain the leakage of fresh water from the main fault barrier leading to the formation of several springs with variable chemical components.

From the results of the localized fractures, it confirms the horizontal orientations of active crustal stresses direction parallel to the main fault system. The coordination of the 9 parallel fractures and the transversally fault are presented in table 7.1.

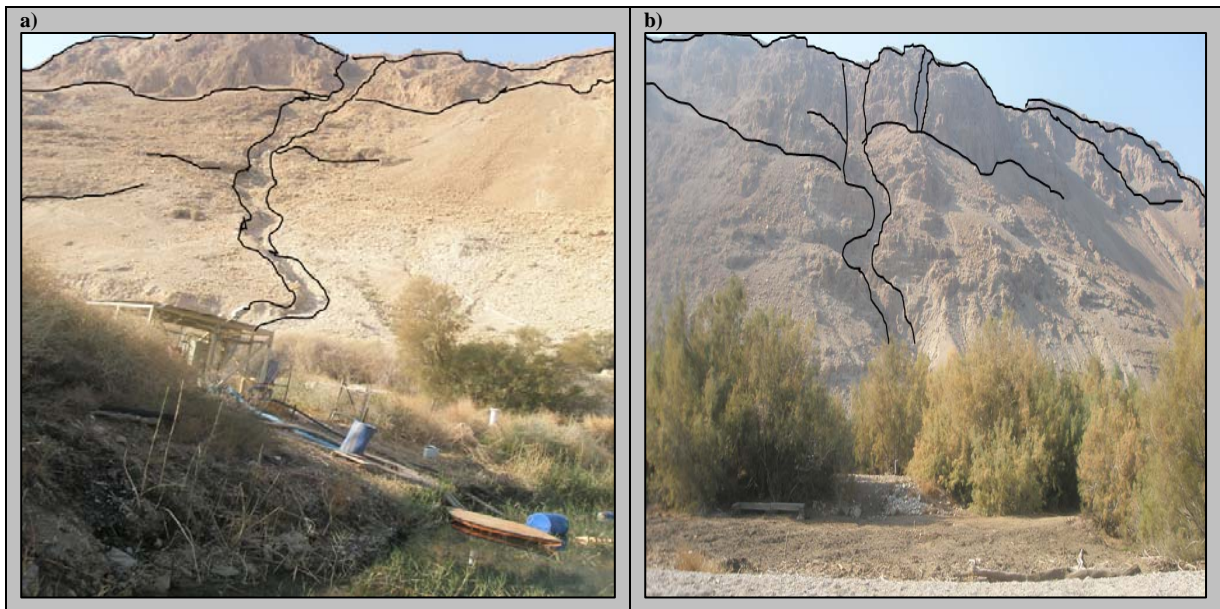


Figure 7.9: Field observations: a) East-West transversal fault crossing the main fault at Ein Feshcha main spring, b) East-West transversal fault at Ras Feshcha.

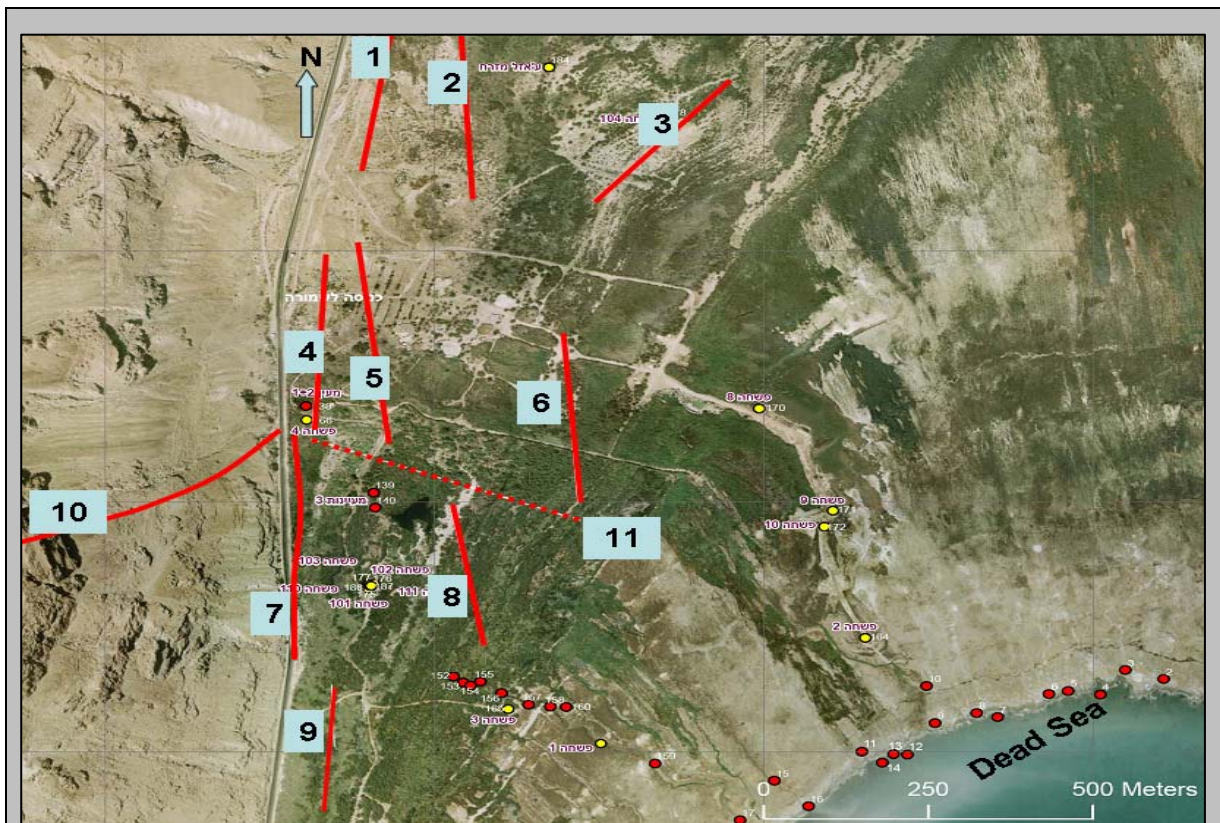


Figure 7.10: Satellite map with the detected faults and fractures localized by the stress variations using NPMEF-method, with the Cereskop instrument.

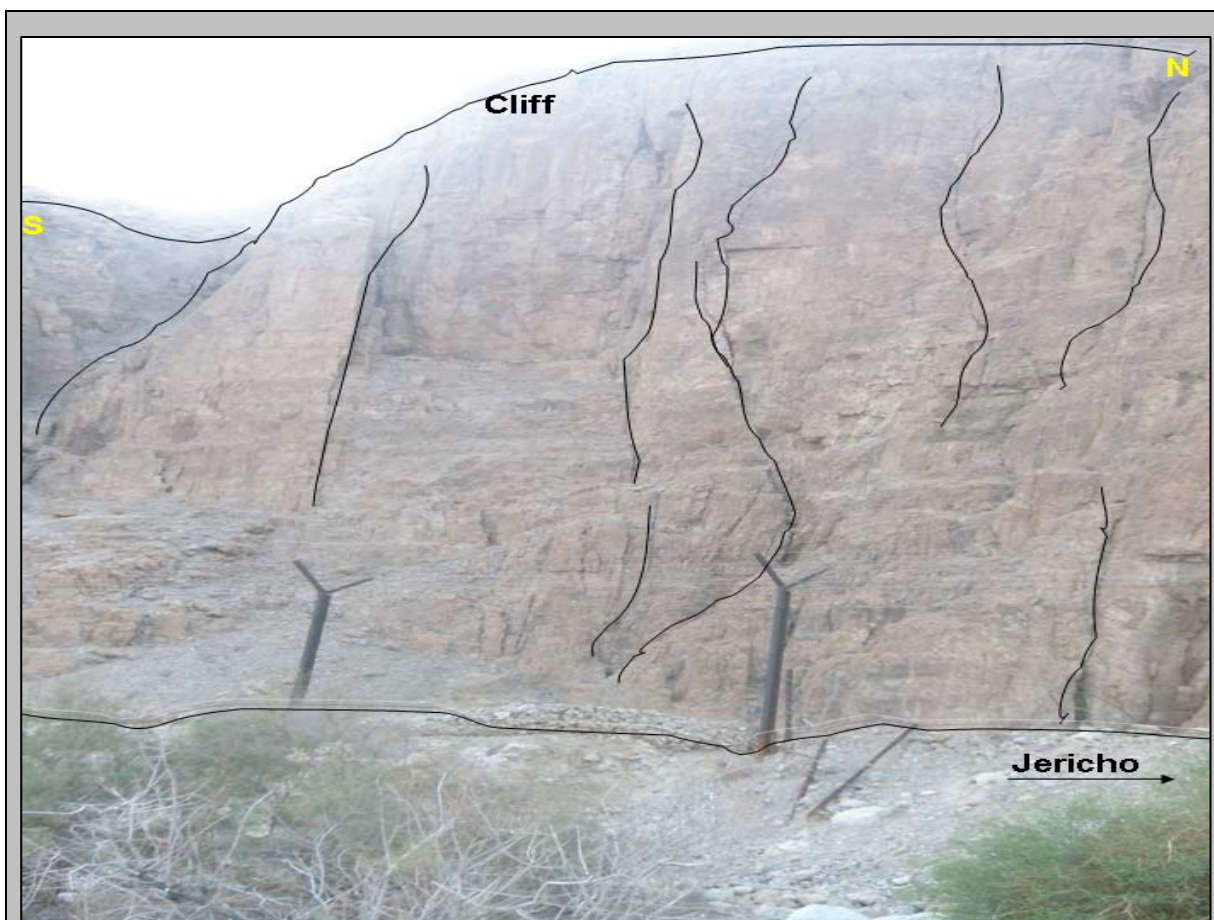


Figure 7.11: East-West directed cracks found in the study area.

Table 7.1: this table presents the coordination, length, beginning and end of the detected fractures

Fracture number	Beginning of the fracture		End of the fracture		Fracture length (m)
	North	East	North	East	
1	625025	243000	624836	242957	189
2	624989	243022	624776	243023	213
3	624876	243289	624700	243143	176
4	624630	242921	624436	242912	194
5	624642	242955	624412	242966	230
6	624518	243122	624300	243145	218
7	624425	242900	624052	242900	373
8	624300	243055	624070	243097	230
9	624053	242914	*ND	ND	>100
10	624437	242888	ND	ND	>400
11	624427	242919	624242	243177	258

*ND: Not Determined

7.3 Summary of Results

The results obtained by the applied geophysical methods (VES and NPEMFE) and the field evidence gave more information about, the interfaces between fresh, brackish and saline waters. The lithological sitting in the study area and localization of the faults and fractures exist in the study area. The combination of these two methods (VES and NPEMFE) with field observations gave more specific information which lead to more understanding of the mixing mechanisms. Figure 7.12 present the combination of the two methods.

The VES measurements detect low resistivity ($<10\text{Ohm/m}$) representing brines and the interface between them (brackish water) as well as the overlying fresher water bodies. In addition, high resistivity values $> 30\text{Ohm/m}$ representing freshwater are also detected, underlying the brines.

The presence of fresh water until a depth of 100m in the area around the main spring (1+2) was shown also by the obtained distribution of the measured resistivities on profile-I (figure 7.4). The only explanation for the fresh water source in Ein Feshcha is from Judea Mountains finding its way through the West-East transversal fault number 10 presented on figure 7.12.

The occurrence of localized low resistivity water bodies ($1-30\text{Ohm/m}$) in sounding points 2 and 12 on profile-I can be interpreted as a result of the existence of fracture number 1 and 2 presented on figure 7.12, these fractures may conduct waters with lower resistivities leading to mixing of the two water types. The source of the brackish water could be related to salt dissolution.

In the Southern direction, immediately South of the main spring on profile-III (figure 7.8), the resistivity values indicate the presence of a limestone block, displaced along a transversal fault, forming probably a barrier in the flow direction of the fresh water, obliging it to flow out and forming the main spring. Such a block was also signalised on profile-I, forming there a barrier in the advancing of the saline water from the Dead Sea toward the West.

The occurrence of low resistivity water bodies until the investigated depth of 100m, on profile-II, (Figure 7.7) can be interpreted as trapped residual brines or salts, related to earlier Dead Sea base levels. These brines are mostly found in the East, closed to the Dead Sea base level and it has a horizontal development.

The combination between all of what have been analyzed and noticed in the field a schematic cross section can be elaborated (figure 7.13). This figure describes the presence of salt diaper, sedimentary rocks and fresh-saline water interaction in the vicinity of the study area.

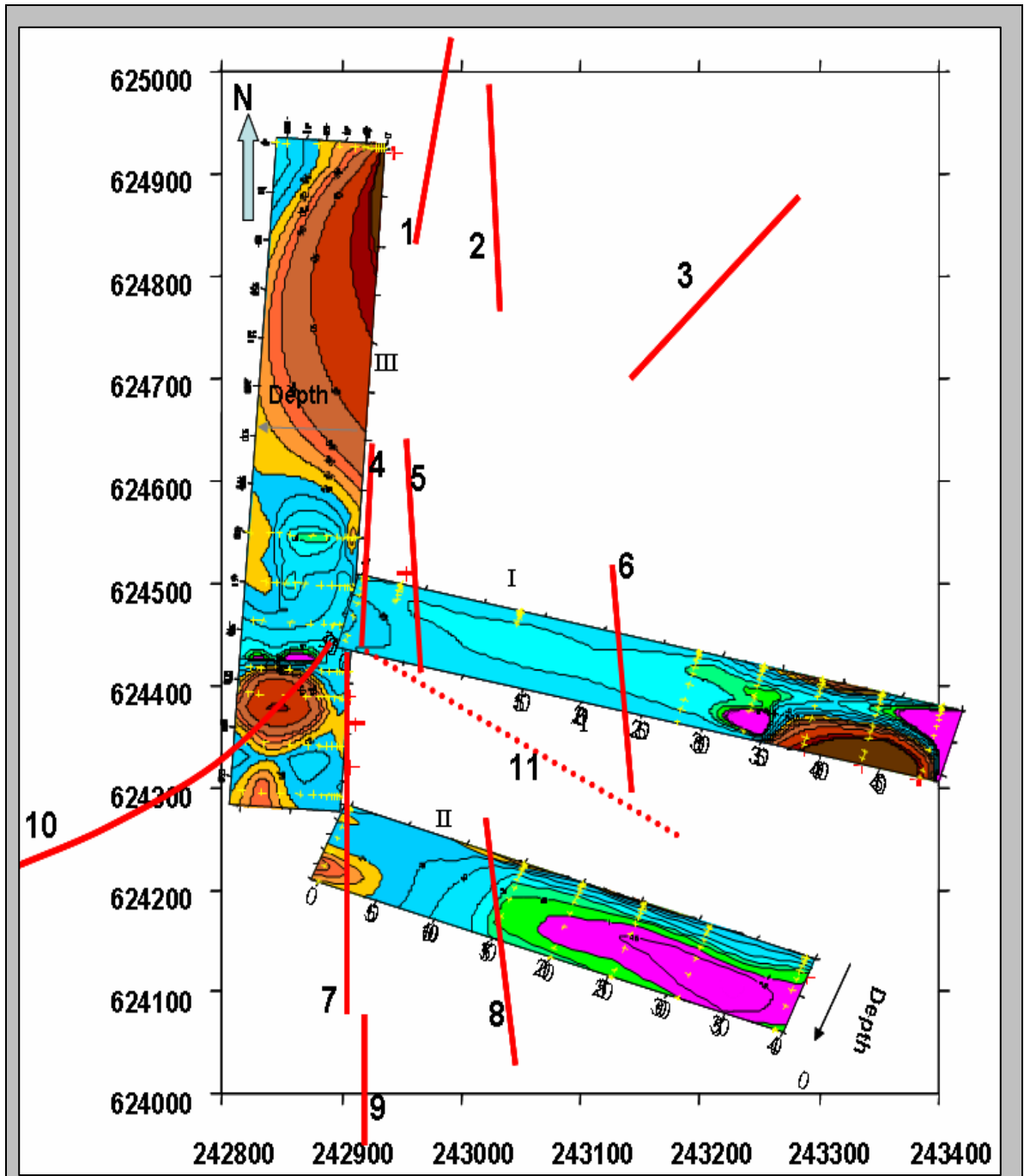
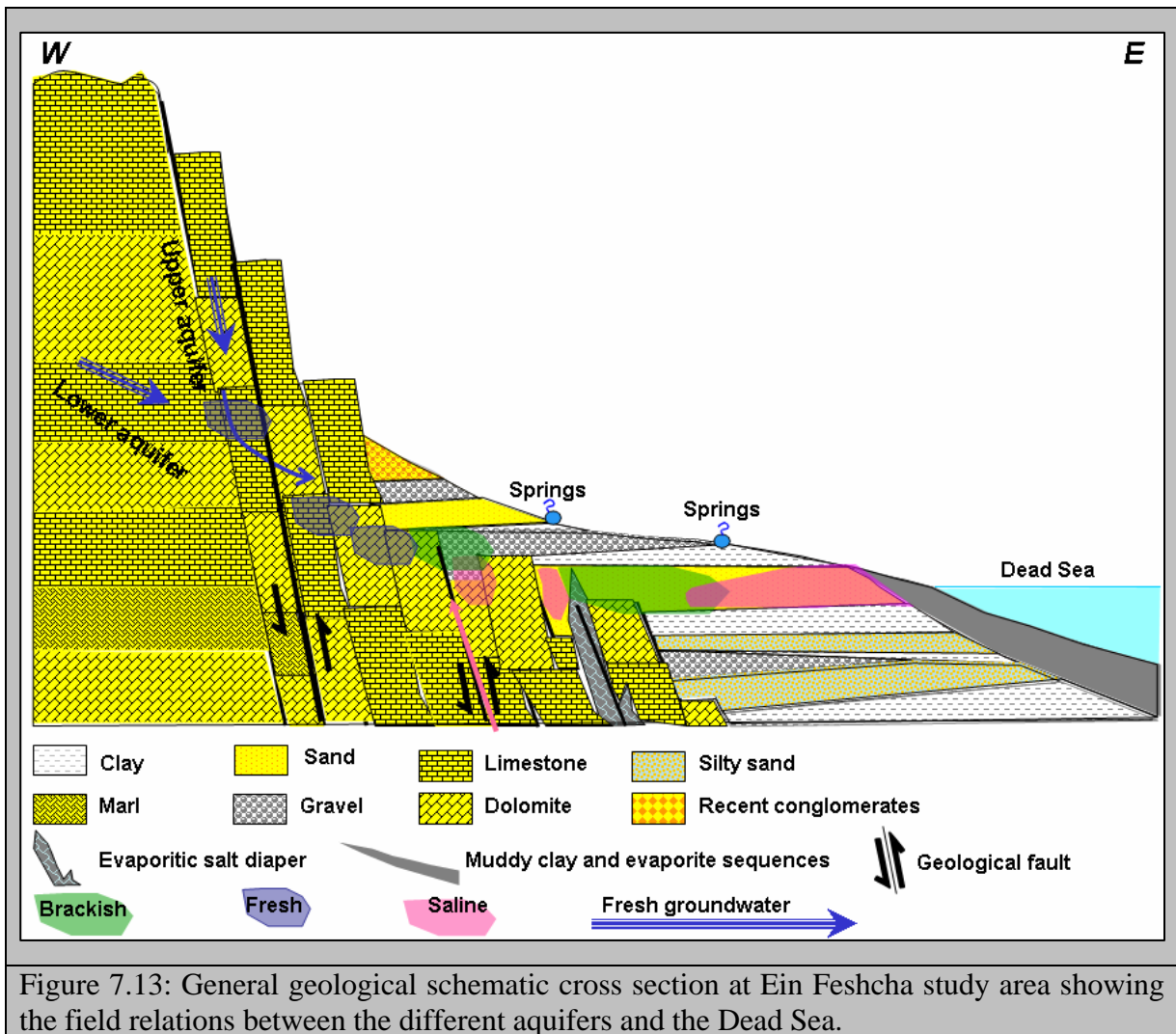


Figure 7.12: presents the results of the combination of the two geophysical methods (VES and NPEMFE)



8 DISCUSSION AND CONCLUSIONS

8.1 Discussion:

This study dealt with an arid area that suffers from an acute shortage of fresh water, in attempt to answer the opened questions and the proposed scenarios. Several scenarios have been proposed regarding water flow directions mixing mechanisms and water origin. In order to answer the opened questions and the proposed scenarios this study summarizes the Geo-hydrochemical and Geophysical investigations carried out in Marsaba-Feshcha area with the aim of improvement of groundwater resources exploitation strategies, through identifying the main sources that affect the groundwater quality and the mechanisms of fresh water deterioration using natural stable isotopes, hydrochemical tracers and electromagnetic measurements, thus tried to define the suitable sites and locations for water extraction before they become salty and flow outside at Ein Feshcha springs.

In order to achieve these aims a total of 65 samples were collected and analyzed during the course of this study. Sample name, description and coordination are summarized in table 4.1. For location on map see figure 4.1 and 4.2. These water samples were analyzed for cations anions, stable and radioactive isotopes. The chemical and isotopic analyses were interpreted using several chemical graphs.

The results for the groundwater of the Judea desert and Jordan Valley show a gradual increase of the Cl content in groundwaters and a concomitant change in the values in the composition of the ionic ratios in either positive or negative dependence of the Cl content. These changes in salinity and ionic ratios occur systematically from the recharge areas to the West through the karstic formation exposed in study area towards Mt.Jericho well field and Ein Feshcha springs to the East, this can be seen in the Cl-excess result of Mt.Jericho-2 well in which the concentration of the ionic ratio of Cl-excess increased from <0.08 in the recharge areas (Herodion field) to the values of $(1.01 - >6.26 \text{ meq/l})$ in Mt.Jericho field.

Whereas at the vicinity of Ein Feshcha springs area three salinization zones can be observed depending on Cl distribution along the springs line. The first zone with Cl concentration ranging between 1400–1999 mg/l the second zone Cl concentration ranges between 1999 – 2500 mg/l and the third one Cl concentration ranges between 3000 – 5000 mg/l (figure 5.1),

this distribution is attributed to localized fractions and faults found in the area affecting the flow direction, quality and quantity for each spring.

The Na-K-Mg diagram of Giggenbach, figure 5.2 shows that the water samples fall in the area of immature water very close to the Mg corner indicating that the water is in partial equilibrium with reservoir rock, the figure suggest that there is mixing between meteoric water with old seated brines, the water springs are slightly thermal.

According to Schoeller diagram figure 5.3, suggests that the groundwater comes from the same aquifer and has passed through similar rock types. This suggests that the groundwaters are mixed with isolated trapped water pockets formed in the geologically recent past, but with separate mechanisms and/or possible up flowing water through the fault system. This leads to mixing between these water types, as a result brackish water appear as an end member at the vicinity of the Ein Feshcha springs area.

Based on the information gained from Durov and Piper Diagram, the water samples broadly fit into three hydrochemical water types with some sub- groupings, in which figure 5.13 shows that water type-III (3b and 3c), fall in the recharge water zone with a dominant Ca-HCO_3 , indicates recharging waters in limestone formation and water type is dominated by Ca and HCO_3 with significant Mg ions, indicates recharging waters in limestone and dolomite aquifers. Whereas water types (1b, 3a, 3c) show no dominant anion or cation, indicates, water exhibiting simple dissolution or mixing. These samples fall in the mixing zone. Water types (1a, 1c, 1d, 1e) and water type 2 fall in the zone of Cl dominant anion and Na dominant cation, indicating that the groundwaters be related to reverse ion exchange of Na-Cl, end-point waters. From figure 5.13 it can be concluded that springs salinization differences are due to evaporation and/or dissolution-precipitation reactions of host rock filing (aragonite, calcite, dolomite and MgCl_2 salts and minor gypsum) which takes place along the water flow path and in the vicinity of the springs. Not only but also due to mixing with variable amounts of originally deep-seated Ca-Mg-Cl brines with meteoric waters through the fractures and the fault system in the vicinity of the study area.

In order to trace the geochemical evolution of different water bodies evolved in the study area, changes in trace elements and ionic ratios were followed and studied, (table 5.10).

The analyzed trace elements (B, Ba, Pb, Sr, Zn and Li), show that these elements are enriched in different rock units of the study area and support the suggestion that these elements originated from different sources. The occurrence of waters saturated with respect to BaSO_4 in the Dead Sea Rift Valley suggests the presence of barite at depth. Lead (Pb) is expected to be leached from rock-forming minerals containing high amounts of Pb (Cerussite- PbCO_3 or Galena-PbS), or from earlier formed ore deposits. It is clear that the composition of the trace elements is altered during the wet season indicating mixing of different water types.

High Strontium (Sr) content in waters associated with high content of Pb and Ba can only be explained by its relevance to Aragonite group dissolution. Strontium (Sr) is thus a good tracer for the existence of evaporates. Ein Feshcha springs are characterized by waters which have transited generally outcrop through the evaporitic Triassic formations since Sr/Ca ratios are $> 1.5\%$, as presented in table 5.10.

Ein Feshcha water acquires a characteristic chemical composition dominated not only by high Cl-Excess (19 – 154) and Ca-Mg-Excess (18 – 154) concentrations but also by low equivalent ratios of Na/Cl < 0.7 and high Q Value > 1 . The groundwater from the Ein Feshcha springs can be identified by their average meq ionic ratios of Sr/Ca (2.4 and 11.3), Mg/Ca (0.27 and 3.0) and Na/Cl (0.37 and 0.65).

Depending on the ionic ratios, figure 5.12 presents two possible zones of water mixing in the vicinity of the Ein Feshcha area with different end members. Mixing zone (A), pointing to a suggested meteoric water type 3c (Azarea-3, PAW-1 and 56 Abu Diea wells). Mixing Zone (B), show two water types of different origins, one of them is meteoric water type 3b (PWA-3 and Azarea-1) the other source is a brine water type 1e (Arab project-66), mixing of these components leads to the saline end member waters at Ein Feshcha springs.

The average saturation indices of the study area show different trends for each mineral, these SI are summarized in table 5.7. All the samples of the study area during the dry and wet season are under saturation with respect to the minerals (Anhydrite, Gypsum, Halite and Siderite). Thus the waters have the potential to dissolve evaporates and calcium sulphate minerals. For Barite which is associated with metal sulfides, solubility of this mineral is variable and in most cases, the minerals are either consistently saturated or consistently under saturated. With respect to barite the water samples of the study area vary from under saturation to saturation. The minerals (aragonite, calcite and dolomite) which represents the major sediments that built-up the geology of the study area, saturation indices are variable and affected by seasonal variation which means mixing with meteoric waters.

The plot of $\delta^{18}\text{O}$ - $\delta^2\text{H}$ vs. TDS, figure 6.4 show mixing between meteoric waters (isotopically lighter) and salty waters (isotopically heavier). The samples in the study area are clustering along the mixing line in which the salinity (TDS) is related to $\delta^{18}\text{O} - \delta^2\text{H}$, which confirm the presence of common seated brine that mixes with groundwater in variable amounts.

Ultra filtration caused by the high clay content found in the area lead to slight enrichment of both $\delta^2\text{H}$ and $\delta^{18}\text{O}$ accompanied with an increase in Ca and Mg concentrations in the water samples and hence it may explain the CaCl_2 and MgCl_2 water types in the area.

With stable isotopes no clear evidence show that evaporation brine play an important role for salinization of groundwater within the rift graben, there is more evidence for dissolution of salts, which may explain the high content of Ba and Pb.

According to the figures 6.3, 6.4 and 6.7 a mixing process between freshwaters of meteoric origin and significantly evaporated and isotopically modified brines ($\delta^{18}\text{O} - \delta^2\text{H}$) because of salts dissolution, seems to better explain the observed $\delta^3\text{H}$, $\delta^2\text{H}$ vs. $\delta^{18}\text{O}$ trend for the water samples.

All water samples contain high activity values of ^{222}Rn over dissolved ^{226}Ra , all waters show disequilibrium between the parent and daughter nuclide, the $^{222}\text{Rn}/^{226}\text{Ra}$ ratio being $\gg 1$. Obviously, the radioactive elements found in these solutions cannot be as ancient as the salts, because they would have decayed long ago to background values, this means that ^{226}Ra isotopes are continuously being replenished in the saline brine end members.

The Ra and Rn inhomogeneity at Ein Feshcha springs attributed to the following factors: a) high ^{226}Ra content appears to be fault controlled for transferring water from depth, b) high ^{222}Rn activity suggests possible presence of a nearby submarine springs, c) the occurrence of very saline brines that desorb ^{226}Ra from the aquifer rocks due to desorption reaction related to ion exchange, and d) continuous mixing of those brines with fresh waters, results in the adsorption of ^{226}Ra to the linings of the aquifer host rocks.

Figure 6.10 summarizes these factors in a schematic cross section, showing ^{238}U in rocks of phosphorite-bearing formations which is considered as the major source of ^{226}Ra . During water up flowing of confined water through fractures and faults it bases a salt mass in its way leading to mineral dissolution (Mn and Fe) close to the mixing point. Close to the main spring exit two types of water mixed to gather (fresh and salt water) leading to precipitation of Mn-Ra-Fe to the lining of the water bath which explains the low concentration of free Ra in aqueous phase. Due to this accumulation of Mn-Ra-Fe to the lining high concentration of ^{222}Rn is noticed.

Through using the VES-method at Ein Feshcha study area, three vertical section profiles (I, II and III) were elaborated analyzed and studied carefully. The geophysical analyses outcome from this method presents the existence of late Pleistocene sediments (tills and clays) block, forming a barrier in the fresh groundwater flow along the North-South oriented main fault system, figure 7.8b. Due to the lowering of the Dead Sea level and the presence of the sedimentary rocks presented by profile-I in figure 7.4 and field observations presented in figure 7.6, these sediments prevents the retreated waters to be moved back forming trapped pockets or zones extending horizontally. The barrier at the main fault system holds the freshwater behind it, allowing large amount of water to flow through East-West cracks and faults functioning like an opening in a dam. These transversally faults may saddle inside Nabi

Musa syncline (Boqea syncline). Guttman et al (2000), noted, “a transitional zone in which the freshwater apparently flows from the lower aquifer to the upper aquifer is somewhere West to the Mt.Jericho well field and however, it is difficult to find field evidence for this assumption”.

Using the NPEMFE-method we managed to localize field evidence for the existence of fractures and transversally faults. The transversally fault, figure 7.9a shows vertical displacement ranging between 0.5m and 0.7m along the fault but it might reach several meters at the cliffs with horizontal displacement ranging between 0.8m up to 1.3m.

A minor transversally faults are also noticeable joining the main one. This fault is heading directly to the main spring which may explain the high water discharge of this spring, in which this fault may work like a tube conducting water from the adjacent upstream aquifers.

The main fault works like a dam holding the water behind. The presence of fresh water with similar chemistry at Mt.Jericho well field to the North and at Ein Gady to the South is explained due to this barrier. Due to the transversally faults and the cracks it works like doors basing the water and distributing it to the springs found at the Dead Sea shore.

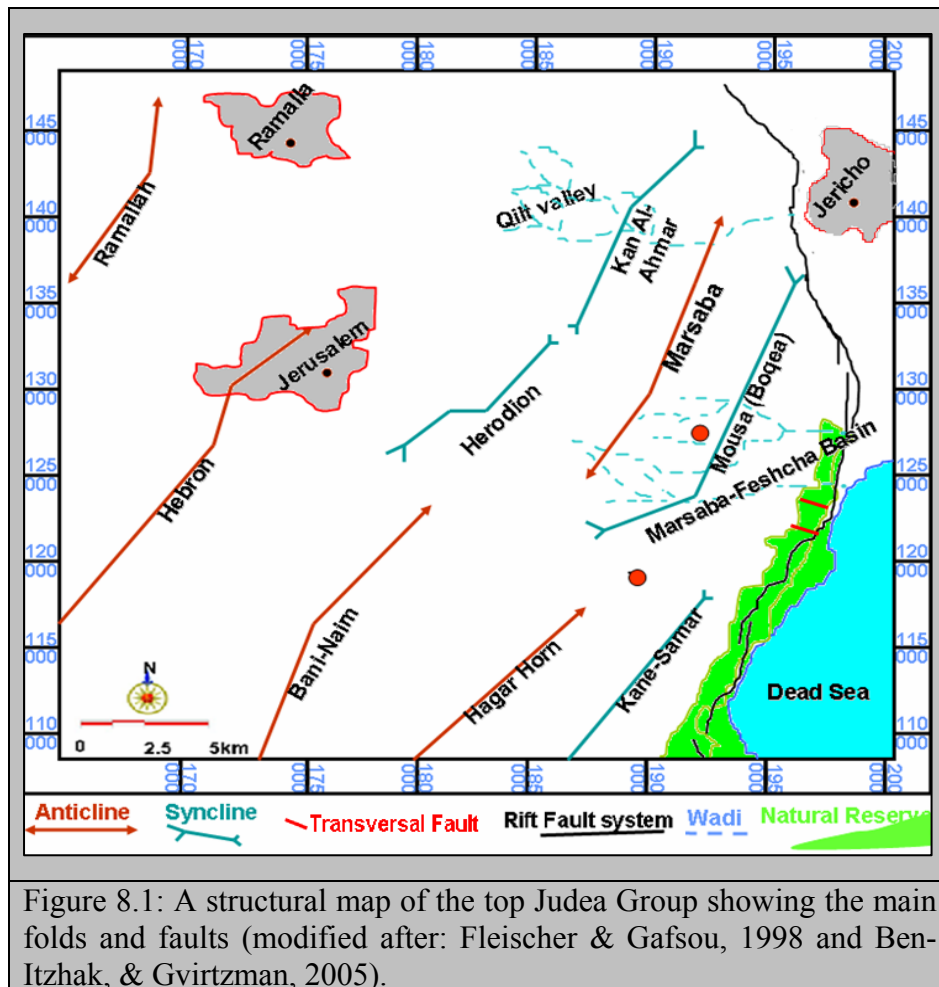
These transversally faults could be the transitional zone, responsible for the hydraulic connection between the lower and upper aquifer in the area.

Guttman, and Zukrman, (1995), Guttman et al (2004), proposed the flow hypothesis: “groundwater flow originating from the West shifts to the North (and apparently also to the South) towards the Mt.Jericho well field located within the saddle inside the Marsaba anticline, from where the flow is channeled towards the Feshcha springs”. This hypothesis is not convenient; therefore, it is still questionable why the groundwater path is changed to the North and to the South and the groundwater drains through the Feshcha springs a few km southern, instead of flowing through the direct and short path to the East into the Rift Valley fill.

The results from this research answer the question about the West-East flow direction, it is important to note that the groundwater flow is also governed by the geological structure of the area, Marsaba anticline and Nabi Musa syncline, as well as fractures and fault systems. The major Western Rift fault is a relatively sealed boundary. This sealed tectonic boundary causes diversion in groundwater flow to the North and to the South but at the same time a major

water leak through the transversally faults presented in figure 8.1 at the boundary of the Feshcha springs explains the West-East flow direction. The fold axes dictate the groundwater flow pattern.

Figure 7.13 represents a schematic cross section showing the field relations between the different aquifers and the Dead Sea. It also shows that the Western part is built of limestone, dolomite and some marl belonging to the Judea Group, while the area between the cliff and the Dead Sea is built of gravel, sand and clay belonging to the Quaternary aquifer. The Kurnub aquifer, which is below the Judea aquifer, is not shown. It also presents a salt diapir recognized in the area which is probably the source of fresh water local salinization and it could be the source for Ba and Pb. This result is consistency with the results obtained by Flexter et al (2000).



8.2 Conclusions:

Depending on the collected data during the course of this study which included: field observations, chemical-, isotopic- and geophysical analysis it can be concluded that the salinization at Ein Feshcha is due to several factors leading to the formation of varies water quality springs with different chemical composition over short distances. Most of these factors take place at the vicinity of Ein Feshcha spring area.

Due to the fractures and faults found in the study area which may create complicated systems of dissolution channels and to the differing nature of the mechanisms of outflow and mixing involved, the quantity and salinity of springs can differ considerably from one spring to the next. The localized fractures and faults found and the limestone barriers explain some of the water mixing mechanisms working as barriers and/or conductors.

It is important to notes that the source of CaCl_2 and MgCl_2 water types in the area is due to ultra filtration caused by the high clay content found in the area which explains the origin of excess Ca and Mg in saline waters. Dead Sea intrusion is not likely due to the existence of the suggested sedimentary rocks overlaid with late Pleistocene sediment blocks. These blocks acts as a barrier in the advancing of saline water intrusion from the Dead Sea but trapped water is more likely.

With the geochemical analysis, radioactive- and stable isotopes no clear evidence show that an evaporation brine play an important role for salinization of groundwater within the rift graben but there is more evidence for dissolution of salts. This salt dissolution is proved by the existence of the recognized salt diaper in the study area. The waters exhibit a wide range of major cations; major anions and trace element concentrations, this is generally due to processes that alter salt concentration, such as dissolution, evaporation and/or precipitation processes which takes place along the water flow path and in the vicinity of the springs.

There is mixing with water from deep confined aquifers containing Ca-Cl brines, which ascend to the surface along the fault lines. In the area of the fault they become mixed with fresh water and become brackish resembling the end member. The existence of fresh waters

has been proved by spring isotopic composition and by VES-method. There is a local mixing between fresh waters and trapped residuals of saline waters in between the exposed clay layers due to the retreat of Dead Sea water, (paleo brines). A mixing process between freshwaters of meteoric origin and significantly evaporated and isotopically modified brines (trapped waters) because of salts dissolution seems to better explain the observed end members.

Radium analysis suggest that ^{226}Ra -rich sources are located at Ein Feshcha study area, on the shore of the Dead Sea and not from the meteoric waters and since ^{226}Ra is enriched continuously at the springs exit the results suggest that the source of ^{226}Ra is from ^{238}U -phosphorite bearing formations, means that the up flowing water arise from a reservoir of brines located below the Dead Sea.

The spring waters have high concentration of dissolved ^{226}Ra that clearly exceeds the EPA standard for water domestic use. The Ein Feshcha springs are an example of a water source whose natural contamination by radium was incidentally discovered before the water to be economically utilized.

The fresh/saline water interface is formed due to the contact between the trapper saline pockets with the conducted fresh waters through the transversally faults. This interface can vary its depth depending on the seasonal precipitation. The rise of saline water is controlled by the head and the discharge of the fresh water. The maximum depth of this interface is ranging between 70 to 80 meters and it is under lined and over lined with brackish waters as a result of the fresh water existence over the whole investigated depth interval of 100m.

The main conclusion is that at the East-West water flow direction at Ein Feshcha natural reserve is due to the transversal faults. The existence of the transversal fault leads to a hydraulic connection between the lower aquifer and the upper aquifer.

Groundwater is being recharged in the mountains in the West, were the aquifer is exposed. It flows to the East, partly confined by the Senonian chinks, these groundwaters due to the existence of tills and limestone blocks, forming a barrier in the fresh groundwater flow along the North-South oriented main fault system hold the water behind it (dam like barrier). This leads to groundwater flow orientation from the West to be shifted to the South toward Ein

Gadi and to the North toward Mt. Jericho well field located within the Marsaba anticline. Due to the East-West transversal fault, the water of the upper and lower aquifer mixed and emerges as springs at Ein Feshcha study area.

It can be concluded that the existence of brackish water above and below the saline domain and the variation of water quality even over short distances implies multiple hydrological aquifer system and a fracture flow system controlling the Ein Feshcha springs. Understanding this concept will help to evaluate the impact of the groundwater extraction on the heads and flow patterns in the aquifer and to locate extraction wells. It is clear that these springs are the outlet for the Eastern drainage of the Judea Mountain aquifer. In order to intercept the fresh water before it becomes mixed with these brines, more wells need to be drilled and more water to be pumped in the Eastern flanks of the Judea anticlinorium.

The outcome of this study will be used as guidelines for researchers, planners and decision makers (Joint Water Committee and Technical Water Committee) to understand the current water situation at the lower Jordan Valley.

8.3 Recommendations:

The main recommendations of this research could be summarized as follows:

- ❖ The saline water could be economically used in a variety of desert enterprises, without any a priori health concerns. Date palm is an increasingly growing sector in the Rift Valley area therefore it is recommended to use spring waters with a Cl content in the range of 1700–2300 mg/l for date palm irrigation.
- ❖ The salt diaper is considered as one of the factors responsible for spring salinization therefore, its geometry and dimension should be studied more since it is essential for conducting an efficient water management.
- ❖ The geographical distribution and the geohydrological interaction of the salt bodies in the area should be identified.

- ❖ The radium might serve as a natural tracer for water origin therefore systematic survey of radium and radon in the Dead Sea springs should be made.
- ❖ In Rift Valley area, drinking water resources are limited and the use of the available water for domestic use requires more attention regarding their chloride content, not only but also, their radio active constituents (Radium).
- ❖ The spring waters have high concentration of dissolved ^{226}Ra , therefore, before its use it is recommended to precipitate the Ra to minimize the health risk.
- ❖ It is a must to establish Palestinian guideline standards for isotope activity in drinking waters and to adapt treatment methods for those waters whom doesn't meet the standards.
- ❖ Production of vulnerability map for the study area in order to localize the assessment actors.
- ❖ Geological field surveys and mapping work is needed to be carry out at the cliff area and along the Dead Sea shore in order to identify and localize: a) the existence of the salt bodies and b) the fractures and transversally faults exposed in the area, using the VES-method and NPEMFE-method, field observations are essential, sinkholes can be used as a primary indicators for fault localization.
- ❖ Small scale dams and infiltration basin is recommended in order to increase ground water recharge in periods with surplus of rain water.
- ❖ It is recommended to construct a new well field at upstream within the synclines, where the thickness of the saturated zone is maximal.

- ❖ It is recommended to construct the suggested wells over a large area in order to monitor their effect on Ein Feshcha and other springs discharge and also to monitor and control the hydrologic drawdown.

- ❖ Dead Sea springs give life to the nature reserve along the sea shore; therefore pumping from the upstream drainage basins would sharply reduce the discharge rates at Ein Feshcha springs, not only but also it would affect Ein Gady spring discharge farther to the South. Therefore it is recommended to develop two well fields with the following coordinates 127500/192500 and 119000/189000 marked with red points on figure 8.1, which explains the location with regard to the tectonic settings. These wells should be drilled activated and monitored. Depending on the aquifer response and how they do affect the discharge downstream, decisions should be made regarding the abstraction rates for each and the possibility for further development of the well field.

9 REFERENCES

- AbdelSalam, A., 1990. Water in Palestine. *Geographic Studies* **1**, 114-116.
- Abdesselam, M., Mania, J., Mudry, J., Gélard, J., Chauve, P., Lami, H., and Aigoun, C., 2000. Hydrogeochemical arguments for a non out cropping Triassic formation in the Djurdjura massif (Kabyle ridge, an element of the Maghrebides range). *Rev. Sci. Eau* **13**, 155-166.
- Abed, A., 1985. The Geology of the Dead Sea. *Dar Al-Urqam*.
- Abelson, M., Baer, G., Shtivelman, V., Wachs, D., Raz, E., Crouvi, O., Kurzon, I., and Yoseph, Y., 2003. Collapse-sinkholes and radar interferometry reveal neotectonics concealed within the Dead Sea basin. *Geoph. Res. Let.* **30**, 1454.
- Alekin, O., 1970. Principles of hydrochemistry. *Hydrometeorology Institute, Leningrad*.
- Ali, M., 1964. Jordan River and the Zionist Conspiracy. *National Publishing and Printing House, Cairo* 54.
- Arad, A. and Michaeli, A., 1964. Hydrogeological Research in the Western Drainage Basin of the Dead Sea Rift. *TAHAL Consulting Engineers Ltd. Report no. 63/4*, 30
- Argaman, Y., 1990. Tel Dan Incident: New Concept in Israeli Tank Warfare. *Israel Defense Forces Journal*.
- ARIJ., 1997. The Status of the Environment in the West Bank. *Water Resources*, 95-107.
- ARIJ., 2000. An Atlas Of Palestine: The West Bank and Gaza Strip. *Research Report. Bethlehem, Palestine* **203**.
- ARIJ., 1995a. Environmental profile for the West Bank - District of Bethlehem. Jerusalem. *Appl. Res. Ins. Of Jerusalem*.
- ARIJ., 1995b. Environmental profile for the West Bank - Hebron District. Jerusalem. *Appl. Res. Ins. Of Jerusalem*.
- Arkin, Y., 1976. Geological Map of Israel, Jerusalem and Vicinity, 1:50,000. *Geo. Surv. Isr.*
- Arkin, Y., Braun, M., Starinski, A., Hamaoui, M., and Raab, M., 1965. Type Sections of Cretaceous Formations in the Jerusalem-Bet Shemesh Area. *Geo. Surv. Isr.*, 42
- Arkin, Y. and Hamaoui, M., 1967. The Judea Group (Upper Cretaceous) in Central and Southern Israel. *Geo. Surv. Isr. Bulletin* **63**.

- Bahat, D., Rabinovitch, A., and Frid, V., 2005. Tensile Fracturing in Rocks: Tectonofractographic and Electromagnetic Radiation Methods. *Springer Berlin Heidelberg*, 569.
- Bajjali, W. and Al-hadidi, K., 2005. Hydrochemical Evaluation of Groundwater in Azraq Basin, Jordan Using Environmental Isotopes and GIS Techniques. *Twenty-Fifth Annual ESRI International User Conference - San Diego, Californi*.
- Bandel, K. and Khoury, H., 1981. Lithostratigraphy of the Triassic in Jordan. *Facies* **4**, 1-26.
- Bartov, Y., Stein, M., Enzel, Y., Agnon, A., and Reches, Z., 2002. Lake levels and sequence stratigraphy of Lake Lisan, the Late Pleistocene precursor of the Dead Sea. *Quat. Res.* **57**, 9 -21.
- Bayer, H., 1986. Map Aquaba-Levant Structure. *Applied Geology*, **Sheet 3**.
- Begin, Z., 1974. Geological Map of Israel, Jericho 1:50,000, with Explanatory Notes. *Geo. Surv. Isr.* **Sheet 9-III**.
- Begin, Z., Ehrlich, A., and Nathan, Y., 1974. Lake Lisan, the Pleistocene precursor of the Dead Sea. *Geo. Surv. Isr.* **Bulletin 63**, 30.
- Ben-Avraham, Z., 1997. Geophysical framework of the Dead Sea: structure and tectonics. *Oxford University Press*, 22-35.
- Bender, F., 1968. Geologie von Jordanien. *Beiträge zur regionalen Geologie der* **7**, 237.
- Ben-Itzhak, L. and Gvirtzman, H., 2005. Groundwater flow along and across structural folding: an example from the Judean Desert, Israel. *Journ. of Hydro.* **312**, 51-69.
- Bensabat, J., Guttman, J., Flexer, A., Hoetzi, H., Ali, W., and Yellin-Dror, A., 2004. Groundwater model of the Marsaba-Feshchah region *Israel, 5th International Symposium on Eastern Mediterranean Geology*, 1487-1490.
- Bentor, Y. and Vroman, A., 1963. The Negev, Nizana, Geological map of Israel, 1:100,000. *Geo. Surv. Isr.* **Sheet 17**.
- Bergelson, G., Nativ, R., and Bein, A., 1999. Salinization and dilution history of ground water discharging into the Sea of Galilee, the Dead Sea Transform. *Isr. Appl. Geochem.* **14**, 91-118.
- Bishop, K., 1991. Episodic increases in stream acidity, catchment flow pathways and hydrograph separation. *Ph.D thesis: Univ. Cambridge, Dept. Geol., Jesus College, Cambridge, U.K.* **246**
- Blake, G. and Goldschmidt, M., 1947. Geology And Water Resources Of Palestine. *Unpublished report*

- Bogoch, R. and Schwartz, M., 1978. Petrogenesis of a Senonian Barite Deposit, Judean Desert. *Israel Mineral. Deposita* **13**, 383-390.
- Braun, M. and Hirsch, F., 1994. Mid Cretaceous (Albian-Cenomanian) carbonate platforms in Israel. . *Cuadernos de Geologia Iberica* **18**, 59-81.
- Bulloch, J. and Darwish, A., 1993. Water wars: coming conflicts in the Middle East. *Victor Gollancz, London, UK. Boston Sunday Globe* **October 18, 1998**.
- Camberato, J., 2001. Irrigation Water Quality, Turf grass Program. *Clemson University, South Carolina*.
- Capaccioni, B., Vaselli, O., Moretti, E., Tassi, F., and Franchi, R., 2003. The origin of thermal waters from the eastern flank of the Dead Sea Rift Valley (western Jordan). *Terra Nova* **15**, 145-154.
- Carmi, I. and Gat, J., 1973. Tritium in precipitation and freshwater sources in Israel. *Isr. Journ. Earth Sci.* **22**, 71-92.
- Carmi, I. and Gat, J., 1978. Changes in the isotope composition of precipitation of the eastern Mediterranean- a monitor of climatic change. *Isr. Meteoro. Res.* **2**, 124- 135.
- CDM/Morganti., 1998. Study Of Sustainable Yield Of The Eastern Aquifer Basin. *Camp Dresser & Mckee International Inc. Task 18 Of The Water Resources Project*.
- CH2M HILL, 2000. Eastern Basin - aquifer modeling. *Geological ections: section D-D', section J-J' Phase III / Task2*.
- CH2M HILL, 2000. West Bank water resources program 2 and Bethlehem 2000 project, Hebron model, final report. *Ground water management modeling Task 7*.
- Chan, L. and Chung, Y., 1987. Barium and radium in the Dead Sea. *Earth Planet. Sci. Lett.* **85**, 41-53.
- Clark, I. and Fritz, P., 1997. Environmental Isotopes in Hydrogeology. *Lewis Publishers, New York, USA*, 328.
- Cole, D. and Vorster, C., 1999. The Metallogeny of the Sutherland Area. *Council for Geoscience, Pretoria* **Explanation of Metallogenic Sheet 3220**.
- Cooley, J., 1984. The War Over Water. *Foreign Policy* **54**, 3-26.
- Coplen, T. and Hanshaw, B., 1973. Ultrafiltration by a compacted clay membrane. I. Oxygen and hydrogen isotopic fractionation. *Geochim. Cosmochim. Acta* **37**, 2295-310.

- Coplen, T., Wildman, J., and Chen, J., 1991. Improvements in the gaseous hydrogen water equilibration technique for hydrogen isotope ratio analysis. *Analyt. Chem. Acta.* **63**, 910-912.
- Craig, H., 1961. Isotopic variations in meteoric waters. *Science* **133**, 1702-1703.
- Daibes, F., 2002. Water the Blue Gold of the Middle East. *PASSIA*, July, 2002.
- Dan, J., Koyumdjisky, H., and Yaalon, D., 1962. Principles of a proposed classification for the soils of Israel. *Trans. Int. Soil Conf. Comm.* **IV and V**, 410-421.
- Dansgaard, W., 1964. Stable isotope in precipitation. *Tellus* **216**, 436-468.
- Davis, J. and Kent, B., 1990. Surface complexation modeling in aqueous geochemistry. *Mineralog. Soci. of Ameri.* **23**, 177-260.
- Davis, U., Antonia, M., and Richardson, J., 1980. Israel's Water Policies. *Jour. of Pales. Stud.* **9**, 3-32.
- Dillman, J., 1989. Water Rights in the Occupied Territories. *Jour. of Pales. Stud.*, 46-48.
- Doherty, K., 1965. Jordan waters conflict. *International Conciliation* **553**, 2-66.
- Dudeen, B., 2000. Land System Classification of the West Bank and Gaza Governorates,. *Land Research Center*, 207.
- Elmusa, S., 1993a. The water issue and the Palestinian-Israeli conflict. *The Center for Policy Analysis on Palestine Washington, DC, USA.*, Information Paper No. 2.
- Environmental., P., 2002. Apartheid Wall Campaign. *NGO Network Report no.1 Fact sheet.*
- EXACT, 1999. Overview of Middle East Water Resources - Water Resources of Palestinian, Jordanian and Israeli Interest. *compiled by U.S. Geological Survey for Executive Action Team Washington, ISBN 0-607-91785-7*, 44.
- Eyal, Y. and Reches, Z., 1983. Tectonic analysis of the Dead Sea Rift Region since the Late-Cretaceous based on mesostructures. *Tectonics Journ.* **2**, 167-185.
- Fink, M., 1973. Possibilities for Groundwater Utilization in the Northwestern Basin of the Dead Sea. *TAHAL Consulting Engineers Ltd. Report no. 01/73/02*, 39.
- Fishelson, G., 1989. The Middle East conflict viewed through water: a historical view. The Armand Hammer Fund for Economic Cooperation in the Middle East. **Bulletin Tel Aviv University, Tel Aviv, Israel.**
- Fleischer, L., 1996. Index of Oil and Gas Wells Drilled in Israel, The Ministry of National Infrastructures. *Earth Sciences Research Administration Report OG/2/96.*

- Flexer, A., 1968. Stratigraphic and facies development of Mount Scopus Group [Senonian-Paleocene] in Israel and adjacent countries. *Isr. Jorun. Earth Sci.* **17**, 85-114.
- Flexer, A., Bensabat, J., Guttman, J., and Yellin-Dror, A., 2001. A 3-D Hydrogeological model of the Marsaba Feshchah Region. **Project No. WT0004.**
- Flexer, A. and Honigstein, A., 1984. The Senonian succession in Israel - lithostratigraphy, biostratigraphy and sea level changes. *Cretac. Res.* **5**, 303-312.
- Flexer, A., Rosenfeld, A., Lipson-Benita, S., and Honigstein, A., 1986. Relative Seal Level Changes During the Cretaceous in Israel. *AAPG Bulletin* **70**, 1685-1699.
- Flexer, A., Yellin-Dror, A., Kronfeld, Y., Rosental, E., Ben-Avraham, Z., Artsztein, A., and Davidson, L., 2000. A Neogene salt body as the primary source of the salinity in Lake Kinneret. . *Arch. of Hydrobio.* **55**, 69-85.
- Freund, R., Garfunkel, Z., Zak, I., Goldberg, M., Weissbord, T., and Derin, B., 1970. The sear along the Dead Sea Rift. *R. Soc. London Phil. Trans* **267**, 107-130.
- Freund, R. and Garfinkle, A., 1980. The Dead Sea Rift. *Tectonophysics* **80**, 1-303.
- Frumkin, A., 2005. Fischhendler, I Morphometry and distribution of isolated caves as a guide for phreatic and confined paleohydrological conditions. *Geomorphology* **67**, 457-471.
- Garbell, M., 1965. The Jordan Valley Plan. *Sci. Ameri.* **212**, 2331.
- Garfinkle, A., 1992. Israel And Jordan In The Shadow Of War: Functional Ties And Futile Diplomacy In A Small Place. *St. Martin Press, New York, U.S.A.*
- Garfunkel, Z. and Ben-Avraham, Z., 1996. The structure of the Dead Sea Basin. *Tectonophysics* **266**, 155-176.
- Gass, I., 1980. Crustal; and Mantle Processes: Red Sea Case Study. *The Open University Department of Earth Sciences.*
- Gat, J., 1971. Comments on the stable isotope method in regional ground water investigations. *Water Resources Research* **7**, 980.
- Gat, J. and Carmi, L., 1970. Evolution of the isotopic composition of atmospheric waters in the Mediterranean Sea area. *Journ. Geophy. Res.* **75**, 3039-3048.
- Gat, J., Mazor, E., and Tzur, Y., 1969. The stable isotope composition of mineral waters in the Jordan Rift Valley. *Isr. Journ. Hydrol.* **7**, 334-352.
- Gavrieli, I., 1997. Halite deposition from the Dead Sea: 1960-1993, in the Dead Sea the lake and its setting. *Oxford University Press*, 145-170.

- Gehre, M., Hoefling, R., Kowski, P., and Strauch, G., 1996. Sample preparation device for quantitative hydrogen isotope analysis using chromium metal. *Analyt. Chem.* **68**, 4414-4417.
- Geological Survey Of Israel, 1990-2002. Geologic Map Sheets For Different Areas Of Israel And Palestine. *Geo. Serv. Isr.*
- Giffin, A., Kaufman, W., and Broecker, S., 1963. Delayed coincidence counter or the assay of action and thoron. *Journ. Geophy. Res.* **68**, 1749-1757.
- Giggenbach, W., 1988. Geothermal solute equilibria. Derivation of Na-K-Mg-Ca geoindicators. *Geochim. Cosmochim. Acta.* **52**, 2749-2765.
- Giggenbach, W. and Goguel, R., 1989. Collection and analysis of geothermal and volcanic water and gas discharges. *Department of Scientific and Industrial Research, New Zealand, Report CD2401*, **81**.
- Gilat, A., 1986. Hydrothermal barite deposits with possible economical value in the Nahal Hever area. *Geo. Surv. Isr. GSI Report.* **86-11**.
- Gilat, A., Mimran, Y., Bogoch, R., and Roth, I., 1978. Circular and tabular (discordant) dolomite bodies in the South Judean Desert, Israel. **In Press**
- Goldschmidt, M., Arad, A., and Neev, D., 1967. The Mechanism of the Saline Spring in the Sea of Galilee Depression. *Isr. Hydrological Service Paper no. 11; Geol. Surv. Bulletin no. 45*.
- Greenboim, J., 1992. Discharge Measurements in the Tsukim Springs in 5-6.8.92. *Isr. Hydrological Service Water Commission (in Hebrew)*.
- Greenboim, J., 1993. Measuring Flow Parameters in the Tsukim Springs (En Fescha). *Isr. Hydrological Service Water Commission (in Hebrew)*.
- Guttman, J., 2006. Geology and Hydrogeology of the Jordan Valley. *Multi-lateral project, within the framework of the German-Israeli-Jordanian-Palestinian joint research program for the sustainable utilization of aquifer systems. Project 02WT9719*.
- Guttman, J., Flexer, A., Hoetzl, H., Ali, W., Bensabat, J., and Yellin-Dror, A., 2000. Hydrogeology of the eastern aquifer in Judea hills and Jordan Valley. *German-Israeli-Palestinian Joint Research. Mekorot Report 468. Project 02WT9719*.
- Guttman, J. and Gotlieb, M., 1996. Hebron boreholes 1 and 2, final report, 5477- R96.253 (E) *TAHAL Consulting Engineering Ltd. Unpublished report*.
- Guttman, Y., 1998. Hydrogeology of the Eastern Aquifer in the Judean Hill and Jordan Valley. *TAHAL Consulting Engineers Ltd. Annual Report 1997, Subproject B: 01/95/66, 6440- R98.006, (in Hebrew)*.

- Guttman, Y., Flexer, A., Hötzl, H., Bensabat, J., Ali, W., and Yellin-Dror, A., 2004. A 3-D hydrogeological model in the arid zone of Marsaba-Feshchah region, Israel. - In: The 5th International Symposium on Eastern Mediterranean Geology. *Thessaloniki Proceedings* **3**, 1510-1513.
- Guttman, Y. and Rosenthal, A., 1991. Mitzpe Jericho Area-Study of Salinization Mechanisms and Water Potential. *TAHAL Consulting Engineers Ltd. Report no. 01/91/46 (in Hebrew)*.
- Guttman, Y. and Simon, A., 1984. Hydrogeological survey of the western shore of the Dead Sea *Mediterranean-Dead Sea project, summary of research reports in Hebrew* **5**, 304-318.
- Guttman, Y. and Zukrman, H., 1995. Flow model in the Eastern Basin of the Judea and Samaria hills. *TAHAL Consulting Engineers Ltd. Report no. 01/95/66 (in Hebrew)*.
- Haddad, M., 1998. Planning Water Supply Under Complex and Changing Political Conditions: Palestine as a Case Study. *Water Policy Journ.* **1**, 177-192.
- Hirzalla, B., 1973. Groundwater Resources Of The Jordan Valley. *Natural resources Authority, Water Resources Division, Groundwater Section, Amman, Jordan*.
- Homer-Dixon, T., 1991. On the threshold: environmental changes as causes of acute conflict. *International Security* **16**, 76-116.
- Hosh, L., Isaac, J., and . 1992. Roots of the water conflict in the Middle East. Paper presented at the Conference on the Middle East Water Crisis: Creative Perspectives and Solutions. *University of Waterloo, Waterloo, Canada. 8-9, May 1992*.
- Hötzl, H., 2008: The Hydrochemical history of the Rift - The Water of the Jordan Valley Handbook, *Springer Scientific Publishing Company, Berlin Hidelberg*.**1**, 75-217
- Hötzl, H., Ali, W., and Rother, M., 2001. Ein Feshkha Springs as a potential reservoir for fresh water extraction, Dead Sea Area. *Le premier colloque national d'hydrogeologie et environment, Fes, Morocco.*, 62.
- Hötzl, H., Ali, W., and Rother, M., 2001. Hydrogeological Investigations for the Development of Sustainable Fresh Water Extraction of the Mar Saba - Ein Feshkha Region. *Annual Report BMBF Project Nr. WT0063 Karlsruhe, Germany*.
- Husary, S., Najjara, T., and Eliewi, A., 1996. Analysis of secondary source rainfall data from the northern West Bank. *PHG, Jerusalem*.
- Inbar, M. and M., J., 1984. Water Resource Planning and Development in the Northern Jordan Valley. *Water International* **9**, 18-25.

- Isaac, J. and Sabbah, W., 1998. Water Resources And Irrigated Agriculture In The West Bank. *Appl. Res. Ins. Of Jerusalem*, 247
- Issar, A., 1993. Recharge and salination processes in the carbonate aquifers. *Isr. Env. Geo.* **21**, 152 -159
- Issar, S., 1993. Recharge and salination processes in the carbonate aquifers in Israel *Isr. Env. Geo.* **21**, 152-159.
- Jacovides, J., 1979. Environmental isotope survey. *Final Report of International Atomic Energy Agency, Vienna*, 81.
- Johnson, P., 1998. Tectonic map of Saudi-Arabia and adjacent areas. *Ministry of Petroleum and Mineral Resources Riad Technical report USGS-TR-98-3*.
- Kafri, U. and Arad, A., 1979. Current subsurface intrusion of Mediterranean seawater - A possible source of groundwater salinity in the rift Valley system. *Isr. Journ. Hydrol.* **44**, 267-287.
- Kafri, U., Goldman, M., and Lang, B., 1997. Detection of subsurface brines freshwater bodies and the interface configuration in-between by the time domain electromagnetic method in the Dead Sea rift, Israel: . *Isr. Env. Geo.* **31**, 42-49.
- Kahhaleh, S., 1981. The Water Problem in Israel and its Repercussions on the ArabIsraeli Conflict. *Beirut: Institute for Palestine Studies*.
- Kaufman, A. and Libby, W., 1954. Natural distribution of tritium. *Phys. Rev.* **93**, 337-1344.
- Kaufman, A., Yechieli, Y., and Gardosh, M., 1992. Reevaluation of the lake sediment chronology in the Dead Sea basin, Israel, based on new $^{230}\text{Th}/\text{U}$ dates. *Quat. Res.* **38**, 292 -304.
- Khayat, S., 2005. Hydrochemistry and Isotope Hydrogeology in the Jericho Area/ Palestine. *Ph.D thesis, University of Karlsruhe, Germany*.
- Khayat, S., Geyer, S., Hötzl, H., Ghanem, M., and Ali, W., 2006. Identification of nitrate sources in groundwater by $\delta^{15}\text{N}$ nitrate and $\delta^{18}\text{O}$ nitrate isotopes: a study of the shallow Pleistocene aquifer in the Jericho area, Palestine. *Hydroch. Hydrobio. Acta.* **34** 27 - 33.
- Khayat, S., Hötzl, H., Geyer, S., Ali, W., Knöller, K., and Strauch, G., 2006. Sulphur and oxygen isotopic characters of dissolved sulphate in groundwater from the Pleistocene aquifer in the southern Jordan Valley (Jericho area, Palestine). *Isotopes in Environmental and Health Studies* **42**, 289 - 302.
- Khouri, F., 1985. The Arab-Israeli dilemma. *Syracuse University Press, Syracuse, NY, USA*.

- Kolodny, Y., Katz, A., Starinsky, A., Moise, T., and Simon, E., 1999. Chemical tracing of salinity sources in Lake Kinneret (Sea of Galilee), Israel *Limnology and Oceanography* **44**, 1035-1044.
- Krenkel, E., 1924. The Syrian arch. Headquarters leaf for mineralogy. *Geologic and paleontology* **9-10**, 274-281 and 301-313.
- Kronfeld, J., Ilani, S., and Strull, A., 1991. Radium precipitation and extreme ²³⁸U-series disequilibrium along the Dead Sea coast, Israel. *Applied Geochem.* **6**, 355-361.
- Ku, T., Luo, S., Hammond, D., and Leslie, B., 1992. Applications of decay-series disequilibria to water-rock interactions and geothermal systems. In: Uranium-Series Disequilibrium: Applications to Marine and Environmental Problems. *Clarendon Press* **2nd**.
- Langmuir, D., 1971. The geochemistry of some carbonate ground waters in central Pennsylvania. *Geochim. Cosmochim. Acta.* **29**, 1023-1045.
- Lerman, A., 1970. Chemical equilibrium and evolution of chloride brines. *Morgan BA (ed) 50th Anniversary Symposium Mineralogical Society Special Paper* **3**, 291-306.
- Levy, Y., 1972. Interaction between brines and sediments in the Bardawil area, northern Sinai. *Ph.D thesis, Hebrew University, Jerusalem.*
- Lloyd, J. and Heathcoat, J., 1985. Natural inorganic chemistry in relation to ground water. *Clarendon Press, Oxford.*
- Lonergan, S. and David, B., 1994. Watershed: The Role of Fresh Water in the Israeli Palestinian-Conflict. Ottawa: International Development Research Centre.
- Lowdermilk, W., 1944. Palestine: land of promise. *Greenwood Press, New York, NY, USA.*
- Lowi, M. and 1992. West Bank water resources and the resolution of conflict in the Middle East. *Peace and Conflict Studies Program, University of Toronto. Project on Environmental Change and Acute Conflict, Occasional* **1**, 29-60.
- Magaritz, M. and Nadler, A., 1980. Re-interpretation of the ¹⁸O and D isotopic composition of the Tiberias subgroup hot waters. *Isr. Geo. Soc. Proceedings, March 1980, 26., Annual Meeting*
- Matsui, E., 1980. A simple method using a disposable syringe to prepare samples for d¹⁸O measurements in water samples. *Analyt. Chim. Acta.* **120**, 423-425.
- Mazor, E., 1962. Radon and radium content of some Israeli water sources and a hypothesis on underground reservoirs of brines, oils and gases in the Rift Valley. *Geochim. Cosmochim. Acta.* **26**, 765- 786.

- Mazor, E. and Mero, F., 1969a. Geochemical tracing of mineral and fresh water sources in the Sea of Galilee Basin. *Isr. Journ. Hydro.* **7**, 276-317.
- Mazor, E. and Mero, F., 1969b. The origin of the Tiberias-Noit mineral water association in the Tiberias-Dead Sea Rift Valley. *Isr. Journ. Hydro.* **7**.
- Mazor, E. and Molcho, M., 1972. Geochemical studies on the Feshcha springs, Dead Sea Basin. *Isr. Journ. Hydro.* **15**, 37-47.
- Mccallin, J., 2002. Israel bans new West Bank wells. *Sunday Herald* **October, 28**.
- Mccarthy, J., 1990. The Population of Palestine. *New York: Columbia University Press*.
- Mekorot., 1987. The water resources of Palestine: Israel National Water Carrier. *Mekorot Water Co. Ltd 1944 50 years of Mekorot*.
- Meybeck, M., 1984. Geographic variability of the natural chemical composition of running waters. *Verh. Internat. Verein. Limnol.* **22**, 1766-1774.
- Migowski, C., Ken-Tor, R., Negendank, J., Stein, M., and J., M., 1999. Post-Lisan record documented in sediment sequences from the western shore area and the central basin of the Dead Sea. *Terra Nostra 98/6: 3rd ELDP Workshop, Ptolemais*, 100-102.
- Moise, T., Starinsky, A., Katz, A., and Kolondy, Y., 2000. Ra isotopes and Rn in brines and ground waters of the Jordan-Dead Sea Rift Valley: Enrichment, retardation, and mixing. *Geochim. Cosmochim. Acta.* **64**, 2371-2388.
- Möller, P., Rosenthal, E., Geyer, S., and Flexer, A., 2007. Chemical evolution of saline waters in the Jordan-Dead Sea transform and in adjoining areas *Internat. Journ. of Earth Sci.* **96**, 541-566.
- Mook, W., 1994. Principles of isotope hydrology: introductory course on isotope hydrology. *Centre of Isotope Research University of Groningen*.
- Moore, S. and Arnold, R., 1996. Measurement of ²²³Ra and ²²⁴Ra in coastal waters using a delayed coincidence counter. *Journ. of Geophy. Res.* **101**, 1321 -1329.
- Moore, S. and Reid, F., 1973. Extraction of radium from natural waters using manganese-impregnated acrylic fibers. *Journ. of Geophy. Res.* **78**, 8880-8886.
- Moser, E. and Reuther, D., 2006. Stress variations determined by measuring electromagnetic emissions along the active Southamerican plate boundary (southern Chile) *Geophysical Research* **8**, 1879.
- Naff, T. and Matson, R., 1984 Water in the Middle East: conflict or cooperation? . *Westview Press Boulder, CO, USA*.

- Naor, H., Katz, D., and Harash, Y., 1987. hydrogeological study to locate production wells in Wadi Zohar area. *TAHAL Consulting Engineering Ltd. Report no. 04/87/17 (in Hebrew)*.
- Nathan, Y., Shuval, S., and Sandler, A., 1992. Clay sediments from the Dead Sea. *Isr. Geo. Sur. Reports no. GSI/21/92*.
- Neal, C. and Shand, P., 2002. Spring and surface water quality of the Cyprus ophiolites. *Hydrology and Earth System Sciences* **6**, 797–817
- Neev, D. and Hall, J., 1976. The Dead Sea geophysical survey, 19 July-1 August, 1974. *Geo. Surv. Isr. Report no. 6/76*, 21.
- Nishri, A., 1982. The geochemistry of manganese and iron in the Dead Sea. *Ph.D thesis, Weizmann Institute of Science, Rehovot*.
- Palacky, G., 1987. Resistivity characteristics of geological targets. In: Nabighian, M. (Ed.), *Electromagnetic Methods in Applied Geophysics-Theory. Society of Exploration Geophysicists Tulsa, OK*, 53-129.
- Parkhurst, D. and Appelo, C., 2001. PHREEQC - A computer program for speciation, batch reactions, one dimensional transport and inverse geochemical calculations. *US Geological Survey*.
- PCBS, 2007. Population Growth rates in the West Bank and Gaza. *Palestinian Central Bureau of Statistics (Unpublished report)*
- Pe`eri, S., Wdowinski, S., Shtibelman, A., Bechor, N., Bock, Y., Nikolaidis, R., and Domselaar, M., 2002. Current plate motion across the Dead Sea fault from three years of continuous GPS monitoring. *Geophy. Res. Lett.* **29**, 14,10.1029/2001GL013879.
- Picard, L., 1937. On the structure of the Arabian Peninsula. *Bulletin Geol. Dept. Hebr. Univ.*
- Picard, L., 1939. Outline of the tectonics of the Earth with special emphasis upon Africa. *Bulletin Geol. Dept. Hebr. Uni. Jerusalem* **2**, 1-66.
- Picard, L., 1943. Structure and evolution of Palestine with comparative notes on neighbouring countries. *Bulletin .Geol. Dept. Hebr. Uni. Jerusalem* **4**, 1-143.
- PWA, 2001. Drinking water standards. *Palestinian Water Authority Personal Communication*
- PWA, 2002. Water Supply in the West Bank. *Palestinian Water Authority Internal report*.
- Qannam, Z. and Merkle, B., 2002. Hydrogeology, hydrochemistry and contamination sources in Wadi Al Arroub drainage basin, Palestine. *Ph.D thesis Technische Universität Bergakademie Freiberg, Germany*, 111-123.

- Quennell, A., 1959. The structural and geomorphic evolution of the Dead Sea Rift *Quart. Journ. Geol. Soc.* **114**, 432-433.
- Ra'anan, U., 1955. The Frontiers of a Nation: A Re-examination of the Forces which Created the Palestine Mandate and Determined its Territorial Shape. *Hyperion Press*.
- Rama, F., Todd, I., and Moore, S., 1987. A new method for the rapid measurement of ^{224}Ra in natural waters. *Mar. Chem.* **22**, 43-54.
- Reichman, S., 1997. The Absorptive Capacity Of Palestine, 1882-1948. *Middle Eastern Studies* **33**, 338-361.
- Reifenberg, A. and Whittles, A., 1947. The Soils of Palestine. *Thomas Murby Co., London, UK*, 16.
- Ritter, O., Ryberg, T., Weckmann, U., Hoffmann-Rothe, A., Abueladas, A., and Garfunkel, Z., 2003. Geophysical images of the Dead Sea Transform in Jordan reveal an impermeable barrier for fluid flow *Geophys. Res. Lett.* **30**, 1741-1744.
- Rofe & Raffety, C. E., 1963. Geological and hydrological report, Jerusalem and district water supply. *Central Water Authority Of Jordan Westminster, London, UK.*, 79.
- Rofe & Raffety, C. E., 1965. Nablus District Water Resources Survey: Geological And Hydrogeological Report. *Central Water Authority Of Jordan Westminster, London, UK.*
- Rofe & Raffety, C. E., 1965. West Bank Hydrology: Analysis Report. *Central Water Authority of Jordan Westminster, London, UK.*
- Rophe, B., 2003. Discharge to Zsukim (Fescha) Springs-Summer 2003. *Isr. Hydrol. Serv. Israel Water Commission.*
- Rosenthal, A., 1978. Non-Equilibrium of $^{234}\text{U}/^{238}\text{U}$ Isotopes in the Water of the Judea Group Aquifer on the Eastern Slopes of the Judea and Samaria Hills. *M.Sc thesis, Tel Aviv University (in Hebrew).*
- Rosenthal, A., 1987. Chemical composition of rainfall and groundwater in recharge areas of the Bet Shean-Harod multiple aquifer system, Israel. *Isr. Journ. Hydrol.* **89**.
- Rosenthal, A., Weinberger, G., and Kronfeld, J., 1999. Groundwater salinization caused by residual Neogene and Pliocene sea water - an example from the Judea Group aquifer, southern Israel. *Groundwater* **37**, 261-270.
- Rozanski, K. and GrÖning, M., 2004. Tritium assay in water samples using electrolytic enrichment and liquid scintillation spectrometry. *TECDOC-1401, IAEA* **195-217**.

- Sabbah, W. and Isaac, J., 1996. An Evaluation Of Water Resources Management In Ramallah District. *Proceedings Of International Seminar On Water Management In Palestine Palestinian Water Authority*, 161-181.
- Sagy, A., 1999. Jointing and Faulting Processes Along the Western Margins of the Dead Sea Basin. *MSc thesis, The Hebrew University, Jerusalem, (in Hebrew)*. 45
- Salameh, E. and El-Naser, H., 2000b. The interface configuration of the fresh -Dead Sea water-Theory and measurements. *Hdrochim. Hydrobio. Acta*. **28**, 323-328.
- Sass, E. and Starinsky, A., 1979. Behaviour of strontium in subsurface calcium chloride brines: Southern Israel and Dead Sea rift valley. . *Geochim. Cosmochim. Acta*. **43**, 885-895.
- Saxena, V., Mondal, N., and Singh, V., 2004. Identification of sea-water ingress using strontium and boron in Krishna Delta, India. *Current Sci. Journ.* **86**, 586-590.
- Scarpa, D., Isaac, J., and Shuval, H., 1994. Eastward groundwater flow from the Mountain Aquifer, Water and Peace in the Middle East. *Elsevier Science*, 193-203.
- Schramm, A., Stein, M., and Goldstein, S., 2000. Calibration of the 14C timescale to >40ka by 234U/ 230Th dating of sediments from Lake Lisan (the paleo- Dead Sea). *Earth Planet. Sci. Lett.* **175**, 27-40.
- Schulman, N., 1959. The geology of the central Jordan Valley. *Bulletin Res. Coun. Isr.* **8G**, 63-90.
- SCIENCES, C. O. A., 2002. Irrigation water quality. *The Pennsylvania State University, USA. (<http://www.cas.psu.edu/docs/casdept/Turf/Education/Turgeon/CaseStudy/OldRanch/IrrWatQual.html>, 01.12.2007)*.
- Segovia, N., Barragan, M., Tello, E., and Alfaro, R., 2005. Geochemical Exploration at Cutzeo Basin geothermal Zone (Mexico). *Journ. of Appl. Sci.* **5**, 1658-1664.
- Shachnai, E., Miro, F., and Meiri, D., 1983. Hydrogeological Survey in Tsukim Springs. *TAHAL Consulting Engineers Ltd. Report no. 01/83/98, (in Hebrew)*.
- Skinner, B. and Porter, S., 1987. Physical Geology. *John Wiley And Sons, New York, USA*.
- Sklash, M. and Farvolden, R., 1979. The role of groundwater in storm runoff. *Jour. of Hydrol.*, **43**, 45-65.
- Sklash, M., Farvolden, R., and Fritz, P., 1976. A conceptual model of watershed response to rainfall, developed through the use of oxygen-18 as a natural tracer. *Can. Journ. Earth Sci.* **13**, 271-283.

- Sneh, A., Bartov, Y., Weissbrod, T., and Rosensaft, M., 1998. Geological Map of Israel. *Geo. Serv. Isr. Sheet 3*.
- Stanislavsky, E. and Gvirtzman, H., 1999. Basin-scale migration of continental-rift brines: paleohydrologic modeling of the Dead Sea Basin. *Geology* **27**, 791-794.
- Starinsky, A., 1974. Relationship between Ca-Chloride Brines and sedimentary Rocks in Israel. *Ph.D thesis, Hebrew University, Jerusalem (in Hebrew)*.
- Stauffer, T., 1982. The Price of Peace: The Spoils of War. *American-Arab Affairs* **1**, 43-54.
- Stein, M., 2001. The sedimentary and geochemical record of Neogene- Quaternary water bodies in the Dead Sea Basin-Inferences for the regional paleoclimatic history. *Journ. of Paleolimnology* **26**, 271-282.
- Steinhorn, I., 1985. The disappearance of the long term meromictic stratification of the Dead Sea. *Limnol. Oceanogr.* **30**, 451-472.
- Steinitz, G., Vulkan, U., and Lang, B., 1995. The radon flux at the northwestern segment of the Dead Sea (Dead Sea Rift) and its relation to earthquakes, during 1992-1994. *Geo. Surv. Isr. Rep. GSI/40/95, and ZD/180/9*.
- Stephen, C. and David, B., 1994. Watershed : the role of fresh water in the Israeli-Palestinian conflict. *Published by the International Development Research Centre PO Box 8500, Ottawa, ON, Canada K1G 3H9*, 195.
- Stoecklin, J., 1968. Speclt deposits of the Middle East. In: R.B. Mattox [ed]. International Conference of Saline Deposits. *Geol. Soc Ameri.* **88**, 157-181.
- Sulin, V., 1946. Waters of petroleum formations in the system of natural waters. *Gostoptekhizdat, Moscow*, 35-96.
- SUSMAQ., 2001. Sustainable Management of the West Bank and Gaza Aquifers Data Review on the West Bank Aquifers. *Data Review working report SUSMAQ-MOD# 02, V2.0, Version 2.0*. (<http://www.ncl.ac.uk/susmaq/library/reports/datareview.pdf>).
- Swan, A. and Sandilands, M., 1995. Introduction to Geological Data Analysis. *Blackwell, Oxford*.
- Taylor, C. and Roether, W., 1982. A uniform scale for reporting low-level tritium measurements in water. *Int. Journ. Appl. Radiat. Isot.* **33**, 377-382.
- Teclaff, L., 1967. The river basin in history and law. *Nijhoff Publishers, The Hague, Netherlands*.
- Todd, D., 1980. Ground water. *Prentice Hall Inc., London*.

- Trottier, J., 1999. *Hydropolitics In The West Bank And Gaza Strip. Ph.D thesis Universite' Catholique de Louvain, Belgium*, 249.
- Vengosh, A. and Rosenthal, A., 1994. Saline groundwater in Israel: Its bearing on the water crisis in the country. *Journ. of Hydro.* **156**, 389-430.
- White, D., Barnes, I., and O'Neil, J., 1973. Thermal and mineral waters of non-meteoric origin, California Coast range. *Bulletin Geol. Soc. Ameri.* **84**, 547-60.
- WHO, 1993. Guidelines for Drinking Water Quality *World Health Organization, Geneva, Switzerland* **1**, 8-29 and 120-130.
- WHO, 1996. Guidelines for drinking water quality. *World Health Organization, Geneva, Switzerland* **2**, 940-949.
- WHO, 1998. Guidelines for Drinking Water: Health criteria and other supporting information. *Geneva, Switzerland:World Health Organization* **2**, 281-3.
- Wilcox, L., 1955. Classification and use of irrigation waters. *US Dept. Agric. Circ. Washington, D.C., USA.*, 19
- Wishahi, S. and Khalid, M., 1999. Hydrochemistry of the Jordan Valley aquifers, Water and Environment. *Palestinian Hydrology Group*, 12-21.
- Wolf, A., 1995. *Hydropolitics along the Jordan River: scarce water and its impact on the Arab-Israeli conflict. United Nation University Press, Tokyo, Japan. (In Press)*.
- Wolf, A., 2000. Trends in Transboundary Water Resources: Lessons for Cooperative Projects in the Middle East. *Ottawa: IDRC*, 137-156 **(In Press)**.
- Wolfer, J., 1998. Hydrogeological investigation along the Jerusalem- Jericho transect (Wadi el Oilt). *Diploma Thesis, Department of Applied geology, Karlsruhe University*.
- Yaghan, R., 1983. Geologic and structural interpretation of Landsat images in North Jordan. *University of Jordan* 61
- Yechieli, Y., Magaritz, M., Levy, Y., Weber, U., Kafri, U., Woelfli, W., and Bonani, G., 1993. Late Quaternary geological history of the Dead Sea area, Israel. *Quat. Res.* **39**, 59-67.
- Yechieli, Y., Ronen, D., and Kaufman, A., 1996. The source and age of groundwater brines in the Dead Sea area as deduced from Cl 36 and C14. *Geochim. Cosmochim. Acta.* **60** 1909-1916.
- Zak, I., 1967. The geology of Mount Sedom. *Ph.D thesis, Hebrew University, Jerusalem*.
- Zarour, H. and Isaac, J., 1993. Nature's apportionment and the open market: a promising solution to the Arab-Israeli water conflict. *Water International* **18**, 40-53.

The Appendices

Appendix 4.2: Sample name, description and coordination of the samples collected during the first campaign from the springs and wells of the catchment area.

Borehole/ Spring	Sample #	Description	Coordination
Spring	10	(Spring 1+2), the main spring at the old entrance of the reserve.	192805/124691
Borehole	11	Mt.Jericho-2	188257/134390
Spring	12	North east, spring branching in between a group of trees and boshes. Under small bridge.	192908/124518
Spring	13	Strong stream of water hading to the Dead Sea.	193061/124396
Spring	14	Strong stream of water hading to the Dead Sea, (beneath a bridge 2m).	193121/124066
Spring	15	A group of variable paths joined together forming stream passing through formations of marlstone.	193335/123977
Spring	16	A small path getting stronger after joining to it a big canyon.	193143/124095
Borehole	17	Feshcha-III, 60m in depth with artesian preacher.	193112/124086
Spring	19	a pool rich with vegetation at the spring exit. Water passing underneath the street.	192764/123395
Spring	20	Water passing underneath the street through a rock canal.	192725/122848
Spring	21	At the southern part of the closed reserve, merging beneath the main street.	192560/122135
Borehole	22	Azarea-1	176610/132018
Borehole	23	Herodion-1	170930/118325
Spring	24	Wade ein al-malh spring	195010/192617
D.S lake	25	At the southern part of the closed reserve.	192830/122698

Appendix 4.3: Sample name, description and coordination of the samples collected during the second campaign from the springs and wells of the catchment area.

Borehole / Spring	Sample #	Description	Coordination
Spring	30	(Spring 1+2), the main spring at the old entrance of the reserve.	192805/124691
Borehole	31	Mt.Jericho-2	188257/134390
Spring	32	North east, spring branching in between a group of trees and boshes. Under small bridge.	192908/124518
Spring	33	Strong stream of water hading to the Dead Sea.	193061/124396
Spring	34	Strong stream of water hading to the Dead Sea, (beneath a bridge 2m).	193121/124066
Spring	35	A group of variable paths joined together forming stream passing through formations of marlstone.	193335/123977
Spring	36	A small path getting stronger after joining to it a big canyon.	193143/124095
Borehole	37	Feshcha-III, 60m in depth with artesian preacher.	193112/124086
Spring	39	North east, spring branching in between a group of trees and boshes.	192911/124520
Spring	40	a pool rich with vegetation at the spring exit. Water passing underneath the street	192764/123395
Spring	41	Water passing underneath the street through a rock canal.	192725/122848
Borehole	42	Azarea-1	176610/132018
Borehole	43	Herodion-1	170930/118325
Borehole	44	Mt.Jericho-2	188257/134390
Spring	45	Wade ein al-malh spring.	195010/192617
Spring	46	Ein Gadi spring at the natural reserve.	164968/128741
D.S lake	47	At the southern part of the closed reserve.	192830/122698
Borehole	50	Azarea-3	173830/112878
Borehole	51	Beit Fajar-1A	169607/115110
Borehole	52	Herodion-4	169460/114087
Borehole	53	JWC-4	170871/121879
Borehole	54	PWA-1	167367/112394
Borehole	55	PWA-3	171255/120265
Borehole	56	Abu Dies Well	174313/124109
Borehole	57	Arab project-66	197030/141050
Spring	58	Ein Samia spring.	181950/154567
Spring	59	Ein Al-Sultan spring.	192155/141952
Spring	60	Ein Al-Dyook spring.	190110/144645
Spring	61	Wade Al-Quilt spring.	185622/138165
Spring	62	Kina spring.	169799/130011
Borehole	63	Fasael-2	183059/130210
Borehole	64	Al-Auja-2	186760/151431

Appendix 4.4: Sample name, description and coordination of the samples collected during the third campaign from the springs and wells of the catchment area.

Borehol/ Spring	Sample #	Description	Coordination
Spring	65	(Spring 1+2), the main spring at the old entrance of the reserve.	192805/124691
Borehole	66	Mt.Jericho-2, 493 m in depth.	188257/134390
Spring	67	North east, spring branching in between a group of trees and boshes. Under small bridge.	192908/124518
Spring	68	North east, spring branching in between a group of trees and boshes.	192911/124520
Borehole	69	Feshcha-III, 60m in depth with artesian preacher.	193112/124086
Borehole	70	Pesometer EZ-5, 6 m in depth.	193143/124095
Spring	71	a pool rich with vegetation at the spring exit, Water passing underneath the street.	192764/123395
Spring	72	Water passing underneath the street through a rock canal.	192725/122848
Borehole	73	Feshcha well 101, 11 m in depth.	192900/124327
Borehole	74	Azarea-1, 827 m in depth.	176610/132018
Borehole	75	Azarea-3, 784 m in depth.	173830/112878
Borehole	76	JWC-4, 788 m in depth.	170871/12189 0
Borehole	77	Herodion-1, 350 m in depth.	170930/11832 5
Borehole	78	Herodion-2, 770 m in depth.	170901/11930 1
Borehole	79	Herodion-3, 743 min depth.	170902/11755 1
Borehole	80	PWA-1, 601 m in depth.	167367/11239 4
Borehole	81	PWA-11, 851 m in depth.	169161/11631 0
Spring	82	At the southern part of the closed reserve, merging beneath the main street.	192560/122135

Appendix 5.2: This table presents the field analysis and the analysis of the cations and anions of the catchmint area during the course of this study.

Sample #	Temp °C	TDS g/l	EC mS/cm	pH	DO mg/l	Cl mg/l	HCO ₃ mg/l	F mg/l	SO ₄ mg/l	NO ₃ mg/l	Na mg/l	K mg/l	Mg mg/l	Ca mg/l	TH mg/l
10	27	2.05	4.39	7.61	0.00	1411	183	0.22	77	28	446	44	153	208	1150
11	31.3	0.31	0.65	6.31	5.90	137	100	0.24	49	27	60	10	27	50	250
12	27.3	2.41	5.28	6.73	6.18	1870	171	0.20	69	29	701	48	155	286	1350
13	28.4	3.05	6.58	6.82	7.00	2461	207	0.17	7	30	893	63	198	375	1750
14	28.4	3.11	6.72	6.85	5.90	3280	207	0.17	82	30	1177	79	184	417	1800
15	28.5	2.93	6.29	7.05	7.84	2037	183	0.17	79	30	693	69	236	292	1700
16	29	2.82	6.24	7.37	7.71	2063	476	0.17	76	30	860	61	249	250	1650
17	26.5	8.10	16.28	8.11	0.00	11048	195	1.56	158	13	3541	137	413	2543	8050
18	0	2.78	5.41	7.61	0.00	1947	171	0.81	77	20	658	54	261	250	1700
19	24.7	7.24	14.48	7.30	12.70	4898	215	0.54	71	36	1602	180	522	287	2866
20	27.4	3.12	6.25	7.10	2.60	1824	246	0.40	112	31	483	60	262	185	1541
21	27.6	3.61	7.23	7.20	4.00	2196	276	0.31	115	31	520	71	238	416	1399
22	*ND	0.29	0.60	7.50	ND	43	320	*<0.01	12	6	15	2	41	44	278
23	ND	0.24	0.51	7.60	ND	23	305	<0.01	3	8	12	2	28	54	247
24	35.6	3.65	6.01	7.12	ND	1730	265	2.30	343	2	755	45	103	379	1370
25	40.9	338	183	6.43	ND	219872	180	<0.01	987	4	33664	7735	47934	20811	249369
30	26.1	1.75	4.10	7.01	5.03	1469	186	ND	72	25	380	46	211	182	1323
31	25.4	0.36	0.72	7.41	5.66	320	183	ND	50	25	58	9	57	94	469
32	24.5	2.20	4.50	7.40	5.77	1720	198	ND	65	27	432	52	232	190	1430
33	23	2.80	5.70	6.80	5.50	2024	183	ND	76	28	517	66	263	208	1602
34	23.7	2.70	5.40	6.60	5.07	2061	195	ND	79	28	538	56	270	203	1619
35	24.7	2.80	5.50	6.80	4.30	1976	186	ND	75	30	444	70	399	191	2120
36	23.5	3.50	7.00	6.90	5.00	1959	192	ND	77	29	525	91	280	217	1695
37	25	9.10	18.30	6.60	5.08	6469	238	ND	176	6.34	2407	344	542	318	3026
40	25	5.80	11.70	6.90	4.65	3823	201	ND	65	29	1474	156	458	274	2570
41	25.2	2.20	4.50	6.50	5.13	1723	220	ND	81	27	470	61	250	200	1529

39	26	3.10	6.50	6.90	6.03	1588	195	ND	70	27	463	60	248	193	1503
42	ND	0.39	0.55	7.40	ND	23	311	<0.01	11	4	19	2	36	54	281
43		0.30	0.55	7.30	ND	22	317	0.40	9	6	19	1	37	50	279
44	24.71	0.59	0.78	7.31	ND	75	253	0.27	33	39	40/1	3	31	76	317
45	34.5	3.53	5.90	7.01	ND	1688	254	2.50	334	3	736	44	99	366	1321
46	28	0.50	0.71	7.41	ND	82	211	0.30	35	29	48	5	29	56	259
47	25.3	321	181	6.23	ND	120050	167	<0.01	117	3	24591	3803	20171	11092	110766
50	ND	0.29	0.59	7.50	ND	43	190	0.18	13	6	17	2	16	45	177
51	ND	0.49	0.59	7.81	ND	32	318	0.21	9	13	25	1	33	55	274
52	ND	0.30	0.61	7.22	ND	21	300	0.31	10	4	18	1	30	56	262
53	ND	0.33	0.51	7.45	ND	23	336	0.31	13	5	20	2	29	69	291
54	ND	0.33	0.56	7.41	ND	24	315	0.17	3	11	13	2	25	65	264
55	ND	0.25	0.48	7.71	ND	24	267	0.21	3	9	7	2	30	48	242
56	23.4	0.44	0.79	7.01	ND	56	269	0.19	20	17	24	2	27	55	248
57	25.9	2.98	5.36	7.41	ND	1451	411	0.21	280	38	560	77	198	168	1231
58	15	0.25	0.46	7.94	ND	23	291	0.20	11	13	17	2	23	52	226
59	24	0.19	0.68	7.39	ND	53	266	0.20	24	48	26	3	28	84	325
60	24.7	0.19	0.68	7.35	ND	46	293	0.20	24	55	26	3	29	86	332
61	16	0.27	0.50	6.73	ND	25	261	0.17	6	9	19	1	20	55	220
62	25.6	1.09	1.94	7.58	ND	400	311	0.60	9	52	138	17	91	103	631
63	25.11	0.44	0.61	7.34	ND	49	267	0.20	15	22	26	2	26	57	249
64	20.1	0.26	0.48	7.21	ND	38	315	0.31	15	21	17	4	31	83	335
65	26.4	1.98	4.10	7.10	0.89	1154	188	ND	ND	ND	ND	ND	ND	ND	ND
66	26	0.21	0.46	7.43	5.66	99	184	ND	ND	ND	ND	ND	ND	ND	ND
67	24.8	2.29	4.97	6.70	2.60	1507	176	ND	ND	ND	ND	ND	ND	ND	ND
68	26.8	2.19	4.82	6.93	2.31	1493	179	ND	ND	ND	ND	ND	ND	ND	ND
69	26.1	10.71	21.20	7.72	4.53	7445	210	ND	ND	ND	ND	ND	ND	ND	ND
70	27.7	3.42	6.13	7.33	1.59	1985	196	ND	ND	ND	ND	ND	ND	ND	ND
71	25.5	6.42	13.11	7.56	4.41	4821	221	ND	ND	ND	ND	ND	ND	ND	ND

72	23.3	6.35	13.12	7.46	4.93	4721	214	ND	ND	ND	ND	ND	ND	ND	ND
73	26.3	2.25	4.36	7.73	ND	2659	179	ND	ND	ND	ND	ND	ND	ND	ND
74	25.7	0.29	0.61	7.39	4.01	43	327	ND	ND	ND	ND	ND	ND	ND	ND
75	24.09	0.27	0.57	7.54	4.02	43	296	ND	ND	ND	ND	ND	ND	ND	ND
76	24.13	0.33	0.53	7.38	3.93	23	332	ND	ND	ND	ND	ND	ND	ND	ND
77	24.1	0.24	0.51	7.60	5.13	32	300	ND	ND	ND	ND	ND	ND	ND	ND
78	22.4	0.20	0.53	7.34	4.04	28	154	ND	ND	ND	ND	ND	ND	ND	ND
79	23.7	0.28	0.61	7.27	3.10	36	257	ND	ND	ND	ND	ND	ND	ND	ND
80	25.5	0.33	0.55	7.41	4.09	25	314	ND	ND	ND	ND	ND	ND	ND	ND
81	24.3	0.29	0.59	7.36	5.07	27	296	ND	ND	ND	ND	ND	ND	ND	ND
82	24.02	2.40	5.04	7.17	4.71	4821	270	ND	ND	ND	ND	ND	ND	ND	ND

*ND: Not determined

*<0.01: below detection limit

Appendix 5.6: The ionic ratios of the sampled wells and springs in the Marsaba-Feshcha area during the years 2005, 2006 and 2007.

SampleID	Sr/Ca	Sr/Cl	HCO3/Cl	SO4/Cl	SO4/HCO3	K/Cl	Na/Cl	Na/Cl	Na/K	Mg/Na	Mg/Ca	Mg/Cl	Ca/HCO3
	%	%	meq/l	meq/l	meq/l	meq/l	meq/l	meq/l	meq/l	meq/l	meq/l	meq/l	meq/l
Lisan	*ND	ND	0.040	0.050	ND	0.050	0.540	0.540	ND	0.650	1.710	0.230	ND
Dead Sea	ND	ND	0.400	0.450	ND	0.050	0.910	0.910	ND	0.833	0.930	0.460	ND
10	2.885	0.754	0.075	0.040	0.533	0.028	0.487	0.487	17.459	0.418	1.211	0.316	3.467
11	4.000	2.591	0.425	0.264	0.622	0.070	0.666	0.666	9.519	0.419	0.856	0.554	1.524
12	2.807	0.758	0.053	0.027	0.511	0.023	0.578	0.578	24.789	0.297	0.893	0.241	5.089
13	2.672	0.720	0.049	0.024	0.484	0.023	0.559	0.559	24.124	0.644	0.871	0.235	5.519
14	2.403	0.540	0.037	0.018	0.504	0.022	0.553	0.553	25.347	0.548	0.731	0.165	6.139
15	3.432	0.870	0.052	0.029	0.550	0.031	0.525	0.525	17.125	0.221	1.333	0.338	4.857
16	4.006	0.859	0.134	0.027	0.203	0.027	0.643	0.643	23.981	0.747	1.642	0.352	1.600
17	1.419	0.578	0.010	0.011	1.025	0.011	0.494	0.494	43.886	0.616	0.268	0.109	39.641
18	3.205	0.728	0.051	0.029	0.568	0.025	0.521	0.521	20.739	1.026	1.713	0.389	4.457
19	7.682	0.796	0.025	0.011	0.420	0.033	0.504	0.504	15.148	0.866	2.999	0.311	4.068
20	5.417	0.972	0.078	0.045	0.578	0.030	0.408	0.408	13.732	5.185	2.336	0.419	2.290
21	2.408	0.807	0.073	0.034	0.460	0.029	0.365	0.365	12.429	4.346	0.943	0.316	4.593

22	ND	ND	4.367	0.208	0.048	0.050	0.542	0.542	10.833	0.258	1.532	2.808	0.420
23	ND	ND	7.813	0.094	0.012	0.063	0.813	0.813	13.000	2.694	0.840	3.531	0.538
24	7.403	2.869	0.089	0.147	1.647	0.024	0.673	0.673	28.557	0.265	0.448	0.174	4.357
25	7.694	1.288	0.000	0.003	6.969	0.032	0.236	0.236	7.400	0.236	3.798	0.636	352.044
30	4.405	0.965	0.074	0.036	0.489	0.028	0.399	0.399	14.008	1.050	1.912	0.419	2.977
31	0.213	0.000	0.332	0.115	0.347	0.025	0.281	0.281	11.043	1.846	1.000	0.519	1.563
32	4.219	0.824	0.067	0.028	0.417	0.027	0.387	0.387	14.128	1.016	2.014	0.393	2.926
33	4.817	0.876	0.053	0.028	0.530	0.030	0.394	0.394	13.308	0.962	2.085	0.379	3.460
34	5.923	1.032	0.055	0.028	0.513	0.025	0.403	0.403	16.364	0.950	2.193	0.382	3.166
35	5.247	0.897	0.055	0.028	0.511	0.032	0.346	0.346	10.788	1.700	3.445	0.589	3.125
36	4.617	0.905	0.057	0.029	0.508	0.042	0.413	0.413	9.803	1.009	2.127	0.417	3.438
37	11.342	0.986	0.021	0.020	0.941	0.048	0.574	0.574	11.898	0.426	2.810	0.244	4.069
39	5.192	1.116	0.071	0.033	0.459	0.034	0.456	0.456	13.340	1.000	2.119	0.456	3.009
40	8.047	1.020	0.030	0.013	0.412	0.037	0.595	0.595	16.070	0.588	2.757	0.350	4.168
41	5.010	1.029	0.074	0.034	0.454	0.032	0.421	0.421	13.103	1.006	2.061	0.423	2.765
42	ND	ND	7.727	0.348	0.045	0.061	1.227	1.227	20.250	3.642	1.105	4.470	0.524
43	ND	ND	8.525	0.311	0.037	0.066	1.344	1.344	20.500	3.756	1.232	5.049	0.481
44	2.639	4.717	1.958	0.325	0.166	0.038	0.821	0.821	21.750	1.466	0.673	1.203	0.913
45	7.667	2.941	0.087	0.146	1.673	0.024	0.672	0.672	28.327	0.255	0.446	0.171	4.389
46	3.584	4.310	1.491	0.310	0.208	0.052	0.905	0.905	17.500	1.138	0.857	1.030	0.806
47	7.624	1.246	0.001	0.001	0.891	0.029	0.316	0.316	10.997	1.552	2.999	0.490	202.015
50	ND	ND	2.570	0.215	0.084	0.050	0.612	0.612	12.333	1.757	0.578	1.074	0.723
51	ND	ND	5.789	0.200	0.035	0.044	1.211	1.211	27.250	2.495	0.986	3.022	0.530
52	ND	ND	8.339	0.356	0.043	0.068	1.322	1.322	19.500	3.154	0.885	4.169	0.565
53	ND	ND	8.609	0.422	0.049	0.078	1.328	1.328	17.000	2.800	0.690	3.719	0.626
54	ND	ND	7.701	0.104	0.014	0.060	0.821	0.821	13.750	3.691	0.625	3.030	0.630
55	ND	ND	6.441	0.088	0.014	0.074	0.441	0.441	6.000	8.133	1.012	3.588	0.550
56	ND	ND	2.791	0.259	0.093	0.032	0.658	0.658	20.800	2.135	0.810	1.405	0.621
57	8.353	1.710	0.165	0.142	0.865	0.048	0.595	0.595	12.365	0.667	1.939	0.397	1.243
58	ND	ND	7.338	0.369	0.050	0.077	1.138	1.138	14.800	2.608	0.745	2.969	0.543
59	ND	ND	2.946	0.338	0.115	0.047	0.757	0.757	16.000	2.054	0.549	1.554	0.961
60	ND	ND	3.692	0.385	0.104	0.054	0.877	0.877	16.286	2.061	0.548	1.808	0.894
61	ND	ND	6.028	0.169	0.028	0.042	1.155	1.155	27.333	2.012	0.602	2.324	0.640
62	5.837	2.660	0.452	0.017	0.037	0.040	0.532	0.532	13.333	1.248	1.457	0.664	1.008

63	3.521	7.246	3.174	0.225	0.071	0.036	0.819	0.819	22.600	1.894	0.754	1.551	0.648
64	ND	ND	4.822	0.290	0.060	0.084	0.682	0.682	8.111	3.493	0.616	2.383	0.802

Appendix 5.6: (continue)

Sample ID	Ca/Na	Ca/Cl	Ca/Mg	Ca/SO4	Ca+Mg/ Na+K	Ca/ (SO4+HCO3)	Ca/ (Ca+SO4)	Ca-(SO4+HCO3) Ca-Excess	Mg/ (Ca+Mg)	Cl-Na/Mg	Cl-(Na+K+Li) Cl-Excess
	meq/l	meq/l	meq/l	meq/l	meq/l	meq/l	meq/l	meq/l	meq/l	meq/l	meq/l
Lisan	0.537	0.150	*ND	3.800	ND	3.680	ND	ND	ND	ND	ND
Dead Sea	0.973	0.490	ND	1.090	ND	0.570	ND	ND	ND	ND	ND
10	0.467	0.261	0.826	6.500	1.122	2.261	0.867	5.800	0.548	1.622	19.290
11	0.482	0.648	1.168	2.451	1.634	0.940	0.710	-0.160	0.461	0.603	1.010
12	0.406	0.270	1.119	9.965	0.851	3.369	0.909	10.020	0.472	1.748	21.000
13	0.483	0.270	1.149	11.409	0.865	3.720	0.919	13.680	0.465	1.877	28.940
14	0.334	0.225	1.367	12.170	0.677	4.080	0.924	15.710	0.422	2.715	39.270
15	0.823	0.254	0.750	8.830	1.066	3.133	0.898	9.920	0.571	1.407	25.540
16	0.436	0.214	0.609	7.899	0.846	1.330	0.888	3.100	0.621	1.014	19.200
17	0.206	0.407	3.733	38.674	1.021	19.576	0.975	120.370	0.211	4.638	153.950
18	0.439	0.227	0.584	7.849	1.129	2.843	0.887	8.090	0.631	1.230	24.890
19	0.918	0.104	0.333	9.676	0.771	2.864	0.906	9.320	0.750	1.594	63.830
20	3.385	0.179	0.428	3.961	1.366	1.451	0.798	2.870	0.700	1.412	28.900
21	5.173	0.335	1.060	9.981	1.651	3.145	0.909	14.160	0.485	2.008	37.480
22	0.576	1.833	0.653	8.800	7.845	0.401	0.898	-3.290	0.605	0.163	0.490
23	0.709	4.203	1.190	44.833	8.839	0.532	0.978	-2.370	0.457	0.053	0.080
24	0.178	0.388	2.230	2.645	0.806	1.646	0.726	7.420	0.310	1.882	14.810
25	0.534	0.167	0.263	50.512	2.998	44.174	0.981	1015.020	0.792	1.201	4538.010
30	0.549	0.219	0.523	6.094	1.493	2.000	0.859	4.540	0.657	1.435	23.730
31	1.846	0.519	1.000	4.510	3.386	1.161	0.818	0.650	0.500	1.384	6.260
32	0.505	0.195	0.497	7.022	1.420	2.065	0.875	4.890	0.668	1.557	28.390
33	0.462	0.182	0.480	6.528	1.324	2.261	0.867	5.790	0.676	1.599	32.890
34	0.433	0.174	0.456	6.177	1.303	2.093	0.861	5.290	0.687	1.563	33.280
35	0.494	0.171	0.290	6.109	2.008	2.067	0.859	4.920	0.775	1.110	34.620
36	0.474	0.196	0.470	6.769	1.346	2.280	0.871	6.080	0.680	1.407	30.070
37	0.152	0.087	0.356	4.324	0.533	2.096	0.812	8.300	0.738	1.744	68.840
39	0.472	0.215	0.472	6.551	1.369	2.062	0.868	4.960	0.679	1.195	22.830

40	0.213	0.127	0.363	10.126	0.754	2.952	0.910	9.040	0.734	1.160	39.640
41	0.488	0.205	0.485	6.085	1.389	1.901	0.859	4.730	0.673	1.369	26.580
42	3.296	4.045	0.905	11.609	6.612	0.501	0.921	-2.660	0.525	-0.051	-0.190
43	3.049	4.098	0.812	13.158	6.488	0.464	0.929	-2.890	0.552	-0.068	-0.250
44	2.178	1.788	1.486	5.493	3.484	0.783	0.846	-1.050	0.402	0.149	0.300
45	0.570	0.384	2.240	2.624	0.797	1.642	0.724	7.140	0.309	1.914	14.470
46	1.329	1.203	1.167	3.875	2.333	0.667	0.795	-1.390	0.461	0.092	0.100
47	0.517	0.163	0.333	226.85	1.897	106.857	0.996	548.340	0.750	1.396	2218.500
50	3.041	1.860	1.731	8.654	4.438	0.668	0.896	-1.120	0.366	0.362	0.410
51	2.532	3.067	1.015	15.333	4.850	0.512	0.939	-2.630	0.496	-0.070	-0.230
52	3.564	4.712	1.130	13.238	6.390	0.542	0.930	-2.350	0.469	-0.077	-0.230
53	4.059	5.391	1.450	12.778	6.478	0.597	0.927	-2.330	0.408	-0.088	-0.260
54	5.909	4.851	1.601	46.429	8.949	0.621	0.979	-1.980	0.384	0.059	0.080
55	8.033	3.544	0.988	40.167	13.857	0.543	0.976	-2.030	0.503	0.156	0.330
56	2.635	1.734	1.234	6.683	4.550	0.568	0.870	-2.080	0.448	0.243	0.490
57	0.344	0.205	0.516	1.437	0.935	0.667	0.590	-4.190	0.660	1.020	14.570
58	3.500	3.985	1.342	10.792	5.722	0.517	0.915	-2.420	0.427	-0.047	-0.140
59	3.741	2.831	1.822	8.380	5.454	0.862	0.893	-0.670	0.354	0.157	0.290
60	3.763	3.300	1.826	8.580	5.488	0.809	0.896	-1.010	0.354	0.068	0.090
61	3.341	3.859	1.661	22.833	5.165	0.623	0.958	-1.660	0.376	-0.067	-0.140
62	0.857	0.456	0.686	27.053	1.958	0.972	0.964	-0.150	0.593	0.705	4.830
63	2.513	2.058	1.327	9.161	4.220	0.606	0.902	-1.850	0.430	0.117	0.200
64	5.671	3.869	1.624	13.355	8.159	0.757	0.930	-1.330	0.381	0.133	0.250

Appendix 5.6: (continue)

SampleID	(Cl-Na-K)/ (SO ₄ +HCO ₃ +NO ₃)	(Cl-Na)/Cl	Cl/Sum Anions	Na/(Ca+Mg)	Na/Na+Cl	(Na+K-Cl)/ (Na+K-Cl+Ca)	HCO ₃ /Sum Anions	Br*1000/Cl
	meq/l	meq/l	meq/l	meq/l	meq/l	meq/l	meq/l	meq/l
Lisan	ND	ND	ND	ND	ND	ND	ND	ND
Dead Sea	ND	ND	ND	ND	ND	ND	ND	ND
10	3.901	0.513	0.904	0.327	0.327	2.167	0.068	7.035
11	0.339	0.334	0.605	0.400	0.400	-0.689	0.257	2.591
12	4.570	0.422	0.930	0.366	0.366	3.105	0.049	6.447

13	5.355	0.441	0.937	0.359	0.359	2.824	0.046	ND
14	7.172	0.447	0.952	0.356	0.356	2.125	0.035	ND
15	5.071	0.475	0.930	0.344	0.344	2.326	0.049	ND
16	1.969	0.357	0.865	0.391	0.391	2.852	0.116	ND
17	19.188	0.506	0.978	0.331	0.331	5.658	0.010	4.749
18	5.371	0.479	0.933	0.343	0.343	2.003	0.048	ND
19	11.700	0.496	0.966	0.335	0.335	1.289	0.025	8.034
20	4.283	0.592	0.901	0.290	0.290	1.469	0.071	22.157
21	5.357	0.635	0.909	0.268	0.268	2.240	0.066	ND
22	0.088	0.458	0.181	0.351	0.351	-0.287	0.789	ND
23	0.016	0.188	0.111	0.448	0.448	-0.031	0.867	ND
24	1.286	0.327	0.857	0.402	0.402	-3.612	0.076	ND
25	192.781	0.764	0.997	0.191	0.191	1.297	0.000	ND
30	4.885	0.601	0.909	0.285	0.285	1.619	0.067	20.265
31	1.436	0.719	0.701	0.220	0.220	3.987	0.233	2.215
32	5.749	0.613	0.918	0.279	0.279	1.501	0.062	13.603
33	6.648	0.606	0.931	0.283	0.283	1.461	0.049	ND
34	6.404	0.597	0.929	0.287	0.287	1.437	0.051	ND
35	6.928	0.654	0.904	0.257	0.257	1.380	0.068	ND
36	5.877	0.587	0.927	0.292	0.292	1.562	0.053	ND
37	8.230	0.426	0.994	0.365	0.365	1.299	0.021	18.304
39	4.561	0.544	0.912	0.313	0.313	1.728	0.065	7.591
40	7.944	0.405	0.960	0.373	0.373	1.525	0.029	11.036
41	4.742	0.579	0.909	0.296	0.296	1.600	0.068	22.840
42	-0.035	-0.227	0.111	0.551	0.551	0.066	0.860	ND
43	-0.046	-0.344	0.102	0.573	0.573	0.091	0.866	ND
44	0.056	0.179	0.904	0.451	0.451	-0.086	0.068	ND
45	1.298	0.328	0.858	0.402	0.402	-3.818	0.075	ND
46	0.022	0.095	0.355	0.475	0.475	-0.037	0.529	ND
47	425.149	0.684	0.998	0.240	0.240	1.332	0.001	ND
50	0.119	0.388	0.267	0.379	0.379	-0.223	0.686	ND
51	-0.041	-0.211	0.141	0.548	0.548	0.077	0.816	ND
52	-0.044	-0.322	0.104	0.569	0.569	0.076	0.865	ND
53	-0.045	-0.328	0.100	0.570	0.570	0.070	0.867	ND

54	0.015	0.179	0.112	0.451	0.451	-0.025	0.858	ND
55	0.073	0.559	0.131	0.306	0.306	-0.159	0.840	ND
56	0.097	0.342	0.246	0.397	0.397	-0.218	0.686	ND
57	1.119	0.405	0.800	0.373	0.373	2.347	0.132	ND
58	-0.027	-0.138	0.114	0.532	0.532	0.051	0.834	ND
59	0.053	0.243	0.221	0.431	0.431	-0.074	0.648	ND
60	0.015	0.123	0.184	0.467	0.467	-0.021	0.679	ND
61	-0.031	-0.155	0.136	0.536	0.536	0.049	0.827	ND
62	0.810	0.468	0.656	0.347	0.347	-15.581	0.296	ND
63	0.040	0.181	0.221	0.450	0.450	-0.076	0.701	ND
64	0.044	0.318	0.161	0.406	0.406	-0.064	0.774	ND

*ND: Not determined

Appendix 5.8: Saturation indices of the end members of water chemistry in the dry season samples of Ein FeshCha.

Sample #	Anhydrite	Aragonite	Barite	Calcite	Dolomite	Gypsum	Halite	Siderite
10	-1.91	0.322	0.017	0.465	1.176	-1.70	-4.88	-3.11
11	-2.282	-1.54	-0.052	-1.399	-2.65	-2.09	-6.68	-1.87
12	-1.89	-0.44	-0.160	-0.298	-0.48	-1.68	-4.58	-2.23
13	-1.79	-0.18	-0.151	-0.038	0.047	-1.59	-4.37	-1.62
14	-1.77	-0.13	-0.150	0.01	0.068	-1.56	-4.14	-1.79
15	-1.87	-0.09	-0.122	0.049	0.406	-1.67	-4.56	-1.42
16	-1.97	0.563	-0.163	0.704	1.81	-1.77	-4.46	-0.84
17	-1.16	1.50	-0.265	1.646	2.91	-0.95	-3.22	-1.28
18	-1.95	0.25	-0.152	0.398	1.11	-1.71	-4.57	-1.49
19	-2.15	0.043	-0.520	0.187	1.01	-1.93	-3.85	-1.76
20	-1.89	-0.106	-0.151	0.036	0.61	-1.68	-4.75	-1.73
21	-1.59	0.358	-0.170	0.5	1.14	-1.38	-4.65	-1.62
22	-2.97	-0.053	*ND	0.094	0.44	-2.73	-7.76	ND
23	-3.51	0.127	ND	0.275	0.54	-3.27	-8.13	ND
24	-1.06	0.342	-0.043	0.478	0.84	-0.89	-4.60	-1.60
25	0.28	0.805	-1.114	0.937	3.27	0.15	0.20	ND
30	-2.03	-0.305	0.025	-0.162	0.115	-1.81	-4.93	-1.90
31	-2.15	-0.048	-0.47	0.095	0.33	-1.93	-6.34	-1.38
32	-2.08	0.086	-0.253	0.231	0.902	-1.86	-4.81	-1.54
33	-2.02	-0.547	-0.160	-0.402	-0.366	-1.79	-4.67	-2.20
34	-2.02	-0.72	-0.131	-0.578	-0.66	-1.79	-4.65	-2.37
35	-2.12	-0.58	-0.0304	-0.432	-0.186	-1.90	-4.76	-2.19
36	-2.01	-0.41	-0.22	-0.261	-0.06	-1.78	-4.68	-2.08
37	-1.77	-0.60	-0.041	-0.456	-0.30	-1.56	-3.57	-2.45
39	-2.05	-0.39	-0.26	-0.25	-0.013	-1.84	-4.82	-2.01
40	-2.16	-0.37	-0.41	-0.226	0.14	-1.95	-3.98	-2.15
41	-1.98	-0.74	-0.19	-0.59	-0.73	-1.77	-4.78	-2.38
42	-2.93	-0.076	ND	0.071	0.25	-2.69	-7.93	ND
43	-3.02	-0.19	ND	-0.048	0.06	-2.78	-7.96	ND
44	-2.33	-0.064	-0.141	0.080	0.117	-2.11	-7.11	-4.97
45	-1.08	0.191	-0.027	0.33	0.53	-0.91	-4.62	-1.73
46	-2.40	-0.115	-0.25	0.027	0.151	-2.20	-6.99	-4.17
47	-1.16	0.058	-1.33	0.20	1.27	-1.05	-0.97	ND
50	-2.86	-0.23	ND	-0.08	-0.335	-2.62	-7.69	ND
51	-3.01	0.347	ND	0.495	1.05	-2.77	-7.67	ND
52	-2.93	-0.246	ND	-0.01	-0.18	-2.69	-7.99	ND
53	-2.75	0.111	ND	0.258	0.424	-2.51	-7.92	ND
54	-3.36	0.029	ND	0.177	0.218	-3.12	-8.09	ND
55	-3.28	0.136	ND	0.283	0.643	-3.28	-8.34	ND

56	-2.65	-0.466	ND	-0.321	-0.62	-2.42	-7.45	ND
57	-1.50	0.358	ND	0.501	1.44	-1.28	-4.78	ND
58	-2.88	0.35	ND	0.5	0.863	-2.63	-7.96	ND
59	-2.43	0.07	ND	0.218	0.298	-2.203	-7.45	ND
60	-2.43	0.091	ND	0.235	0.337	-2.206	-7.51	ND
61	-3.14	-0.848	ND	-0.697	-1.61	-2.896	-7.879	ND
62	-2.94	0.351	ND	0.494	1.296	-2.72	-5.89	ND
63	-2.75	-0.100	ND	0.043	0.0979	-2.534	-7.476	ND
64	-2.63	-0.086	ND	0.061	-0.02	-2.396	-7.773	ND

*ND: Not determined

Author Curriculum VitaeAuthor Addressee:

Postal address:

Salah Al-Dien st.

P.O.Box 67793, East Jerusalem

Israel.

E-mail: jhassan@ccba.alquds.edu

Mob:++972-508573714



Mr. Jawad Hasan was born on June, 01, 1974 in Jerusalem, Palestine. Between 1987 and 1993 he attended the Arab Institute secondary School, where he obtained his General Secondary Certificate- Scientific Stream (Tawjihi) in 1993. In the same year he joined the Life Sciences Department at Al-QUDS University, Palestine. Mr. Hasan was awarded his B.Sc. degree in Biology in the year 1998. Between 1998 and 1999 he worked as undergraduate researcher, research assistant and as a researcher at the faculty of science and technology, life science department, Al-QUDS University.

Between 1999 and 2002 he joined the team of the Center for Chemical and Biological Analysis (CCBA), Al-QUDS University. During his work in the Center he managed to be the head of the quality control unit (QCU) in the center from 2002 up to 2005. During the years 1998 – 2005 he was involved in several projects:

- Wastewater treatment and agricultural reuse.
- Varietals tests and quality evaluation of tomatoes for the processing industry.
- Environmentally safe approach to plant disease control in the Middle East.
- Fate of Pesticides in Soil Irrigated with Treated Wastewater: interactions with organic matter and plant materials.
- Adsorption and determination of Cr(VI) and Cr(III) in industrial wastewater using ICP-AES

Mr. Hasan joined the Faculty of Graduate Studies, AL-QUDS University, Palestine in 2002 and was awarded M.Sc. in the Environmental Studies with cumulative average of 88.1% (a rating Very Good) in 2005. From 2005 to 2008 he was a PhD student at Karlsruhe University, Baden-Württemberg, Germany, department of Civil Engineering, Geo- and Environmental Sciences. During this time he attended the following courses: Hydrogeology – Groundwater Regions; Integrated Watershed Management and Watershed Modeling; Groundwater; Water Supply and Sanitation; Waste Analysis and Waste Treatment; Hydrogeology of Fractured Rocks and International Nature Conservation.

Mr. Hasan mother tongue is Arabic. In addition, he is fluent in speaking, reading and writing English and Hebrew.